SAND81-1045
Unlimited Release
September 1981

Strategic Petroleum Reserve (SPR) Geological Site Characterization Report Big Hill Salt Dome

R. J. Hart
Terri Smith Ortiz
Thomas R. Magorian-Consultant

Prepared by Sandia National Laboratories,
Albuquerque, NM 87185 and Livermore, CA 94550
for the United States Department of Energy under
Contract DE-AC04-76DP00789.

Sandia National Laboratories

SF 2900-Q(3-80)

Sandia Laboratories

Albuquerque, New Mexico
Livermore, California

date: December 2, 1981

to: Distribution

from: J. F. Ney, 4543

subject: Replacement Pages for Strategic Petroleum Reserve (SPR) Geological Site Characterization Report Big Hill Salt Dome, SAND81-1045

The color overlays of Figures 5-1, 5-2, and 6-5 were shifted slightly when printed the first time. Therefore, we have had these figures reprinted and have enclosed them for your use. Please remove the old Figures 5-1, 5-2, and 6-5 and replace them with the new ones.

We are sorry for any inconvenience this may cause you.

TSO:4543:jmu

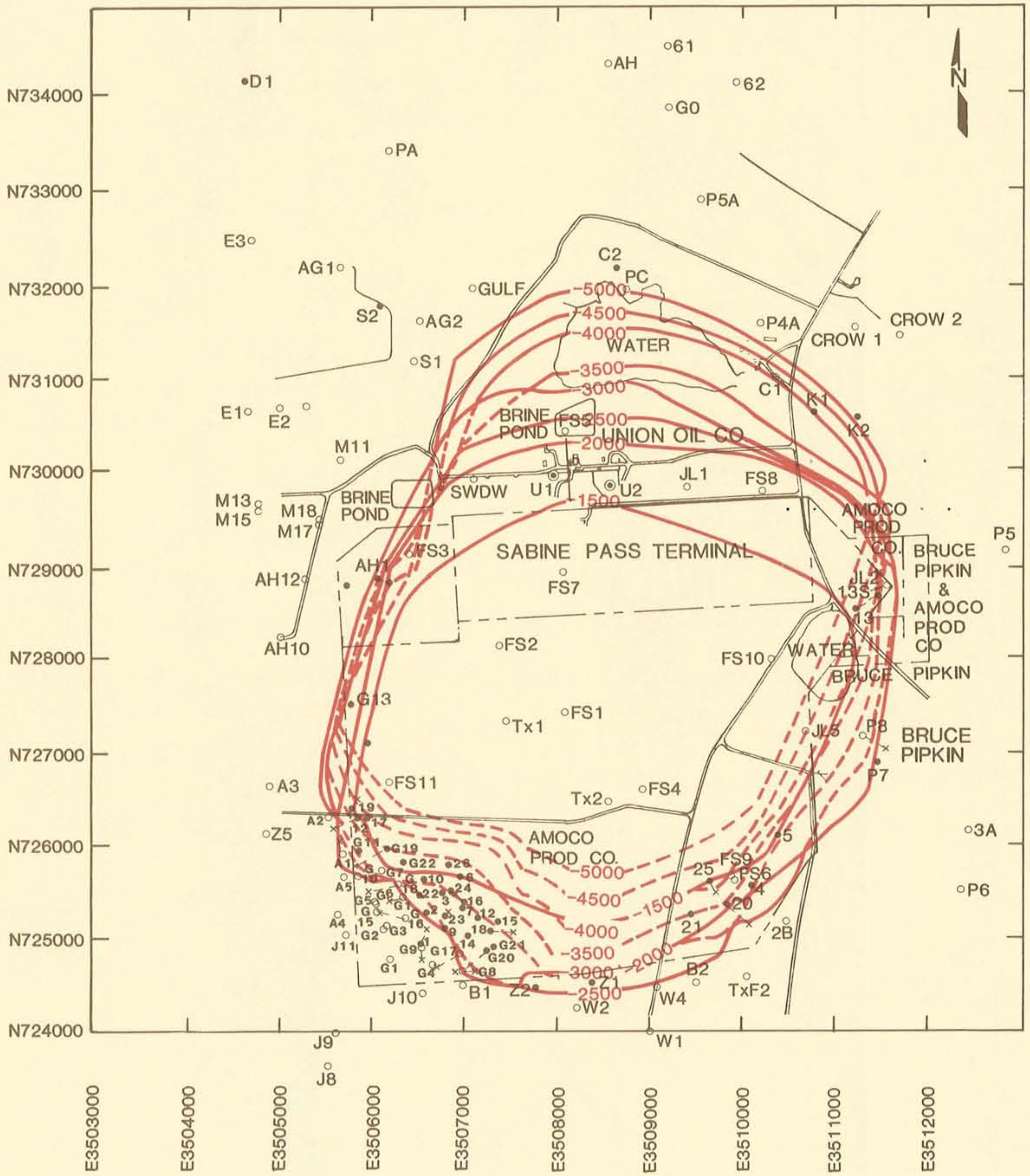

NOTES

1. SEE APPENDIX B FOR EXPLANATION OF WELL NUMBERS AND WELL LOCATIONS.
2. CONTOURED DEPTHS MEASURED IN FEET BELOW DRILLING FLOOR.

LEGEND

- U1 UNION OIL LPG CAVERN.
- SURFACE LOCATION OF WELL.
- G2 BOTTOM HOLE LOCATION OF WELL.
- G2 BOTTOM HOLE LOCATION OF SIDETRACK HOLE.
- G2 DRILLED AS VERTICAL HOLE. NO BOTTOM HOLE LOCATION AVAILABLE.
- G2 LOCATION OF WELL PENETRATING SALT.
- SALT DEPTH CONTOURS

1000 500 0 1000 2000

DISTANCE IN FEET

BIG HILL SALT DOME
STRUCTURE MAP-SALT

Sandia National Laboratories

T. R. MAGORIAN

SEP 1981 FIG. 5-1

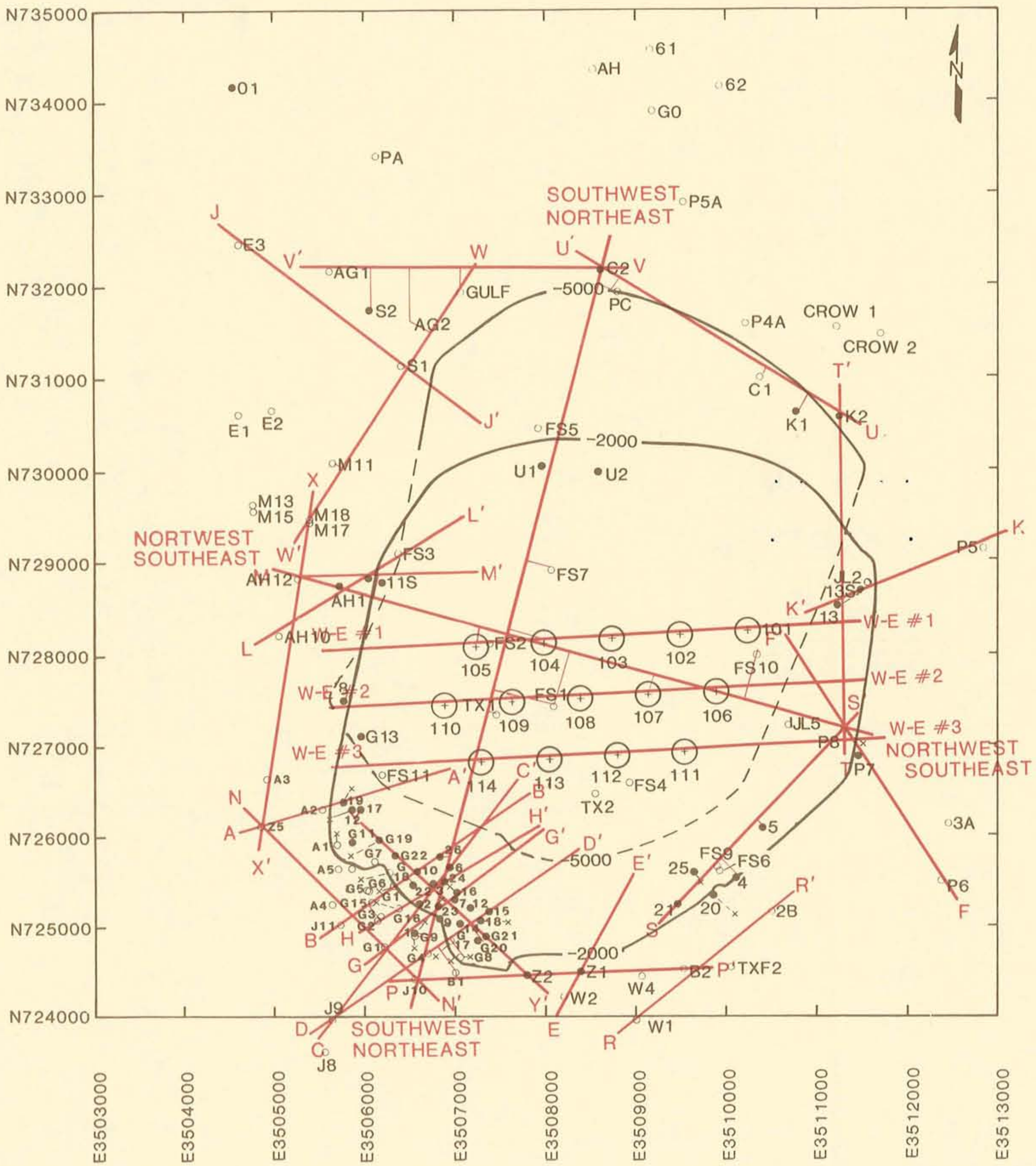

NOTES

1. SEE APPENDIX B FOR EXPLANATION OF WELL NUMBERS AND WELL LOCATIONS.

LEGEND

UI UNION OIL LPG CAVERN

SURFACE LOCATION OF WELL.

G2 BOTTOM HOLE LOCATION OF WELL.

G2 BOTTOM HOLE LOCATION OF SIDETRACK HOLE

G2 DRILLED AS VERTICAL HOLE. NO BOTTOM HOLE LOCATION AVAILABLE

101 PROPOSED SPR CAVERNS

SECTION LINE

WELLS PROJECTED TO SECTION LINE

BIG HILL SALT DOME SECTION REFERENCE MAP

Sandia National Laboratories

SEP 1981

FIG. 5-2

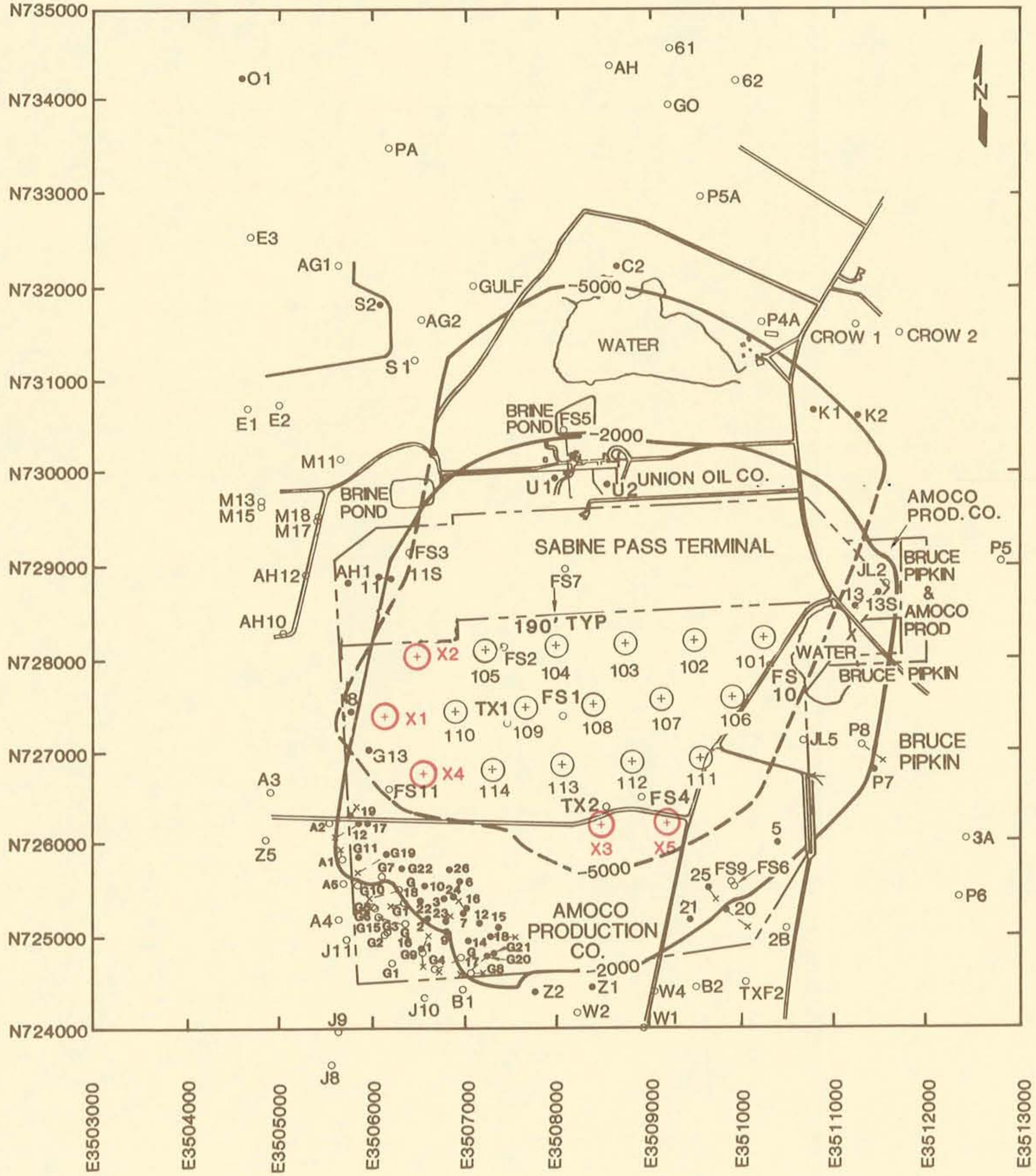

CAVERN LOCATION TABLE

CAV #	NORTH	EAST
101	728250.45	3510231.68
102	728214.66	3509482.52
103	728178.87	3508733.39
104	728143.09	3507984.23
105	728107.30	3507235.09
106	727583.79	3509888.10
107	727548.00	3509138.95
108	727512.21	3508389.79
109	727476.43	3507640.64
110	727440.65	3506891.51
111	726917.14	3509544.51
112	726881.34	3508795.35
113	726845.56	3508046.23
114	726809.77	3507297.08
X1	727404.86	3506142.36
X2	728071.52	3506485.95
X3	726214.68	3508451.79
X4	726773.99	3506547.09
X5	726250.46	3509201.77

1000 500 0 1000 2000
DISTANCE IN FEET

POTENTIAL EXPANSION
CAVERN LAYOUT
BIG HILL SALT DOME

Sandia National Laboratories

SEP 1981 FIG. 6-5

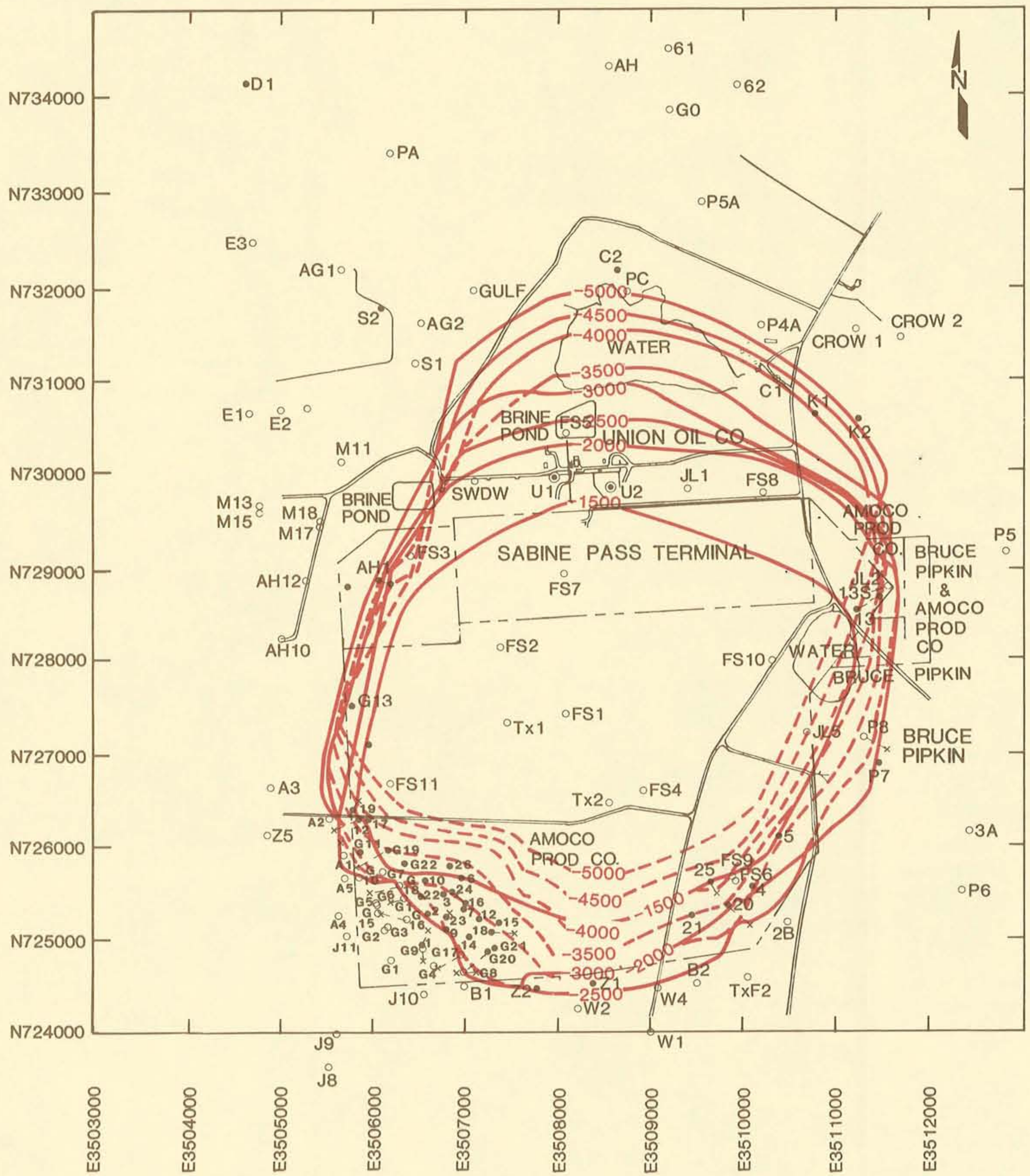

NOTES

1. SEE APPENDIX B FOR EXPLANATION OF WELL NUMBERS AND WELL LOCATIONS.
2. CONTOURED DEPTHS MEASURED IN FEET BELOW DRILLING FLOOR.

LEGEND

- U1 UNION OIL LPG CAVERN.
- \+ SURFACE LOCATION OF WELL.
- G2 BOTTOM HOLE LOCATION OF WELL.
- G2 BOTTOM HOLE LOCATION OF SIDETRACK HOLE.
- ○ G2 DRILLED AS VERTICAL HOLE. NO BOTTOM HOLE LOCATION AVAILABLE.
- • G2 LOCATION OF WELL PENETRATING SALT.
- SALT DEPTH CONTOURS

1000 500 0 1000 2000

DISTANCE IN FEET

BIG HILL SALT DOME
STRUCTURE MAP-SALT

Sandia National Laboratories

T. R. MAGORIAN

SEP 1981 FIG. 5-1

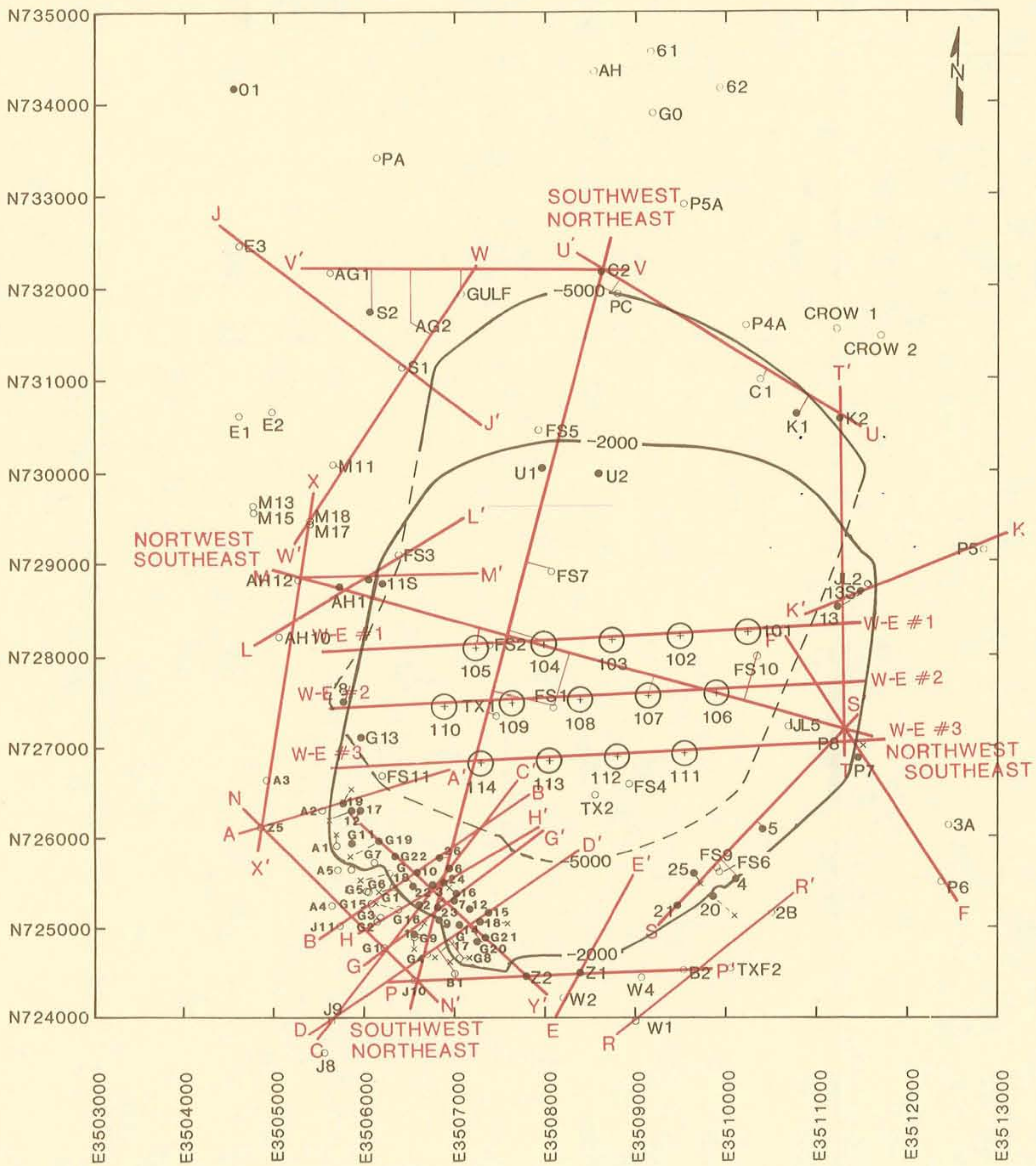

NOTES

1. SEE APPENDIX B FOR EXPLANATION OF WELL NUMBERS AND WELL LOCATIONS.

LEGEND

- UI — UNION OIL LPG CAVERN
- × — SURFACE LOCATION OF WELL.
- G2 — BOTTOM HOLE LOCATION OF WELL.
- G2 — BOTTOM HOLE LOCATION OF SIDETRACK HOLE
- ○G2 — DRILLED AS VERTICAL HOLE. NO BOTTOM HOLE LOCATION AVAILABLE
- 101 — PROPOSED SPR CAVERNS
- SECTION LINE
- WELLS PROJECTED TO SECTION LINE

1000 500 0 1000 2000

DISTANCE IN FEET

BIG HILL SALT DOME
SECTION REFERENCE MAP

Sandia National Laboratories

SEP 1981

FIG. 5-2

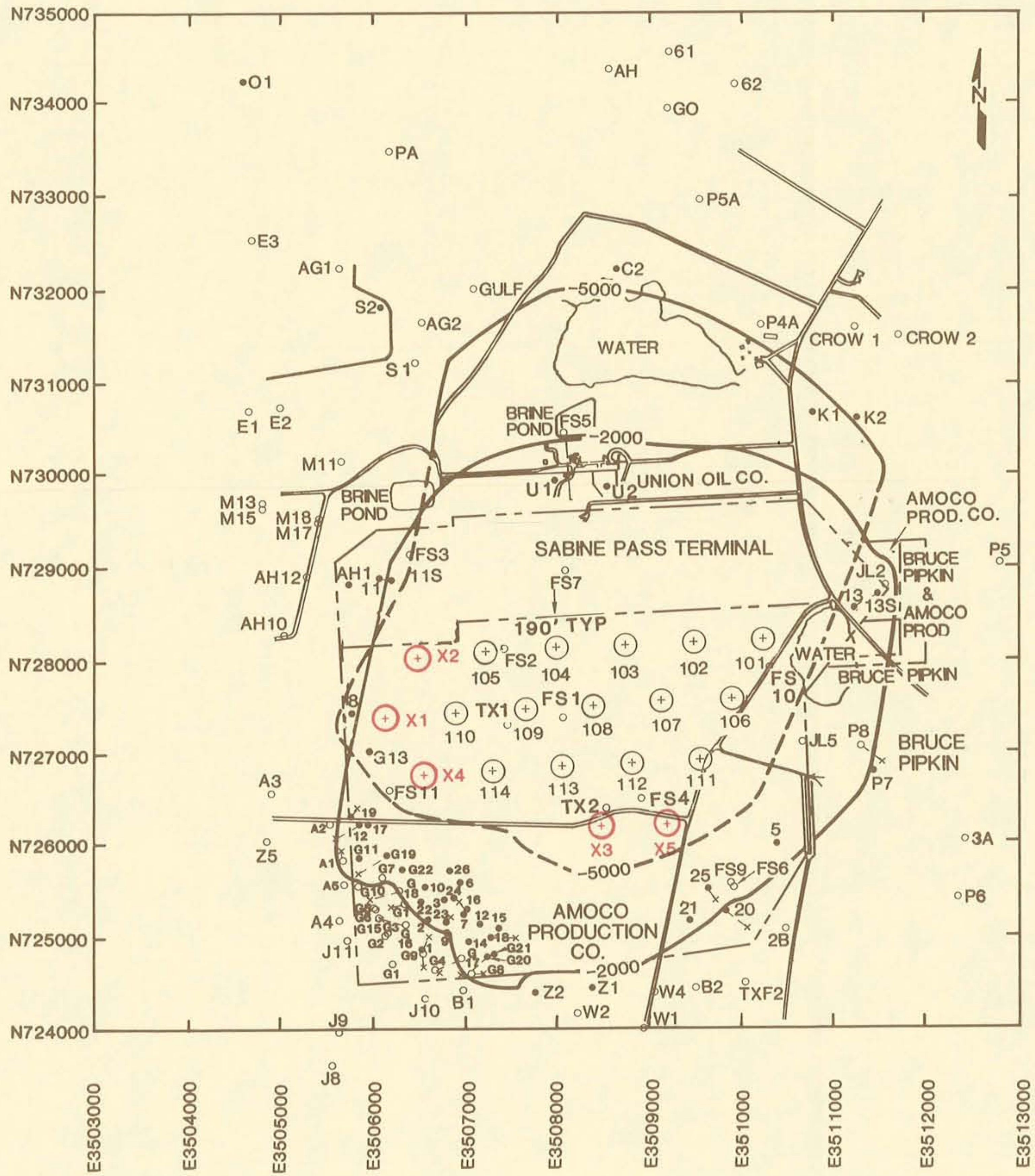

CAVERN LOCATION TABLE

CAV #	NORTH	EAST
101	728250.45	3510231.68
102	728214.66	3509482.52
103	728178.87	3508733.39
104	728143.09	3507984.23
105	728107.30	3507235.09
106	727583.79	3509888.10
107	727548.00	3509138.95
108	727512.21	3508389.79
109	727476.43	3507640.64
110	727440.65	3506891.51
111	726917.14	3509544.51
112	726881.34	3508795.35
113	726845.56	3508046.23
114	726809.77	3507297.08
X1	727404.86	3506142.36
X2	728071.52	3506485.95
X3	726214.68	3508451.79
X4	726773.99	3506547.09
X5	726250.46	3509201.77

1000 500 0 1000 2000

DISTANCE IN FEET

POTENTIAL EXPANSION CAVERN LAYOUT
BIG HILL SALT DOME

Sandia National Laboratories

SEP 1981 FIG. 6-5

Sandia Laboratories

Albuquerque, New Mexico
Livermore, California

date: December 2, 1981

to: Distribution

from: J. F. Ney, 4543

subject: Replacement Pages for Strategic Petroleum Reserve (SPR) Geological Site Characterization Report Big Hill Salt Dome, SAND81-1045

The color overlays of Figures 5-1, 5-2, and 6-5 were shifted slightly when printed the first time. Therefore, we have had these figures reprinted and have enclosed them for your use. Please remove the old Figures 5-1, 5-2, and 6-5 and replace them with the new ones.

We are sorry for any inconvenience this may cause you.

TSO:4543:jmu

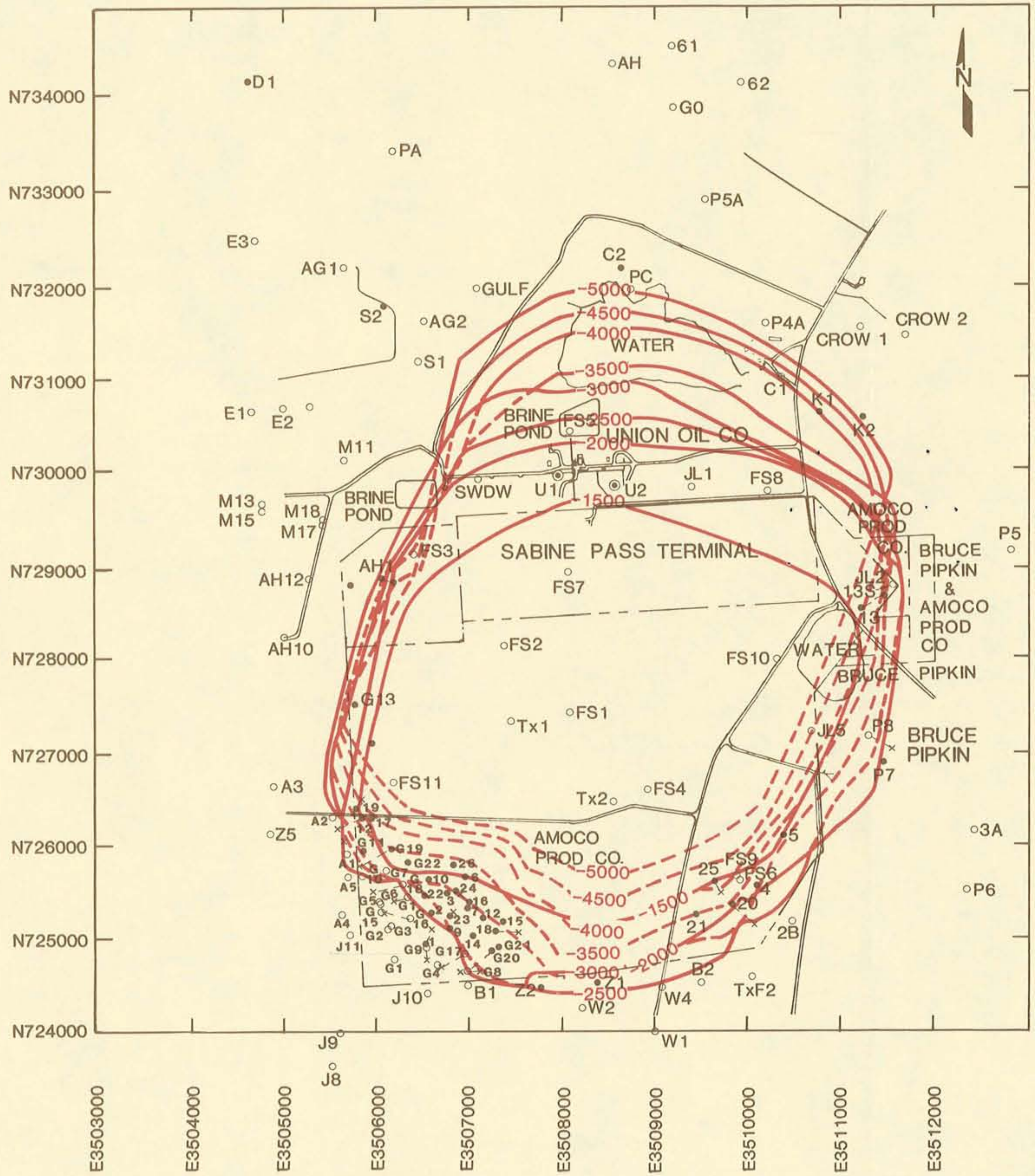

NOTES

1. SEE APPENDIX B FOR EXPLANATION OF WELL NUMBERS AND WELL LOCATIONS.
2. CONTOURED DEPTHS MEASURED IN FEET BELOW DRILLING FLOOR.

LEGEND

- U1 UNION OIL LPG CAVERN.
- SURFACE LOCATION OF WELL.
- G2 BOTTOM HOLE LOCATION OF WELL.
- G2 BOTTOM HOLE LOCATION OF SIDETRACK HOLE.
- G2 DRILLED AS VERTICAL HOLE. NO BOTTOM HOLE LOCATION AVAILABLE.
- G2 LOCATION OF WELL PENETRATING SALT.
- SALT DEPTH CONTOURS

1000 500 0 1000 2000

DISTANCE IN FEET

BIG HILL SALT DOME
STRUCTURE MAP-SALT

Sandia National Laboratories

T. R. MAGORIAN

SEP 1981 FIG. 5-1

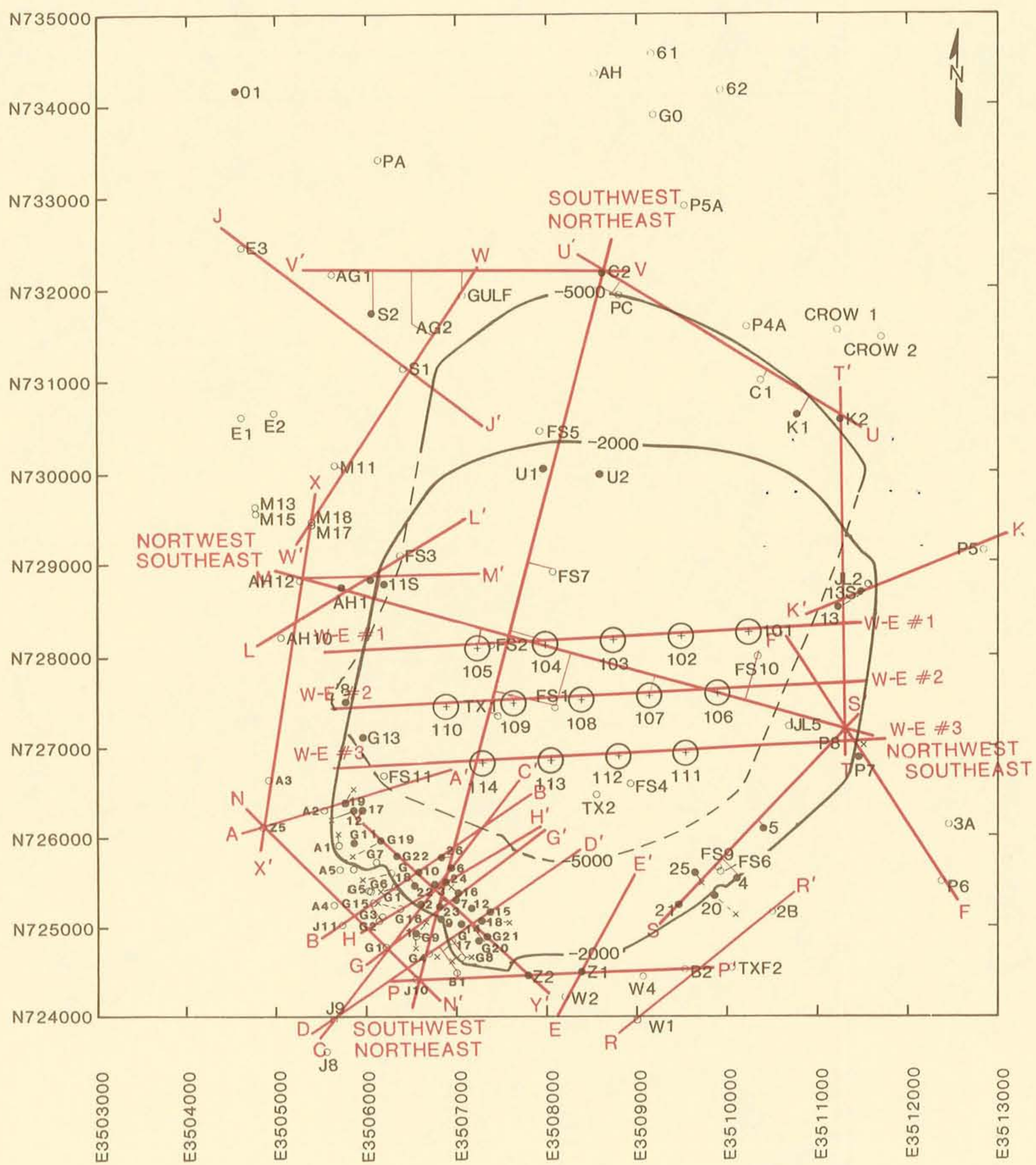

NOTES

1. SEE APPENDIX B FOR EXPLANATION OF WELL NUMBERS AND WELL LOCATIONS.

LEGEND

- UI UNION OIL LPG CAVERN
- SURFACE LOCATION OF WELL.
- BOTTOM HOLE LOCATION OF WELL.
- G2 BOTTOM HOLE LOCATION OF SIDETRACK HOLE
- G2 DRILLED AS VERTICAL HOLE. NO BOTTOM HOLE LOCATION AVAILABLE
- 101 PROPOSED SPR CAVERNS
- SECTION LINE
- WELLS PROJECTED TO SECTION LINE

BIG HILL SALT DOME
SECTION REFERENCE MAP

Sandia National Laboratories

SEP 1981

FIG. 5-2

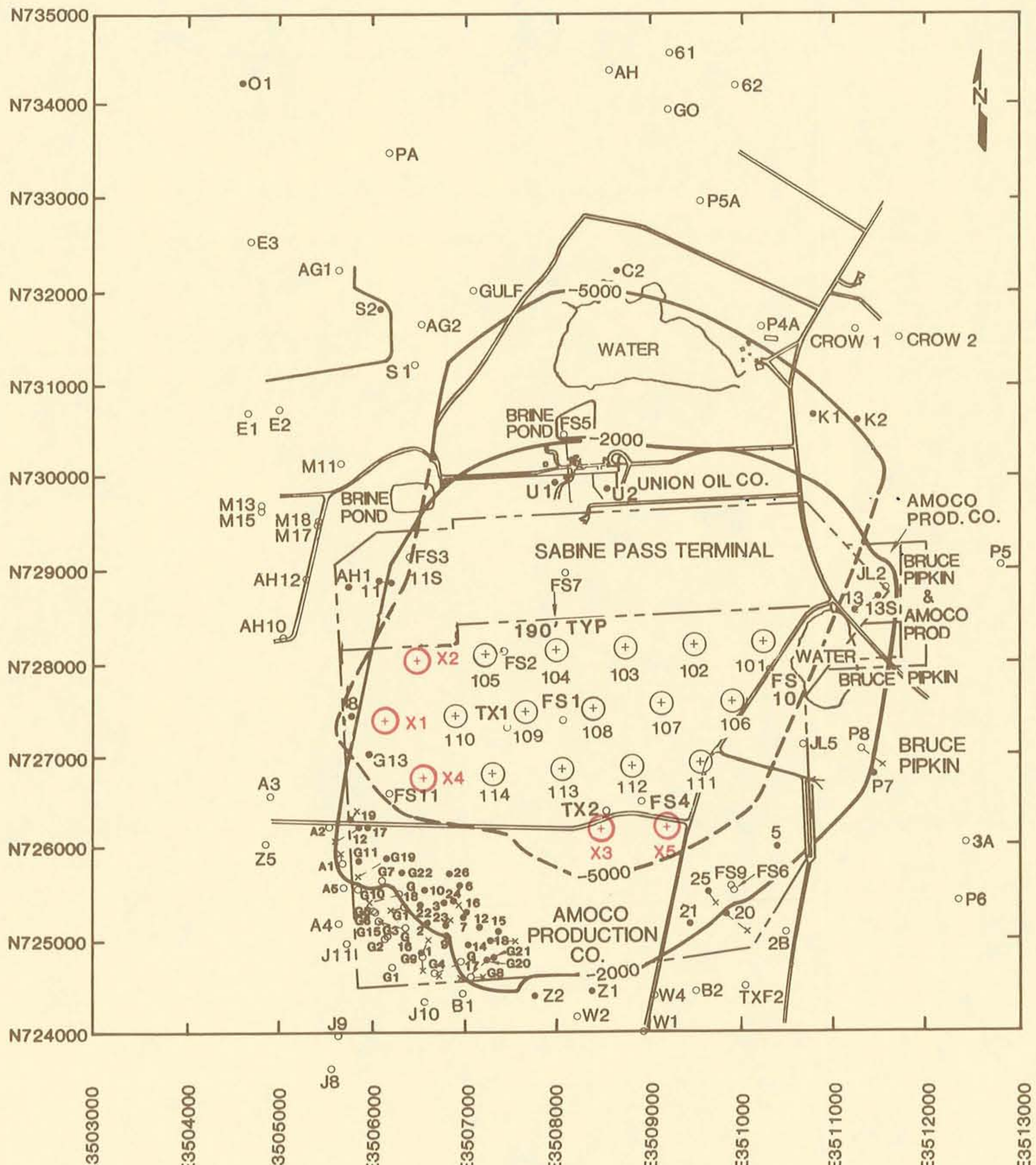

CAVERN LOCATION TABLE

CAV #	NORTH	EAST
101	728250.45	3510231.68
102	728214.66	3509482.52
103	728178.87	3508733.39
104	728143.09	3507984.23
105	728107.30	3507235.09
106	727583.79	3509888.10
107	727548.00	3509138.95
108	727512.21	3508389.79
109	727476.43	3507640.64
110	727440.65	3506891.51
111	726917.14	3509544.51
112	726881.34	3508795.35
113	726845.56	3508046.23
114	726809.77	3507297.08
X1	727404.86	3506142.36
X2	728071.52	3506465.95
X3	726214.68	3508451.79
X4	726773.99	3506547.09
X5	726250.46	3509201.77

1000 500 0 1000 2000
DISTANCE IN FEET

POTENTIAL EXPANSION
CAVERN LAYOUT
BIG HILL SALT DOME

Sandia National Laboratories

SEP 1981 FIG. 6-5

SAND81-1045
Unlimited Release
Printed September 1981

Distribution
Category: UC-94e

STRATEGIC PETROLEUM RESERVE (SPR)
GEOLOGICAL SITE CHARACTERIZATION REPORT
BIG HILL SALT DOME

R. J. Hart
Terri S. Ortiz
SPR Geotechnical Division
Sandia National Laboratories
Albuquerque, NM 87185

Thomas R. Magorian
Consulting Geologist-Geophysicist
Amherst, NY

Printed in the United States of America

Available from
National Technical Information Service
U. S. Department of Commerce
5285 Port Royal Road
Springfield, VA 22161

NTIS price codes
Printed copy: $10.00
Microfiche copy: A01

CONTENTS

CONTENTS (Cont)

FIGURES

FIGURES (Cont)

TABLES

GLOSSARY OF ABBREVIATIONS

AB	*Amphistigina* "B"
bbl	barrels
DOE	US Department of Energy
DR	*Discorbis* (restricted)
EPA	Environmental Protection Agency
fps	feet per second
HUD	Department of Housing and Urban Development
ICW	Intracoastal Waterway
LPG	liquefied-petroleum gas
MMB	million barrels
mg/L	milligrams per litre
msl	mean sea level
NOAA	National Oceanic and Atmospheric Administration
P/D	pillar-to-diameter ratio
ppm	parts per million
RL	Robulus "L"
SD	*Siphonina davisi*
S/D	Salt roof thickness-to-diameter ratio
SNL	Sandia National Laboratories
SPR	Strategic Petroleum Reserve
USGS	US Geological Survey
WIPP	Waste Isolation Pilot Project

CHAPTER 1 - SUMMARY AND RECOMMENDATIONS

Summary

Introduction

Sandia National Laboratories is responsible for the geotechnical program of the Strategic Petroleum Reserve (SPR) project for the Department of Energy (DOE). The overall scope of the Sandia program includes geological characterization of all existing and planned SPR sites. Development of 140 million barrels (MMB) of storage capacity in the Big Hill salt dome is planned as part of the SPR expansion to achieve 750 MMB of storage capacity.

This Phase 1 geological characterization of the Big Hill salt dome was done in association with Dr. Thomas R. Magorian, consulting geologist and geophysicist who provided the geological and geophysical analyses and interpretations that define the salt and the surrounding geology. Objectives of the study were to

1. Acquire, evaluate, and interpret existing data pertinent to geological characterization of the Big Hill dome

2. Characterize the surface and near-surface geology and hydrology

3. Characterize the geology and hydrology of the overlying cap rock

4. Define the geometry and geology of the dome

5. Determine the feasibility of locating and constructing 14 10-MMB storage caverns in the south portion of the dome

6. Assess the effects of natural hazards on the SPR site

The Big Hill salt dome in southwestern Jefferson County, Texas, was discovered in 1901 when the first oil exploration hole (a dry hole) was drilled into cap rock. The first producing well was drilled into the flank of the dome in 1923, but commercial production did not begin until 1949. No significant amount of oil or gas has been found in the cap rock overlying the dome. The Big Hill dome has been extensively explored for sulphur since 1917, but none has been produced. Through 1975, cumulative oil and gas production associated with the dome was 15,030,000 barrels (bbl) and 55,559 million cubic feet, respectively (Halbouty, 1979). A few producing wells on the southwest flank of the dome continue in operation.

The Union Oil Company operates two liquefied-petroleum gas (LPG) storage caverns on the northern part of the dome. The capacity of these two caverns, which were leached in 1957 and 1960, is ~400,000 bbl each.

Local Geology and Hydrology

Big Hill salt dome is ~20 mi southwest of Port Arthur, Texas, and 5.3 mi north of the Intracoastal Waterway (ICW). The surface expression of the dome is a mound ~1 mi in diameter rising to a maximum elevation of 37 ft mean sea level (msl), or 27 ft above the surrounding flat terrain. The soils at the site are Pleistocene silty loams and clays.

The site is within the Gulf Coast geosyncline, which is characterized by a thick accumulation of sediments. Big Hill, like other salt domes, formed as a result of plastic upward movement of deeply buried salt initiated by the tremendous weight of the denser overlying sediments.

Faulting in the region occurs on two scales: (1) large-scale regional faulting, or growth faulting associated with basin fill, and (2) small-scale, localized faulting associated with the growth of salt domes.

The surface water system at the site includes two freshwater ponds and a good drainage system. In addition, Union Oil Company has two brine ponds at Big Hill. Water for brining the SPR caverns will be taken from the Intracoastal Waterway to the south of the site (PB/KBB, 1979).

The subsurface hydrologic units near the site are the Miocene Burkeville aquiclude, the Pliocene Evangeline aquifer containing saline water, and the Pleistocene Chicot aquifer containing fresh water at very shallow depths grading to saline water with depth.

Cap-Rock Geology and Hydrology

The cap rock at Big Hill is comprised of two distinct layers: an upper layer of limestone and gypsum, and a lower layer of anhydrite. The top of the cap rock is roughly dome-shaped, rounded on top and steepening at the edges. Near the periphery of the dome the top of the cap rock is encountered below a depth of 1000 ft. Over the center of the dome, the cap rock is encountered at a depth of <300 ft. The thickness of the cap rock at Big Hill varies from 850 to 1350 ft, making it one of the thickest known cap rocks of the Gulf Coast salt domes. The cap rock at Big Hill is vuggy, and the lithology is complex. Faults and fractures caused by dissolution of the salt and collapse at the salt/cap-rock interface result in a highly permeable, discontinuous unit. Drilling logs indicate difficulty with stuck tools and with lost circulation (Table 4-1).

Salt-Dome Geology

Because of sparse drillhole data, geological interpretative methods based on strata convergence and faulting were used to define the geometry of the Big Hill salt dome. Interpretation of the dome geometry and surrounding geology was based on four seismic profiles and on 145 wells drilled on and around the dome, 46 of which penetrated salt.

The Big Hill dome is shaped like a cylindrical column tilted to the south. The top of the salt lies between 1300 and 1800 ft below the surface. The north flank of the dome dips gently downward to 2000 ft, where the dip increases to 60° between 2000 and 10,000 ft. The south flank is overhung below 2000 ft at about 60° dip. Both the east and west sides at the center of the dome are nearly vertical.

The Big Hill dome is overlain with Pleistocene sediments. Sediments flanking the dome are steeply dipping sands and shales of Pliocene, Miocene, and Oligocene age. Sediments around the dome have been faulted by radial and tangential faults caused by the upward movement of the dome.

Big Hill shows a consistent history of central domal uplift without the formation of any large rim synclines or other evidence of salt exhaustion or stagnation.

Cavern Locations and Geotechnical Considerations

The SPR Phase III expansion program calls for constructing 140 MMB of storage capacity at Big Hill. The objective of the cavern location study was to determine the feasibility of constructing 14 10-MMB caverns on the south part of the dome by using the dome definition developed in this site characterization study, the DOE-specified guidelines, and the geotechnical criteria necessary to assure cavern structural integrity and stability.

Caverns 270 ft in diameter and 2000 ft high at the end of five withdrawal cycles were assumed, based on SPR Phase II cavern leaching analyses. The following geotechnical criteria for cavern design were used:

Pillar-to-Diameter (P/D) Ratio	≥ 1.78
Salt Roof Thickness-to-Diameter (S/D) Ratio	≥ 1.0
Edge of Cavern-to-Edge of Dome	≥ 300 ft

Based on these geotechnical criteria and a cavern-to-property-line spacing of 190 ft, we determined that it is feasible to construct 14 10-MMB caverns on the south part of the dome. No separate exploratory-well or geophysical programs are required to proceed with cavern construction, according to this baseline cavern layout. Because of the sparse data forming the basis of geological interpretations of the salt contours, an exploratory extension of three of the cavern wells combined with a comprehensive well-logging and coring program are required to dispel uncertainties about the distance to the edge of the dome at the bottom of the caverns.

The potential for expanding the Big Hill site by constructing additional caverns was also investigated. The results of that study indicate that, with some additional exploration, the number of caverns on the site can be expanded to 19.

Natural Hazards

Ground water withdrawal in the area has caused some minor, regional subsidence (0.2 to 1 ft); and minor subsidence because of oil withdrawal around the periphery of the dome can be expected. However, it appears that subsidence of this type will pose no threat to SPR facilities. The possibility of subsidence caused by formation of the storage caverns has not yet been adequately determined.

The National Oceanic and Atmospheric Administration (NOAA) has classified the Big Hill area as having no reasonable expectancy of seismic risk. The two types of faults that occur in the area, regional growth faults and faults related to the upward movement of the salt dome, are both considered aseismic. Movement along these faults is gradual and should have no adverse effect on the site.

The 100-yr flood plain in the Big Hill area covers land up to 15 ft msl, completely encircling Big Hill. Hurricane-induced flooding could be somewhat higher because of the added impact of storm surge.

Recommendations

To ensure that SPR storage caverns at Big Hill meet the desired standards for structural integrity and stability at the lowest overall cost, the following recommendations are made.

1. Because of the high sulfate ion concentration in the groundwater at Big Hill and its corrosive nature, we recommend the use of sulfate-resistant cement in the casing program.

2. We recommend application of the geotechnical criteria specified in Chapter 6 to the design and construction of the caverns, and location of the caverns as shown in Figure 6-2, 6-3, and 6-4. These criteria are:

   $P/D \geq 1.78$
   $S/D \geq 1.0$
   Cavern-to-Dome Edge $\geq$ 300 ft
   Cavern-to-Property line = 190 ft

3. We recommend implementation of the exploratory extension drilling and coring program outlined in Chapter 6 for one of the wells for Caverns 101, 111, and 114 as shown in Figure 6-9.

4. We recommend, as a part of the cavern well-drilling program, the implementation of a comprehensive well-logging and coring program and a cap-rock water sampling program, as outlined in Chapter 6.

5. We recommend a comprehensive materials test program, as outlined in Chapter 6, to support the cavern leaching plan and the analytical efforts to evaluate structural stability and long-term creep of the caverns.

6. We recommend design and construction of the surface facilities of the site, including wellheads, to withstand potential effects of hurricanes.

7. We recommend location of all surface facilities at elevations above the 100-yr flood plain as shown in Figure 7-2, or their construction to withstand flooding.

8. We recommend updating the site characterization as data from future development and/or exploration of the dome become available, and addition of a section on materials properties when the results of the materials test program become available.

CHAPTER 2 - INTRODUCTION

Purpose and Scope of Study

Sandia National Laboratories is responsible for the geotechnical program of the Strategic Petroleum Reserve (SPR) project for the Department of Energy (DOE). The overall scope of the program includes all geotechnical investigations needed to support continued SPR development. Among these investigations is a comprehensive geological characterization of all existing and planned SPR sites. The Big Hill salt dome has been proposed as part of the SPR expansion program from 500 MMB to 750 MMB of storage capacity. This report is the Phase 1 geological characterization of the Big Hill salt dome/SPR Site. Phase 1 consists of the compilation, analysis, and interpretation of existing geological and geophysical data.

Specific tasks associated with preparation of this Phase I report were as follows:

1. Acquisition, evaluation, and interpretation of existing data for the geological characterization of the Big Hill dome. All known data from public and private sources were obtained under this task.

2. Characterization of the surface and near-surface regional and local geology and hydrology with respect to its impact on SPR objectives and facilities.

3. Characterization of the geology, hydrology, and mineralogy of the cap rock overlying the dome.

4. Characterization of the salt dome, including mapping of its boundaries to the depths of concern for storage cavern construction.

5. Determination of the feasibility of constructing 14 10-MMB storage caverns on the south part of the dome by using the geotechnical criteria necessary to assure cavern structural integrity and stability.

6. Assessment of the effects of natural events (i.e., hurricanes, earthquakes, and natural subsidence) on the SPR site.

Data Acquisition and Analysis

Two previous reports on the Big Hill dome have been prepared during the course of the SPR program (PB/KBB, 1979 and Fenix & Scisson, 1973). PB/KBB included preliminary geotechnical investigations, and Fenix & Scisson addressed the feasibility of the Big Hill salt dome as an SPR site. To avoid duplication of effort, these two previous studies and associated data and analyses were reviewed and used as a starting point for this study. Most of the work presented in this report continues and expands these previous studies, with the objective of providing a comprehensive geologic characterization of Big Hill. Data from AMOCO Texas Exploration Well 26, which was drilled in a strategic location has become available since the Conceptual Design Study was prepared. All well logs have been analyzed to accurately define the critical geometry of the salt and cap rock and the geology surrounding the dome. All analyses and data interpretations were based on existing material collected from other sources.

Site History

Unlike the other SPR sites, no brine-production wells have been drilled at Big Hill. Therefore, all SPR caverns will be formed especially to store crude oil. Hydrocarbons have been developed around the periphery of the dome, and considerable unsuccessful sulphur exploration has been carried out in the cap rock. In addition, two small storage caverns are operating in the northern part of the dome. Figure 2-1 is a site development map showing locations of all the wells and the two storage caverns.

Hydrocarbon Exploration

The topographic high at Big Hill was recognized as a potential salt dome by J. M. Guffey, who drilled the first well to cap rock in 1901. It was a dry hole. (Guffey later discovered oil at Spindletop dome.) In 1923, Houston Oil Company drilled the first producing well. Although several wells were later drilled that showed signs of oil, the first commercial production was not until 1949 (Dollison, 1965). A drilling program to define the Miocene and Oligocene reservoirs followed. Most of the Miocene production has come from the overhang area on the southwest flank. Cumulative production of oil through 1975 was 15,030,000 bbl, and total production of gas was 55,559 million cubic feet (Halbouty, 1979).

Sulphur Exploration

Although there has been extensive sulphur exploration at Big Hill, no sulphur has been produced. Texas Exploration Company drilled four holes into the cap rock in 1917-18, with two reports of uneconomic quantities of sulphur. In 1927-28, Freeport Sulphur Company drilled 16 exploratory sulphur wells without locating economic deposits. Jefferson Lake Sulphur Company drilled five holes in 1962, again finding no economic quantity of sulphur.

Union Oil Storage Caverns

Union Oil Company operates two LPG (isobutane and normal butane) storage caverns on the northern part of the dome (Figure 2-1). Cavern 1 was leached in 1957 by the Pure Oil Company (presently the Union Oil Company). A 9-5/8-in. production casing was cemented to -1998 ft, which is 328 ft into the salt. The cavern was leached through 7-in. and 5-in. strings. The 7-in. string was later removed and the 5-in. string left in place as a brine production string for product recycling. A leak in 1971 above the top of the salt resulted in a loss of butane. A new cemented 7-in. casing solved the problem. The latest sonar survey, which was run in 1978 (see Figure 2-2), showed the cavern as almost cylindrical and extending from 2650 to 3430 ft below the surface, with a maximum diameter of ~90 ft. Total volume in 1978 was 406,000 bbl. The salt roof over the cavern was 980 ft thick.

Cavern 2 was leached by the Pure Oil Company in 1960 to store propane. The well was cased by using 16-in. and 13-3/8-in. casings with the 13-3/8 in. set at -2288 ft, 588 ft into the salt. The cavern was leached through 10-3/4 in. and 7-in. suspended casings. Both strings were removed and replaced by an 8-5/8-in. string to be used as the brine string during propane cycling. The 8-5/8-in. casing has been replaced at least once because of corrosion; the cemented casings have remained pressure-tight. The latest sonar survey on this cavern was run in 1978 (Figure 2-3) and indicated that the top of the cavern was 2602 ft below the surface, and the bottom 3203 ft below the surface with a maximum diameter of 100 ft and a total volume of 403,000 bbl. The salt roof was 900 ft thick, and the cavern was nearly cylindrical.

Propane withdrawal from both storage caverns is done with nearly saturated brine; growth of the caverns since the sonar surveys of 1978 should therefore be minimal.

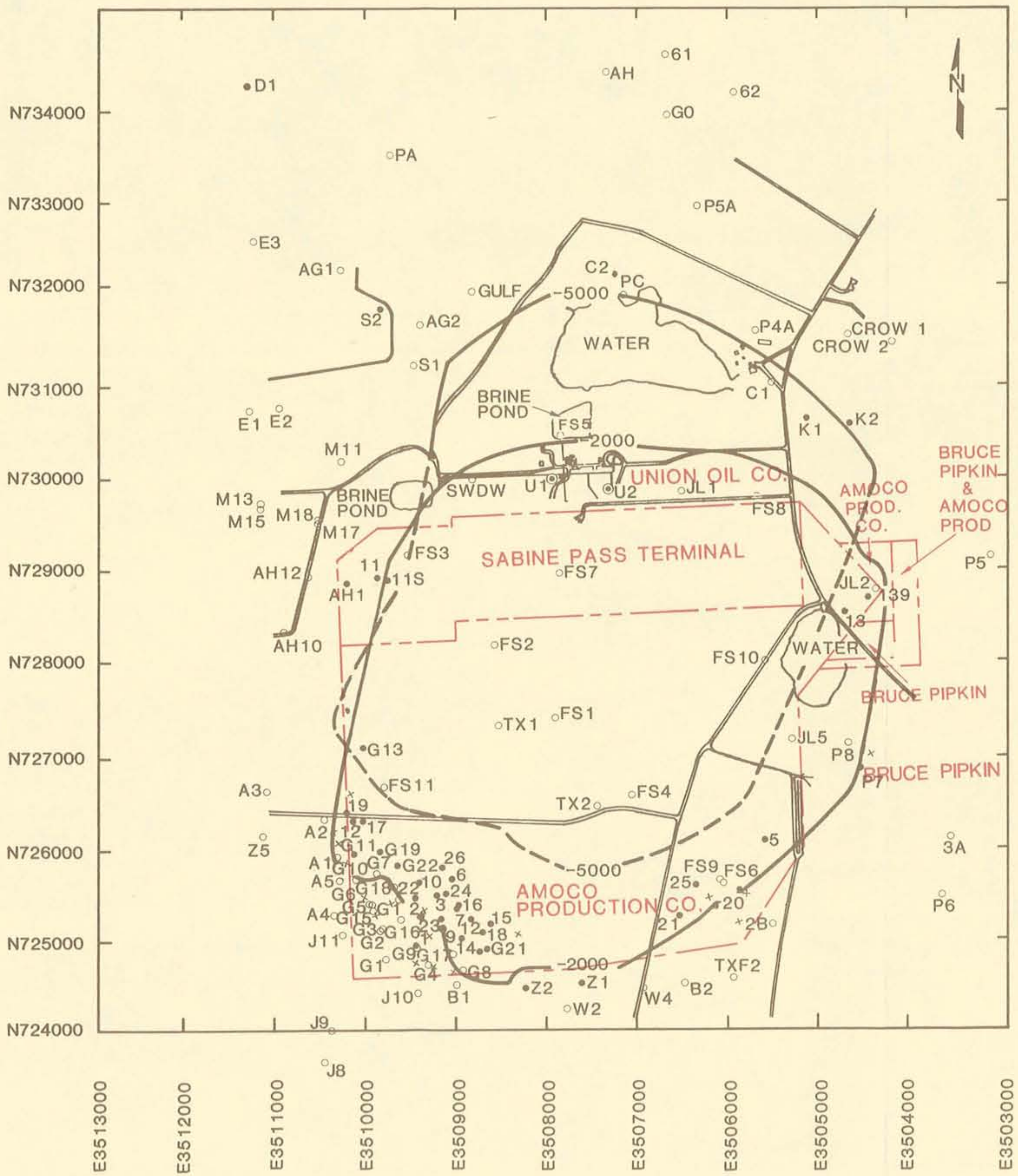

NOTES

1. SEE APPENDIX B FOR EXPLANATION OF WELL NUMBERS AND WELL LOCATIONS

LEGEND

- ◉U1 UNION OIL LPG CAVERN.
- SURFACE LOCATION OF WELL.
- • G2 BOTTOM HOLE LOCATION OF WELL.
- • G2 BOTTOM HOLE LOCATION OF SIDETRACK HOLE.
- ○ G2 DRILLED AS VERTICAL HOLE. NO BOTTOM HOLE LOCATION AVAILABLE.
- • G2 LOCATION OF WELL PENETRATING SALT.
- PROPERTY LINE.
- SALT CONTOUR
- SALT CONTOUR BENEATH OVERHANG
- ROADS

1000 500 0 1000 2000

BIG HILL SALT DOME
SITE DEVELOPMENT MAP

Sandia National Laboratories

SEP 1981 FIG. 2-1

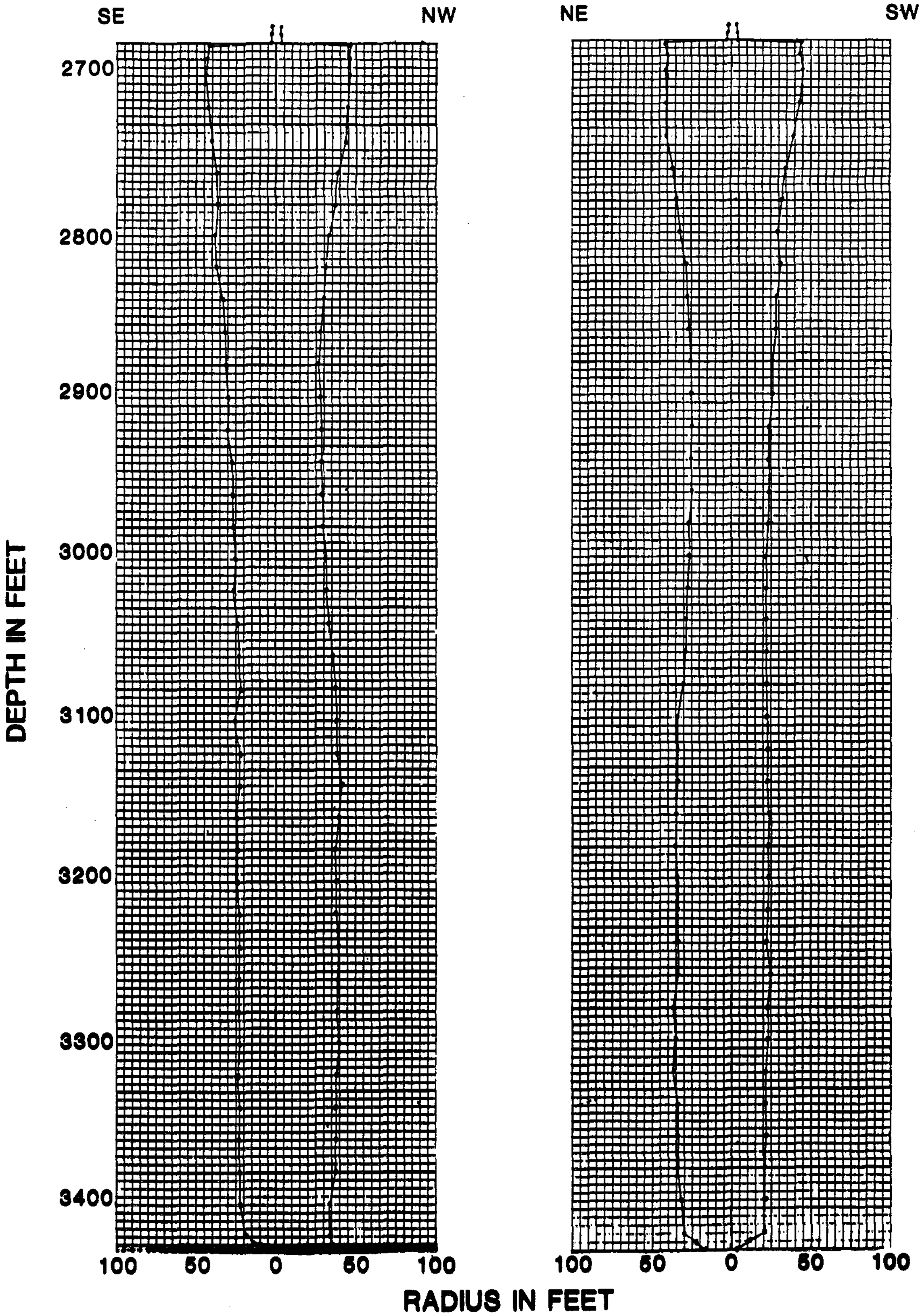

BIG HILL SALT DOME
DOWELL SONAR SURVEY
UNION OIL LPG #1 1978

Sandia National Laboratories

SEPT 1981

FIG. 2-2

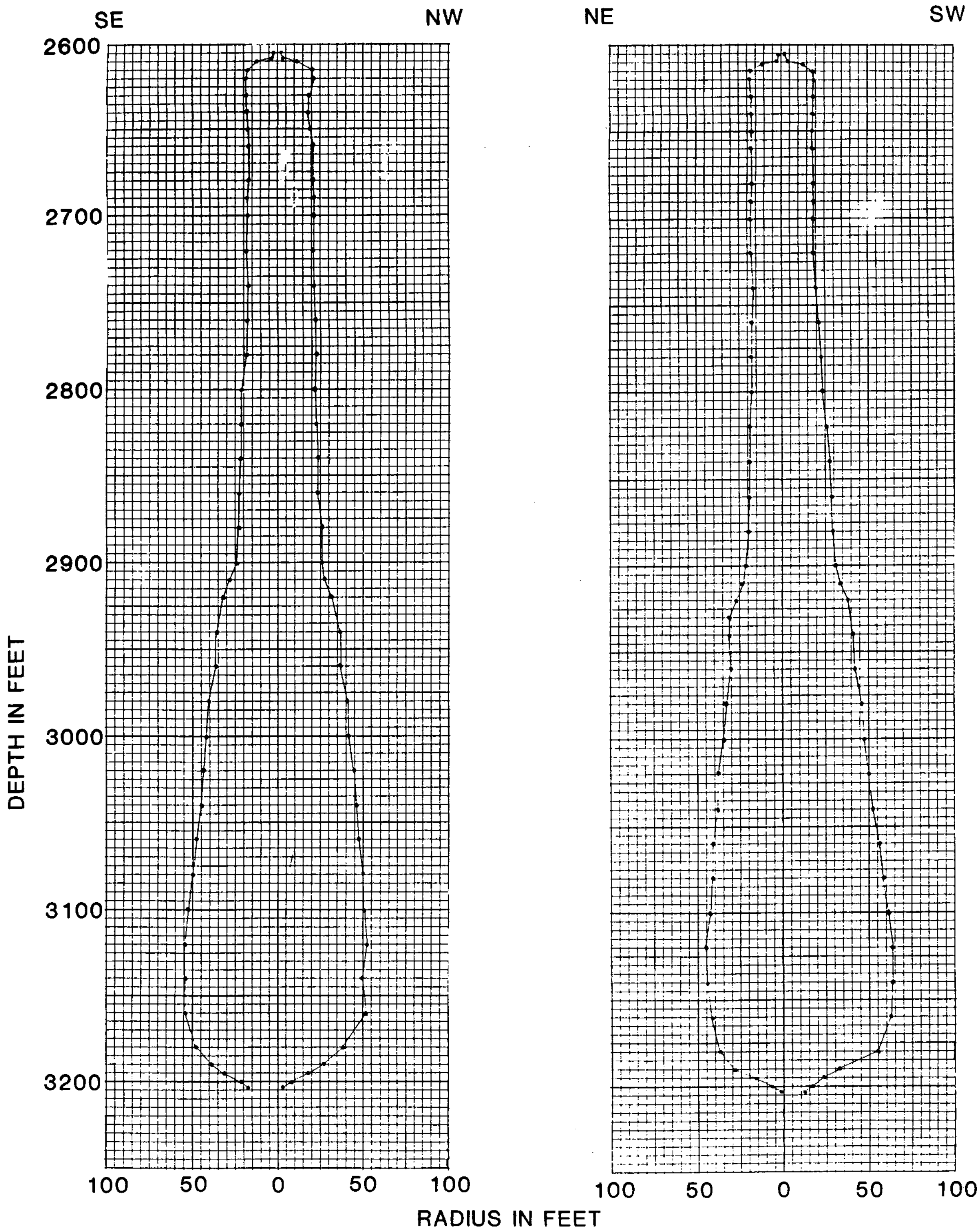

BIG HILL SALT DOME
DOWELL SONAR SURVEY
UNION OIL LPG #2 1978

Sandia National Laboratories

SEP 1981 **FIG. 2-3**

CHAPTER 3 - LOCAL GEOLOGY AND HYDROLOGY

Physiography

Big Hill is in southwestern Jefferson County ~20 mi southwest of Port Arthur, 70 mi east of Houston, and 9 mi north of the Gulf of Mexico. The site is 5.3 mi north of the ICW and 1 mi due north of Spindletop Marsh (Figure 3-1).

The site is in the West Gulf Coastal Plain Physiographic province, which is characterized by low, flat, featureless terrain. Marshes and meandering bayous are common. The plain dips toward the coast at ~1-1/2 ft/mi.

The surface expression of Big Hill salt dome is a roughly circular mound ~1 mi in diameter with a valley incised on the northwest edge (Figure 3-2). The maximum relief is 27 ft above the surrounding sediments, which is 37 ft above msl. Big Hill is covered by grass fields with some densely wooded areas.

Pimple mounds--small, circular mounds of sandy and silty materials--are common in the area surrounding the dome. Pimple mounds are 30 to 50 ft in diameter and up to 1 ft high. They seem to be soil-development features; however, their origin has never been satisfactorily determined.

Geologic Setting

Big Hill is located in the Gulf Coast Geosyncline, which is characterized by a thick accumulation of sediments. In vertical section, the geologic formations of the area form a series of gently dipping truncated wedges that thicken coastward, causing each wedge to dip slightly steeper than the overlying wedge. The lithology reflects depositional environments including continental (alluvial plain), transitional (delta, lagoon, beach), and marine (continental shelf).

Salt domes within the geosyncline occur in two belts. One extends through northern Mississippi, Louisiana, and Texas; the other extends along the Gulf Coast and offshore. Big Hill is in the Southern Belt (Figure 3-3). Salt domes are a result of upward movement of deeply buried salt by means of plastic flow. This flow is initiated by the tremendous weight of the overlying sediments on the less-dense salt. Many salt domes, like Big Hill, have a surface expression; however, they are minor structural features of the region (Wood et al, 1963).

Geologic History

The relevant history of the site begins with the deposition of the thick sequence (1000 to 5000 ft) of post-Permian (Table 3-1) Louann (salt and anhydrite) evaporites in a desert basin much like today's Red Sea area. After deposition of the Louann evaporites, carbonates and eventually clastic sediments of late Jurassic and Cretaceous age (see Table 3-1) were deposited.

Eocene

The base of the Tertiary in this area is the Marine Midway Shale of Lower Eocene Age. The Laramide Orogeny in western North America during middle Eocene gave rise to the Rocky Mountains, which in turn supplied the clastic sediments of the Wilcox Formation in the Gulf basin. The basin, or geosyncline, has subsided in response to the deposition of sediments. The rate of subsidence almost equals the rate of deposition. The shallow beds dip toward the Gulf, with both dip and structural complexity increasing with depth. The formations represent alternating marine transgressions (thick marine shales) and regressions (thick marine shales) and regressions (deltaic sands with interbedded lagoonal or backswamp muds) resulting in very complex stratigraphy.

Oligocene

There is no evidence from drilling to indicate the presence of the usual sheath of overpressured Vicksburg-Jackson shale around the salt, although it may be present on the south side below 4000 ft and on the north side below 10,000 ft. However, the limited production of oil close to the dome suggests that this sheath, which is a major source of oil, is also absent at depth.

Oligocene deep-water shales are the oldest sediments penetrated by drilling near the dome. A regional structure map of the Anahuac Shale is included as Figure 3-4. The continuous shale sequence of clays and organic-rich rocks is broken by the few thin sands of the underlying Frio Formation, deposited by submarine slides or turbidity currents flowing down the steep slope of the continental shelf from the north. The lower Frio (Hackberry sands) are the deep-gas pay sands of the Big Hill Northwest Field.

Miocene

The Miocene sediments consist of a pile of deltaic sands approximately 1/2 mile thick with some individual sand units on the order of hundreds of feet thick.

The usual breakdown of the Miocene subsurface stratigraphy in Texas is a letter designation of deltaic sandgroups A through E that are separated by shales. The lowermost Planulina or E sand overlies the top of the deepwater, overpressured shale sequence marked by the Discorbis (restricted) fauna (DR shale), which is the upper Anahuac Shale. Above the E sand is the Siphonina davisi (SD) shale, representing a marine transgression. The D sand, the main pay sand, is in turn separated from the C sands by the Robulus "L" (RL) shale, representing another marine transgression. The C sand is the lowest sand above the deepwater shale. The *Amphistigina* "B" (AB) shale (marine transgression) overlies the C sand. The Oakville, or B, sand overlies this shale. A major mid-Miocene unconformity between the B and C sands marks the end of rapid sedimentation near the edge of the continental shelf. Above the B sand is the Lagarto shale (*Bigerina florida*). The A sand is a thin group of sands at the top of the Miocene.

Table 3-2 is a breakdown of the Miocene stratigraphy in and around the dome. The Miocene sands represent a typical delta regression sequence that is divisible into a number of distinct sand types based on mode of deposition. Each type has a typical orientation and extension so that, once its type is known, a particular sand can be mapped or predicted in lateral extent with great accuracy. In addition, at particular places in the deltaic sequence, the sand types can be identified or confirmed by permeability variations that are readily detectable on the electric logs.

The two main contrasting sand types are beach and channel sands. Figure 3-5, a sample log of a typical Miocene sequence, shows an interpretation of the sediment types.

These sands are in turn overlain by muds that are often highly organic. These lagoonal muds are succeeded by a relatively thin sequence of river-channel sands that are gravely at the base and finer toward the top. These channel sands are highly permeable because of high-velocity sorting and cross-bedding of fluvial currents. Most channel sands were deposited inside meandering river beds as point bars. Thus these sands are formed into crescent-shaped deposits and are generally limited in extent.

Pliocene

Sediments of Pliocene age consist of silty clay with thin, lignitic sands that were deposited onshore in a backswamp area (Jones, et al, 1954). Much of the cap-rock material is of Pliocene age.

Pleistocene

Pleistocene sediments are related to recurring glacial advances and retreats (Table 3-1). Sea levels lowered during periods of glacial ice accumulation. As the glaciers melted, sea levels rose, resulting in the deposition of sands and gravels. Later in the interglacial periods the carrying capacity of the stream decreased as a result of decreased gradient. The glaciers melted and the sea level increased causing a decrease in the grain size of sediment to silt and clay (Bernard and LeBlanc, 1965).

The Lafayette Gravel marking the base of the glacial Pleistocene sediments includes some material of upper Pliocene age (Figure 3-6 and Table 3-3). The gravel is associated with the deep-stage erosion of the interior of the continent, and is 200 to 500 ft thick. It is prominent on much of the Gulf Coast and lies unconformably over the Pliocene marine silts. This gravel forms the base of the Chicot aquifer and is in turn overlain by clays of Kansan and Nebraskan age (Tables 3-1 and 3-3).

The Willis (Williana) Formation overlying the Lafayette gravel is of Nebraskan age. It is a sequence of sands, silts, and clay ~300 to 600 ft thick in the Big Hill area.

The Lissie (Bentley) Sand is the most prominent bed in the lower Pleistocene section and is 100 to 600 ft thick. It has a highly variable thickness typical of alluvial channel deposits during the glacial low stages of sea level. The sand was deposited at the beginning of the Yarmouth interglacial stage.

An unnamed clay of Yarmouthian age (Table 3-1), deposited as an interglacial backswamp sediment, overlies the Lissie Sand. Away from the dome, this unit lies at a depth of ~700 ft. Over the dome, it was found to overlie the cap rock in some wells. The clay thickens to >100 ft away from the dome. It is likely that the limestone and gypsum cap rock has incorporated much of this unit.

The Montgomery Sand (Table 3-3, Figure 3-6) is a thick sequence (200 to 400 ft) of sands deposited by glacial meltwaters during the Sangamon interglacial stage. Sand and gravel with minor silt and clay were deposited by coalescing point bars as rivers meandered around the dome. Clayey or silty layers accumulated near the top of the Montgomery as the stream neared base level. At the site, these sands formed the edge of the Trinity River delta. This and the overlying sand are the major freshwater aquifers in southeastern Texas.

The Beaumont Clay was deposited over the Montgomery after the Sangamonian interglacial period. The formation is a backswamp deposit of clay and silt. The Beaumont forms the surface sediments at Big Hill and extends 200 to 300 ft below the surface. It was partially oxidized and desiccated during a low-sealevel stage of the last ice age (Fisk, 1944). The clay is underlain in part by a variable or stray sand of Peorian age, often termed the Prairie Sand. Recent back-swamp marsh with sticky (bentonitic) black clay is ~5 ft above mean low water (sea level).

Regional Structure

Faulting in the Gulf Coast region occurs on two scales: large-scale regional faulting associated with basin filling, and small-scale localized faulting associated with the upward movement of salt domes. The regional faults can be mapped for miles and have displacements on the order of hundreds to thousands of feet.

The Gulf Coast geosyncline is typified by large-scale, east-west-trending normal faults (Figure 3-3). The faults are generally parallel to the present Gulf Coast or to one of the older Gulf Coast geosynclinal axes that are subparallel to the present coast. These faults are frequently referred to as "growth" faults since their origin was caused by the long-term, continuing subsidence of the geosynclinal basin. Gulf Coast growth faults are downthrown to the south in the direction of the major area of basin filling. The larger structures may have up to thousands of fault displacement. The faults dip at ~60° in the near-surface sediments but tend to flatten out at depth.

The local faulting associated with salt domes is restricted to the immediate dome area, seldom extending more than a few miles. Displacements of domal faults are normally on the order of tens to hundreds of feet, but can extend up to 1000 ft. Domal faulting at Big Hill is discussed in detail in Chapter 5.

Soils

The major soil groups present at Big Hill include the Hockley, Crowley, and the Morey silt loams (Crout, et al, 1960). The distribution of soils, which are all modifications of the Beaumont Clay, is shown in Figure 3-7.

The Hockley silt loam is typical over salt domes having a topographic expression. This soil covers most of the hill and is 14 to 30 in. thick. The upper horizon of this soil type is very pale brown and can hold a moderate amount of moisture for plants. The lower silt horizon absorbs water readily.

The Crowley silt loam (the Prairie Formation, in Louisiana) is present on the east side of the site. The upper 12 in. is granular, but the subsoil is very compacted.

The Morey silt loam can hold a moderate amount of moisture for plant use, but common surface crusts and impermeable subsoil make it difficult for water to enter the soil. The surface is a silt loam in most places, but clay loam or very fine sandy loam with yellowish-brown mottles is also present. The subsoil is olive gray with red and yellow-brown mottles. Large concretions of calcium carbonate are common in the lower subsoil.

The unmodified Beaumont marine clay is present in the extreme southwest and northeast corners of Big Hill. The soil is a dark-gray silty clay loam, or clay. The subsoil is mottled with brown by partial oxidation.

Oil wasteland occurs in the southern portion of Big Hill and to a lesser extent at former drilling sites.

As part of the conceptual design study, PB/KBB (1979) took several soil borings and tested samples. In general, the soil profile at Big Hill consists of a surface layer 1 to 3 ft thick composed of silt and fine sand underlain by medium stiff to stiff clays of varying composition interbedded with silty fine sand extending to the depth of the boring, 100 ft. Locally a silty sand layer <5 ft thick exists at depths of 8 to 10 ft below the surface.

The shear strength of cohesive soils ranges from 700 to 1300 lb/ft^2 for the first 10 ft of the soil profile. From 10 to 25 ft the value ranges from 450 to 700 lb/ft^2. Samples collected from this interval have slickenside surfaces on which the soil could have failed. Below 25 ft, the shear strength increases to 1000 to 2000/lb/ft^2.

Results of consolidation tests indicate that clays are generally overconsolidated and of low compressibility. The natural moisture contents of all soils are lower than the liquid limits.

Swelling clays are common in the Beaumont clay and associated soils. Soils that may swell are those subject to seasonal moisture change and that have an overburden pressure less than the swelling pressure of the soil. The local depth of seasonal moisture change is 8 ft below the surface. The plasticity index of soil in the upper 10 ft varied from 20 to 50, indicating soils of medium to high swelling potential. However, swell-pressure tests of two samples resulted in swell pressures of 66 to 233 psf. A swell pressure <400 psf indicates low swelling potential. Swell-potential tests of two samples resulted in volume changes of 1.5% and 2.8%. A volume change of 1.5% to 5% indicates a medium swelling potential. In general, PB/KBB concluded that, based on the lab tests, these soils show a low potential for swelling. An overburden of only 2 to 3 ft would be enough to restrain swell-induced displacements.

A complete description of the soil profiles, the testing procedures, and results can be found in PB/KBB (1979). This report also includes information on soils at the ICW water source location.

Hydrology

The surface water system is shown in Figures 3-8 and 3-2. There are two brine ponds on the Union Oil Company property, one with a capacity of 320,000 bbl, the other 380,000 bbl. Two freshwater ponds are also located close to the site. One pond, on the north side of the dome, covers 50 acres; it has been modified somewhat for rice field irrigation. The other pond to the southeast covers 20 acres. It appears to have been built up on the south side. The freshwater ponds do not seem to be related to subsidence. Surface drainage is good, and erosion is negligible because of permanent ground cover. A discussion of the regional water system is presented in DOE (1978).

Water for leaching the SPR caverns (up to 1,400,000 bbl/day) will be taken from the ICW south of the site (PB/KBB, 1979). This segment of the waterway extends from the Sabine-Neches Canal southwest along the Gulf Coast toward Galveston. It is ~250 ft wide with a maintained depth of 12 ft. Flow is influenced by winds and tides but is generally to the northeast. Spindletop Ditch joins the ICW about 5-1/2 mi southeast of the Big Hill dome. The ditch is 150 ft wide with a depth of <6 ft. Water quality data and sediment quality data for the ICW south of the dome are included in DOE (1978).

The subsurface hydrologic units of the Big Hill area are the Chicot and Evangeline Aquifers and the Burkeville Aquiclude. The units are composed of gravel, sand, silt, and clay of Miocene, Pliocene, and Pleistocene age (Table 3-3). Hydrologic cross sections through the dome are shown in Figures 3-9 and 3-10.

The southwest-northeast hydrologic section (Figure 3-9) shows the convergence and pinchout of Pliocene and lower Pleistocene sands. The later Montgomery formation thickens slightly to form the permeable fresh and slightly saline water zones over the cap rock.

The Burkeville Aquiclude is the lowermost hydrologic unit and corresponds to the Miocene Lagarto Clay (Table 3-3).

The Evangeline Aquifer overlies the Burkeville Aquiclude and includes the lower Pliocene Goliad Sand and the silts and sands of the upper Pliocene (Table 3-3). The total thickness of the aquifer is 1000 to 1100 ft near the dome. The Evangeline Aquifer contains saline water in the Big Hill area.

The Chicot Aquifer overlies the Evangeline Aquifer and consists of the Pleistocene Lafayette Gravel, Willis Sand, Bentley Formation, Montgomery Formation, and the Praire Formation, (Beaumont Clay) (Table 3-3). Water in the upper Chicot is fresh but grades to saline at depth. The total thickness of the aquifer is 1250 to 1350 ft. The Chicot is more permeable than the Evangeline and differs in grain size, cementation, and compaction.

The Chicot can be divided into an upper unit that may correspond to the 200-ft sand in southwestern Louisiana, and a lower unit that may correspond to the 500 and 700-ft sands. In some places the two units are separated by clay. However, determination of the boundary is especially difficult around salt domes. Interconnection of aquifers is indicated by electric logs and water quality data near Big Hill (Wesselman and Aronow, 1973).

While boring for soil profile determinations, PB/KBB (1979) noted that the groundwater surface varied from a depth of ~6 ft below the surface near the center of the hill (elevation +37 ft msl) to about ground level near the base of Big Hill (10 ft msl). The groundwater level generally follows the topography of the site.

Fresh water (<1000 mg/L dissolved solids) is limited to the Upper Chicot in the Big Hill area. Over the dome, fresh water is limited to the zone extending from near the surface to a depth of slightly less than -100 ft msl (Figures 3-9 and 3-10). Less than 2 mi northwest of the dome, fresh water extends to -200 ft msl. Slightly saline (1000 to 3000 mg/L dissolved solids) water is present below the fresh water to ~-300 ft msl over the dome (Figures 3-9 and 3-10) and to ~-500 ft msl near Winnie (Figure 3-11). Saline water is probably introduced into the shallower sands by dissolution of the salt dome or from vertical movement of deeper saline water around the flanks of the dome (Wesselman and Aronow, 1973).

Major centers of groundwater withdrawal from the Lower Chicot are at Baytown, 40 mi west of Big Hill and in the Beaumont/Port Arthur area, 22 mi northeast of the site. The decline in water at Beaumont/Port Arthur affects water levels at Big Hill and produces a movement of groundwater southeast to eastward from Big Hill (Wesselman and Aronow, 1973).

The major center for groundwater withdrawal in the Upper Chicot is at Winnie, 8 mi northwest of Big Hill. Withdrawals at Winnie have two major results. First, the saline/freshwater interface in the Upper Chicot is drawn northwest toward Winnie. Second, the reduction in aquifer pressure may cause some minor regional subsidence. From 1951 to 1965, the water level had declined a few feet at Big Hill (Table 3-4).

Table 3-5 summarizes the aquifer tests in the Big Hill area. Table 3-6 gives the accompanying chemical analyses of the water wells in the area.

Table 3-1

Geologic Timetable

ERA	PERIOD	EPOCH	GLACIATION	INTERGLACIATION	MILLIONS OF YEARS AGO
CENOZOIC	QUATERNARY	HOLOCENE			0 012
		PLEISTOCENE	WISCONSINIAN		
				SANGAMONIAN	0.215
			ILLINOIAN		
				YARMOUTHIAN	0 70
			KANSAN		
				AFTONIAN	1 3
			NEBRASKAN		
				(BLANCAN ?)	1 8
	TERTIARY	PLIOCENE			10
		MIOCENE			22 5
		OLIGOCENE			40
		EOCENE			55
		PALEOCENE			70
MESOZOIC	CRETACEOUS				141
	JURASSIC				195
	TRIASSIC				230
PALEOZOIC					

From Van Eysinga, 1975.

Table 3-2

Big Hill SPR Site Tertiary Geologic Units

Age	Formation	Map Symbol	Stratigraphic Unit	Biostratigraphic Zone	Sediment Type	Depositional Environment	Transport Mode	Comment
Pliocene	Goliad	PL			Sand Over Clay	Alluvial Levee and Backswamp	River Channel	
				Buliminella	Sand Over Shale	Alluvial Levee	Sitty Mud/Overbank	
Miocene	Fleming (Miocene)	A	Clovelly		Sand	Delta	Distributary Channel	
	Largarto	BF	Lagarto	Bigenerina Florida	Shale	Backswamp		
	Oakville	B	Duck Lake	Bigenerina Humblei	Sand	Delta	Beach/Bar	Highly Mineralized Close to Salt
		AB		Amphistegina B	Shale	Marine Transgression	Suspended Mud	Major Unconformity
	Catahoula	C	Duck Lake		Sand	Delta	Distributary Channel	
		RL		Robulus L	Shale	Marine Transgression	Suspended Mud	
	Main	D	Napoleonville	Discorbis Bolivarensis	Sand	Delta	Shoreline Beach/Bar	Main Producing Sand
		SD		Siphonina Davisi	Shale	Marine Transgression		
	Lower	E		Planulina Palmerae		Delta	Distributary Channel	
Oligocene	Anahuac	DR		Discorbis "restricted"	Shale	Deep Water	Pelagic and Suspended Mud	Overpressured
		M		Marginulina	Thin Erratic Sand	Shelf Edge	Turbidity Current Proximal End	Slumps
	Frio	F	Upper		Sand	Deep Water	Turbidity Current	Slumps
	Frio		Lower	Hackberry Assemblage	Sand	Deep Water	Turbidity Current	Slumps Near Lithostatic Pressure

Table 3-3

Big Hill SPR Site Hydrologic Units

SYSTEM	SERIES	FORMATION	HYDROLOGIC UNIT
Quaternary	Pleistocene	Beaumont Clay	Upper Chicot Aquifer
		Montgomery Sand	Lower Chicot Aquifer
		Lissie Sand	
		Willis Formation	
		Lafayette Gravel	
Tertiary	Pliocene	Goliad Sand	Evangeline Aquifer
	Miocene	Fleming Formation	Burkeville Aquiclude

Table 3-4

Water Levels in Wells at
Big Hill, 1951-1965*

Well PT-64-22-301

Owner: Pipkin Ranch
Elevation: 5

Date	Water Level
May 17, 1951	0.67
June 5, 1952	2.47
May 22, 1953	6.16
May 28, 1954	9.99
December 14, 1955	8.91
May 16, 1956	7.74
May 29, 1957	9.80
May 21, 1958	9.42
October 19, 1959	7.72
October 11, 1960	14.64
March 20, 1963	10.48
May 7, 1965	9.73

Well PT-64-23-103

Owner: Pipkin Ranch
Elevation: 5

Date	Water Level
June 5, 1952	1.06
May 27, 1953	2.67
May 28, 1954	2.43
December 14, 1955	3.54
May 16, 1956	3.53
May 29, 1957	4.37
May 21, 1958	5.01
October 19, 1959	4.75
October 11, 1960	6.58
May 10, 1962	7.42
March 20, 1963	8.01
February 6, 1964	7.82
May 7, 1965	7.69

*From Wesselman and Aronow, 1973.

Table 3-5

Summary of Aquifer Tests,
Upper Chicot*

Well	Date	Coefficient of Transmissibility (GPD/ft)	Coefficient of Permeability (GPD/ft^2)	Coefficient of Storage	Specific Capacity (GPM/ft of Drawdown)	Remarks
PT-64-15-704	September 22, 1966	21,300	207	-	-	Recovery observation well
PT-64-15-705	-	21,600	216	-	1.7	Recovery pumped well; 23-h test

*From Wesselman and Aronow, 1973.

Table 3-6

Chemical Analyses of Water*

Well	Depth of Producing Interval (ft)	Date of Collection	Silica (SiO_2)	Iron (Fe)	Calcium (Ca)	Magnesium (mg)	Sodium (Na)	Potassium (K)	Bicarbonate (HCO_3)	Sulfate (SO_4)	Chloride (Cl)	Fluoride (F)	Nitrate (NO)	Dissolved Solids	Hardness as $CaCO_3$	Specific Conductance (µmho at 25°C)	pH
901	162	1-28-42	-	-	50	15	503	-	665	2	518	-	1.0	1,416	184	-	-
902	200	8-26-41	-	-	+5	18	348	-	427	2	340	-	20	923	74	-	-
Pure 2	170-191	7-17-56	52	20	1170	330	5300*	-	300	2420	9250	-	-	18,850	4300	26,400	7.9
Pure 2	291-307	7-19-56	145	1.1	1350	310	6880*	-	253	2390	12,000	-	-	23,350	4650	28,240	7.9
Pure 3 (705)	315-330	7-26-56	22	0.34	21	11	456*	-	622	3	380	-	-	1,550	98	11,650	7.62
Pure 3 (705)	392-406	7-24-56	17	2.15	250	104	2183*	-	478	587	3,400	-	-	7,030	1050	2,135	8.62
Pure 3 (705)	415	9-23-66	18	0.04	72	26	782	6.9	660	96	980	0.4	1.5	2,310	286	4,090	7.3
301	327	8-26-41	-	-	18	11	417	-	622	2	345	-	20	1,099	92	-	-
101	327	8-26-41	-	-	18	11	494	-	653	2	445	0.4	20	1,291	92	-	-
103	250	8-26-41	-	-	28	17	568	-	695	2	570	-	20	1,527	141	-	-
104	250	8-26-41	-	-	38	17	624	-	702	2	670	0.3	20	1,696	166	-	-
201	178	8-26-41	-	-	61	39	934	-	659	2	1,280	-	20	2,640	314	-	-

*Na+K

(Analyses given are in mg/L except SAR, RSC, specific conductance, and pH

Pure 2 170-191

Free Carbon Dioxide CO_2-5 ppm
Total Sulfide, S, 25 ppm
Noted sulphur odor and salty taste

Pure 2 291-307

Free Carbon Dioxide, CO_2-4 ppm
Total Sulfide, S, -10 ppm
Noted sulphur odor and salty taste

Pure 4 315-330

No odor
Free Carbon Dioxide, CO_2-0
Total Sulfide, S-ND

Pure 3 392-406

Slight sulphur odor
Free Carbon Dioxide, CO_2-17 ppm
Total Sulfide, S - 0 ppm

From Wesselman and Aronow, 1973.

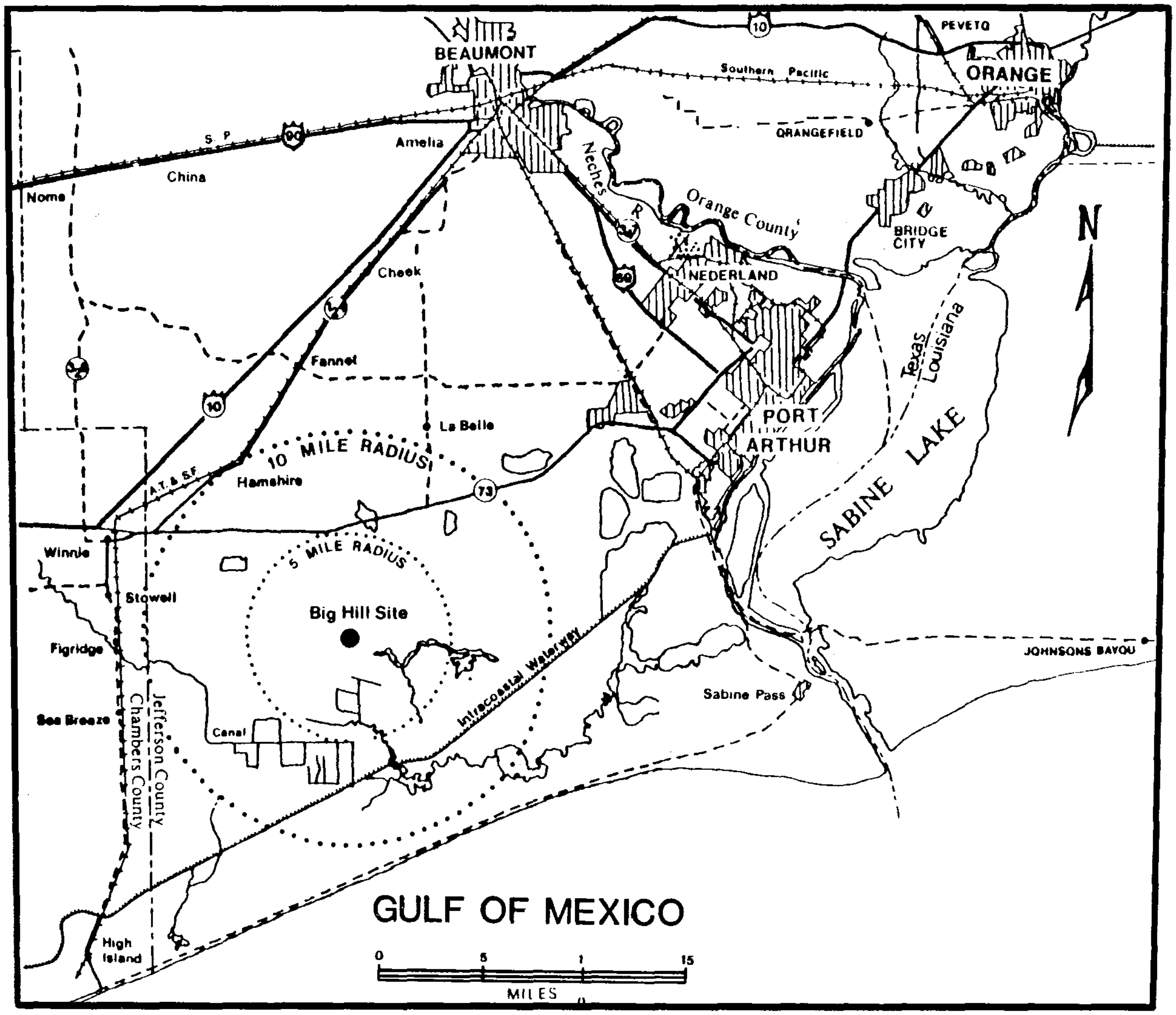

FROM DOE, 1978.

BIG HILL SALT DOME
SITE LOCATION MAP

Sandia National Laboratories

SEP 1981 FIG. 3-1

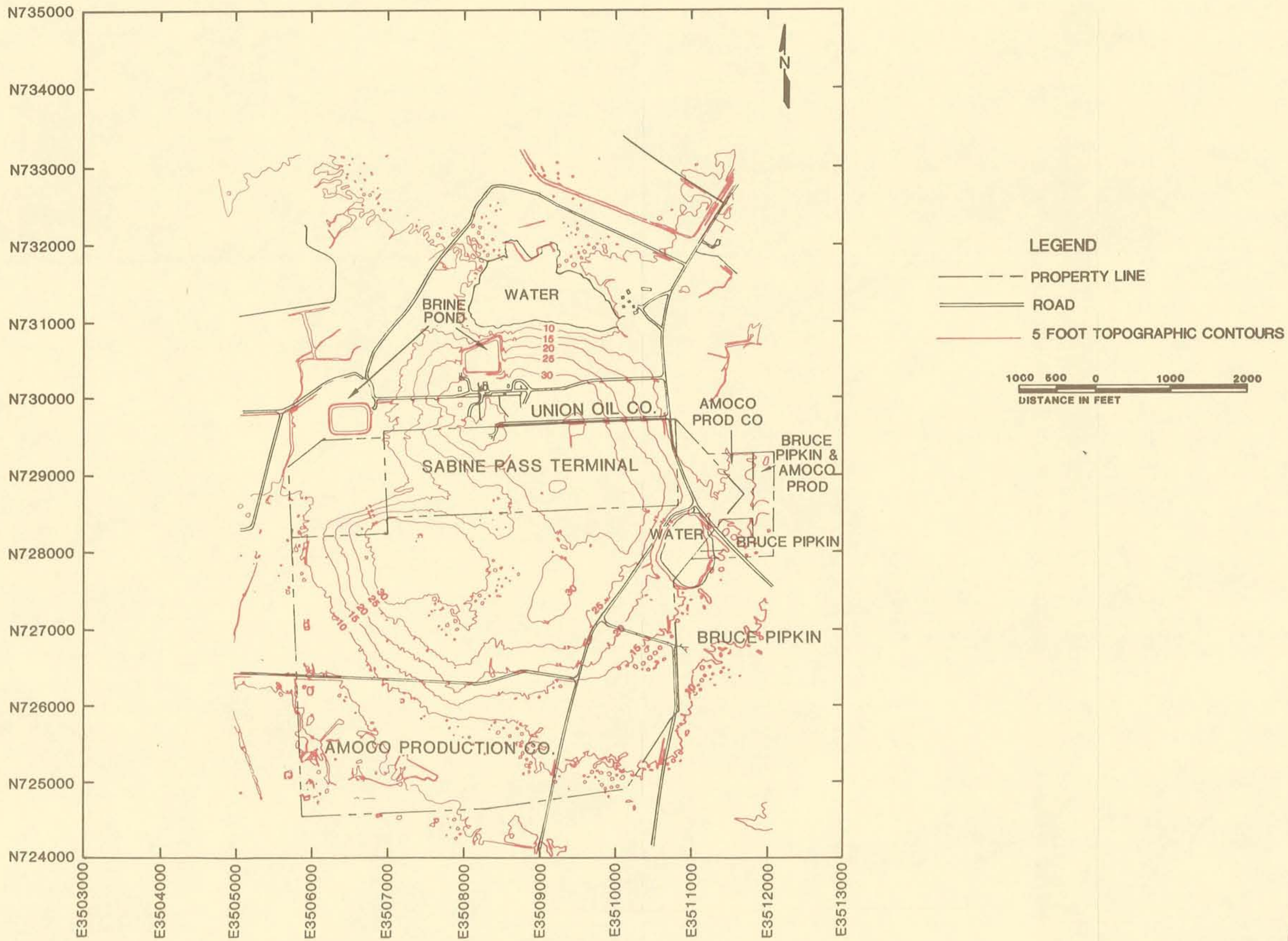

BIG HILL SALT DOME
TOPOGRAPHIC MAP

Sandia National Laboratories

SEP 1981 FIG. 3-2

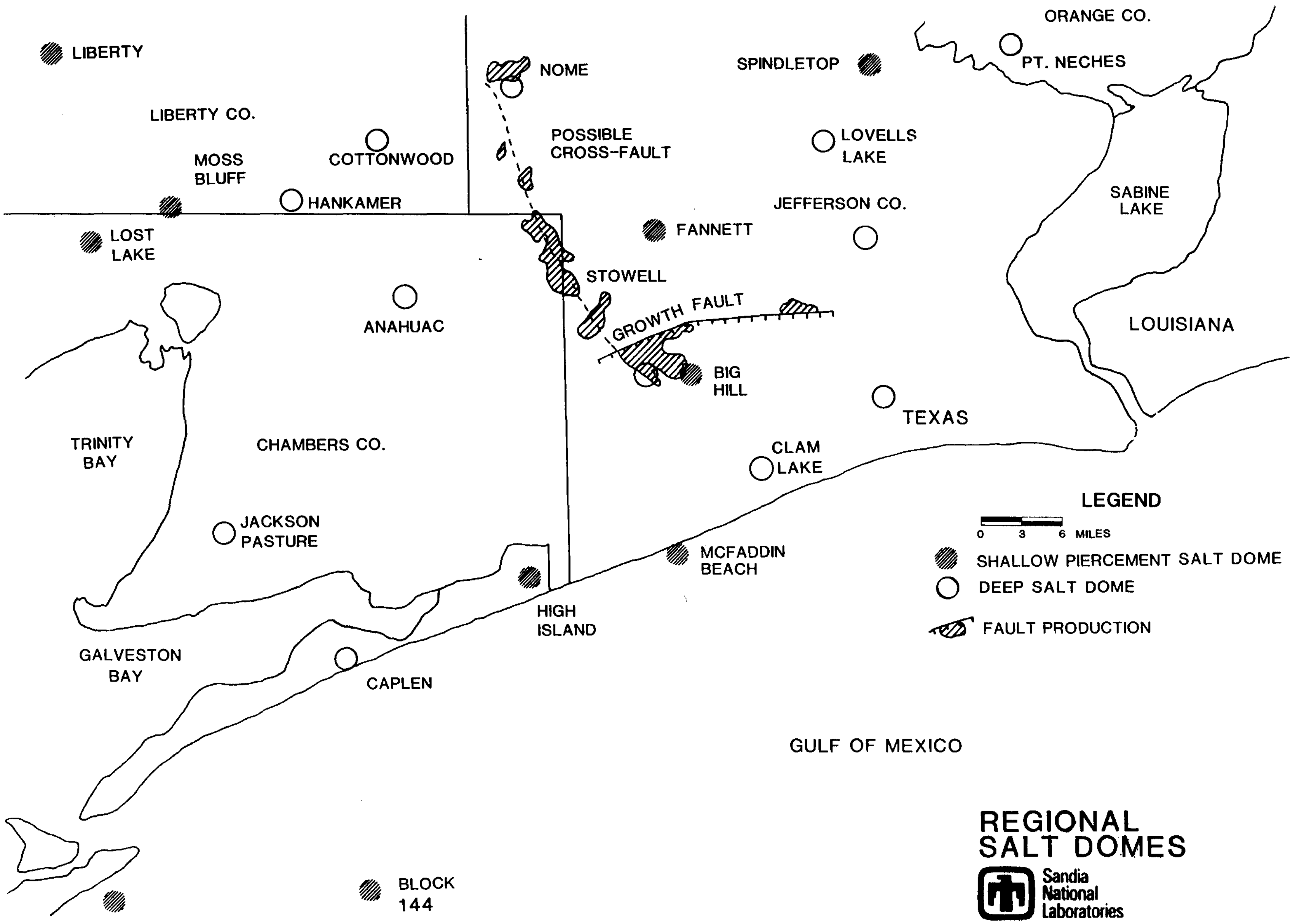

REGIONAL SALT DOMES

Sandia National Laboratories

T. R. MAGORIAN

SEP 1981 FIG.3-3

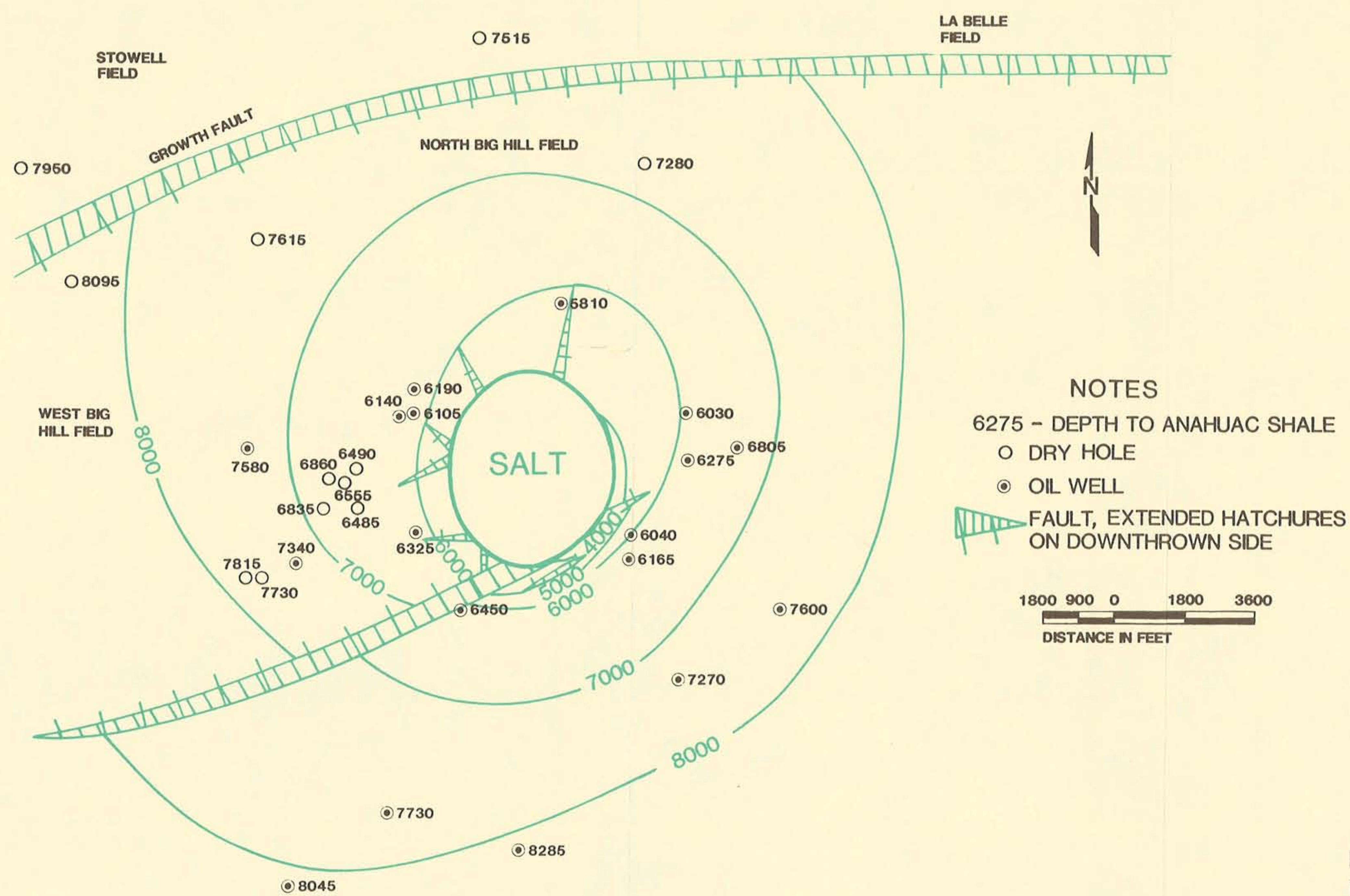

BIG HILL SALT DOME
REGIONAL STRUCTURE
ANAHUAC SHALE

Sandia National Laboratories

T. R. MAGORIAN

SEP 1981 FIG. 3–4

JAYRED
FITZHUGH #9

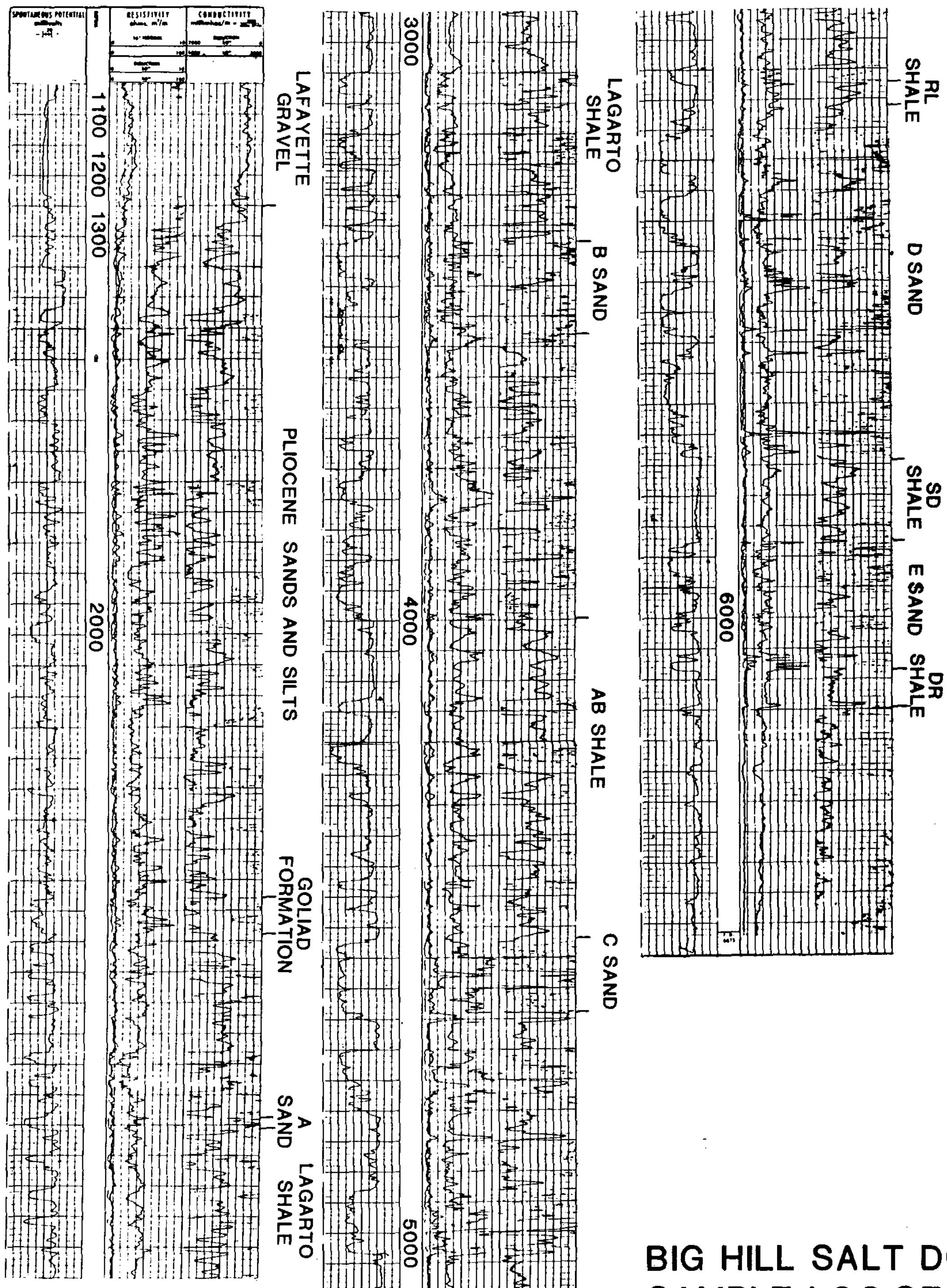

BIG HILL SALT DOME SAMPLE LOG OF DEEP SEDIMENTS

Sandia National Laboratories

T.R. MAGORIAN

SEP 1981 FIG. 3-5

GOODALE BERTMAN &COMPANY,INC.
PAN AM #3

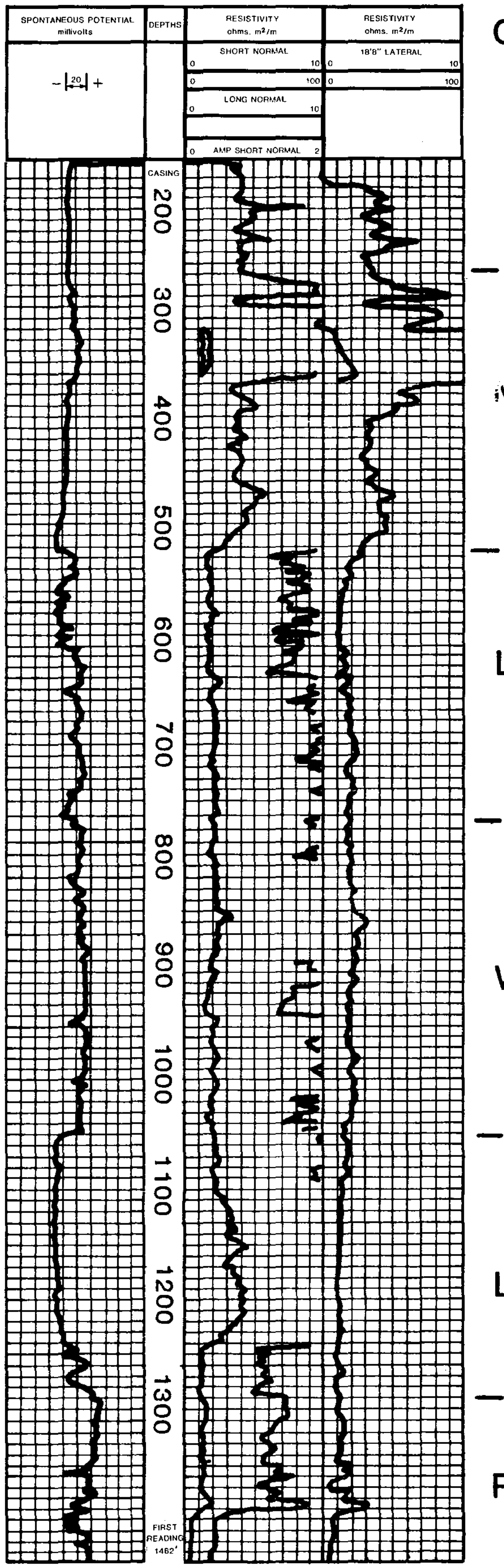

BEAUMONT CLAY

MONTGOMERY SAND

LISSIE SAND

WILLIS FORMATION

LAFAYETTE GRAVEL

PLIOCENE

BIG HILL SALT DOME
SAMPLE LOG OF NEAR-SURFACE SEDIMENTS

Sandia National Laboratories

T.R. MAGORIAN

SEP 1981

FIG.3-6

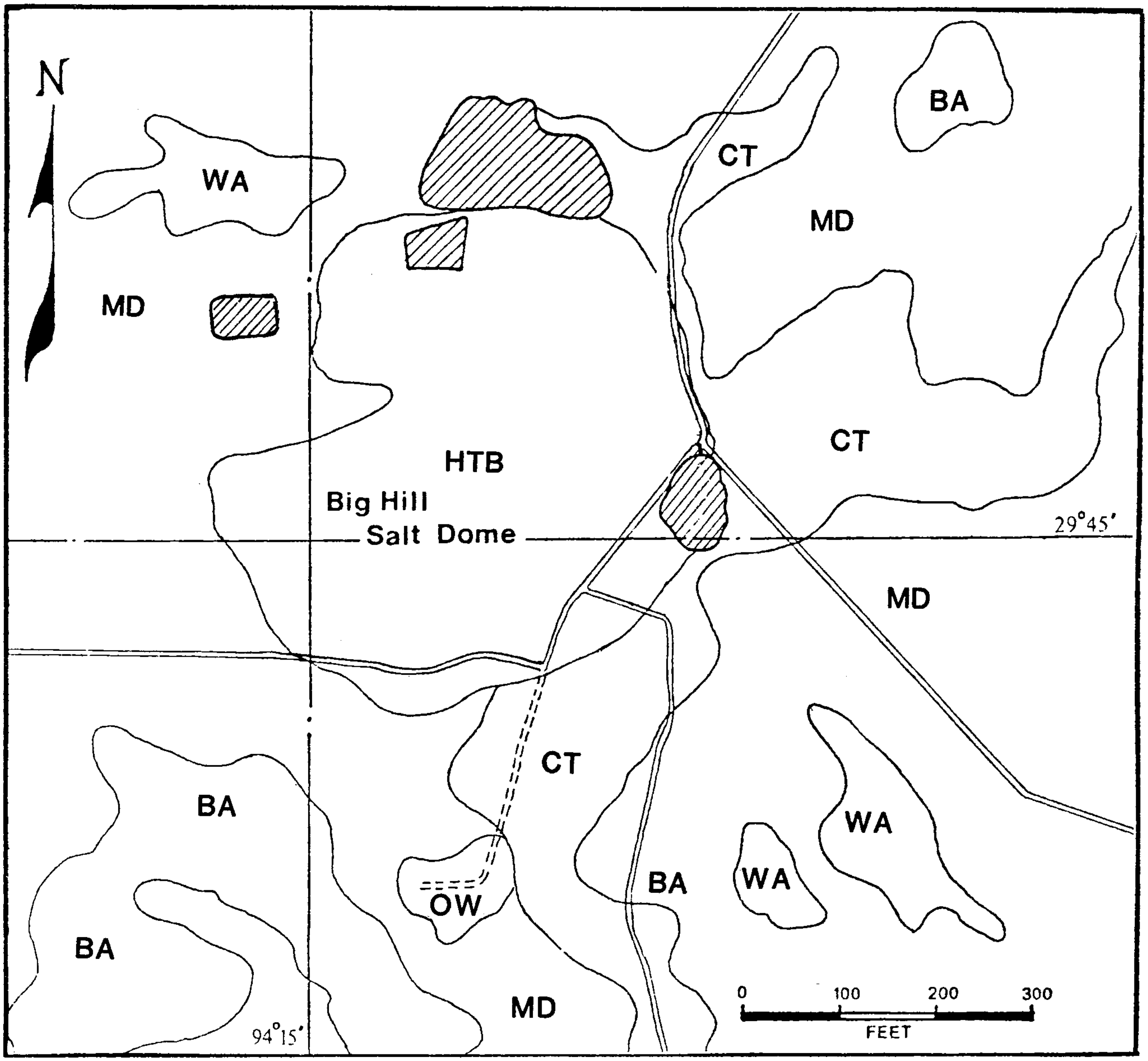

HTB	HOCKEY SILT LOAM	BA	BEAUMONT CLAY
MD	MOREY SILT LOAM	OW	OIL WASTE LAND
CT	CROWLEY SILT LOAM	WA	WALLER SOILS
▨	WATER		

FROM CROUT, et al, 1965.

BIG HILL SALT DOME
SOIL DISTRIBUTION MAP

Sandia National Laboratories

SEP 1981 FIG. 3-7

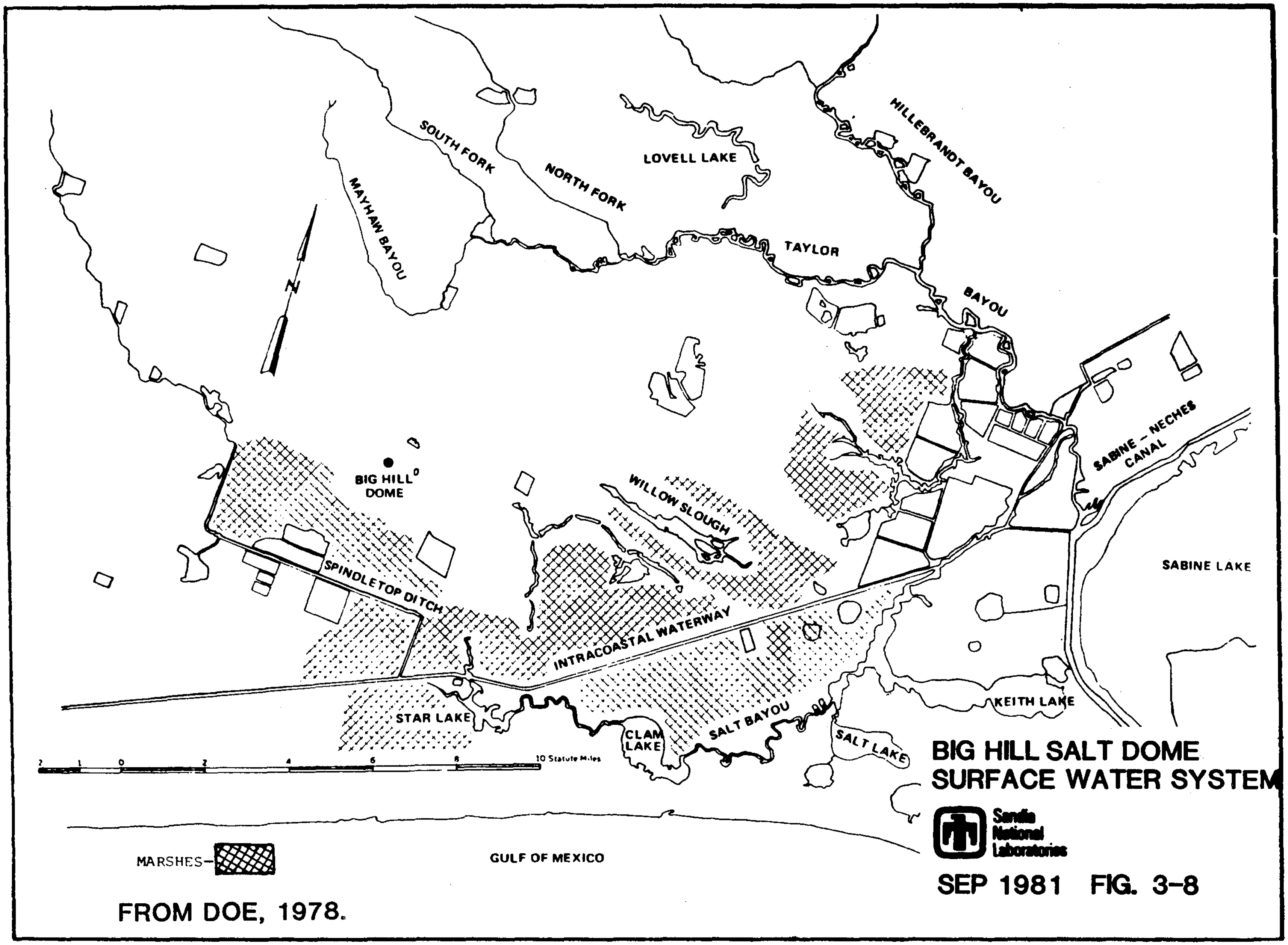

BIG HILL SALT DOME SURFACE WATER SYSTEM

SEP 1981 FIG. 3-8

FROM DOE, 1978.

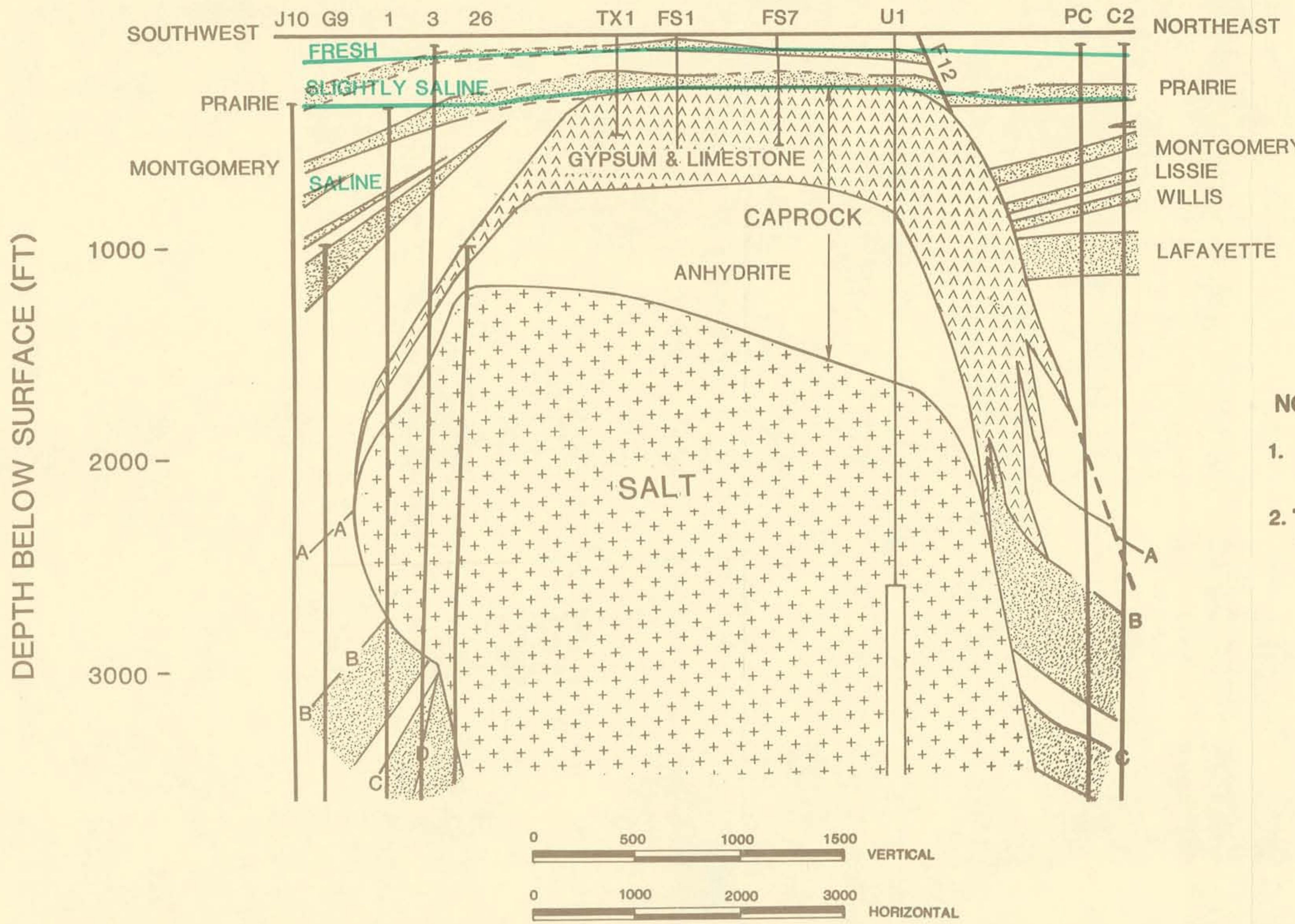

NOTES

1. SEE FIGURE 5-2 FOR SECTION LINE
2. T – INDICATES LOGGED INTERVAL

BIG HILL SALT DOME
SOUTHWEST-NORTHEAST
HYDROLOGIC CROSS SECTION

Sandia National Laboratories

T. R. MAGORIAN

SEP 1981

FIG.3-9

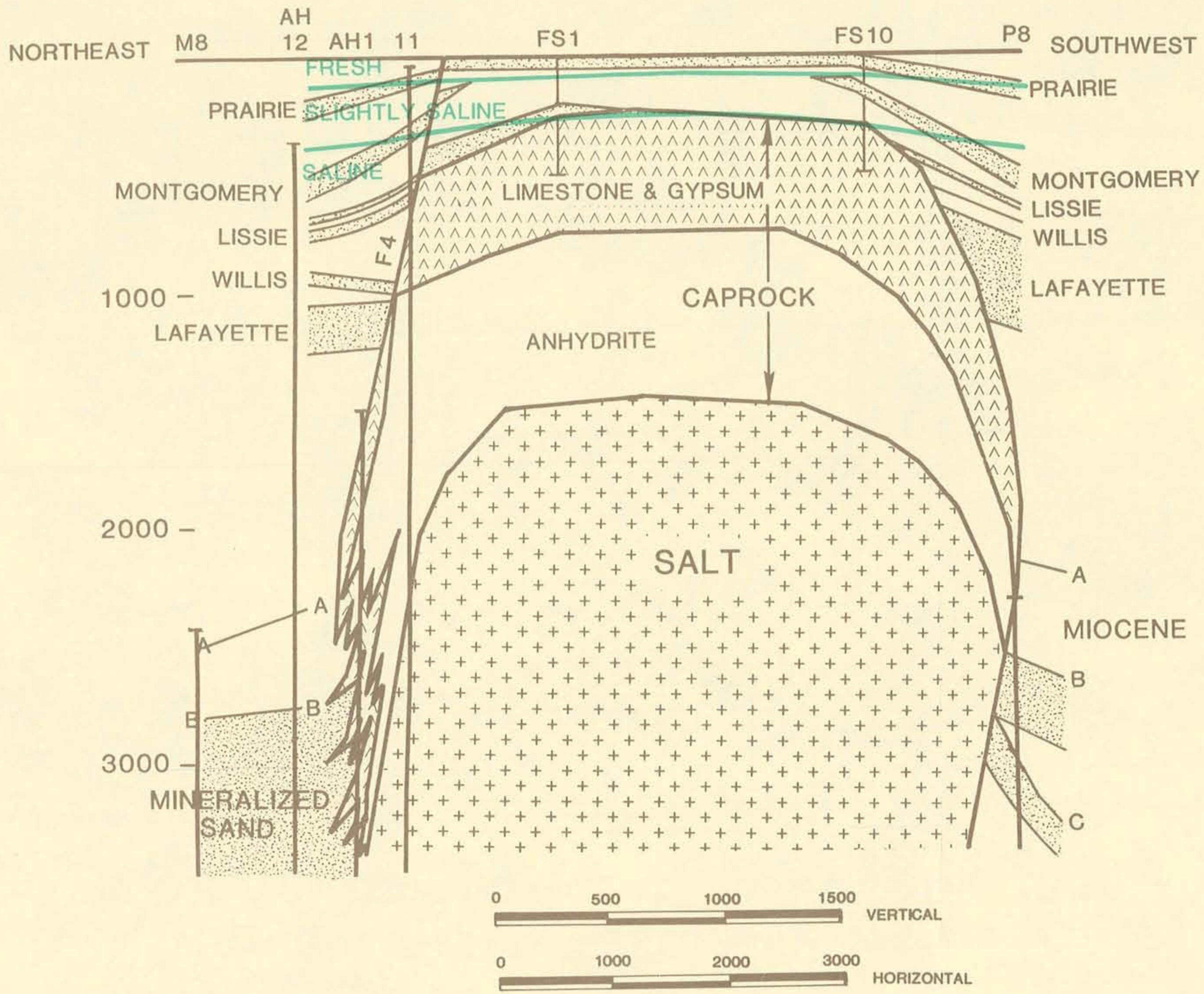

NOTES

1. SEE FIGURE 5-2 FOR SECTION LINE
2. T – INDICATES LOGGED INTERVAL

BIG HILL SALT DOME
NORTHWEST-SOUTHEAST
HYDROLOGIC CROSS
SECTION

Sandia National Laboratories

T. R. MAGORIAN

SEP 1981

FIG. 3-10

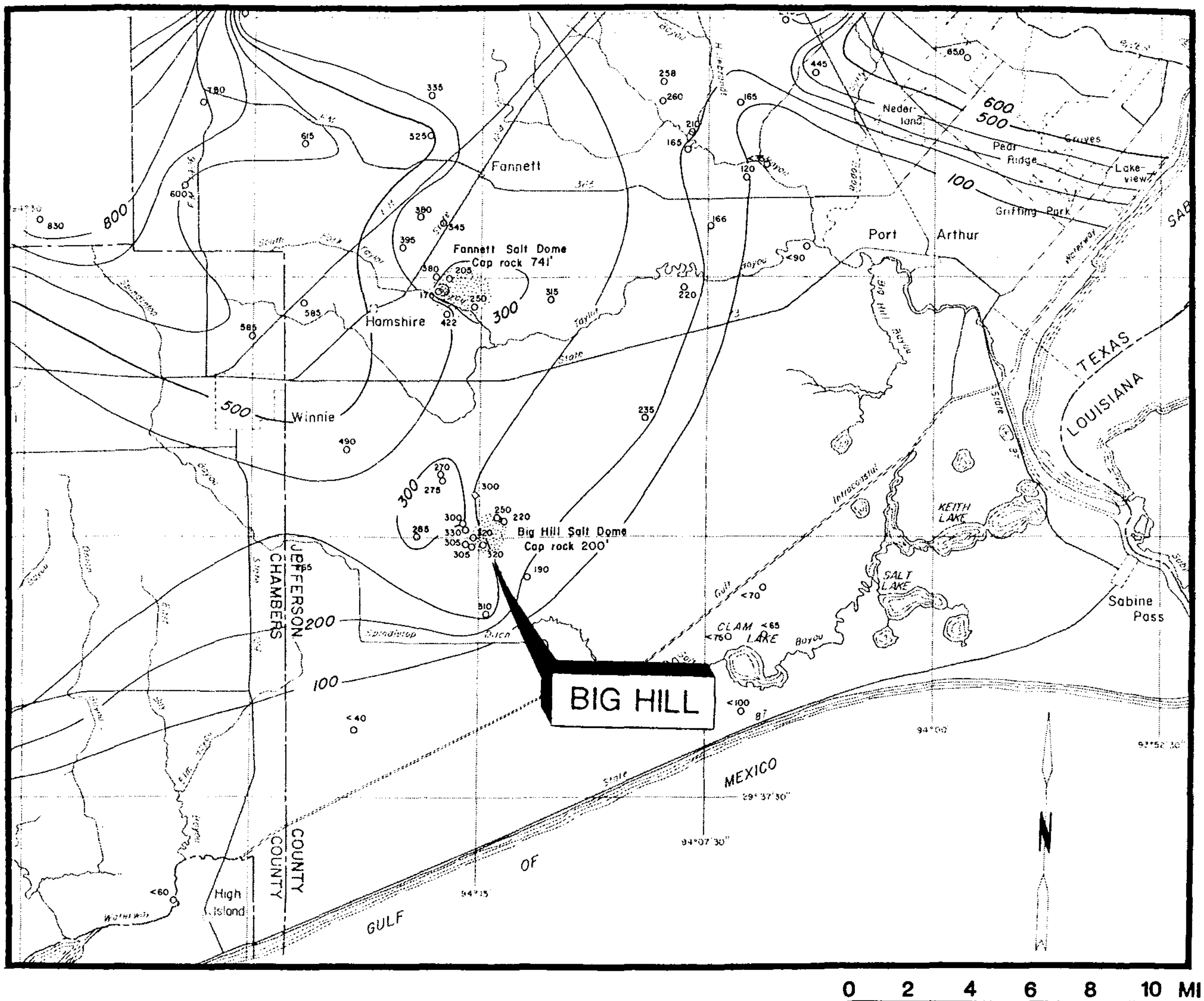

LEGEND

o<80

Well used for control
Number indicates altitude of base
of slightly saline water below mean sea level
"<" indicates value less than number shown

———100———

Water-interface contour
Shows approximate altitude of base
of slightly saline water below mean sea level

Contour interval 100 feet
Datum is mean sea level

Big Hill Salt Dome
Cap rock 200'

FROM WESSELMAN AND ARONOW, 1973.

BASE OF SLIGHTLY SALINE WATER

Sandia National Laboratories

SEP 1981 FIG. 3-11

CHAPTER 4 - CAP-ROCK GEOLOGY AND HYDROLOGY

Cap-Rock Geology

It is now commonly accepted that cap rock represents the product of a residual accumulation of anhydrite from a salt stock (Martinez, et al, 1978). Secondary alteration of anhydrite ($CaSO_4$) yields gypsum ($CaSO_4 \cdot 2H_2O$), calcite or limestone ($CaCO_3$), hydrogen sulfide (H_2S), and free sulphur. Carbon for the reaction comes from the oxidation of hydrocarbons or organic matter. Free sulphur and hydrogen sulfide result from the action of sulphate-reducing bacteria (Desulfovibrio desulfuricans). A typical reaction is:

$CaSO_4$	+	CH_4	→	$CaCO_3$	+	H_2S	+	H_2O
anhydrite	+	methane	→	limestone	+	hydrogen sulfide	+	Water

During periods of dome growth, solutioning of the salt occurs faster than uplift, resulting in formation of cavities at the salt/cap-rock contact. As cavities enlarge, overlying cap rock collapses into the voids. This process is repeated, yielding a complex sequence of lithologies in the cap rock.

Cap-Rock Lithology

Drillers' logs from sulphur-exploration wells indicate that the upper cap rock at Big Hill is composed largely of gypsum and limestone (Figure 4-2). This interval can be soft to hard, competent to fractured, and porous to nonporous. Selenite (transparent crystalline gypsum) is noted often on the core logs. Over the center of the dome, where cap rock is encountered at shallower depth, the limestone is slightly thinner. A layer of anhydrite underlies the thick gypsum and limestone sequence (Figure 4-3). The exploratory sulphur wells were abandoned when massive anhydrite was encountered because sulphur is typically found only above the anhydrite. Cap rock terminates smoothly on all flanks except the north and the west where it grades into mineralized "B" sand. A sample log of the cap rock is included as Figure 4-1.

Attempts to correlate seismic reflection data with actual depths to beds recorded in well logs indicate that the average velocity of cap rock varies considerably. The usual causes for these velocity variations are discontinuities and variations in rock type. Both well logs and seismic data indicate that the lithology of the cap rock at Big Hill is highly variable.

Cap-Rock Structure and Geometry

The cap rock is ~200 to 300 ft below the surface over the center of the dome, dropping off rapidly at the flanks. The gypsum and limestone layer is 400 to 450 ft thick over the center of the dome, increasing to 500 to 600 ft away from the center. This upper layer of the cap rock thins rapidly to 100 ft, then pinches out on the south flank. The layer thickens to 750 to 800 ft on the north side before grading into mineralized B sands. The underlying anhydrite is ~150 ft thick in the southern portion of the dome where it drapes over the salt and thickens to ~750 ft thick on the north side before pinching out. The total thickness of the cap rock is therefore >1000 ft over the center of the dome, increasing to 1350 ft in the northern part of the dome and decreasing to 200 ft in the southern half. The cap rock can be expected to be 850 to 1350 ft thick in the SPR storage cavern area (Figure 4-4).

The top of the cap rock is roughly dome-shaped, rounded on the top and steeper on the edges. The shape of the massive anhydrite layer (Figure 4-3) roughly follows that of the surface of the overlying gypsum and limestone (Figure 4-2). However, the internal structure of the cap rock is very complicated. No one particular horizon in the cap rock can be followed for a large distance because of how the cap rock was formed.

Cap-Rock Hydrology

Water in the cap rock occurs in the pores or vugs of the cap rock and can be expected to be of very poor quality. One well drilled on the Union Oil Property in 1956 penetrated to a depth very near cap rock (Table 3-6, Pure 2). Water samples taken from the interval 170 to 191 ft in this well contained 18,850 parts per million (ppm) dissolved solids, and a sample from 219 to 307 ft contained 23,350 ppm dissolved solids. Both samples were very high in sulfate, calcium, magnesium, sodium, and chloride compared to other wells in the area and would be classified as very saline at 10,000 to 35,000 mg/L (or roughly equivalent to 35,000 ppm dissolved solids). Water in the cap rock can be expected to be of much poorer quality. Because cap-rock hydrology can affect drilling circulation and casing corrosion, water samples from the cap rock should be taken and analyzed as discussed in Chapter 6.

Lost Circulation

For the thick cap rock expected, drilling times are estimated to start at 15 days and to decrease with drilling experience. The problems that are encountered in cap-rock drilling relate to lost-circulation zones (vugs and caverns) that are found principally at the top of the cap rock, throughout the gypsum-limestone interval, and at the base of the cap rock just above the salt. Stuck pipe has occurred only at the top of the cap rock in the more recently drilled holes. Table 4-1 is a summary of cap-rock drilling records that include the thickness of the cap rock drilled, lost-circulation zones and stuck pipe, and total drilling time in the cap rock.

Various methods are available to overcome lost-circulation problems. In view of the nature of the cap rock, preparation for circulation problems should be made and problems anticipated.

Casing Corosion Potential

The hydrogen sulfide present in the cap rock can corrode the casing in forms such as hydrogen blistering, embrittlement, and stress cracking (Hogan, 1980b). Sulfate attack on casing cement can be a serious problem unless sulfate-resistant cement is used. Retrieval and analysis of water samples from the cap rock during drilling of the SPR wells is recommended so that potential corrosion can be evaluated. Chapter 6 outlines the coring and sampling program.

Table 4-1

Cap-Rock Drilling Summary

Date Drilled	Well	Well Symbol	Thickness of Cap-Rock Interval (ft)	Lost Circulation	Stuck Pipe	Total Drilling*** Time in Cap Rock (days)
1951	Texaco Masterson 1	K1	1720	*		55
1953	Texaco Pipkin 7	P7	400			13
1966	Goodale Bertman Fitzhugh A1	A1	370			9
1967	AMOCO TX Exploration 1	1	220		7 days	9
1966	AMOCO TX Exploration 2	2	345	Top Cap Rock		
1967	AMOCO TX Exploration 3	3	330	Top Cap Rock for 2 days	7 days	7
1967	AMOCO TX Exploration 4	4	580			4
1967	AMOCO TX Exploration 5	5	500			3
1967	AMOCO TX Exploration 6	6	450	Top Cap Rock, Base Cap Rock		7
1967	AMOCO TX Exploration 7	7	325			8
1967	AMOCO TX Exploration 8	8	630			3
1967	AMOCO TX Exploration 9	9	300			2
1967	AMOCO TX Exploration 10	10	500			2
1967	AMOCO TX Exploration 11	11	375	Base Cap Rock		4
1967	AMOCO TX Exploration 12	12	430	Base of Gypsum and Limestone, Base of Cap Rock	**	11
1967	AMOCO TX Exploration 13	13	390	Top Cap Rock		6
1967	AMOCO TX Exploration 14	14	350	Base of Gypsum and Limestone		2
1967	AMOCO TX Exploration 15	15	450	Base of Cap Rock		4
1967	AMOCO TX Exploration 16	16	450			5
1967	AMOCO TX Exploration 17	17	500	Base of Cap Rock for 3 days	1+	8
1967	AMOCO TX Exploration 18	18	350			2
1967	AMOCO TX Exploration 19	19	650	Top of Cap Rock		14
1967	AMOCO TX Exploration 20	20	1090	3 Times at Top of Cap Rock, Base of Cap Rock		11
1967	AMOCO TX Exploration 21	21	1005			9
1967	AMOCO TX Exploration 25	25	550		1+	-
	SPR Wells		1400			<15

*All limestone

**Accidental sidetrack

***Drilling time only. Does not include casing and cementing time. Wells were not underreamed.

PAN AM (AMOCO)
TEXAS EXPLORATION #1

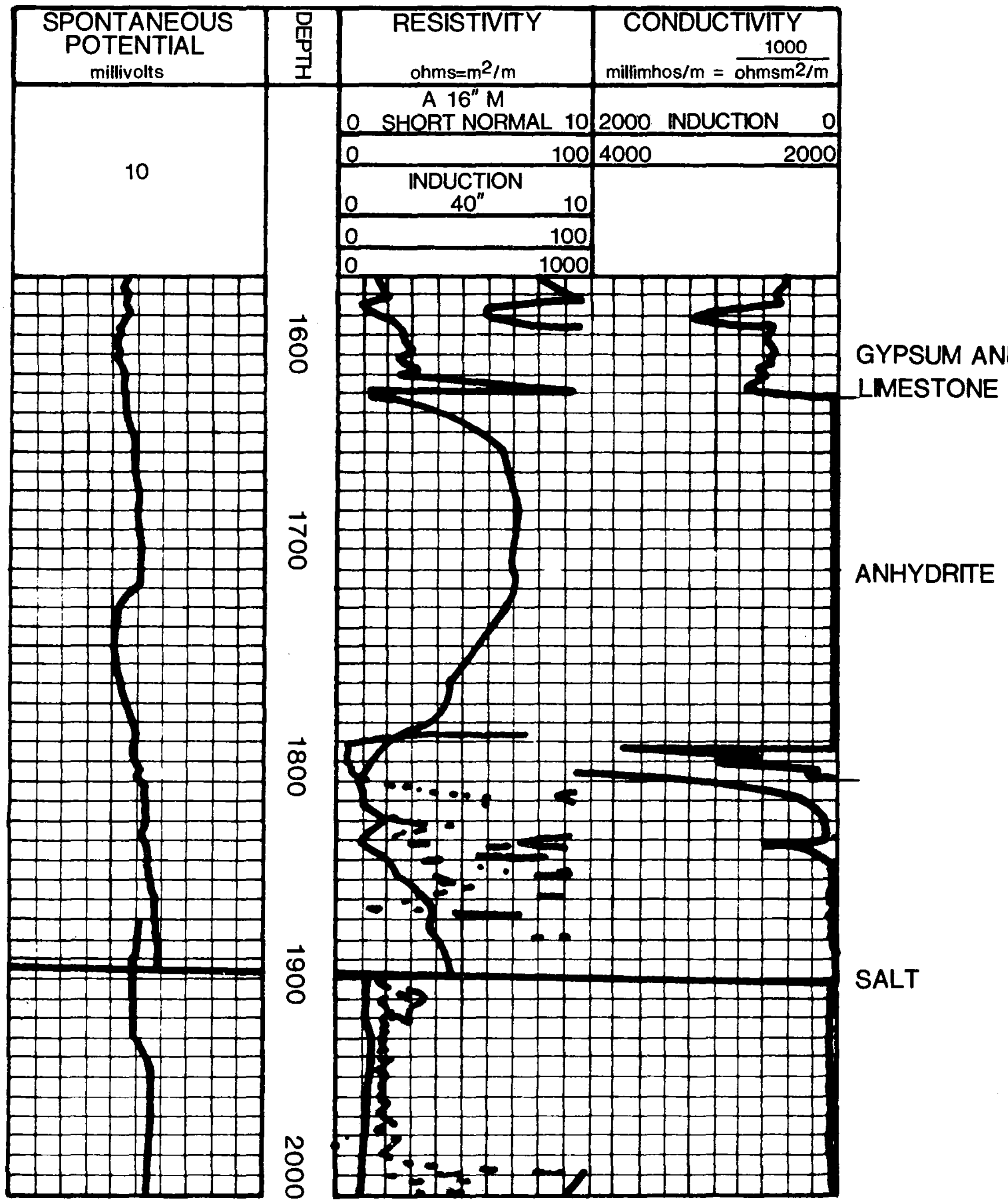

BIG HILL SALT DOME
SAMPLE LOG OF
CAPROCK

Sandia National Laboratories

T. R. MAGORIAN

SEP 1981 FIG. 4-1

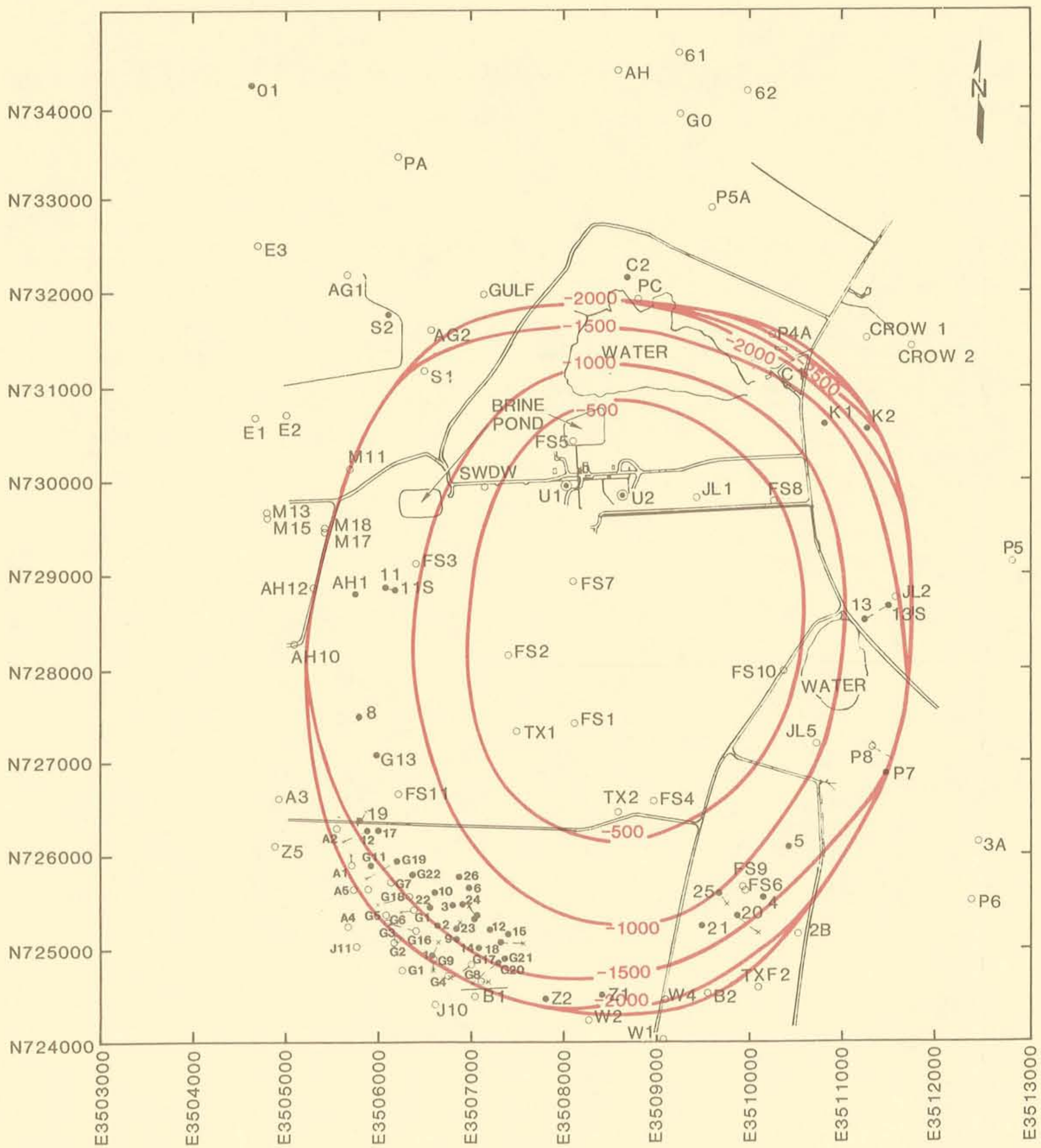

NOTES

1. SEE APPENDIX B FOR EXPLANATION OF WELL NUMBERS AND LOCATIONS.
2. CONTOURED DEPTHS MEASURED IN FEET BELOW DRILLING FLOOR.

LEGEND

- U1 — UNION OIL LPG CAVERN.
- SURFACE LOCATION OF WELL
- G2 — BOTTOM HOLE LOCATION OF WELL.
- G2 — BOTTOM HOLE LOCATION OF SIDETRACK HOLE.
- G2 — DRILLED AS VERTICAL HOLE NO BOTTOM HOLE LOCATION AVAILABLE.
- G2 — LOCATION OF WELL PENETRATING SALT.
- DEPTH CONTOURS IN FEET.

1000 600 0 1000 2000

DISTANCE IN FEET

BIG HILL SALT DOME
STRUCTURE MAP
-CAPROCK

Sandia National Laboratories

T. R. MAGORIAN

SEP 1981 FIG. 4-2

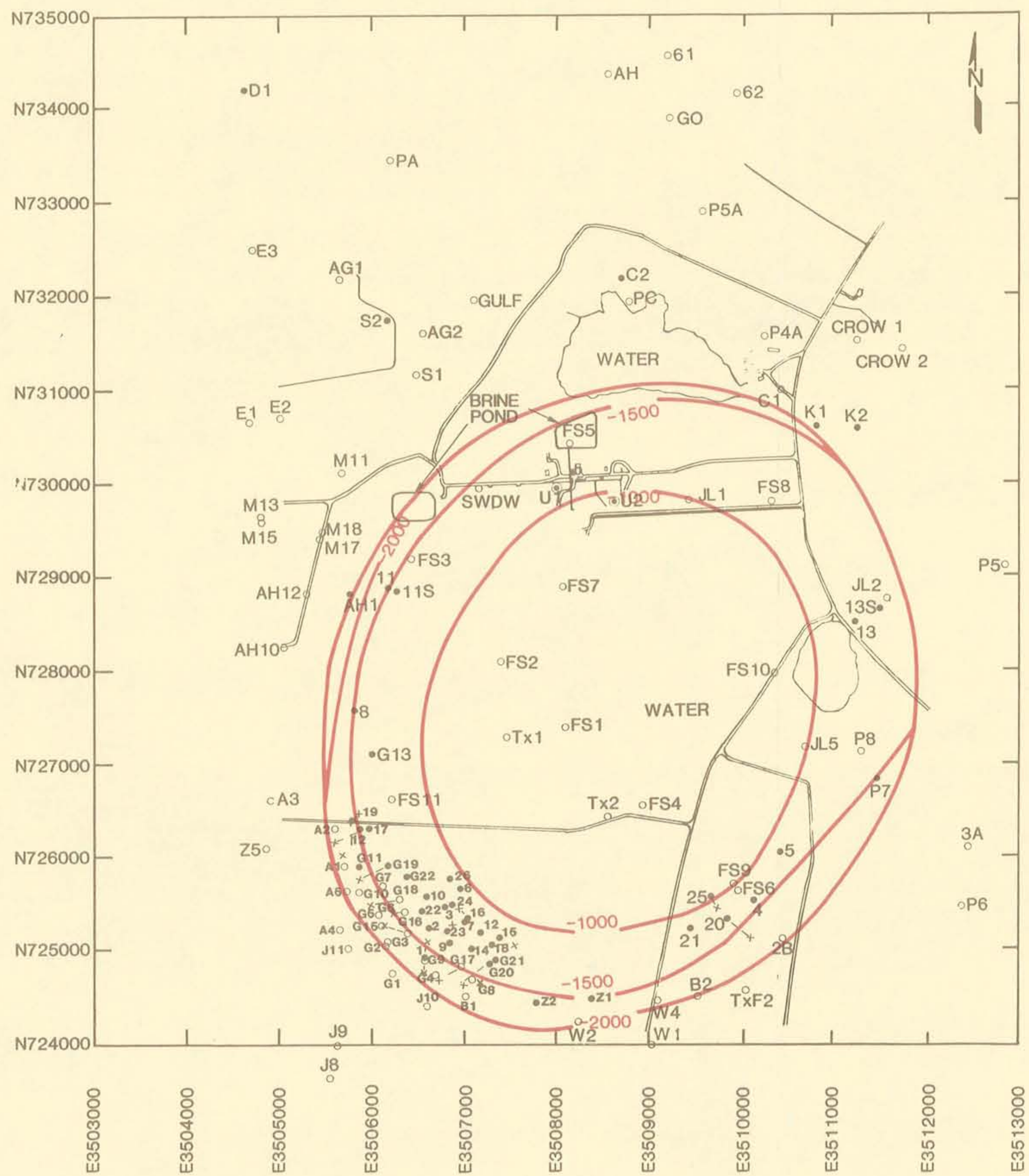

NOTES

1. SEE APPENDIX B FOR EXPLANATION OF WELL NUMBERS AND WELL LOCATIONS.
2. CONTOURED DEPTHS MEASURED IN FEET BELOW DRILLING FLOOR.

LEGEND

U1	UNION OIL LPG CAVERN
	SURFACE LOCATION OF WELL
G2	BOTTOM HOLE LOCATION OF WELL.
G2	BOTTOM HOLE LOCATION OF SIDETRACK HOLE
G2	DRILLED AS VERTICAL HOLE. NO BOTTOM HOLE LOCATION AVAILABLE
G2	LOCATION OF WELL PENETRATION
	500 FOOT ANHYDRITE DEPTH CONTOURS

100 500 0 1000 2000

DISTANCE IN FEET

STRUCTURE MAP
ANHYDRITE

Sandia National Laboratories

T. R. MAGORIAN

SEP 1981 FIG. 4-3

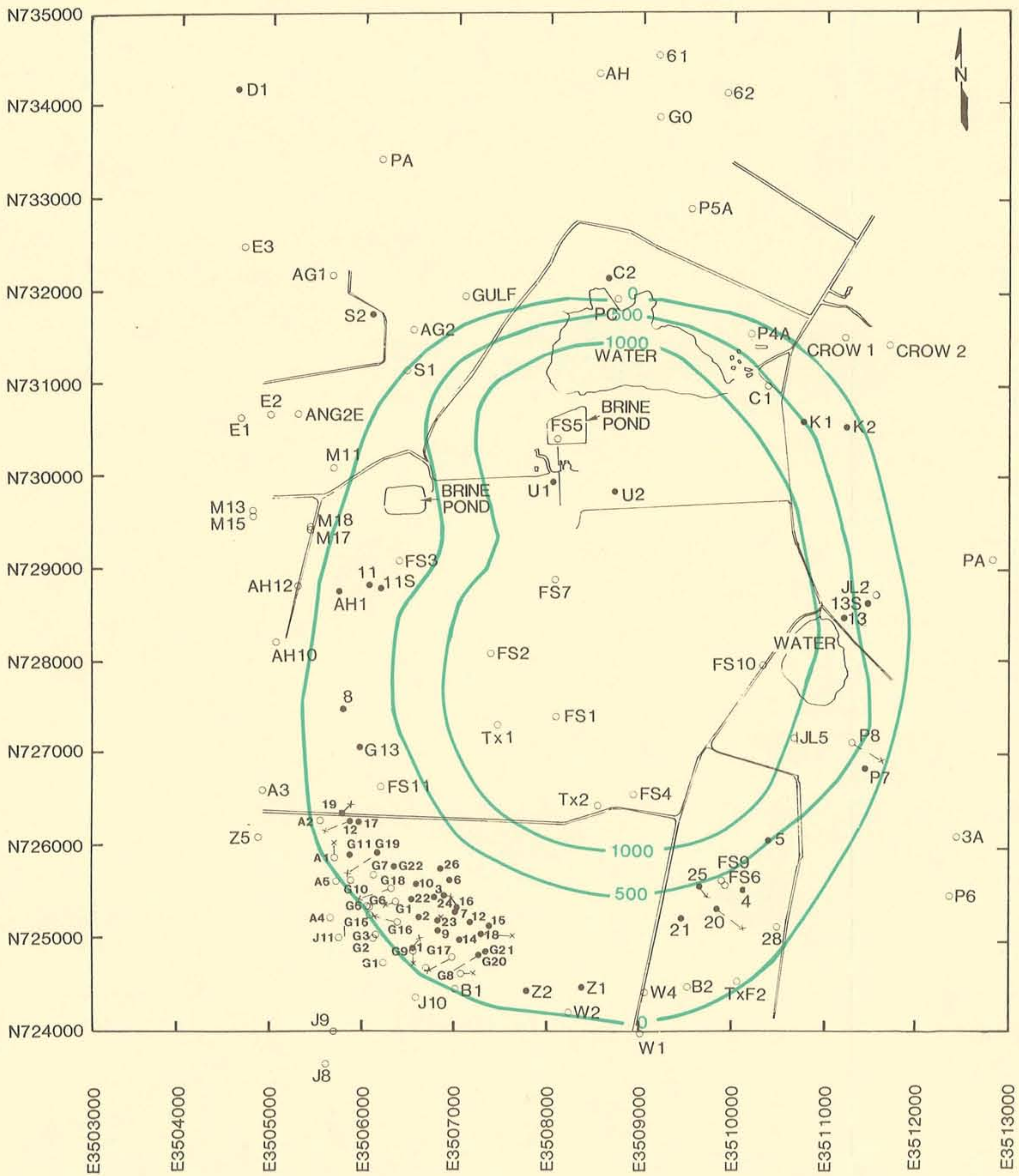

NOTES

1. SEE APPENDIX B FOR EXPLANATION OF WELL NUMBERS AND WELL LOCATIONS.
2. CONTOURED DEPTHS MEASURED IN FEET BELOW DRILLING FLOOR.

LEGEND

- U1 — UNION OIL LPG CAVERN
- SURFACE LOCATION OF WELL
- G2 — BOTTOM HOLE LOCATION OF WELL.
- G2 — BOTTOM HOLE LOCATION OF SIDETRACK HOLE
- G2 — DRILLED AS VERTICLE HOLE NO BOTTOM HOLE LOCATION AVAILABLE
- G2 — LOCATION OF WELL PENETRATING SALT
- ISOPACH CONTOURS

1000 500 0 1000 2000

DISTANCE IN FEET

BIG HILL SALT DOME
ISOPACH MAP OF CAPROCK

Sandia National Laboratories

T. R. MAGORIAN

SEP 1981

FIG. 4-4

5

CHAPTER 5 - SALT-DOME GEOLOGY

Origin of the Dome

The Big Hill salt dome is a diapiric, piercement structure formed from the Louann salt formation. The depth of the Louann salt is estimated as >30,000 ft in the Big Hill area, although this has never been confirmed by drilling.

The most generally accepted theory on the origin of salt domes is the upward intrusion of salt into overlying sediments caused by the difference in density between the salt and sediments overlying the salt. Since salt has a specific gravity of 2.2, and the sediments vary in specific gravity from 1.7 to 2.0 at the surface to 2.4 to 2.8 at depth, at some depth the salt becomes gravitationally unstable. When the density of the overlying sediments exceeds that of the salt, the plastic behavior of salt at the high temperatures and pressures existing at depth allow the salt to migrate upward through the overlying sediments. In the Big Hill area of the Gulf Coast, the salt becomes buoyant below a depth of 5,000 ft. The additional pressure and temperature required to initiate salt movement at this depth are quite small (Ode, 1968). The overlying beds that are pierced by the intruding salt are dragged upward along the salt body resulting in their being pinched out, smeared along the salt edge, incorporated into the salt, and faulted. When the salt rises to a level where the density is greater than that of the surrounding sediments, overhangs develop and the salt "slumps" back or breaks off into the lighter surrounding sediments. The mode of salt-dome emplacement is well described by Kupfer (1974) and elsewhere; it is not considered necessary here to detail this previous work.

Dome Geometry

The geometry of the Big Hill dome was defined by geologic interpretations of available seismic and well-log data. The geometry is shown by a combination of depth contours on the salt surface, a series of radial and tangential cross sections, and structure maps of key marker beds surrounding the dome. Figure 5-1 shows the salt contours to a depth of 5000 ft. Figure 5-2 is the cross-section reference map showing the location of the cross sections and the 14 SPR storage caverns planned for Big Hill. Figures 5-3 through 5-7 show the major cross sections through the dome, including the planned SPR storage caverns. Figures 5-8 through 5-19 and Figures 5-20 through 5-29 are the radial and tangential cross sections, respectively, that were constructed to define the structure on the key marker beds (Figures 5-30 through 5-35). Accuracy of the dome geometry as shown in the salt contour map and the cross sections is ±100 ft at the 5000-ft depth.

Big Hill shows a consistent history of central domal uplift without the formation of any large rim synclines or other evidence of salt exhaustion or stagnation. The overall shape of the dome is that of a cylindrical column tilted to the south. The top of the salt lies between 1300 and 1800 ft below the surface. The salt surface over the top of the dome is relatively flat, sloping gently outward to a depth of ~2000 ft, where the angle steepens sharply. The north flank dips gently downward to 2000 ft, where the dip increases to ~60° between 2000 and 10,000 ft. The south flank of the dome is overhung below 2000 ft at the same dip. The steepest dips are found on the east and west flanks. Another small overhang is indicated on the northwest flank.

The 60° overhang on the south flank has developed in the thick Anahuac shale (Table 3-2) section underlying the Miocene sand pile. The Anahuac is overpressured and of abnormally low density so that the salt is unstable above it. Frio sands (Table 3-2) are present only on the north side of the dome, apparently thick enough to help push the salt mass southward into the mud.

The weight of the cap rock, which is one of the thickest in the Gulf Coast, has also pressed the salt down. The dip of the overhang is matched by Cote Blanche and several offshore domes.

The massive salt overhang along the southern flank of the dome is documented from drillholes to a depth of -3740 ft (in Amoco Well 25). All salt contours below -4000 ft are projected from shallow data points except the -5000-ft contour on the west flank, which is confined by Amoco-Texas Exploration Well 8. There is no way to verify from existing drilling records how far the southern flank of the dome continues to dip northward below -3740 ft. Thus exploratory extension drilling of SPR cavern wells on the periphery of the dome is recommended, as outlined in Chapter 6.

Because oil production along the southeast flank has been limited (and the wells are now abandoned), it was long believed that the south overhang was separated by a salt outlier of some sort in the middle of the south side. Interpretation of seismic reflection data shows clearly, however, that the entire south side of the dome is a single overhang with a large fault separating the areas of oil production.

Geological Interpretation

Logs from drillholes that have penetrated the salt would ideally provide the data necessary to accurately define dome geometry. To obtain a complete definition of the dome to the depths of interest for SPR storage caverns, many wells strategically located on the dome and around its periphery are required. If the dome is not upright and of fairly simple geometry, then a much larger number of wells are required to define the geometry. At Big Hill only 46 drillholes have penetrated the salt; and, oil exploration, not definition of the geometry of the salt, was the objective in drilling the holes, except for the Union Oil storage cavern wells. Thus, most of the drill holes are not strategically located to define the dome geometry. In addition, the Big Hill dome is not a simple, upright, geometrical shape.

With the limitation of sparse drillhole data at Big Hill, geological interpretative methods based on strata convergence and faulting were used to define the geometry of the salt dome. The methods are based on the assumption that dome shape can be determined from the properties of the surrounding sediments and their deformational characteristics. It is well established that the dip of shales and thin-sand units next to a dome tend to be asymptotic (near vertical) to the salt at the edge of the dome. Therefore, by projecting the increasing dip of two or more beds towards the salt, a point where the beds converge can be plotted on a geologic section. This geometric relationship allows more accurate prediction of the salt edge. Similarly, detailed evaluation of the fault geometry in the adjacent sediments also assists in defining the salt-dome boundaries.

Using well-log data, a series of sections were constructed on and around the dome to detail the subsurface structures to a depth of 5000 ft. Lists of the depths to the tops of the geologic units used in constructing the sections are in Appendix B.

Well Control

The interpretation of the dome geometry and surrounding geology was based on 145 wells drilled on and around the dome, 99 of which did not penetrate salt. The wells of primary value in the interpretations are discussed below, with locations shown in Figures 2-1 and 5-1.

AMOCO-Texas Exploration Well 8 -- The AMOCO-Texas Exploration Well 8 (8) is on the west flank of the salt dome. It penetrated salt at -1850 ft and reached a total depth of 5200 ft, still in salt. This is the only well at Big Hill to penetrate the complete vertical interval in which the proposed caverns are to be constructed.

Stanolind-Davidson Well 1 -- The Stanolind-Davidson Well 1 (D1) is located ~1.5 mi northwest of the center of the surface expression of the Big Hill dome. It intersects salt at 10,114 ft and is the deepest salt penetration on the Big Hill dome. This and a few other wells show the northern flank of the dome to be a sloping surface dipping to the north.

Stanolind-Fitzhugh Wells 1 and 2 -- The Stanolind-Fitzhugh Wells 1 (Z1) and 2 (Z2) are the only wells giving control for the salt in the middle one-third of the southern flank of the dome. Well 1 penetrated a salt overhang from -2200 ft to -2670 ft. Below the salt, productive oil sands were encountered down to -5447 ft. Well 2 confirmed the overhang.

AMOCO-Texas Exploration Wells 6, 26, and 25 -- AMOCO-Texas Exploration Wells 6 (6) and 26 (26) penetrate the salt overhang along the southwest flank of the dome. Well 25 (25) is on the southeast flank and is the deepest confirmation of the overhang with a base of salt at -3800 ft.

AMOCO-Texas Exploration Well 13 -- The AMOCO-Texas Exploration Well 13 (13) is on the eastern flank of the salt dome. This well, which defines the eastern edge of the salt dome, penetrated a shale inclusion between two separate salt overhangs. The overhangs were between -1720 and -3710 ft and between -4120 and -4350 ft.

AMOCO-Texas Exploration Well 11 and Adams and Haggarty Well 1 -- AMOCO-Texas Exploration Well 11 (11) defines the slight overhang on the west flank next to the Sabine Pass Terminal Property. Adams and Haggarty Well 1 (AH1) confirmed the overhang.

Seismic Interpretation

Four seismic profiles, located on Figure 5-36, aided in the interpretation of the general structural information for the Big Hill area. Profiles 18 and 19 were shot in 1969 by AMOCO Oil Company, and profiles F36 and F37 were run in 1976 by Shell Oil Company. The data from these four profiles were reinterpreted in 1979 by T. R. Magorian for PB/KBB to give the results presented here.

The interpretation of the seismic record was effected by using several different digital playback filters in conjunction with a simple velocity model to "migrate" the data and form a depth section of the seismic records.

The reflector locations as shown on this depth section were then interpreted in terms of the geologic structure of the area. The velocity model used for the migration has a surface P-wave velocity of 5000 feet per second (fps), which increases linearly with depth to 7500 fps at 5000 ft. This gives an average velocity of 6250 fps for the sediments as contrasted to the constant 15,000-fps velocity used for the salt.

Based on the above interpretation schemes alone, the limits of the dome have been established to within ±400 ft, and the overhang in the southern quadrants of the dome has been shown to extend to at least 5000 ft. In addition, two faults, possibly of Hackberry age, F5 and F6, Figure 5-12, have been delineated.

The complicated structure of the Big Hill dome makes it very difficult to define an absolute vertical or horizontal profile. The resultant large error, however, has been significantly reduced by using other information in conjunction with the seismic interpretation.

Structure and Stratigraphy

The dome is overlain with Pleistocene sediments. The sediments flanking the dome are steeply dipping sands and shales of Pliocene, Miocene, and Oligocene age. As in other types of intrusions, the salt dome must displace the overlying sediments as it is emplaced. When uplift proceeds, any sediment deposited over the top of the dome must be either pushed aside or eroded away. On domes with a surface expression such as Big Hill, sediments are eroded off the top of the dome as it rises. As each layer of sediment was deposited over the dome, the upward movement of the salt stretched it to the point of failure, essentially pulling the layer apart in a series of normal faults. The mechanical failure of the sediments surrounding the dome has caused the faults to develop radially from, and tangentially to, the dome in a series of graben and horst structures.

Radial and tangential sections and structural maps were constructed from well-log data and used to define the subsurface structure surrounding the salt dome. The structure contour maps on the surfaces of the major marker horizons, as shown in Figures 5-30 through 5-35, were drawn to define the salt edge at different elevations and show the lateral extent of faulting. Because the faults are created by the intruding salt, their pattern helps predict the location of the salt dome. The hatched areas on the structural maps show where the key marker units are absent. Their absence is caused by the structural offset of the unit by normal faulting. As the structure maps show, the extent and magnitude of faulting increase with depth. Fault offsets of Pliocene age are on the order of 10 to 30 ft; those of the Anahuac are up to 1000 ft. Sections were drawn radially and tangentially to the dome in order to orient them as near normal as possible to both the radial and tangential faults. If a section is not oriented normal to the fault, the apparent dip of the fault plane will be less than the true dip of the fault.

Major Cross Sections

The section reference map, Figure 5-2, shows five major cross sections cutting completely across the dome. These sections show the overall shape of the dome and the relationship of the planned SPR storage caverns to the dome boundaries. Two of these five sections, the southwest-northeast and the northwest-southeast sections, were taken through control wells to provide good definition of the overall shape of the dome and the salt boundaries. The other three sections were constructed through the three rows of planned SPR caverns in a nearly west-east direction. These sections were taken to show the steep east and west flanks of the dome at critical depths and the relationship of the planned SPR caverns to the salt boundaries. These three sections, however, lack the well control for a high-confidence definition of the dome edges or the cap rock. The simpler appearance of the cap rock in these three sections compared to the SW-NE and the NW-SE sections simply indicates a lack of enough data to accurately define the cap–rock structure.

Southwest-Northeast Cross Section (Figure 5-3) -- This north-south section extends completely across the dome and is shown to the total depth of available well control. The rounded lip of the salt on the south side underlies the convergence and pinchout of the Pliocene and lower Pleistocene sands.

Growth Fault F12 causes the abnormal dip of the Montgomery and underlying Pleistocene sediments in the PC and C2 wells. This section shows the location of planned SPR Cavern 114 relative to the edge of the dome on the southwest flank.

Northwest-Southeast Cross Section (Figure 5-4) -- This section extends completely across the dome and is shown to the total depth of available well control. The rounded blunt end of the overhang on the east side is very close to the P8 well. Cap rock terminates smoothly without extensive mineralization of sands. On the west side, however, the cap rock grades into mineralized B sands just above the unconformity. Planned SPR Caverns 104, 105, 106, and 107 are projected into this section. The proximity of SPR Cavern 106 to the edge of the southeast flank of the dome is shown. Because very little well data are available to define salt contours on the southeast flank, the proximity of SPR 106 to the dome edge is of concern. An extension drilling program as outlined in Chapter 6 is recommended to alleviate this concern.

West-East Cross Section No. 1 (Figure 5-5) -- This section was constructed to show the relationship of the first row of the planned SPR caverns to the east and west flanks of the dome and the top of the salt. Projecting from AMOCO Well 11 south to AMOCO 8 shows that the salt is nearly vertical on the west side. AMOCO Well 13 and its sidetracked hole give control to the definition of the east flank in the interval from -1730 ft to -3710 ft. The Lafayette gravel is almost entirely cut out in Well 13. Other wells that penetrate the Lafayette close to the dome show a constant thickness for the Lafayette; the cutout in Well 13 is therefore interpreted to be a fault, and is shown in this cross section as F14. This section shows the potential space remaining on the west side for an additional cavern (see Chapter 6).

West-East Section No. 2 (Figure 5-6) -- This section through the middle row of planned SPR caverns also illustrates the steep east and west flanks and the relationship of the SPR caverns to the top of the salt and the edge of the dome. In this section it is also clear that space remains on the west side for an additional cavern beyond the baseline, as discussed in Chapter 6. Definition of the cap rock from Well G13 on the west side of this section is uncertain. The top of the limey material may be as shown or as deep as 1300 ft. The anhydrite is thin but a reliable marker. The top of the salt is reliable. There is no control for the east flank or for the sediments on either flank.

West-East Section No. 3 (Figure 5-7) -- This section through the bottom row of planned SPR caverns, like the previous two sections, graphically illustrates the SPR cavern-salt dome relationship. Construction of this row of SPR caverns involves the greatest geological risk because the caverns are the farthest out in the overhang on the south flank. The recommended extension drilling program outlined in Chapter 6 will reduce the risk of a cavern leak in the future. Control is available on both the east and west flanks through the cap rock (A2 and P7) and through the salt on the west flank (AMOCO 19). The dome narrows as the overhang converges on the south flank.

Radial Sections

Construction of radial cross sections is needed for accurate estimation of the salt's geometry. The controlling tectonic stresses and resultant salt geometry are observed in the fault patterns that appear on both radial and tangential sections. Both types of sections are needed to define the salt dome in three dimensions.

The extent of the south overhang can be seen in the radial sections taken around the south flank of the dome from A-A' (Figure 5-8) just south of the steep west side at Well 8, through Section H-H' (Figure 5-15).

Section A-A' (Figure 5-8) -- The southwest radial section through brine disposal Well 19 shows the steepening of the overhang as it swings around from the south flank of the dome into the near-vertical west side. The vertical salt wall extends upward from the mid-Miocene *Amphistegina* B shale.

Section B-B' (Figure 5-9) -- The radial section across the producing area west of F1 (Figure 5-34) shows the same projection of the salt overhang as A-A', with matching dips of the lower Miocene sands. The deep wells (10 and 26) allow interpretation of the *Marginulina* sand within the geopressured Anahuac Shale. Both beds dip at the same steep angle up to the salt. The Marginulina sand was unproductive in both wells but has produced high-pressure gas over several square miles to the west (the Big Hill Northwest field). The risk of a gas blowout during the drilling and leaching program will require detailed evaluation as information is obtained from the proposed wells.

Section C-C' (Figure 5-10) -- This radial section across the middle of the producing area shows a rounded salt edge above the D sand and a simple overhang surface below. The well control available in this small area assures the simplicity of this interpretation. The maximum extent of the salt coincides with the top of the Miocene, marked A in the section. Beds below the salt bulge are uplifted at the same 60° angle as the salt overhang.

Section D-D' (Figure 5-11) -- The radial section across the southeast end of the producing area shows a linear overhang. The abundant well control assures the linearity of the overhang, and thus confidence in its extension to the bottom of the proposed caverns. Thinning and convergence of all the Miocene beds is observable because they are uplifted at the same 60° angle formed by the salt overhang itself.

Section E-E' (Figure 5-12) -- This short radial section, located at the middle of the south flank, shows a sharp stratigraphic convergence against the salt overhang and two faults, marked F5 and F6, parallel to the overhang. The shallow salt edge is rounded by dissolutioning and extends farthest east at the top of the Miocene. The locations of Faults F5 and F6 have been confirmed by the north-south shell seismic line.

Section F-F' (Figure 5-13) -- This radial section across the southeast flank shows the linearity of the south-flank overhang, and the convergence of the beds confined to the lower Miocene. The lower Miocene sands are uplifted to 45° dip; the upper Miocene B sands are nearly flat.

Section G-G' (Figure 5-14) -- This detailed radial section through the middle of the southwest producing area shows a sharp change in slope of the salt overhang at the level of intersection with the main D sand. A fault, F13, which is parallel to a 300-ft array from the salt edge, has allowed ~300 ft of lower Miocene sediments to slip downward against the salt, forming a sort of graben in the salt-contact zone.

Section H-H' (Figure 5-15) -- This detailed radial section across the southwest flank shows truncation of Fault F1 close to the salt. The transition in slope of the salt overhang here occurs at the unconformity between the B and the C sands. A wedge of sediments is apparently trapped between the steep salt wall and F1; there is no evidence, however, that this extends farther into the salt mass as an inclusion. No inclusions have been found in any of the overhang salt penetrations, unlike the near-vertical salt on the east side of the dome (Well 13). Steeper 80° overhangs very commonly contain inclusions, but this 60° overhang appears too heavy and massive to allow their survival.

Section J-J' (Figure 5-16) -- This northwest radial section shows a smooth northward slope of the salt from cavern Well U1, one of the existing storage caverns, down to Well S2. The graben, or down-dropped block, between Fault F8 and the salt does not seem to affect the salt surface, insofar as available well control indicates. The graben is filled with lower Miocene sands, particularly the main D sands, during which F8 acted as a growth fault.

Section K-K' (Figure 5-17) -- The east radial section shows a 100-ft-thick inclusion that has separated a long wedge of salt from the main mass of the overhang at the point where it steepens along the near-vertical east side. Although this sliver of salt is not entirely loose, it is probably trapped along Fault F5.

Section L-L' (Figure 5-18) -- The section through the northwest overhang and the steep west flank shows the maximum extent of the salt occurring opposite the upper Miocene B sands. These sands are highly mineralized. Both D and E sands thin dramatically and are pulled up into a near-vertical position. There is not enough control to determine any probable faulting that complicates this situation. The overpressured Anahuac shale, marked by its top, the *Discorbis*, restricted (DR), is dragged up, but the shale sheath common to Gulf Coast salt domes has not yet been found at Big Hill. The geodynamics of a large 60° overhang make survival of the shale sheath or diapir very difficult. That is, the weight of the salt overhang has probably squeezed any shale out at the shallow depths to which the dome has been drilled. If the south flank overhang steepens up to yield space for additional storage caverns, this flank may also be protected by a shale sheath.

Section M-M' (Figure 5-19) -- This radial section through the northwest overhang shows protruding salt that has dropped into the sediments. The overhang is limited to the area north of Well 8 and may steepen with depth. There is no control, however, to clarify the details of this complex area.

Shales are relatively impermeable and will be added protection to the oil stored in caverns near the edge of the salt in contrast to more permeable sands. The shale-sand sequence at the depth of the proposed caverns can be noted in the radial sections (Figures 5-8 through 5-19). Shale "squeezeouts" or sand convergences against the salt are also shown on these radial sections. Ideal cases appear in Wells 23 (Figure 5-10) and G20 (Figure 5-11). The convergence of sands defined from well control near the salt edge is a useful tool for defining the location of the salt edge. One or more tangential faults dipping away from the dome often occur where the converging sediments have been steeply uplifted.

Tangential Sections

The tangential sections provide the details of the salt dome needed to delineate radial faults and to correlate the radial sections. Many of these faults are actually parallel to tangentials at the edge of the dome. The tangential sections complete the three-dimensional picture of the dome for a more accurate description of the salt boundaries. They should be used in association with the radial sections and the structure maps showing the tops of the various marker beds.

A complete traverse around the dome is shown in tangential sections N-N' through Y-Y' (Figures 5-20 through 5-29). All of the major radial faults as well as the largest tangential faults are revealed in these sections, making the discovery of additional overhangs much less likely.

Section N-N' (Figure 5-20) -- The outside tangential section across the southwest-producing area shows the Faults F1 and F2 that form the hydrocarbon-producing structure: a horst or block between the intersecting normal faults below the mid-Miocene unconformity. Inside the horst, the C-sand dips northwest and the basal E-sand dips southeast because of growth in the D-sands along F1.

Section P-P' (Figure 5-21) -- The east-west tangential section across the south side of the dome shows the large fault, F5, which extends upward at least through the Miocene. F5 has ~1000 ft of throw at the top of the Anahuac. This fault dominates the section, cutting the lower salt in Well W4. The salt dome structure is broken by the fault dipping east and west at 60° angles below the fault and 30° angles above. Fault F6, forming the graben parallel to the salt overhang, may displace F5 where the two faults cross. Fault F6 also displaces the salt in Well 22.

Section R-R' (Figure 5-22) -- This tangential section along the southeast flank shows two parallel faults, F6 and F7, in the lower Miocene. The arch structure found in all of the beds in this section is simply caused by the intersection of the tangential section with the dome. The faults are tangential and parallel to the salt overhang as shown in the radial sections.

Section S-S' (Figure 5-23) -- This section tangent to the southeast flank of the dome shows a fault across the section at an oblique angle. The salt is displaced by F5, as shown in Well 25. The thickening of the D-sand is associated with reversal of dip in Well 5. This structure produced oil for some years. The beds, which show drag near Fault F5, also steepen toward Well P8, indicating a structural high to the east.

Section T-T' (Figure 5-24) -- The tangential section running north-south along the east side of the dome shows the north end of the isolated salt finger found in Well 13 where it joins the main salt mass and dips steeply northward. Fault F5 has no observable displacement on the salt, although that is probably only because of lack of well control. In this section, the Miocene beds below F5 appear to dip into the salt overhang. The dip away from the salt is normal on the north flank.

Section U-U' (Figure 5-25) -- The section tangent to the northeast flank shows a small but sharp uplift in Well C2. The top of the salt is displaced by Fault F11. A gentle dome over the salt ridge in Well K1 extends to the top of the Miocene Sediments.

Section V-V' (Figure 5-26) -- The tangential section across the north side of the dome shows a simple, rather gentle west dip. The E-sand, and to a lesser extent, the D-sand, thicken to the west, particularly on the down side of F8 (as shown in the graben discussed in the northwest radial section). The mid-Miocene shale (AB) also thickens in Wells S2 and AG1.

Section W-W' (Figure 5-27) -- The section tangent to the dome across the northwest flank shows lower Miocene beds dipping steeply to the southwest near the fault that cuts through the Gulf well. The salt domal structure to the southwest is mostly caused by thickening in the *Siphonina davisi* shale and the underlying E-sands in Well M11. In general there is almost no dip here. The B sands are thicker in Well M17. This amount of stratigraphic variation is normal and traps oil both against the salt and in other fault contacts and bed pinchouts.

Section X-X' (Figure 5-28) -- The tangential section running north-south on the west side of the dome shows a gentle southward dip interrupted by Fault F9. The fault extends upward to the mid-Miocene unconformity. The eastward extension of F9 into the salt mass helps create the small northwest overhang shown in the radial sections K-K' and L-L' through Well 11.

Section Y-Y' (Figure 5-29) -- This inner tangential section across the southwest producing area shows the intersection of F1 and F2 with the salt overhang. The lower Miocene sands in the productive horst are dipping northwest at 60°. Curvature of the underside of the salt is partly a function of available well control, because any slight deviation from the ideal line of section will produce an anomaly when the dip of the sediments is steep.

Structure Contour Maps

Figures 5-30 through 5-35 show structure contour maps on the tops of the A through E sands and Anahuac shale. These maps, essentially slices through the dome, were drawn to define the salt edge at the level of the particular unit being mapped. The maps show the dip of the salt northward with depth. The amount of displacement on the top of the units also increases with depth, showing the effect of dome uplift on the surrounding sediments. Many of the sands close to the dome have produced gas and oil. These reservoirs tend to be segmented by faulting associated with dome growth. Mappable fault displacement stops at the dome since any displacement becomes indistinguishable because of the plastic, self-healing nature of the salt.

Dome-Related Faulting

Mapping faults is useful in defining the edge of the salt since dips on fault planes depend on lithology. Faults through loose sands generally dip at 60°; steeper dips occur in the more consolidated sediments. The salt edge is technically a fault surface. In the silty, consolidated turbidites of the Frio Formation, which is overpressured, dips of faults can range down to horizontal. Once a fault is formed, it continues to grow as additional sedimentary layers are deposited and the dome continues to rise. Therefore, the fault offset decreases upward along the fault plane. Although the displacement of some of these dome-related faults is on the order of hundreds of feet at the dome edge, the faults die out rapidly away from the dome, generally in less than 1 mi.

Mapping of the dome-related faults has been based on electric log data. Faults can be interpreted from the logs by correlation of the major stratigraphic horizons such as the Miocene A through E sands. Offset of these major units infers faulting. Because of the sparse well control on and around the dome, only some of the faults can be correlated with those in the surrounding wells to determine the orientation of the fault planes. The accuracy of determining the amount of offset depends on the lithology of the sediments the fault passes through. In shales, for example, the resolution of an electric log is good to within 2 ft; while in coarse, cross-bedded levee or channel sands, a fault with 200 ft of offset may be obscured. Where the sediments show a linear drop on the downthrown side of the fault, the salt shows a curved updrag.

Fourteen major faults (labeled F-1 through F-14, Figures 5-3 through 5-35), have been defined around the dome. Many more small-scale faults (displacement in the tens of feet) probably exist, but are not considered critical to defining the salt dome. The remaining faults offset only Miocene and older sediments and are considered "inactive."

Faults F4 (Figure 5-4) and F12 (Figure 5-3) on the dome appear "active" in the sense that they continue to grow with increased sedimentation and salt-dome uplift. Movement along this type of fault is a gradual slippage that will have no adverse effect on the SPR site. Fault F4 on the west side of the dome has been cut on the top of the Pliocene and appears to reflect the area of maximum salt uplift today, forming the active margin of the dome.

Oil is produced from the associated trap in Well M17. There is an anomalous dip down toward growth Fault F12 on the north flank. This fault displaces sediments to the surface (Figure 5-3).

The major faults are both radial from, and tangential to, the dome. The radial faults appear on many of the structure maps to strike through the salt mass. For example, Fault F-7 on the A-Sand structure map (Figure 5-30) strikes out of the northwest and southeast flanks of the dome. This is because many radial faults originally formed tangential to the dome. As the salt dome moved upward, it passed through the fault plane, destroying it but leaving traces of the plane away from the dome intact.

Salt Mineralogy

Most salt domes in this area of the Gulf Coast are nearly pure halite. The major impurity found is anhydrite, which is generally present in amounts from 1% to 10%. Studies of salt mines at other domes have revealed inclusions of sediments, gas, brine, and petroleum within the salt mass (Kupfer, 1974). Although no core of the Big Hill salt dome is available for testing, salt was cored from Pure Oil #1 (now Union Oil #1) and analyzed for insolubles. The average of three samples taken from the top, middle, and bottom of that well was 3.2% insolubles. A detailed coring and logging program as well as a materials testing program are outlined in Chapter 6.

Several thin salt sections have been logged along the western and eastern edges of the dome where the salt overhangs into the soft sediments (Figure 5-17). These sections are either inclusions of sediment in the salt mass, or pieces of detached salt that have separated from the main body of salt. Salt inclusions in the sediments are eventually dissolved; however, sediment inclusions inside the main salt mass are better preserved. No inclusions have been found on the south side.

The AMOCO-Texas Exploration Well 8 on the west flank of the dome penetrated salt at -1850 ft and reached a total depth of 5200 ft, still in salt. This is the only well to penetrate the complete interval where the proposed SPR caverns are to be constructed. An electric log is the only log available for this well, as is the case for most wells (see Appendix B). The electric log indicates that the salt is of good quality throughout the entire interval of the proposed caverns. However, an electric log can give only a partial analysis of salt quality, and a testing program as outlined in Chapter 6 should be carried out. Also, the quality of the salt may vary from place to place on the dome.

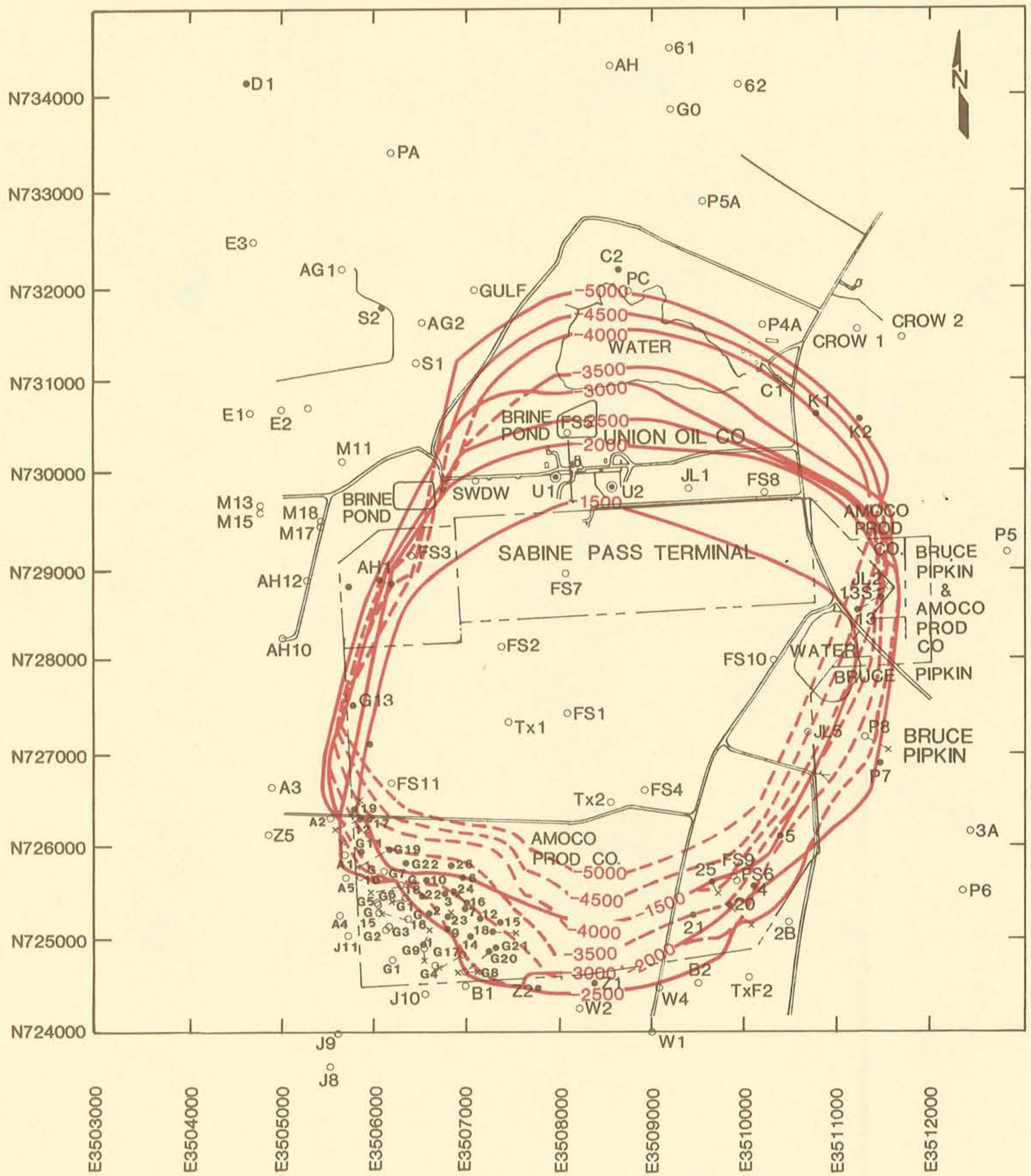

NOTES
1. SEE APPENDIX B FOR EXPLANATION OF WELL NUMBERS AND WELL LOCATIONS.
2. CONTOURED DEPTHS MEASURED IN FEET BELOW DRILLING FLOOR.

LEGEND
- U1 UNION OIL LPG CAVERN.
- + SURFACE LOCATION OF WELL.
- G2 BOTTOM HOLE LOCATION OF WELL.
- G2 BOTTOM HOLE LOCATION OF SIDETRACK HOLE.
- ○ G2 DRILLED AS VERTICAL HOLE . NO BOTTOM HOLE LOCATION AVAILABLE.
- • G2 LOCATION OF WELL PENETRATING SALT.
- SALT DEPTH CONTOURS

1000 500 0 1000 2000
DISTANCE IN FEET

BIG HILL SALT DOME
STRUCTURE MAP-SALT

Sandia National Laboratories

T. R. MAGORIAN

SEP 1981 FIG. 5-1

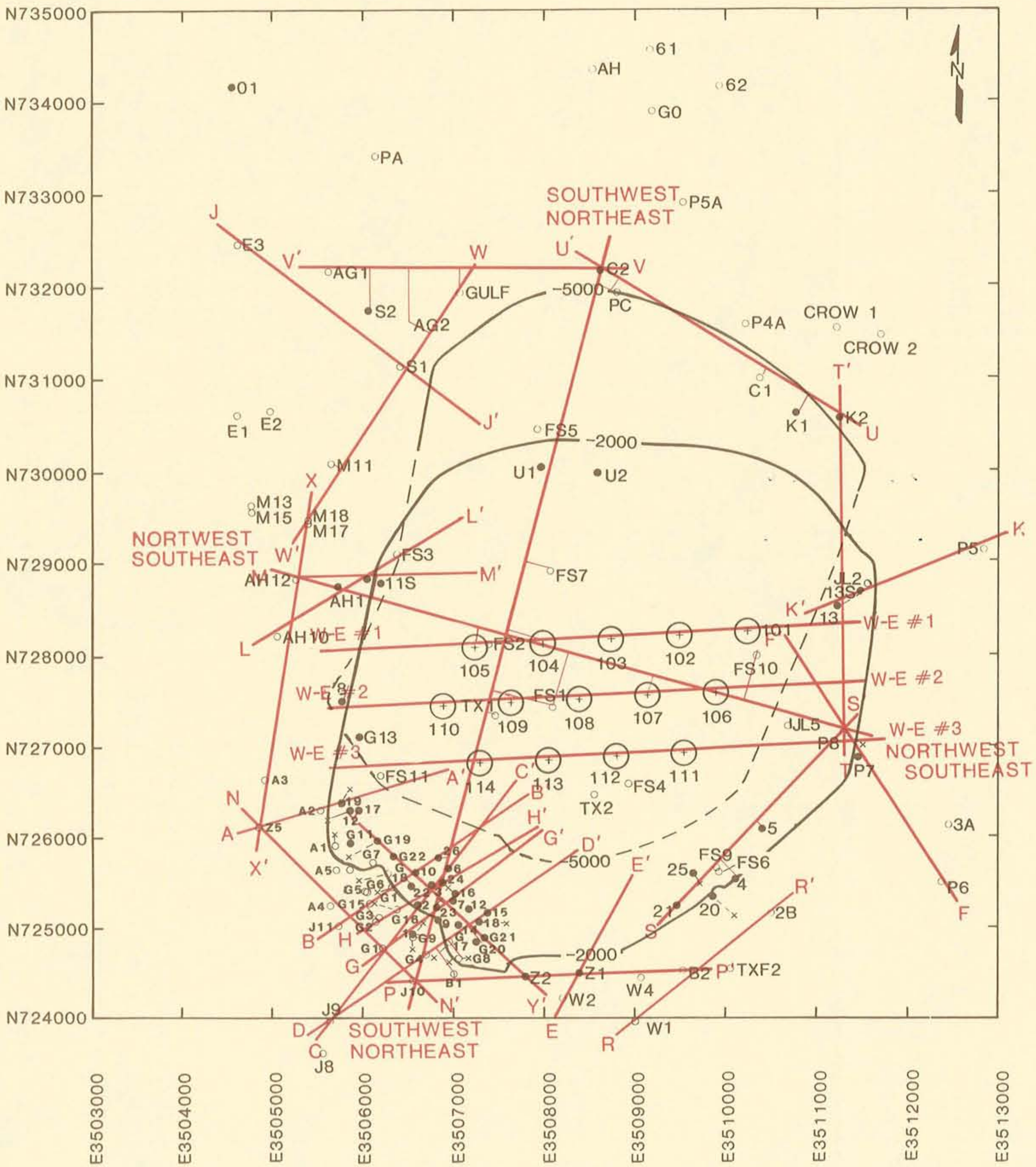

NOTES

1. SEE APPENDIX B FOR EXPLANATION OF WELL NUMBERS AND WELL LOCATIONS.

LEGEND

- UI UNION OIL LPG CAVERN
- SURFACE LOCATION OF WELL.
- G2 BOTTOM HOLE LOCATION OF WELL.
- G2 BOTTOM HOLE LOCATION OF SIDETRACK HOLE
- G2 DRILLED AS VERTICAL HOLE. NO BOTTOM HOLE LOCATION AVAILABLE
- 101 PROPOSED SPR CAVERNS
- SECTION LINE
- WELLS PROJECTED TO SECTION LINE

1000 500 0 1000 2000

DISTANCE IN FEET

BIG HILL SALT DOME
SECTION REFERENCE MAP

Sandia National Laboratories

SEP 1981

FIG. 5-2

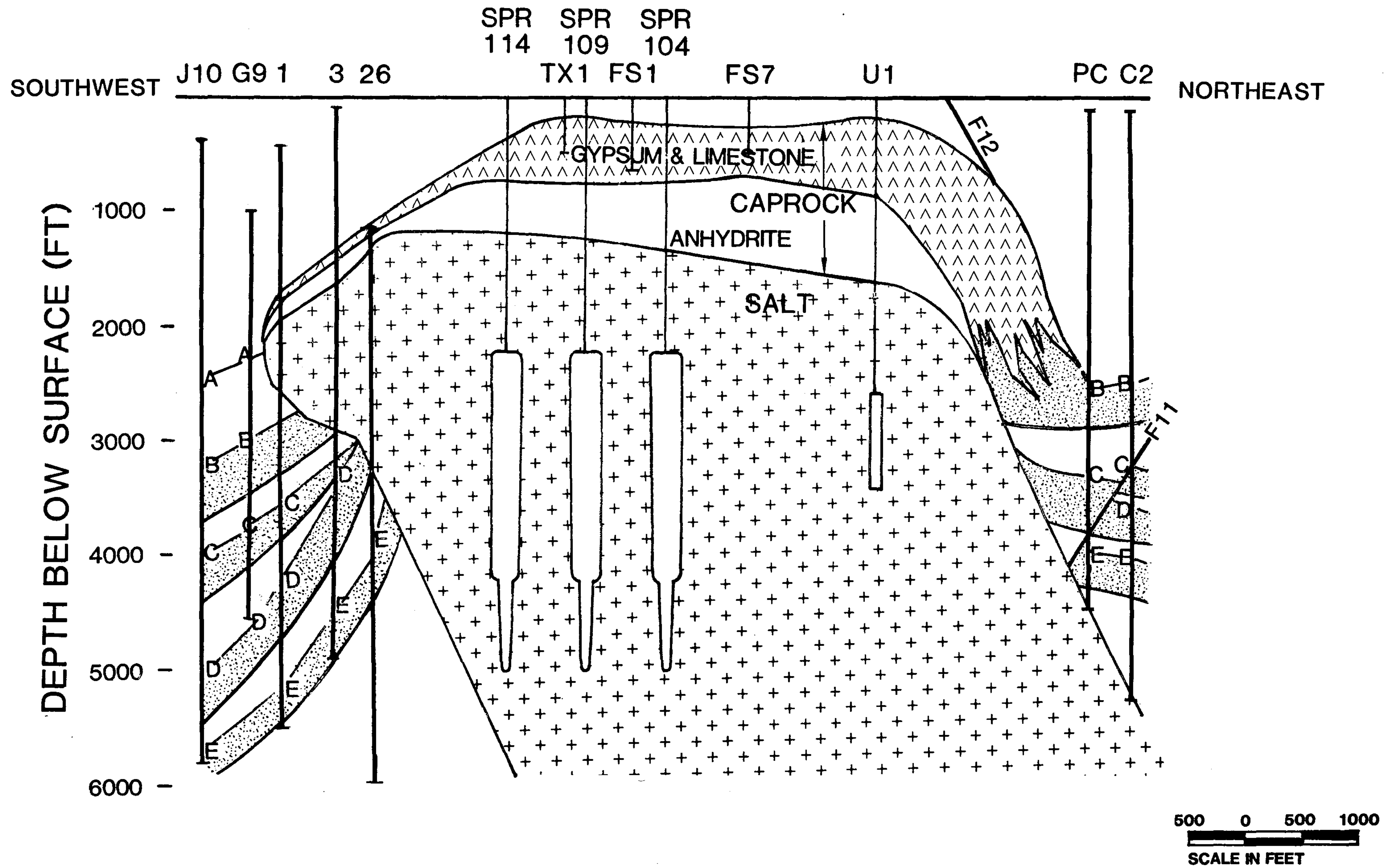

BIG HILL SALT DOME
SOUTHWEST-NORTHEAST
CROSS SECTION

Sandia National Laboratories

T.R. MAGORIAN

SEP 1981 FIG. 5-3

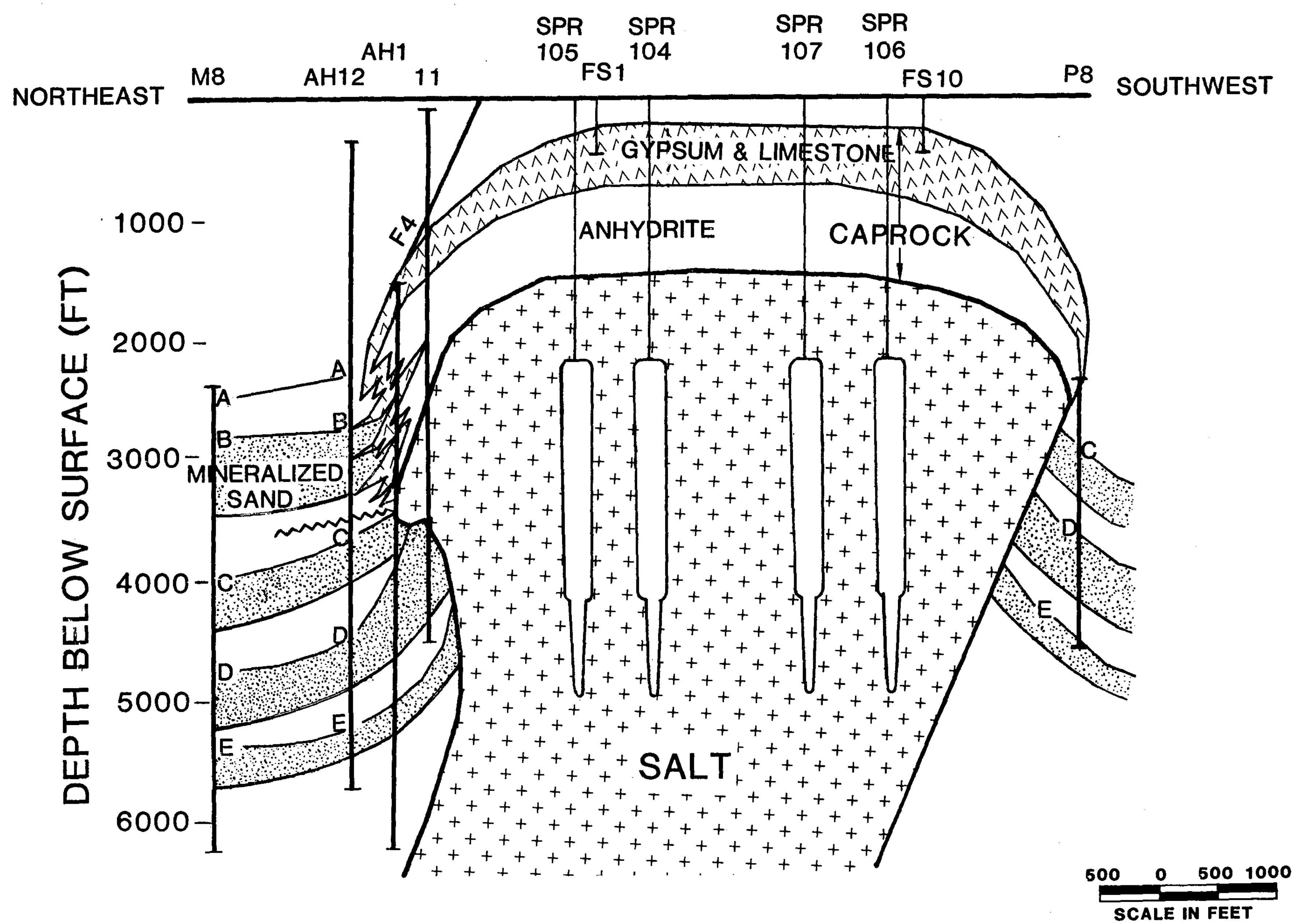

BIG HILL SALT DOME
NORTHWEST-SOUTHEAST
CROSS SECTION

Sandia National Laboratories

T.R. MAGORIAN

SEP 1981 FIG. 5-4

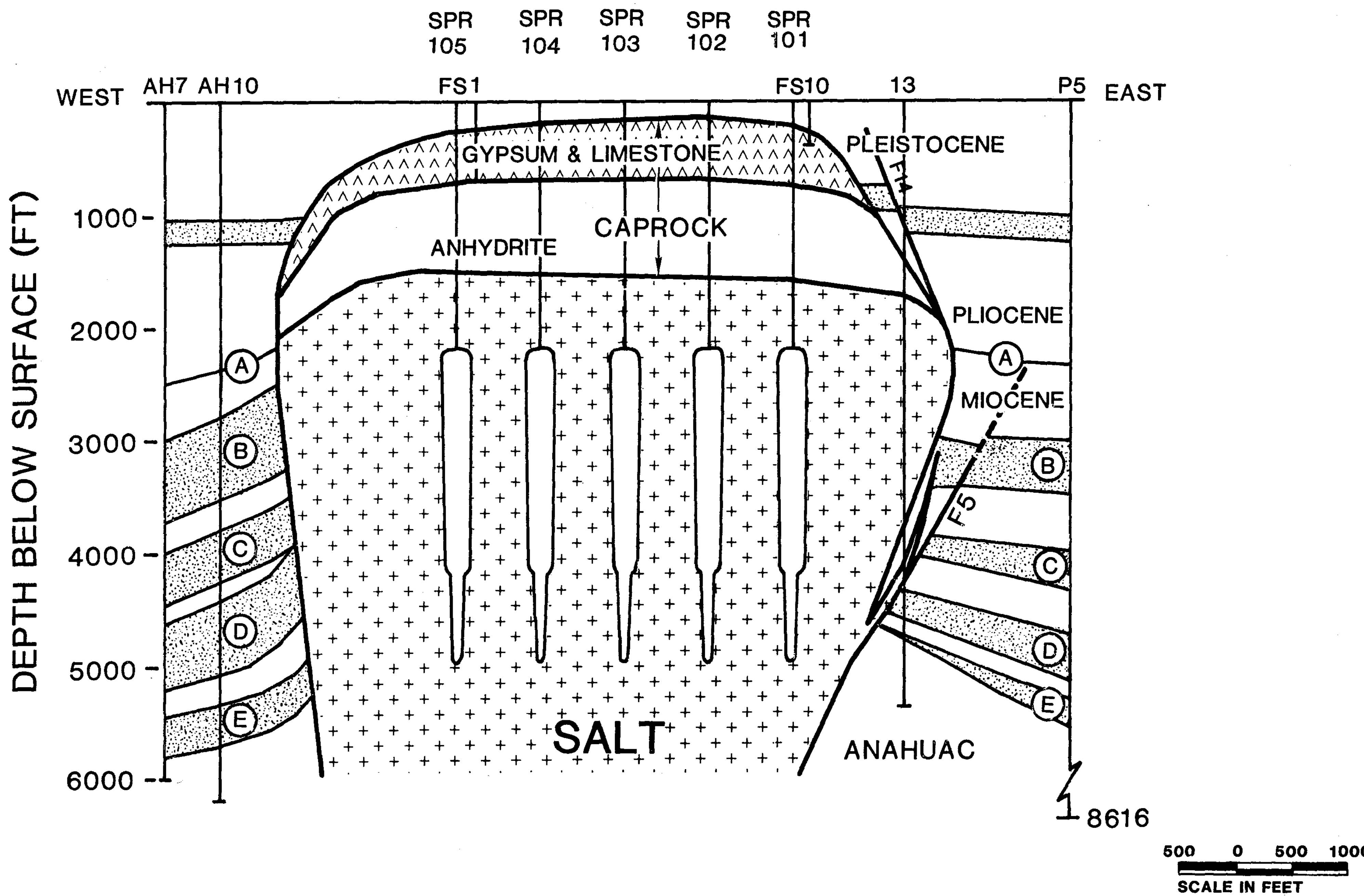

BIG HILL SALT DOME
WEST-EAST CROSS
SECTION NO.1

Sandia National Laboratories

T.R. MAGORIAN

SEP 1981 FIG. 5-5

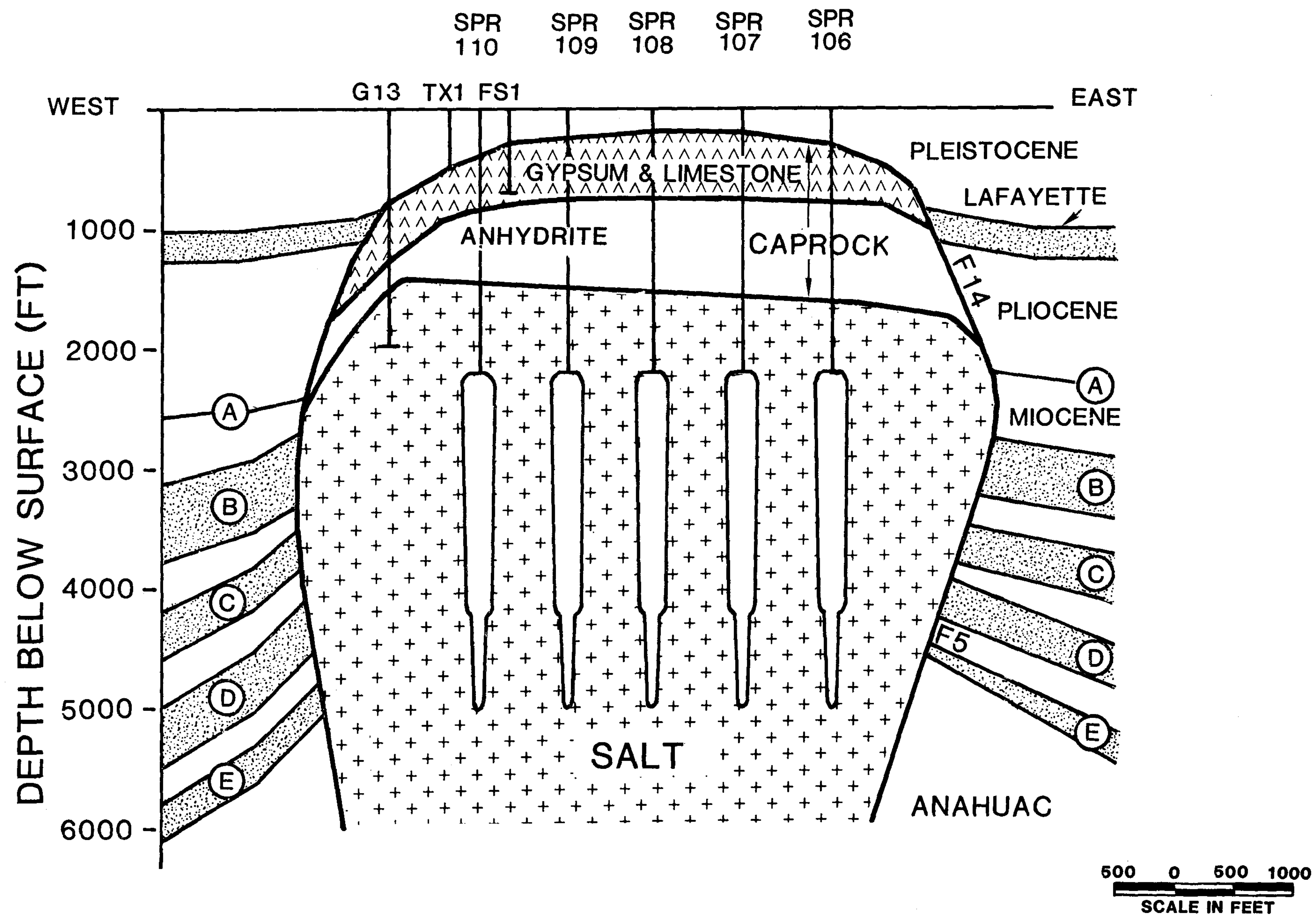

BIG HILL SALT DOME
WEST-EAST CROSS
SECTION NO.2

Sandia National Laboratories

T.R. MAGORIAN

SEP 1981 FIG.5-6

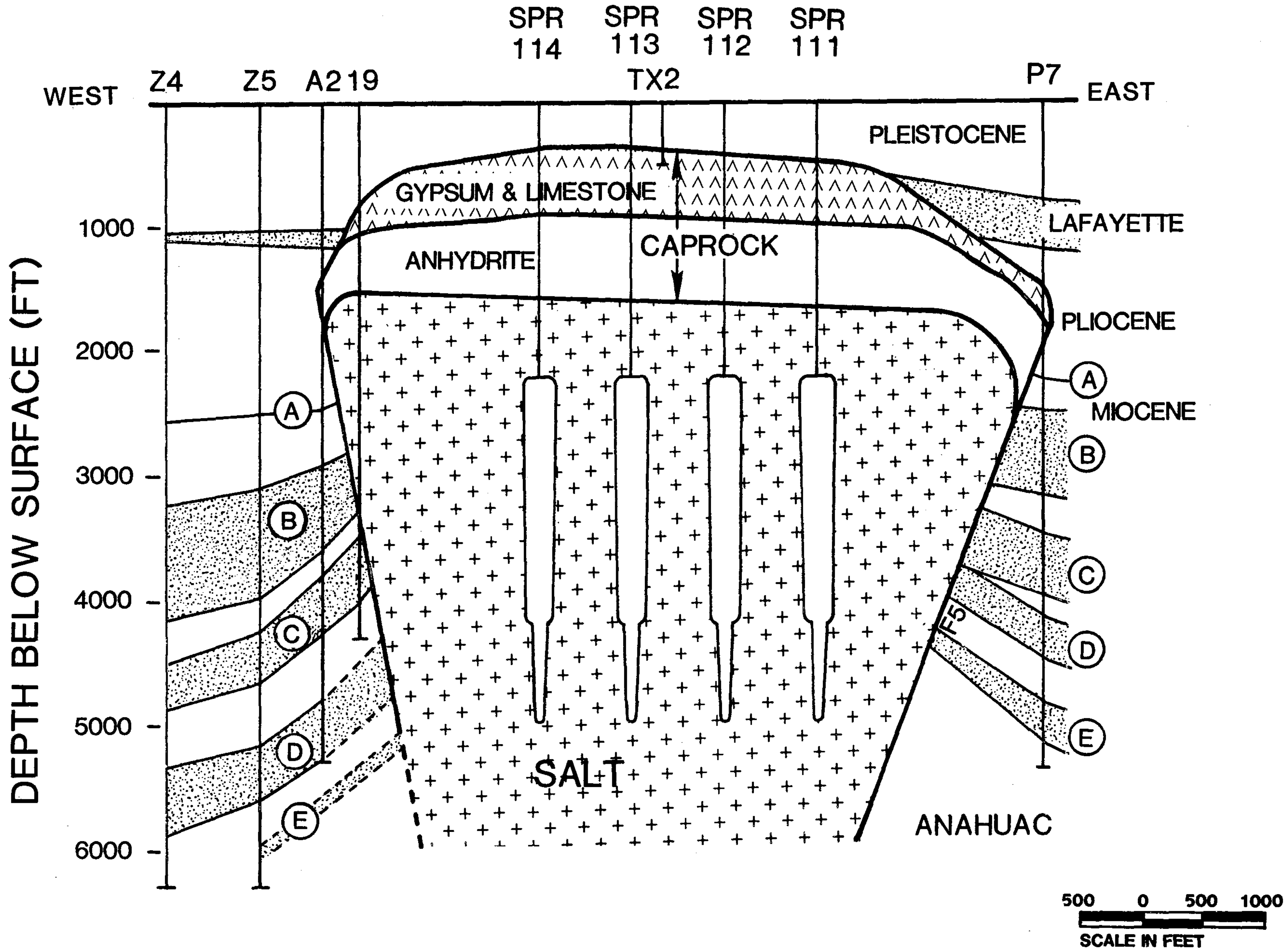

BIG HILL SALT DOME
WEST-EAST CROSS
SECTION NO.3

Sandia National Laboratories

T.R. MAGORIAN

SEP 1981 FIG. 5-7

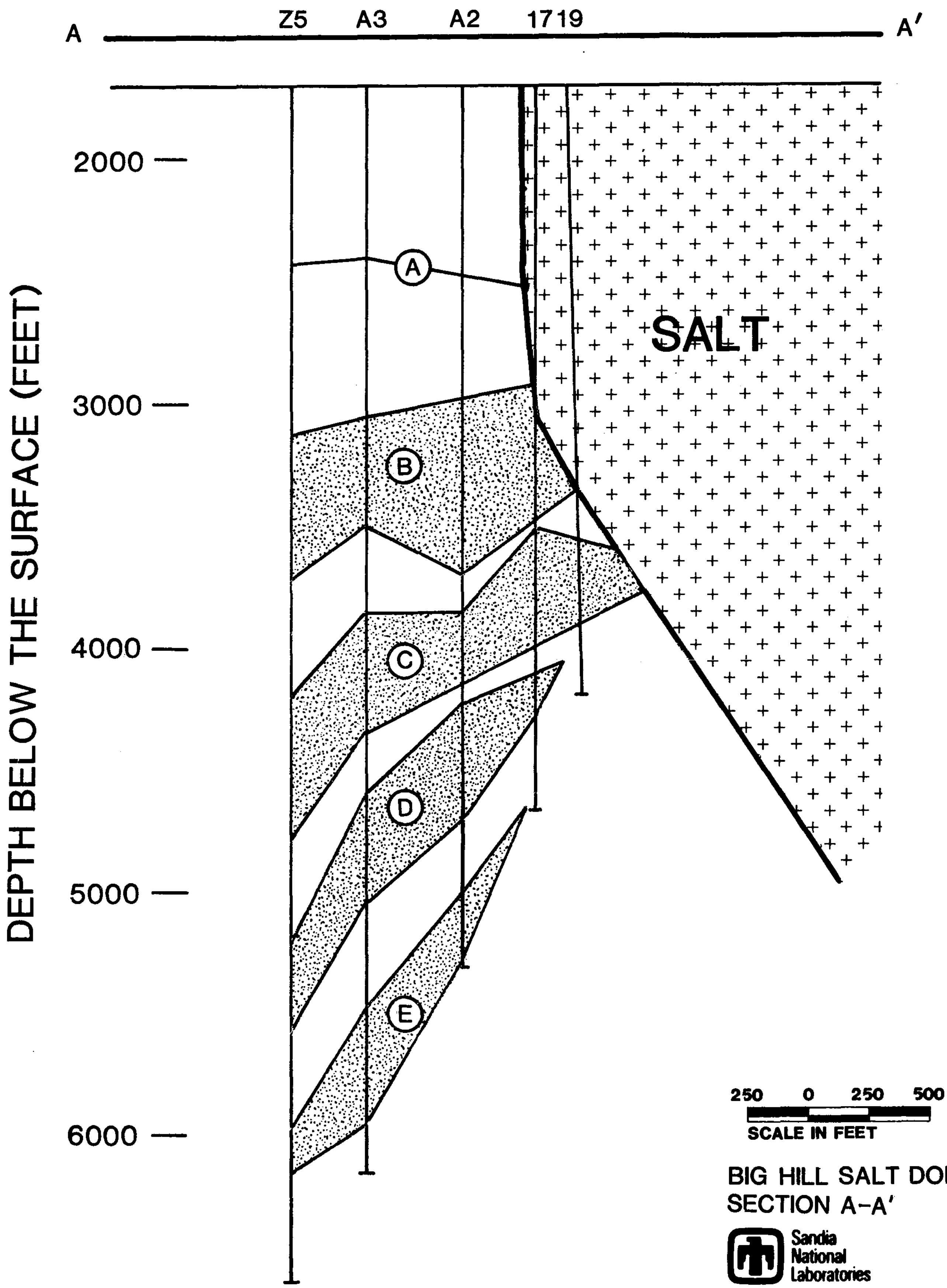

BIG HILL SALT DOME
SECTION A–A′

Sandia National Laboratories

T. R. MAGORIAN
SEP. 1981 FIG. 5-8

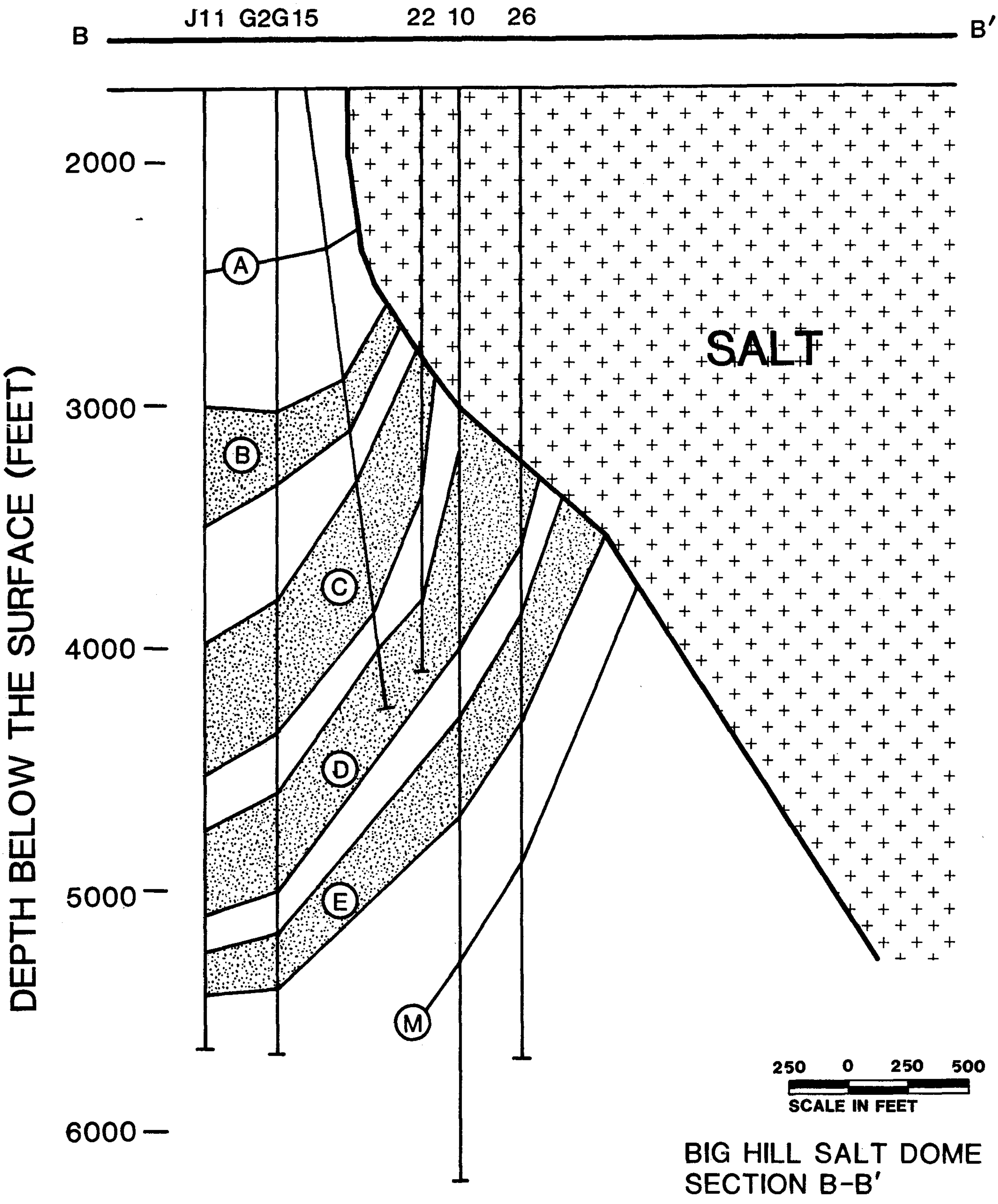

BIG HILL SALT DOME
SECTION B-B′

Sandia National Laboratories

T. R. MAGORIAN

SEP. 1981 FIG. 5-9

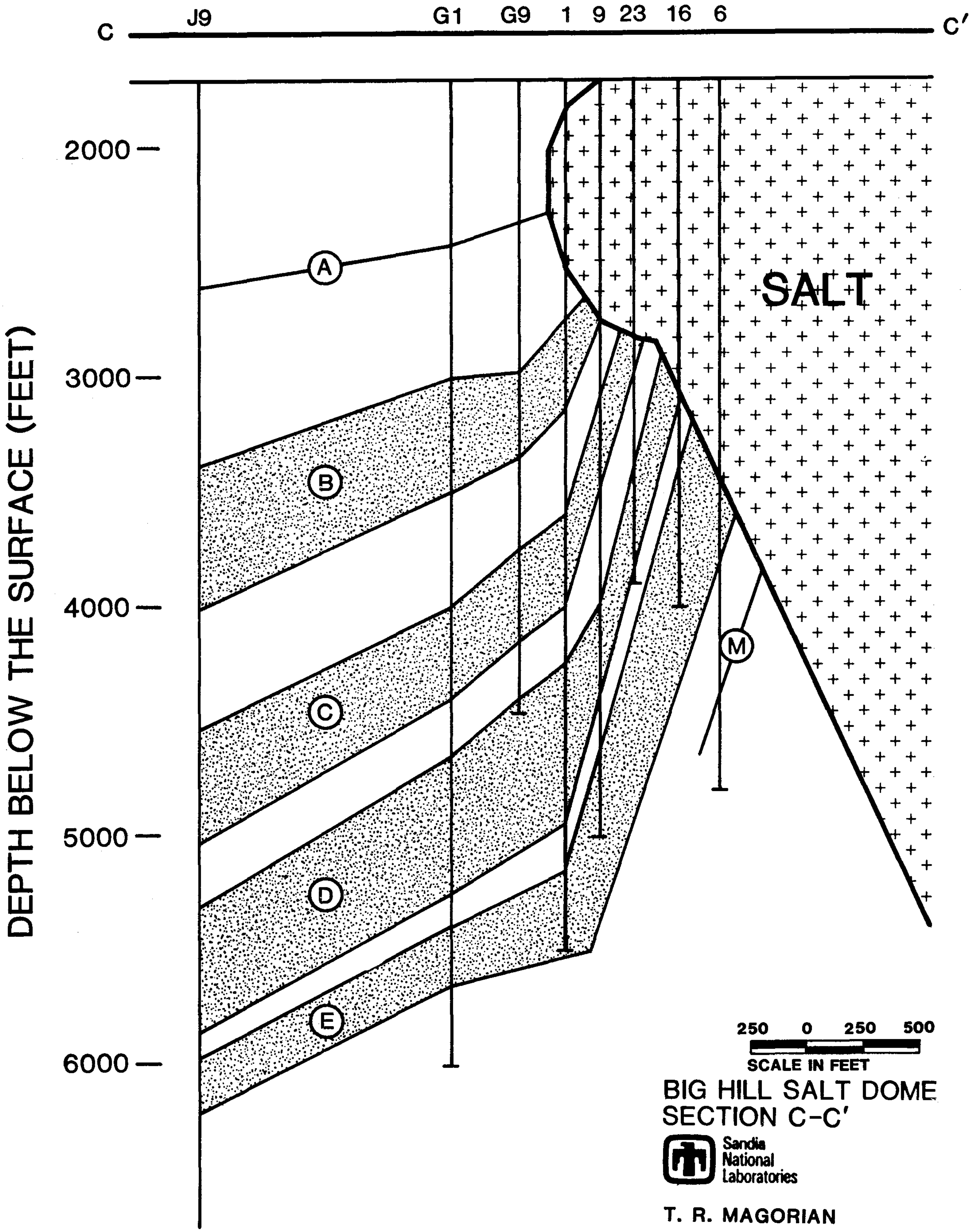

BIG HILL SALT DOME
SECTION C–C′

Sandia National Laboratories

T. R. MAGORIAN

SEP 1981 FIG. 5-10

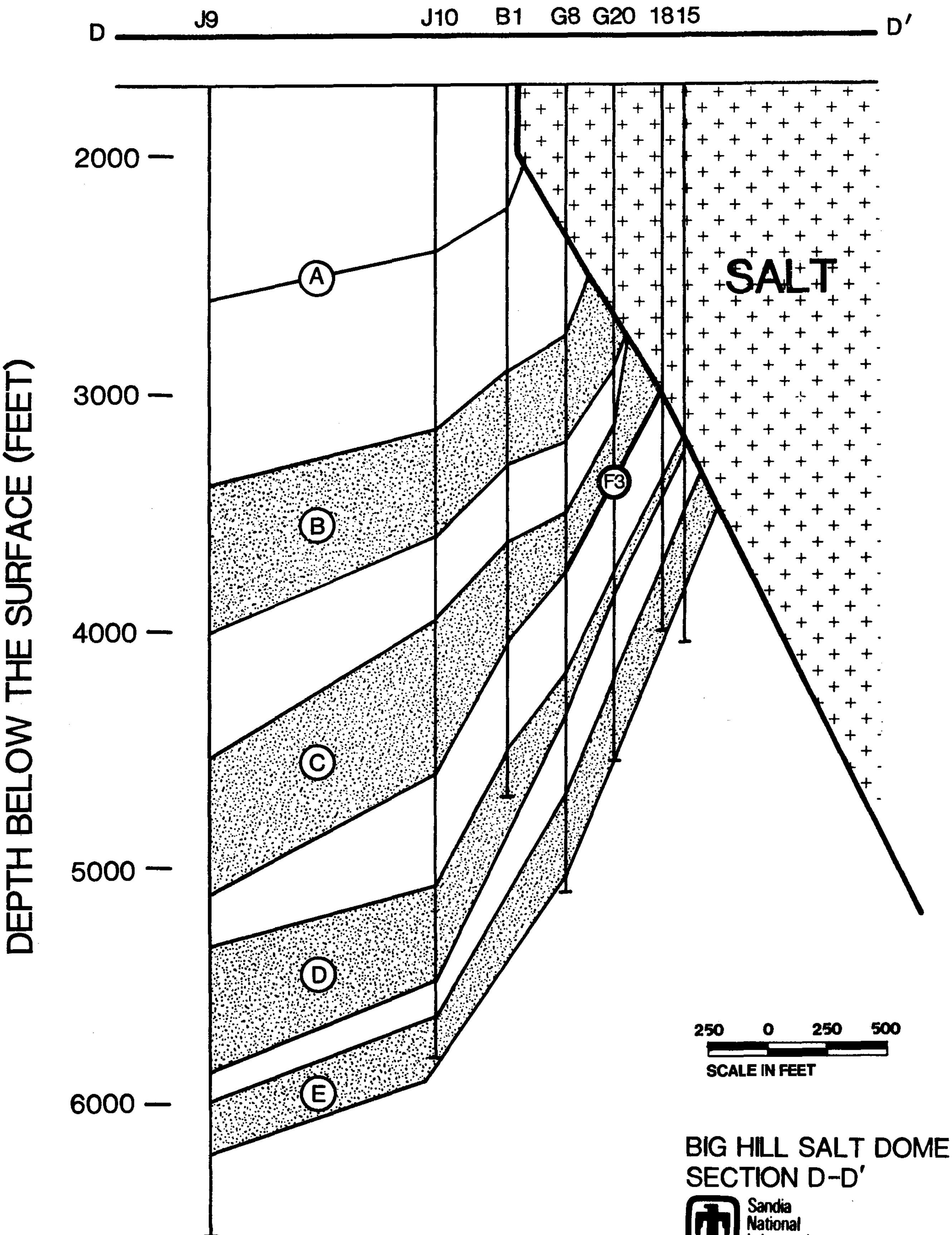

BIG HILL SALT DOME
SECTION D-D′

Sandia National Laboratories

T.R. MAGORIAN

SEP. 1981 FIG. 5-11

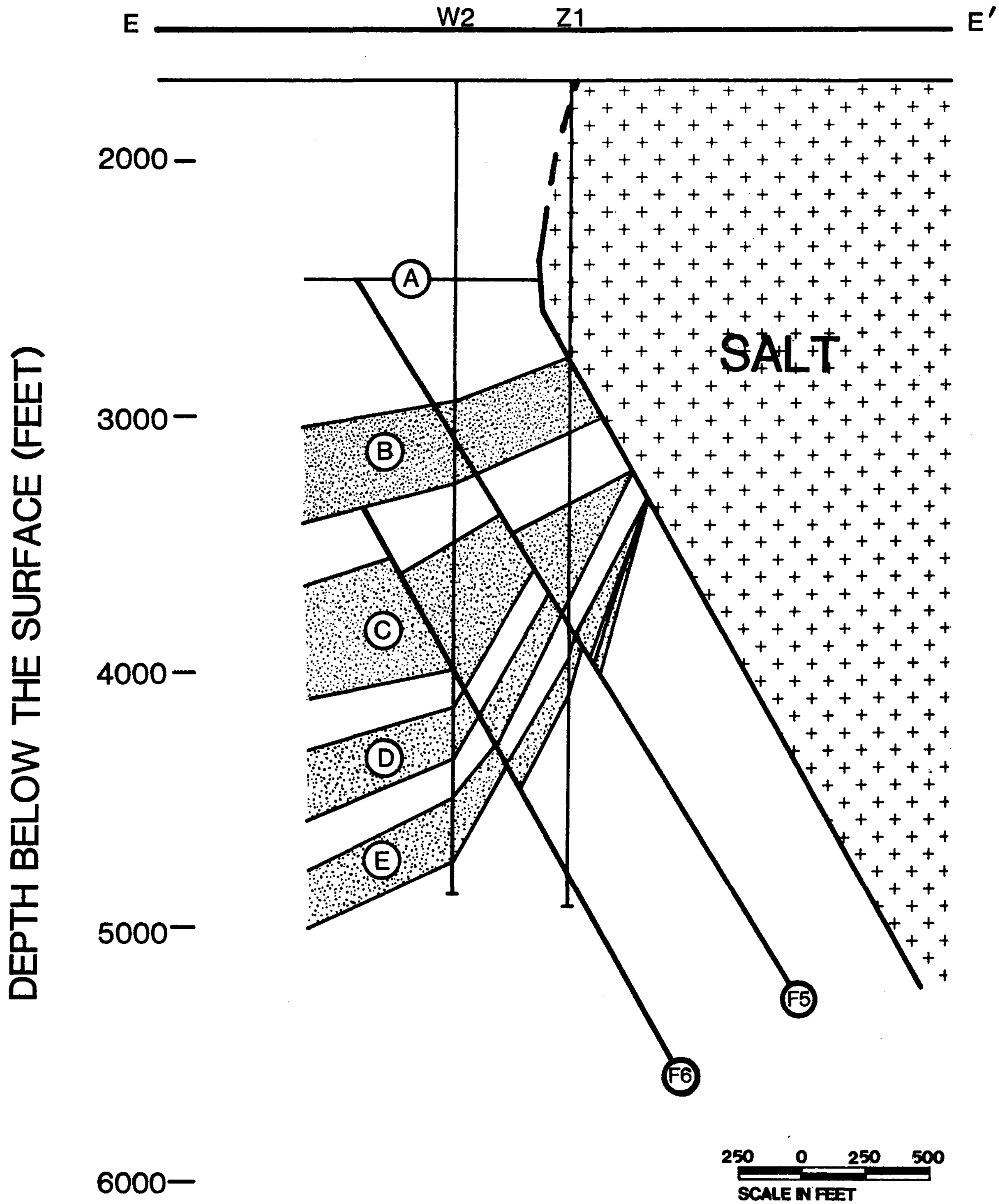

BIG HILL SALT DOME
SECTION E-E′

Sandia National Laboratories

T. R. MAGORIAN

SEP. 1981 FIG. 5-12

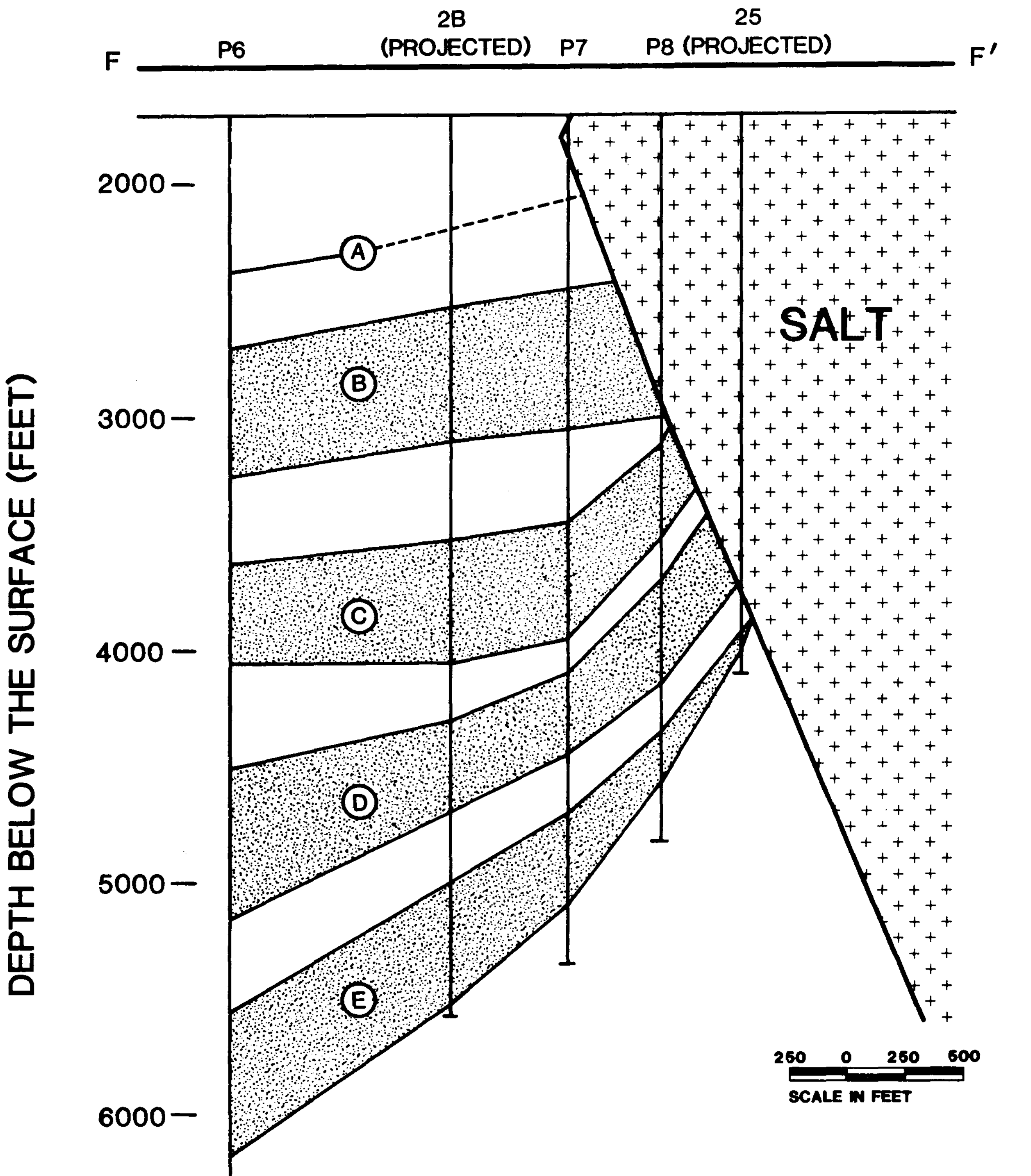

BIG HILL SALT DOME
SECTION F-F′

Sandia National Laboratories

T.R. MAGORIAN

SEP 1981 FIG. 5-13

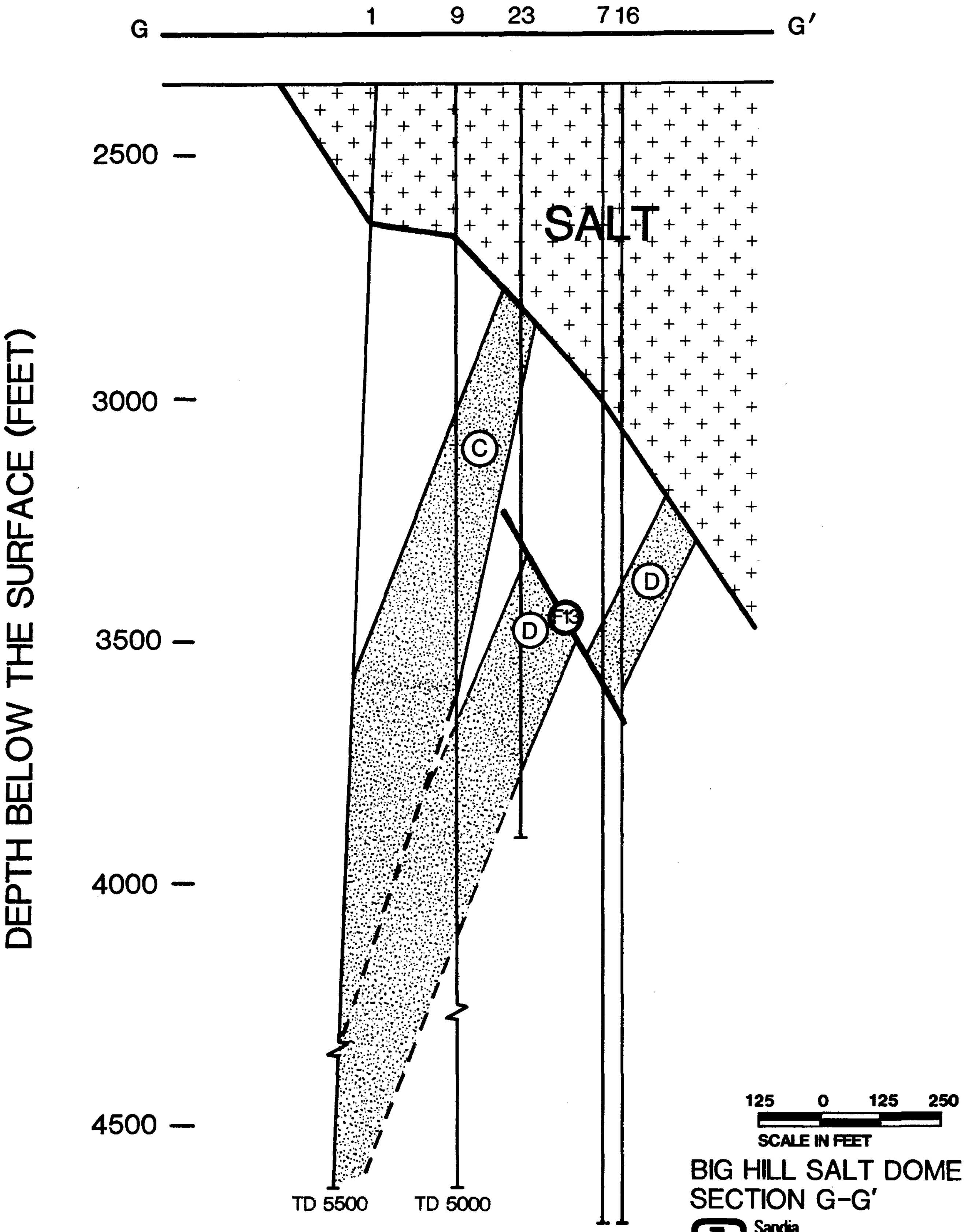

BIG HILL SALT DOME
SECTION G–G′

Sandia National Laboratories

T. R. MAGORIAN

SEP 1981 FIG. 5–14

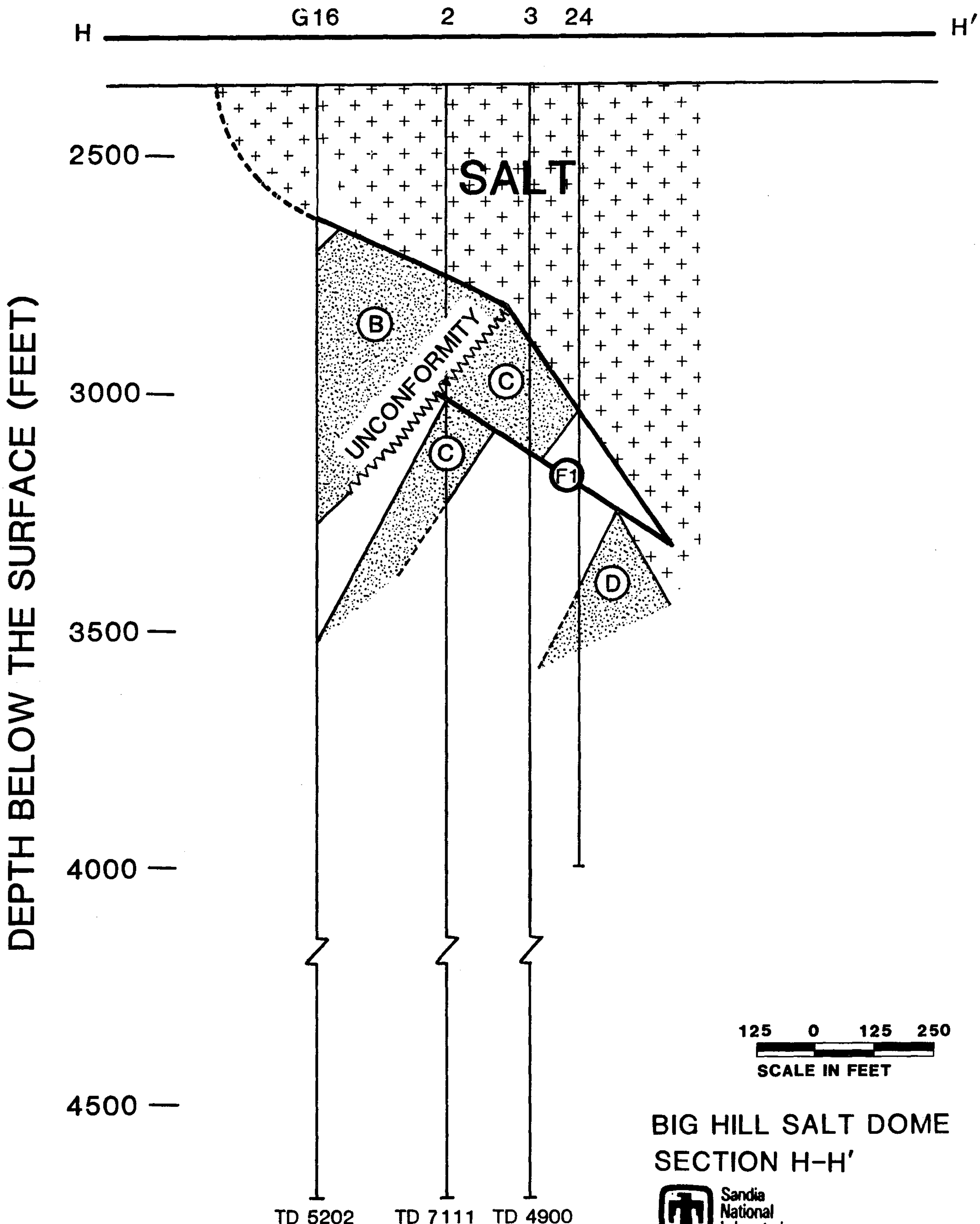

BIG HILL SALT DOME
SECTION H-H′

Sandia National Laboratories

T. R. MAGORIAN

SEP. 1981 FIG. 5-15

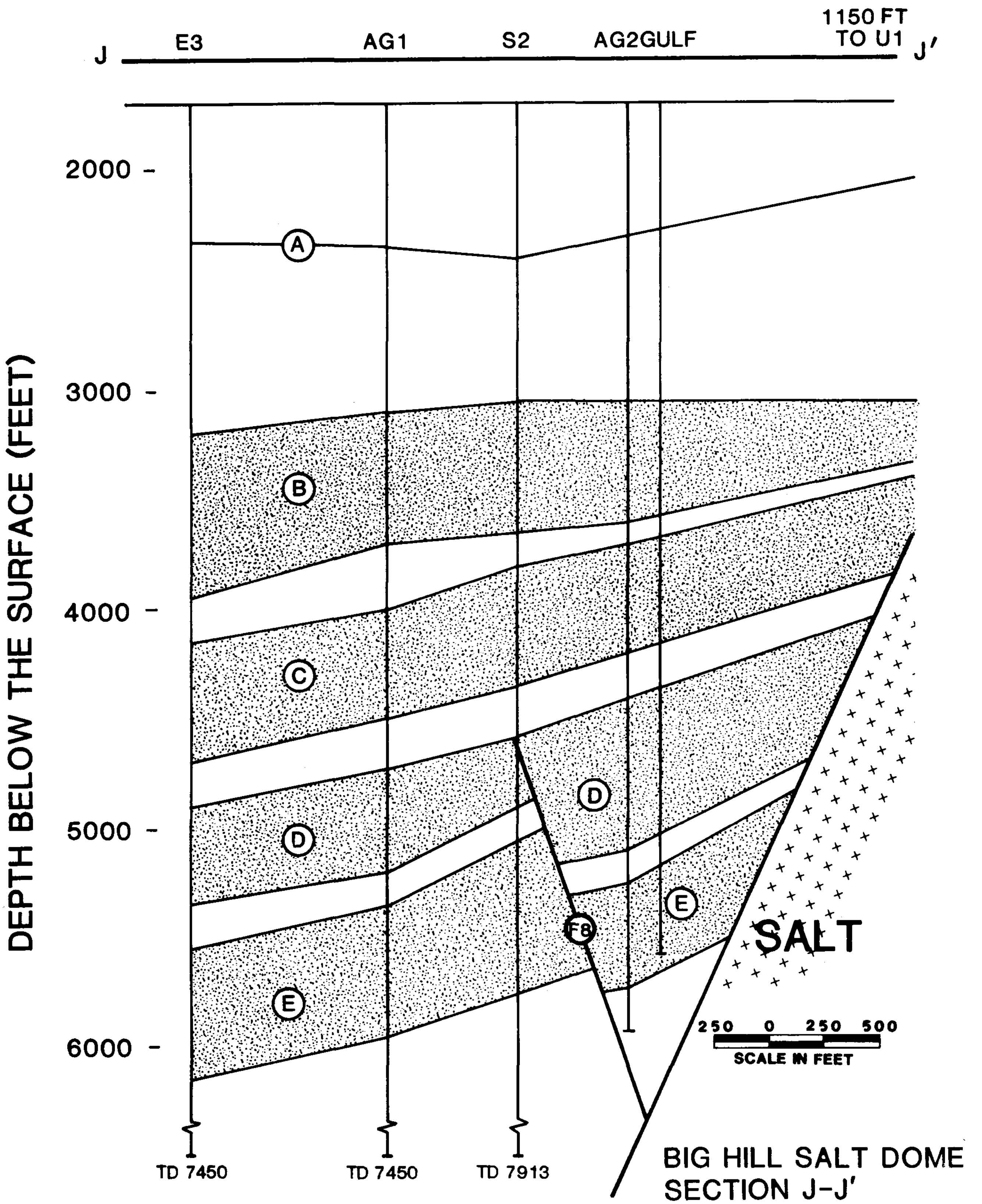

BIG HILL SALT DOME
SECTION J–J'

Sandia National Laboratories

T.R. MAGORIAN

SEP. 1981 FIG.5-16

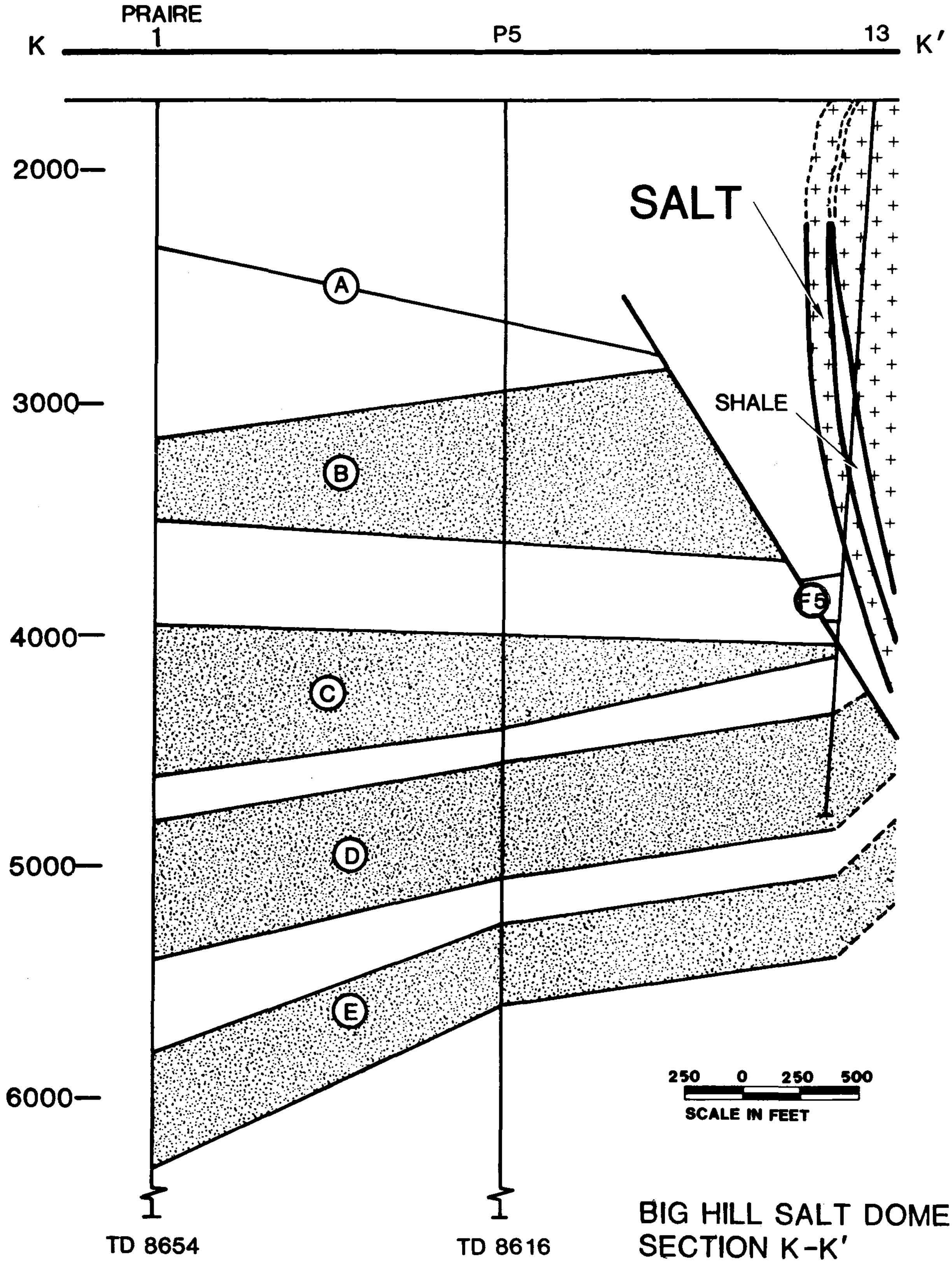

BIG HILL SALT DOME
SECTION K-K'

Sandia National Laboratories

T.R. MAGORIAN

SEP. 1981 FIG. 5-17

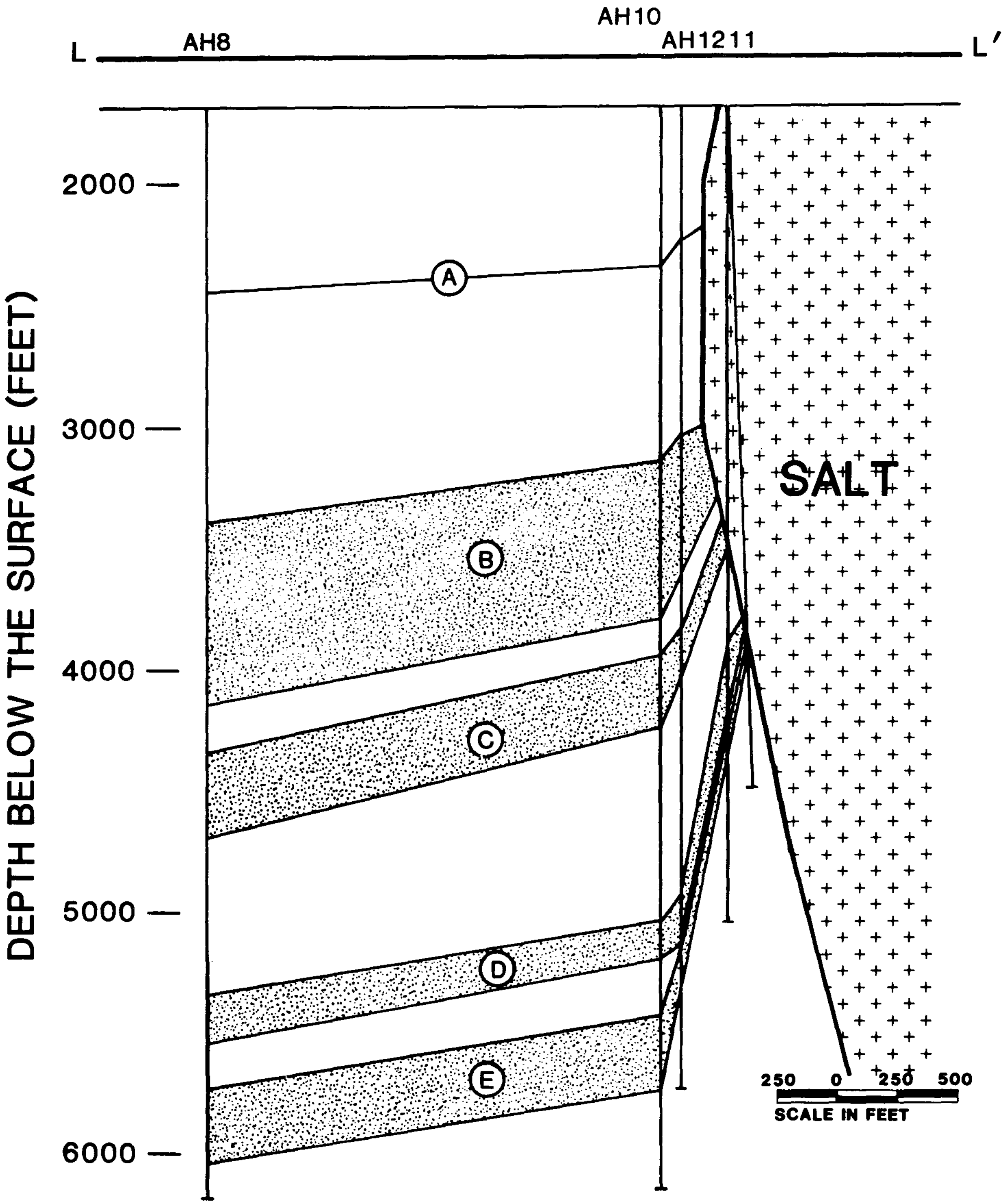

BIG HILL SALT DOME
SECTION L-L′

Sandia National Laboratories

T.R. MAGORIAN

SEP 1981 FIG. 5-18

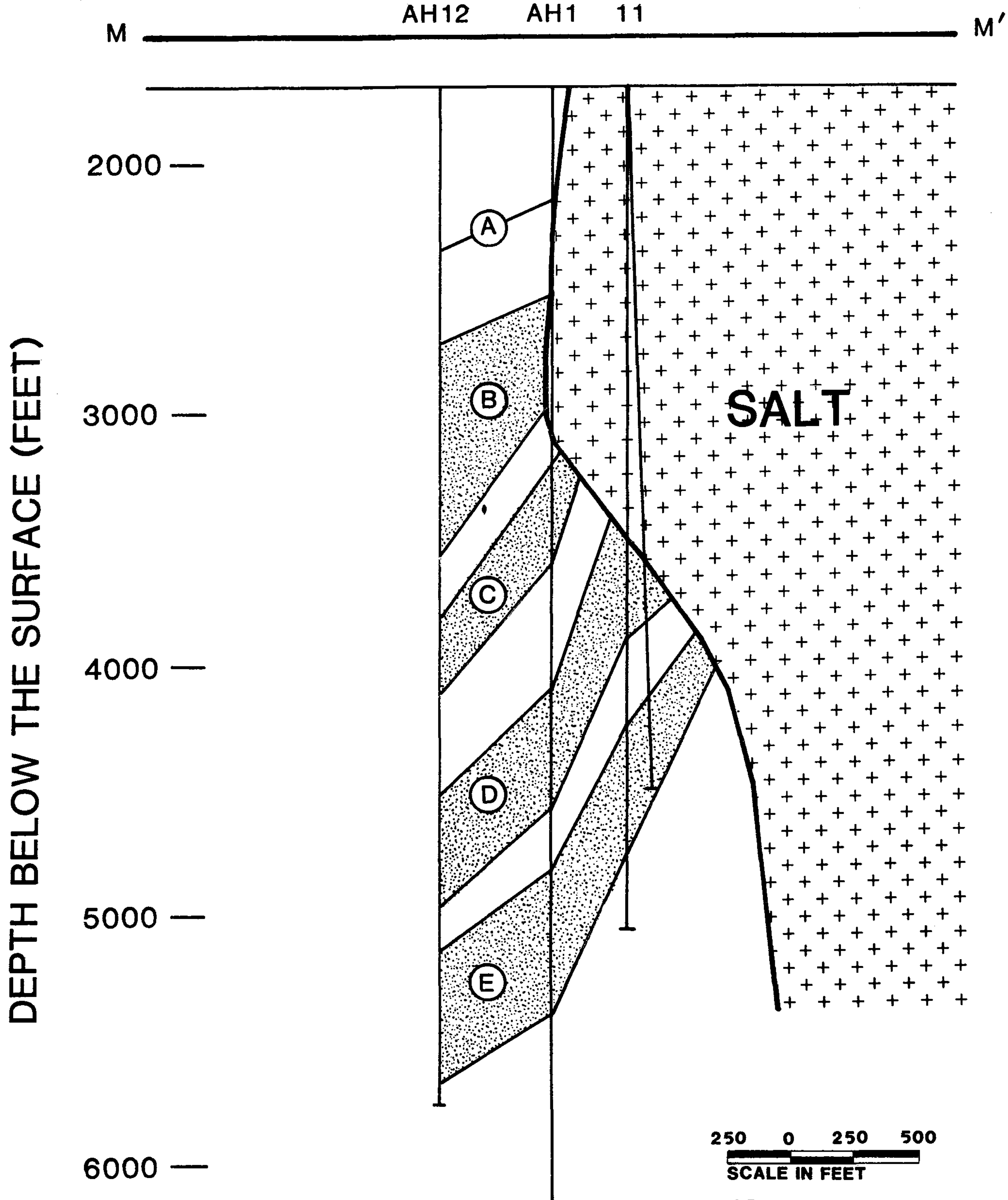

BIG HILL SALT DOME
SECTION M-M′

Sandia National Laboratories

T. R. MAGORIAN

SEP. 1981 FIG. 5-19

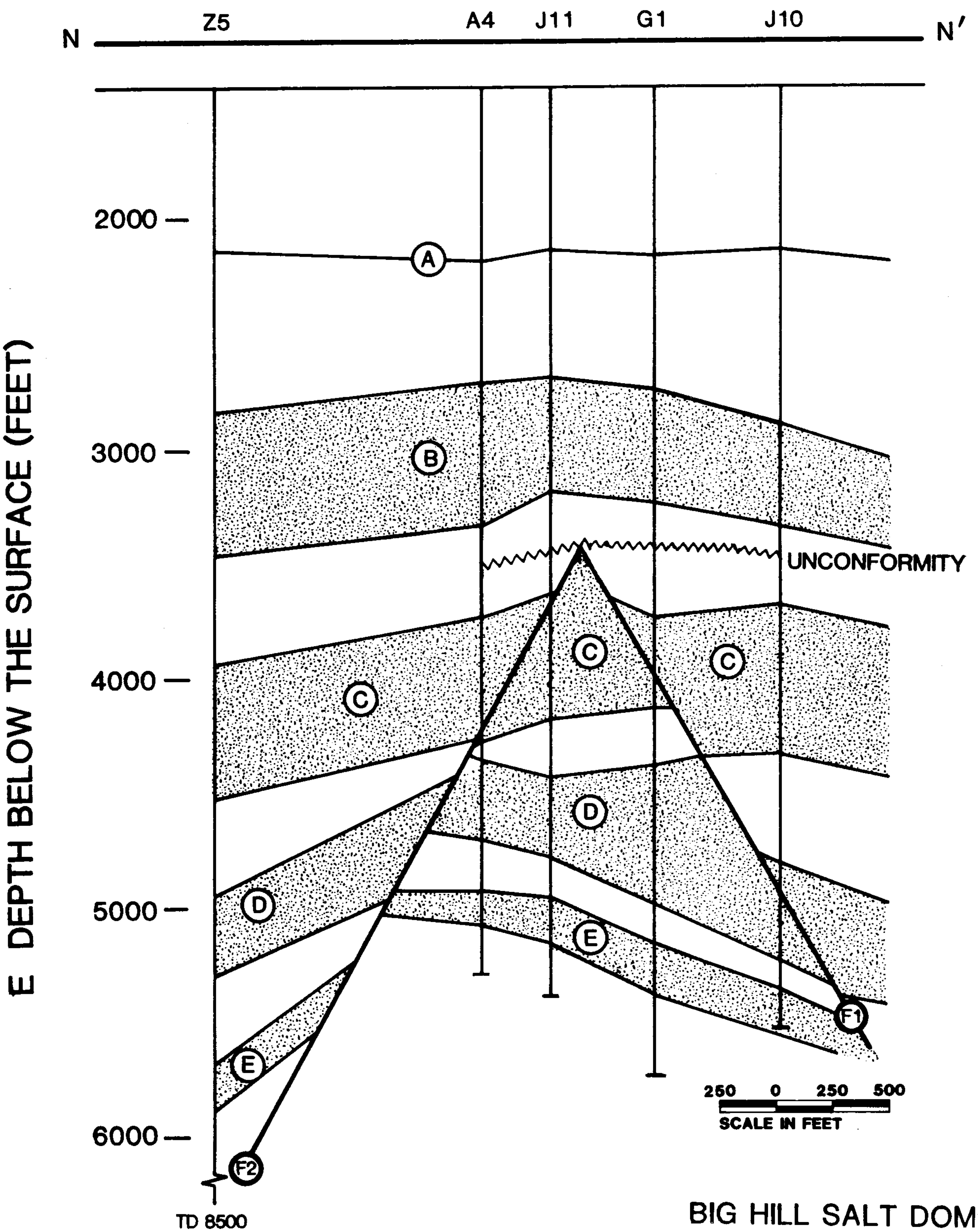

BIG HILL SALT DOME
SECTION N-N′

Sandia National Laboratories

T.R. MAGORIAN

SEP 1981 FIG. 5-20

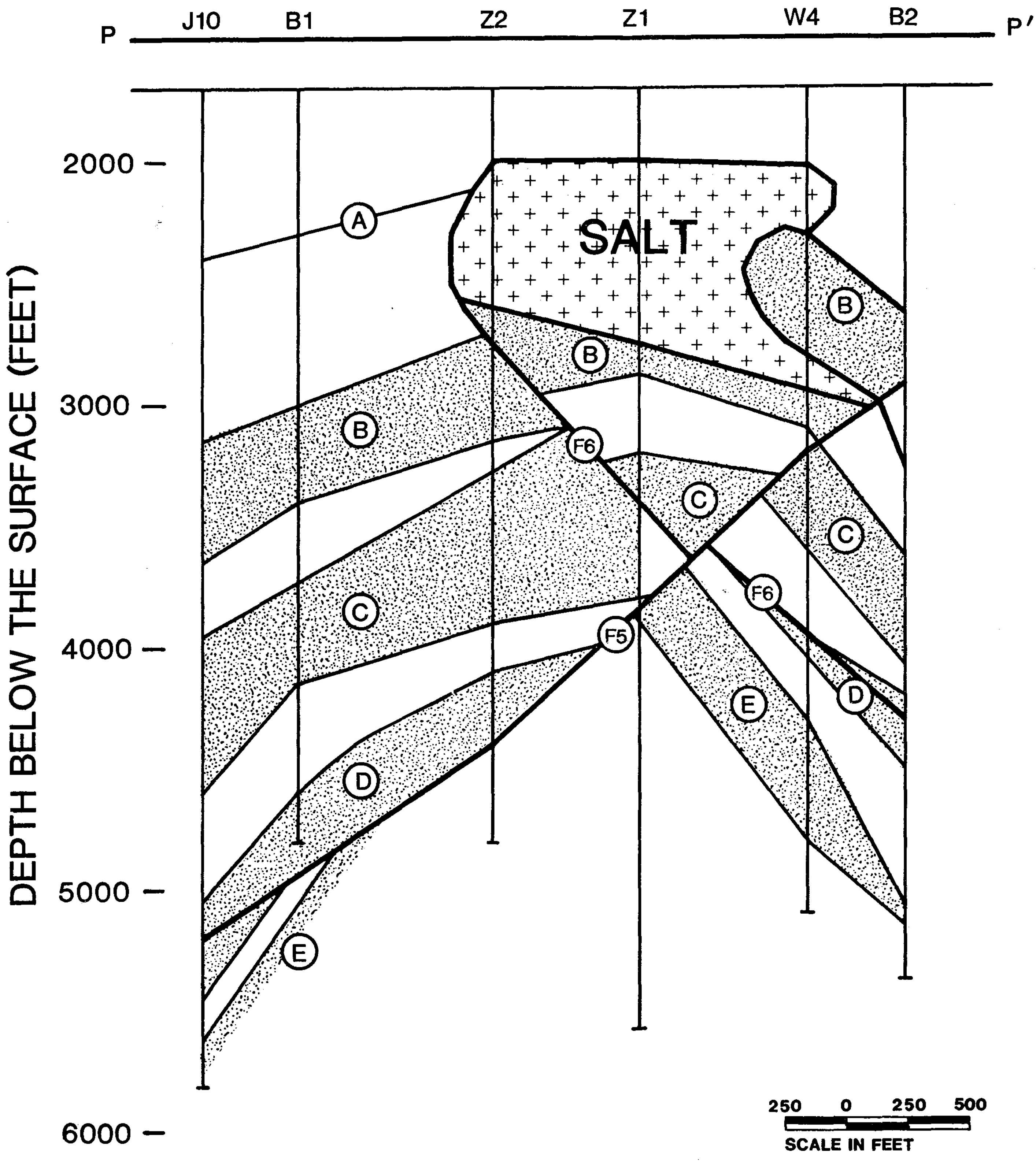

BIG HILL SALT DOME
SECTION P-P′

Sandia National Laboratories

T. R. MAGORIAN

SEP 1981 FIG. 5-21

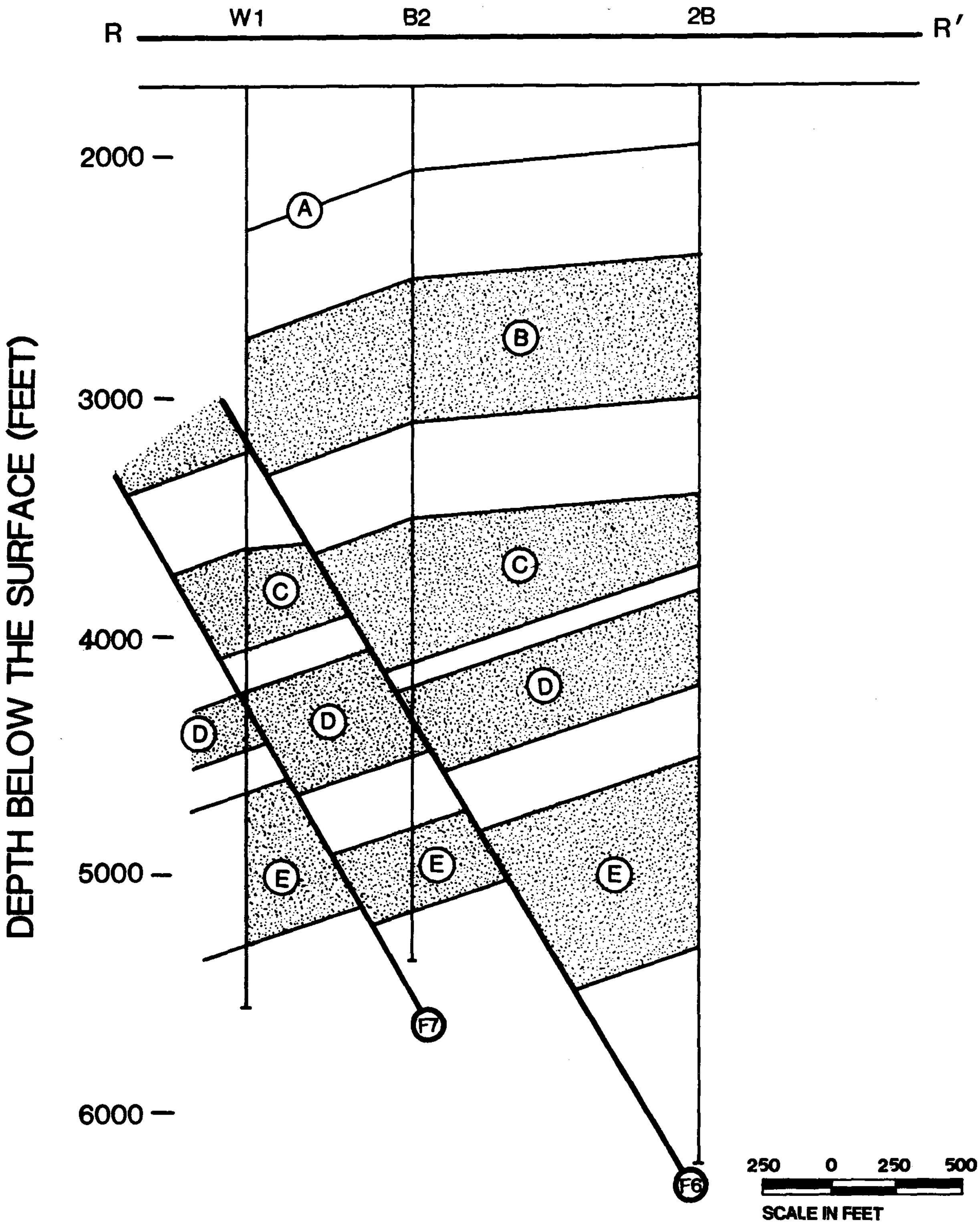

BIG HILL SALT DOME
SECTION R-R′

Sandia National Laboratories

T. R. MAGORIAN

SEP 1981 FIG. 5-22

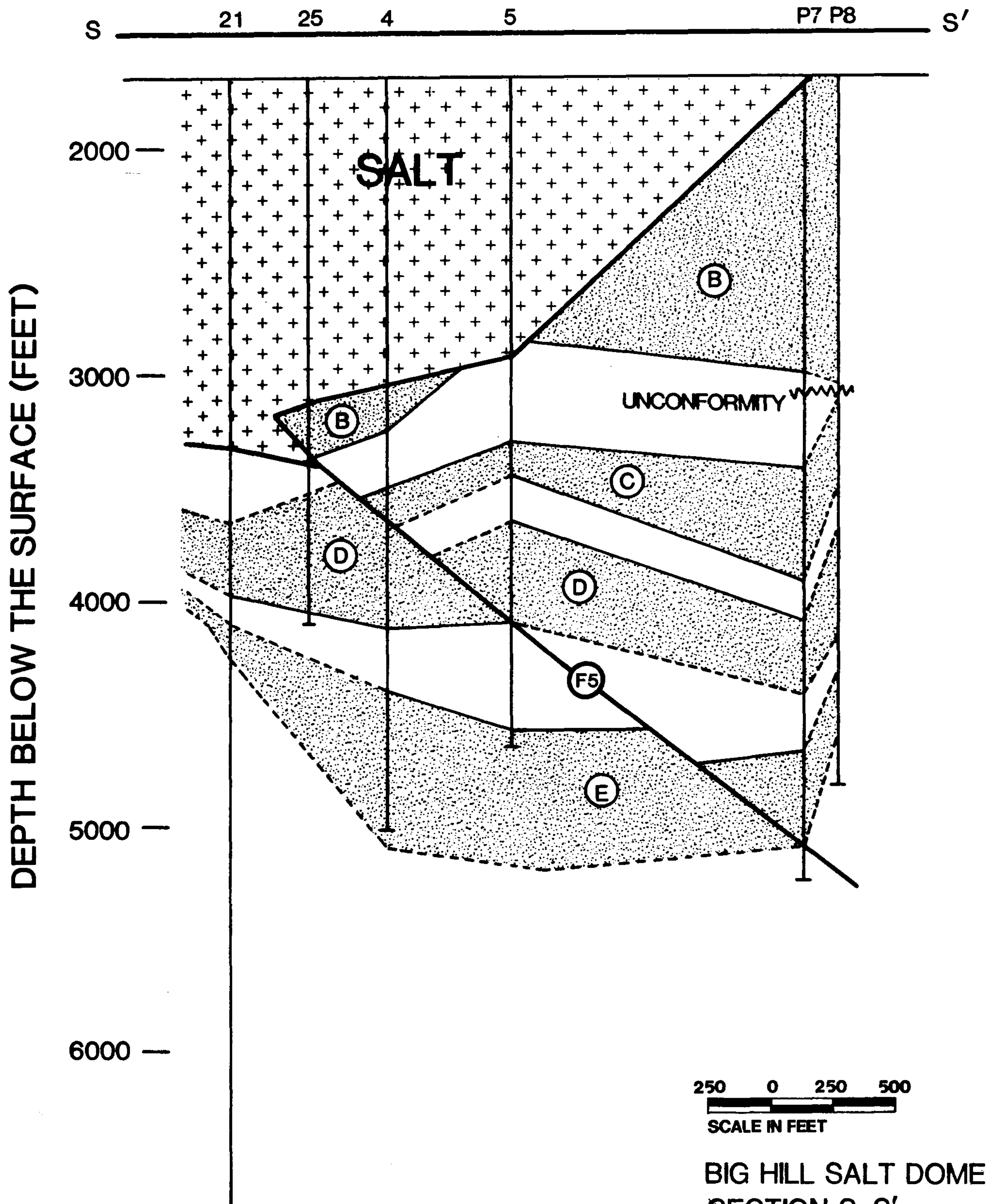

BIG HILL SALT DOME
SECTION S-S′

Sandia National Laboratories

T. R. MAGORIAN

SEP. 1981 FIG. 5-23

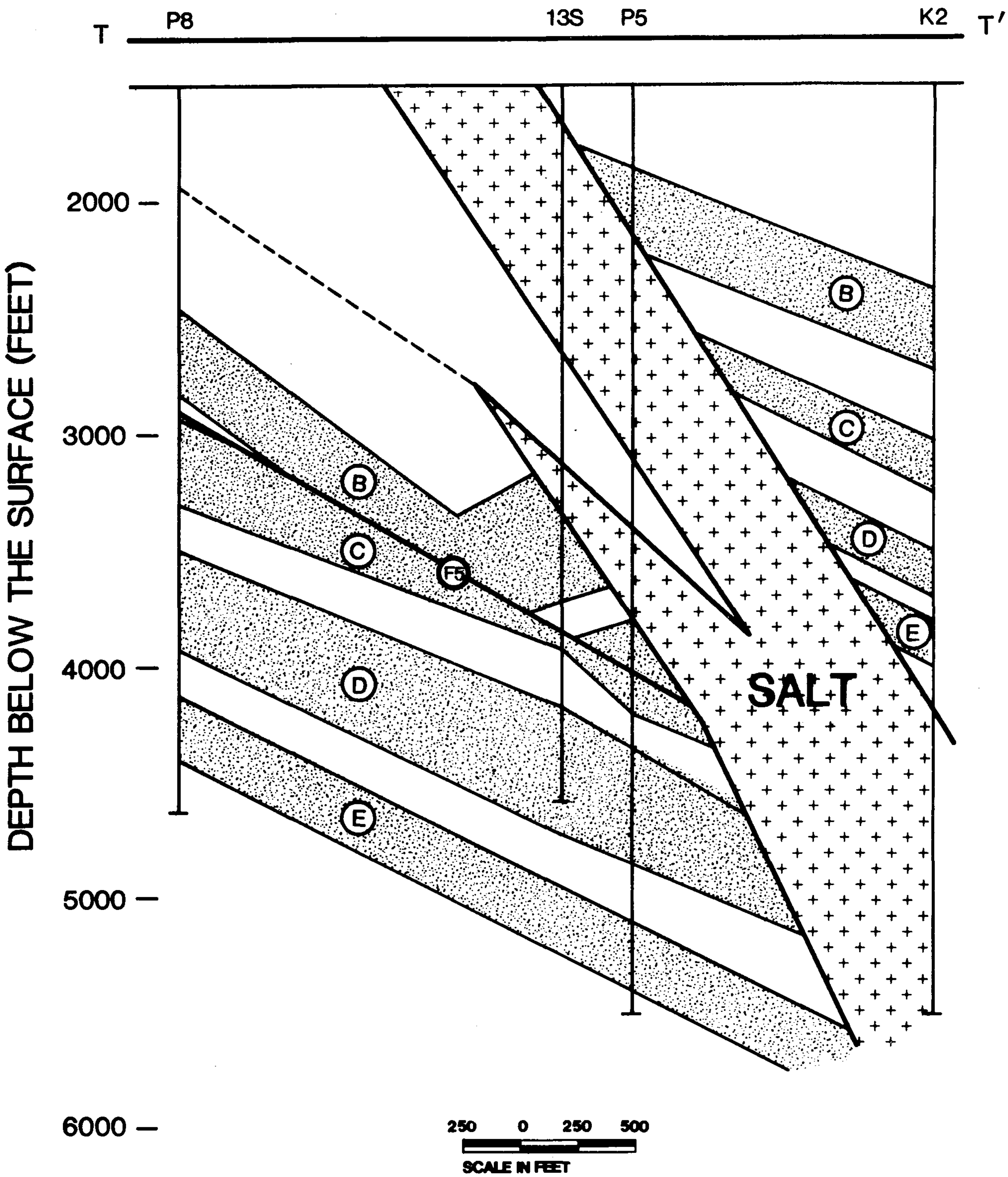

BIG HILL SALT DOME
SECTION T-T'

Sandia National Laboratories

T.R. MAGORIAN

SEP 1981 FIG 5-24

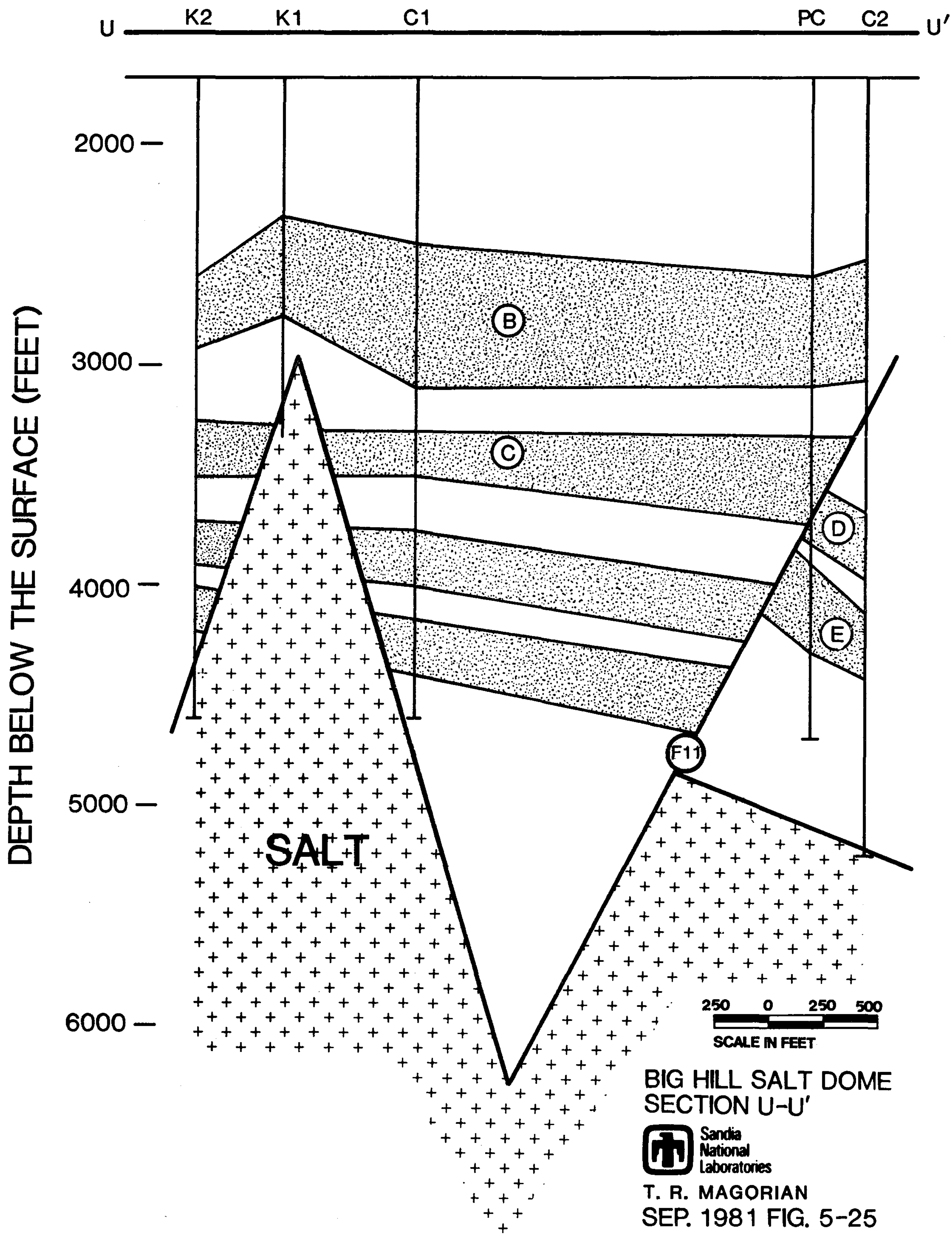

BIG HILL SALT DOME
SECTION U-U′

Sandia National Laboratories

T. R. MAGORIAN
SEP. 1981 FIG. 5-25

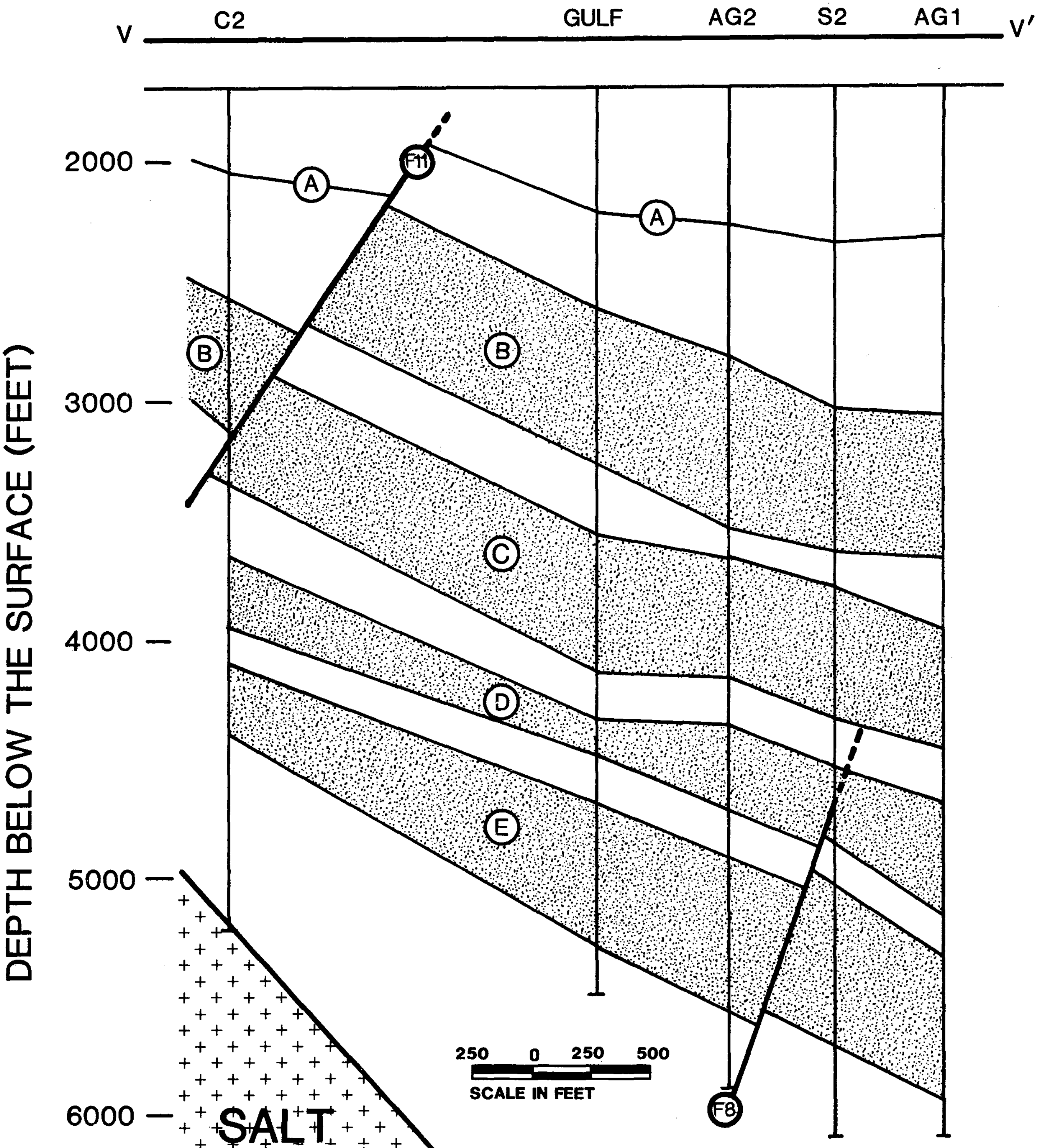

BIG HILL SALT DOME
SECTION V-V′

Sandia National Laboratories

T. R. MAGORIAN

SEP 1981 FIG. 5-26

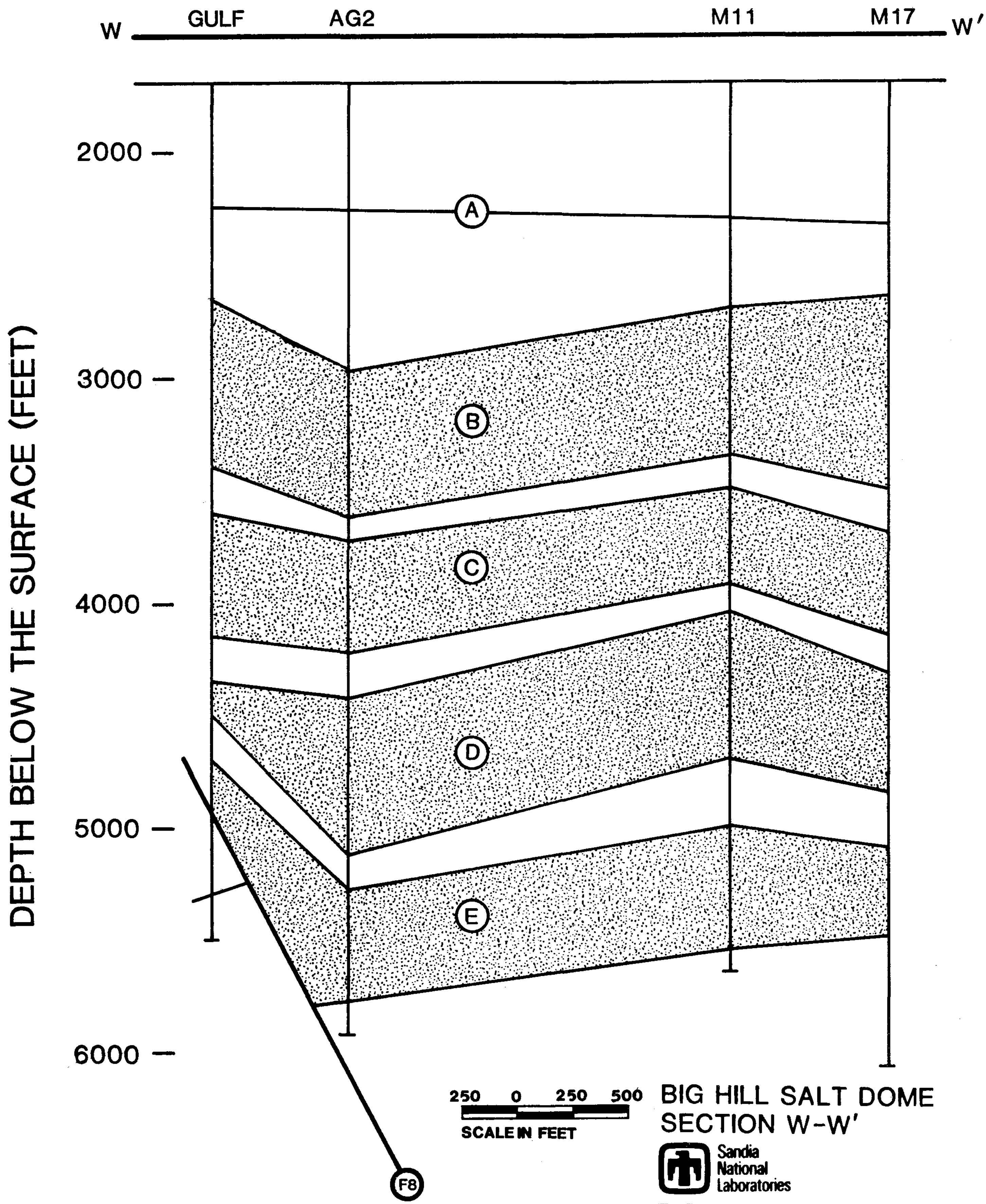

BIG HILL SALT DOME
SECTION W-W′

Sandia National Laboratories

T. R. MAGORIAN
SEP. 1981 FIG. 5-27

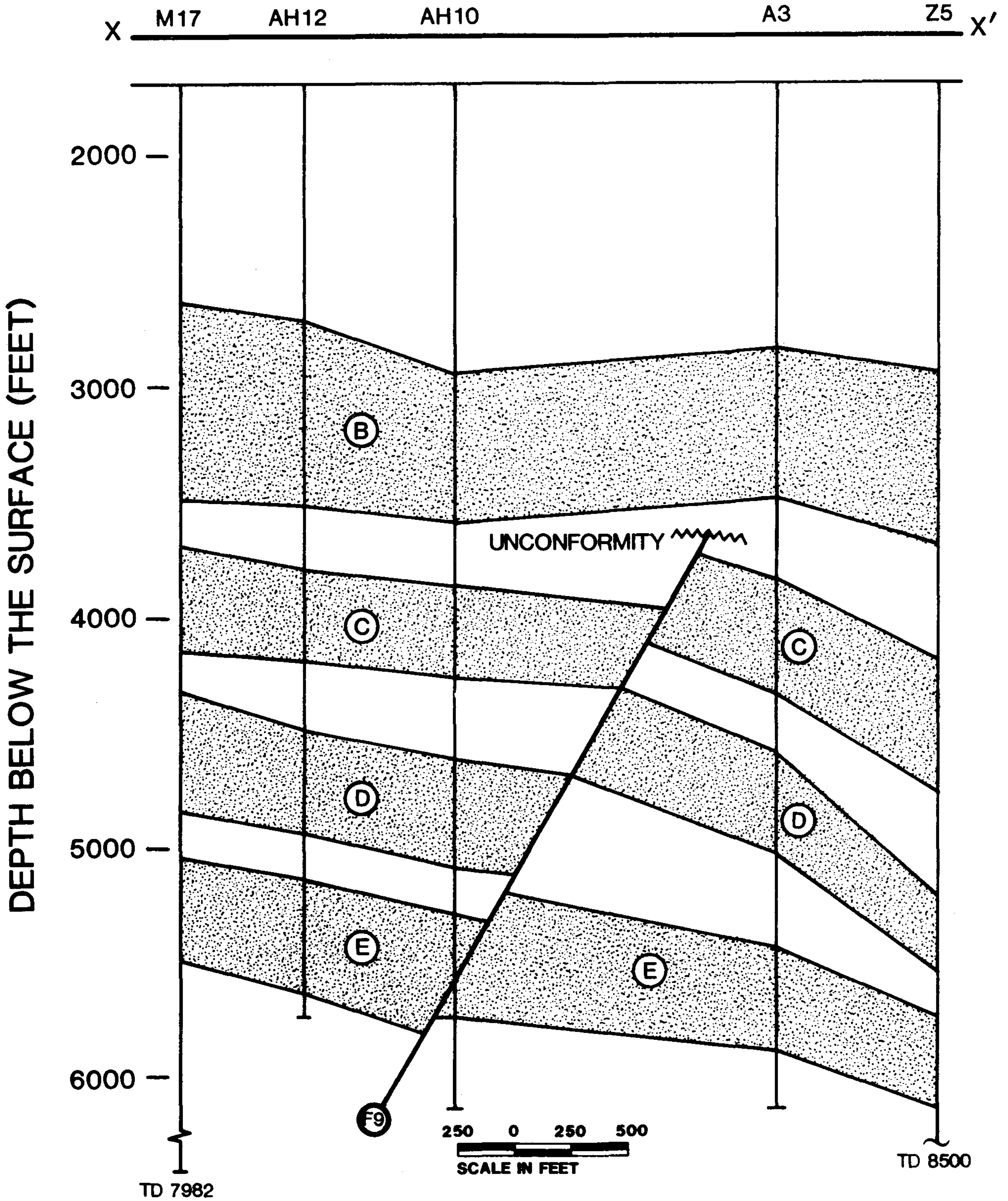

BIG HILL SALT DOME
SECTION X-X′

Sandia National Laboratories

T. R. MAGORIAN

SEP 1981 FIG. 5-28

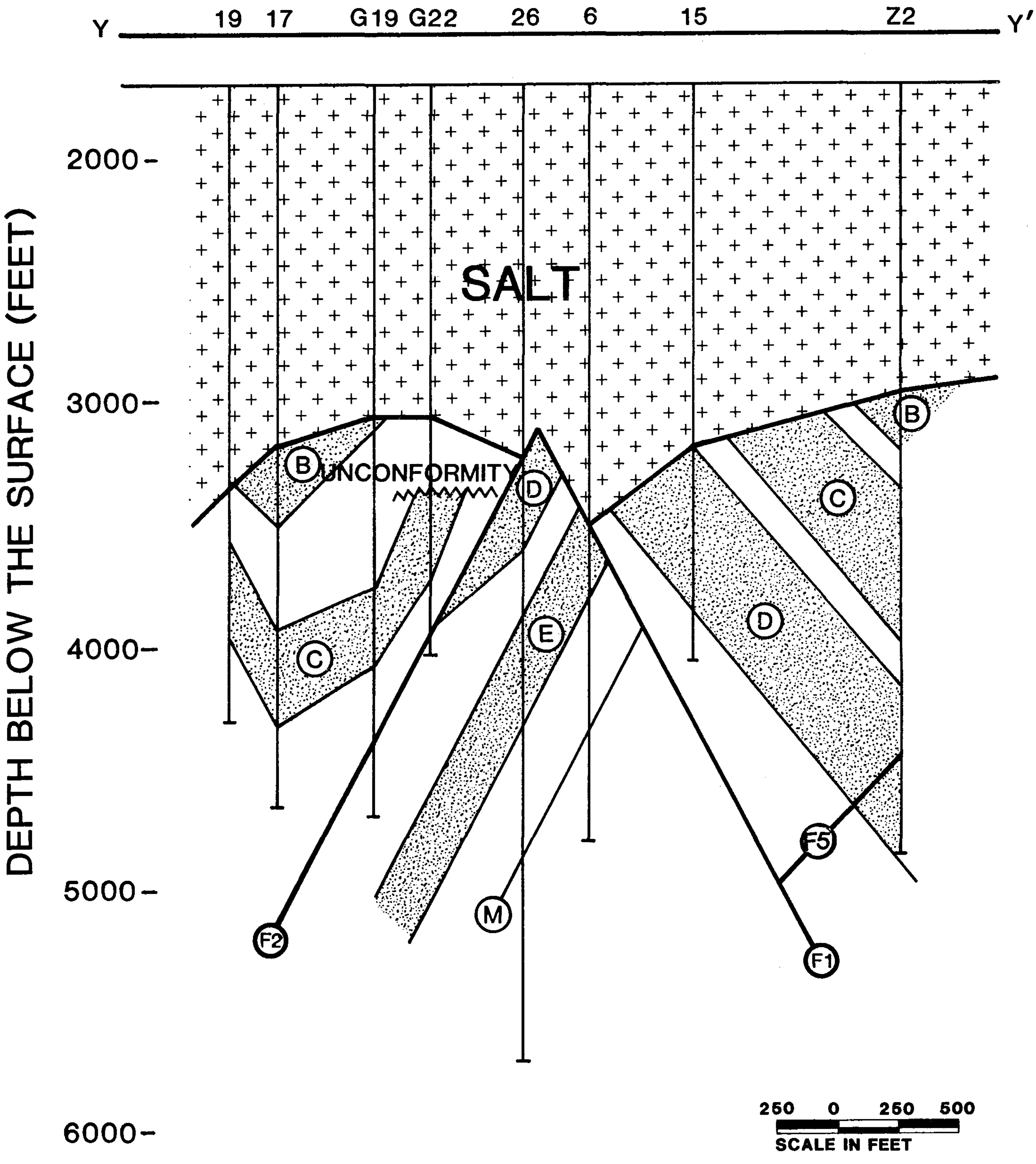

BIG HILL SALT DOME
SECTION Y-Y'

Sandia National Laboratories

T. R. MAGORIAN

SEP 1981 FIG. 5-29

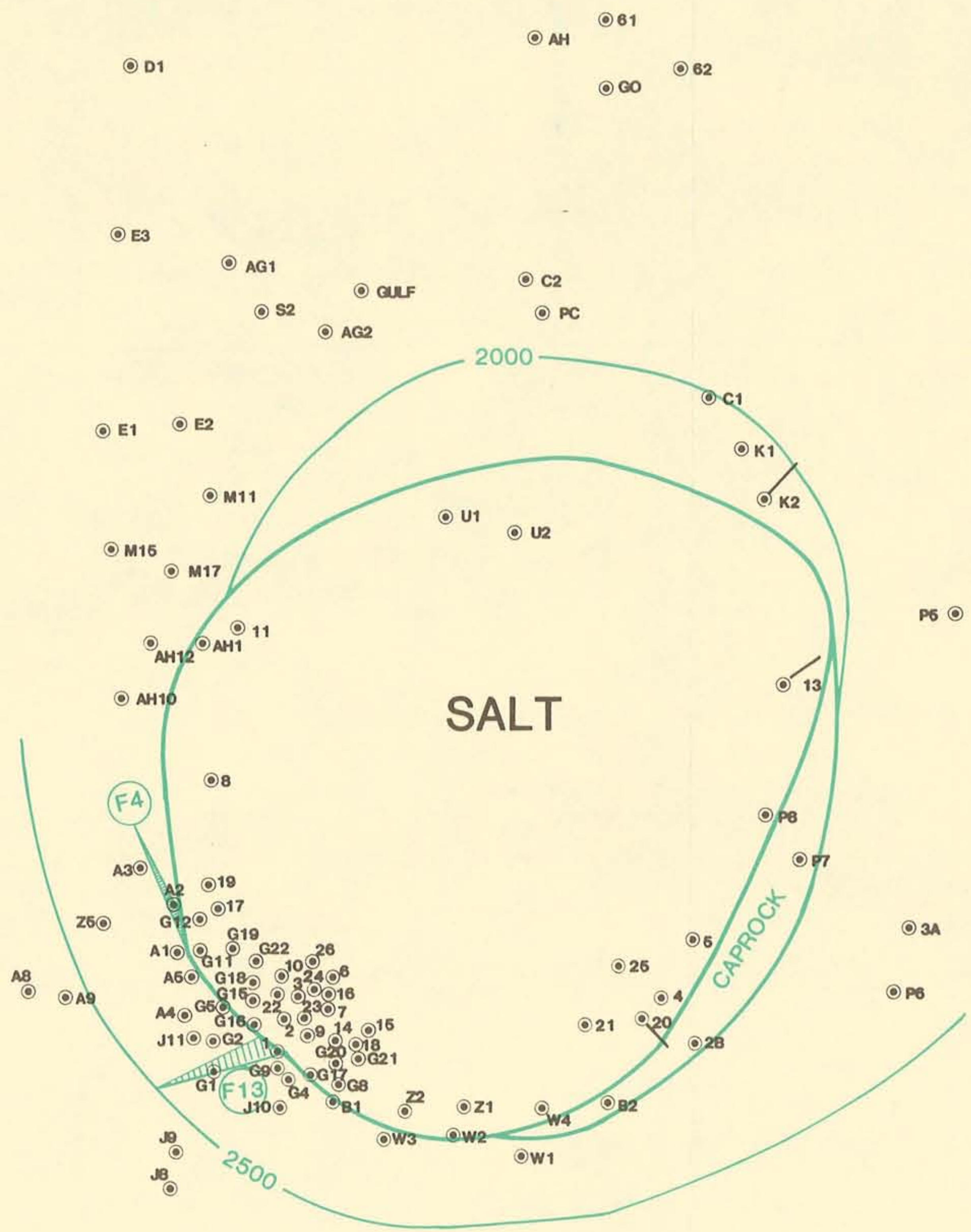

NOTES

1. SEE APPENDIX B FOR EXPLANATION OF WELL NUMBERS
2. CONTOURED DEPTHS MEASURED IN FEET BELOW DRILLING FLOOR

LEGEND

FAULT , EXTENDED HATCHURES ON DOWN SIDE

DEPTH CONTOURS IN FEET

CONTACT WITH SALT

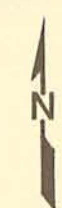

BIG HILL SALT DOME
STRUCTURE MAP
A SAND

Sandia National Laboratories

T. R. MAGORIAN

SEP 1981 FIG. 5-30

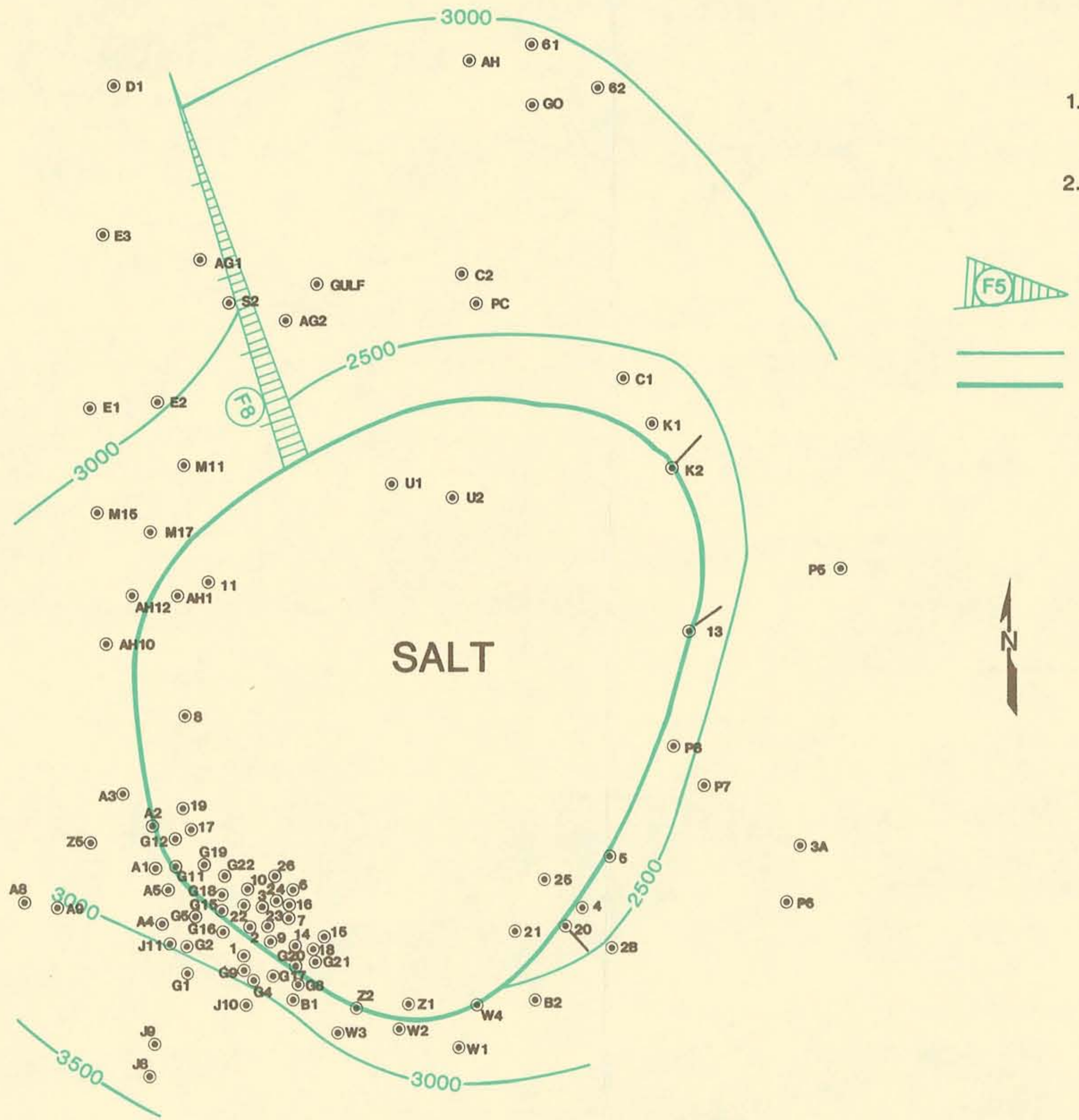

NOTES

1. SEE APPENDIX B FOR EXPLANATION OF WELL NUMBERS
2. CONTOURED DEPTHS MEASURED IN FEET BELOW DRILLING FLOOR

LEGEND

F5 FAULT, EXTENDED HATCHURES ON DOWN SIDE

DEPTH CONTOURS IN FEET

CONTACT WITH SALT

600 300 0 600 1200

DISTANCE IN FEET

BIG HILL SALT DOME
STRUCTURE MAP
B SAND

Sandia National Laboratories

T. R. MAGORIAN

SEP 1981 FIG. 5-31

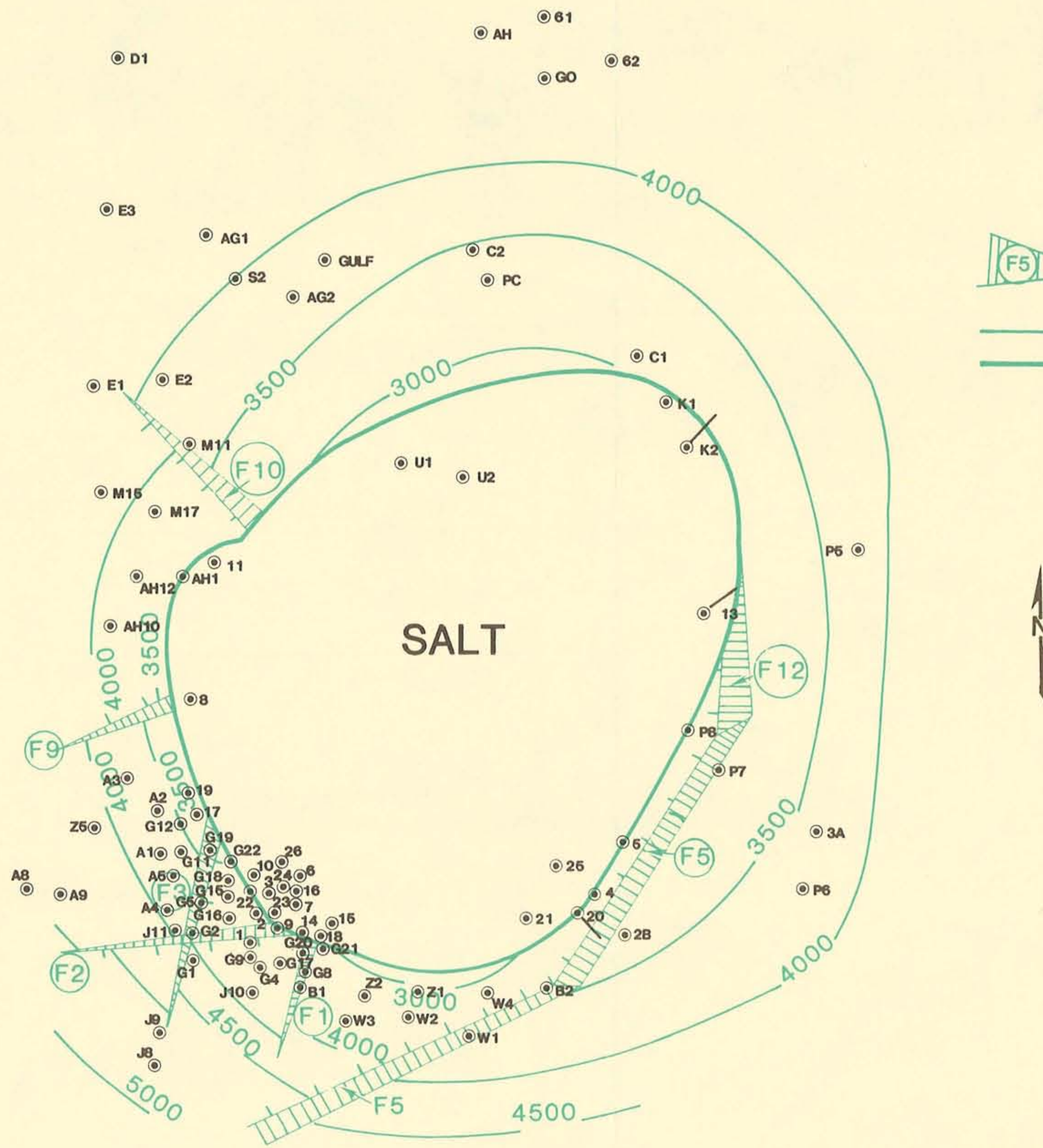

NOTES

1. SEE APPENDIX B FOR EXPLANATION OF WELL NUMBERS
2. CONTOURED DEPTHS MEASURED IN FEET BELOW DRILLING FLOOR

LEGEND

F5 FAULT, EXTENDED HATCHURES ON DOWN SIDE

DEPTH CONTOURS IN FEET

CONTACT WITH SALT

600 300 0 600 1200

DISTANCE IN FEET

BIG HILL SALT DOME
STRUCTURE MAP
C SAND

Sandia National Laboratories

T. R. MAGORIAN

SEP 1981 FIG. 5-32

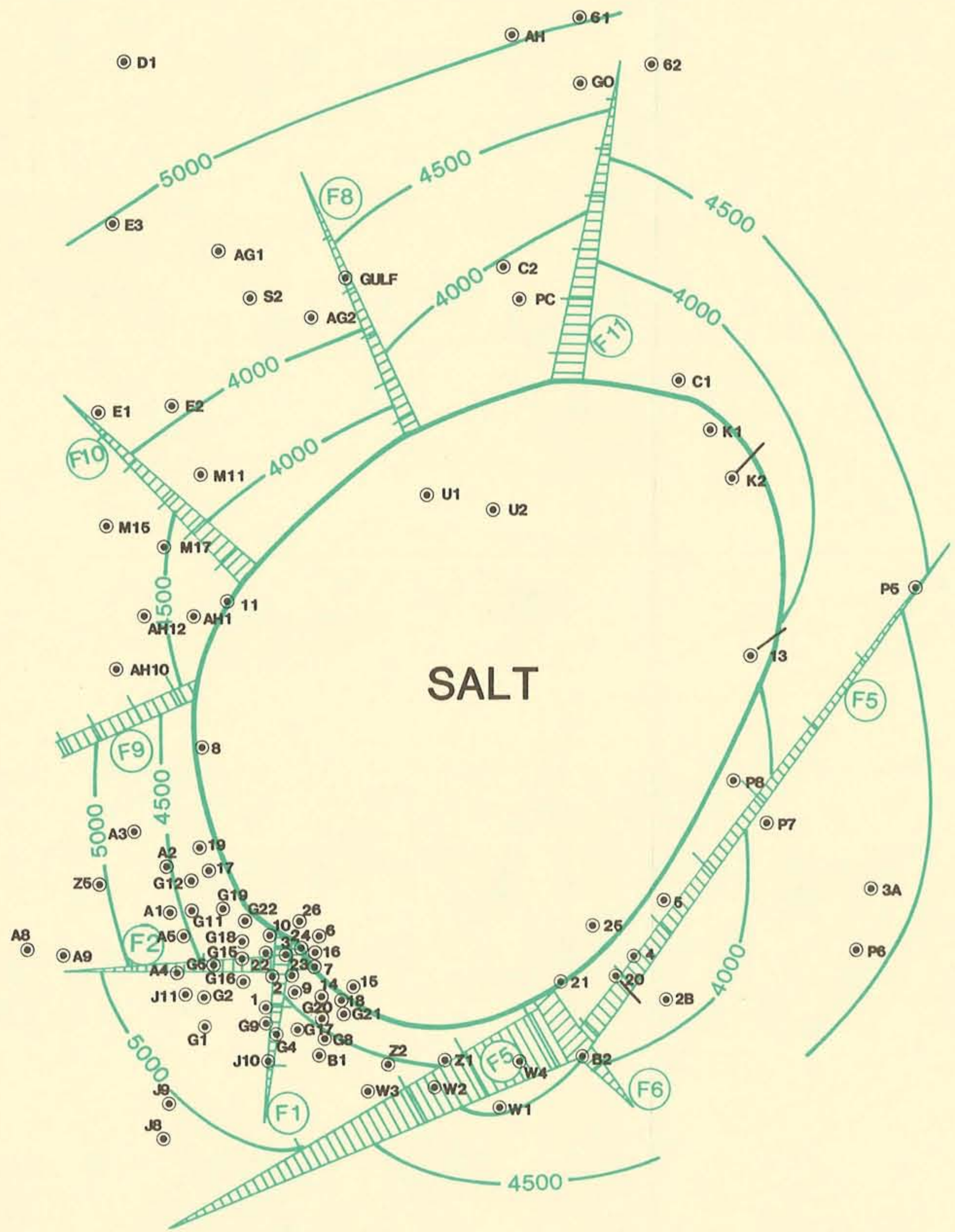

NOTES

1. SEE APPENDIX B FOR EXPLANATION OF WELL NUMBERS
2. CONTOURED DEPTHS MEASURED IN FEET BELOW DRILLING FLOOR

LEGEND

FAULT , EXTENDED HATCHURES ON DOWN SIDE

DEPTH CONTOURS IN FEET

CONTACT WITH SALT

BIG HILL SALT DOME
STRUCTURE MAP
D SAND

Sandia National Laboratories

T. R. MAGORIAN

SEP 1981 FIG. 5-33

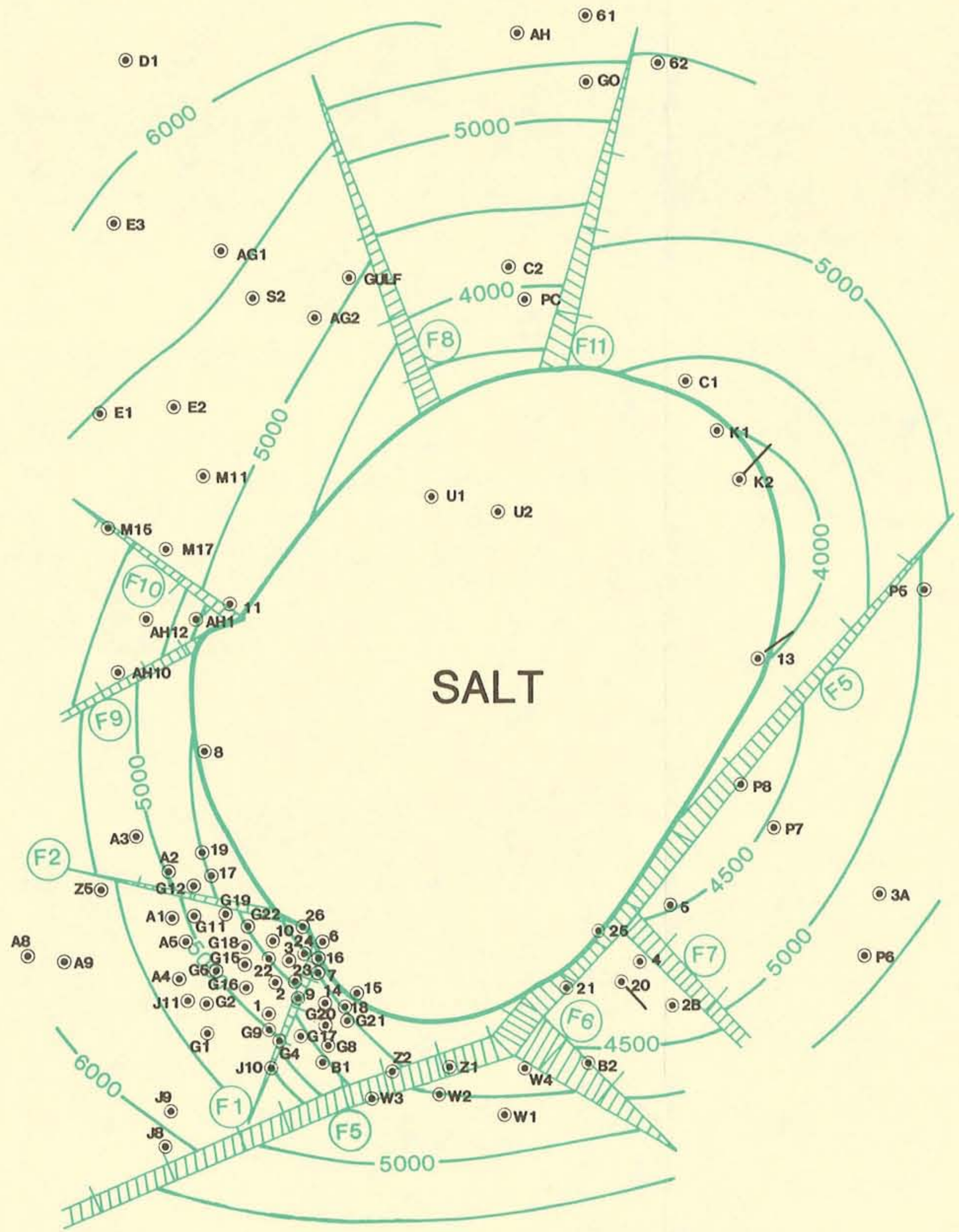

NOTES

1. SEE APPENDIX B FOR EXPLANATION OF WELL NUMBERS
2. CONTOURED DEPTHS MEASURED IN FEET BELOW DRILLING FLOOR

LEGEND

F5 FAULT, EXTENDED HATCHURES ON DOWN SIDE

DEPTH CONTOURS IN FEET

CONTACT WITH SALT

600 300 0 600 1200

DISTANCE IN FEET

N

BIG HILL SALT DOME
STRUCTURE MAP
E SAND

Sandia National Laboratories

T. R. MAGORIAN

SEP 1981 FIG. 5-34

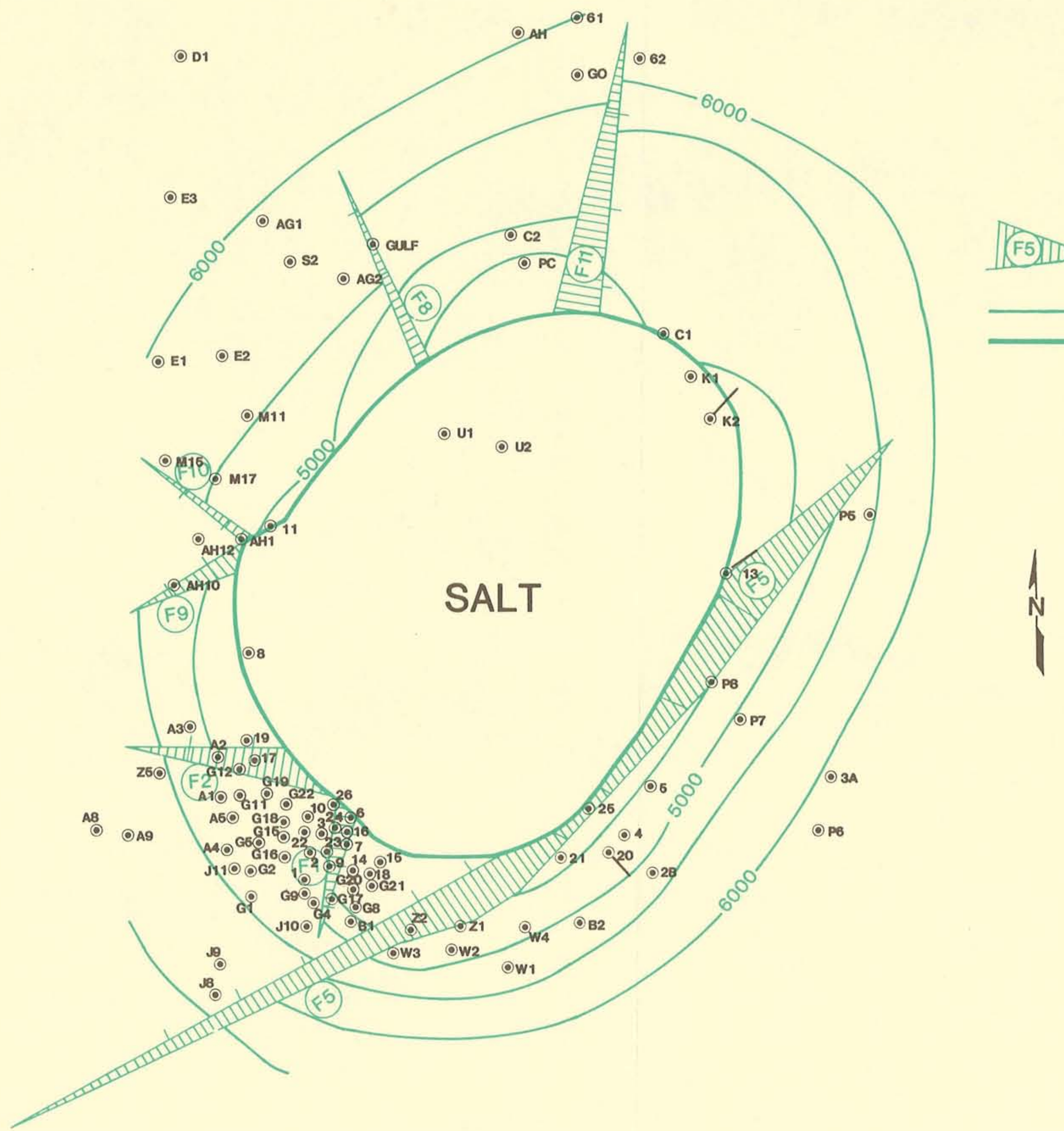

NOTES

1. SEE APPENDIX B FOR EXPLANATION OF WELL NUMBERS
2. CONTOURED DEPTHS MEASURED IN FEET BELOW DRILLING FLOOR

LEGEND

F5 FAULT, EXTENDED HATCHURES ON DOWN SIDE

DEPTH CONTOURS IN FEET

CONTACT WITH SALT

600 300 0 600 1200

DISTANCE IN FEET

BIG HILL SALT DOME
STRUCTURE MAP
ANAHUAC SHALE

Sandia National Laboratories

T. R. MAGORIAN

SEP 1981 FIG. 5-35

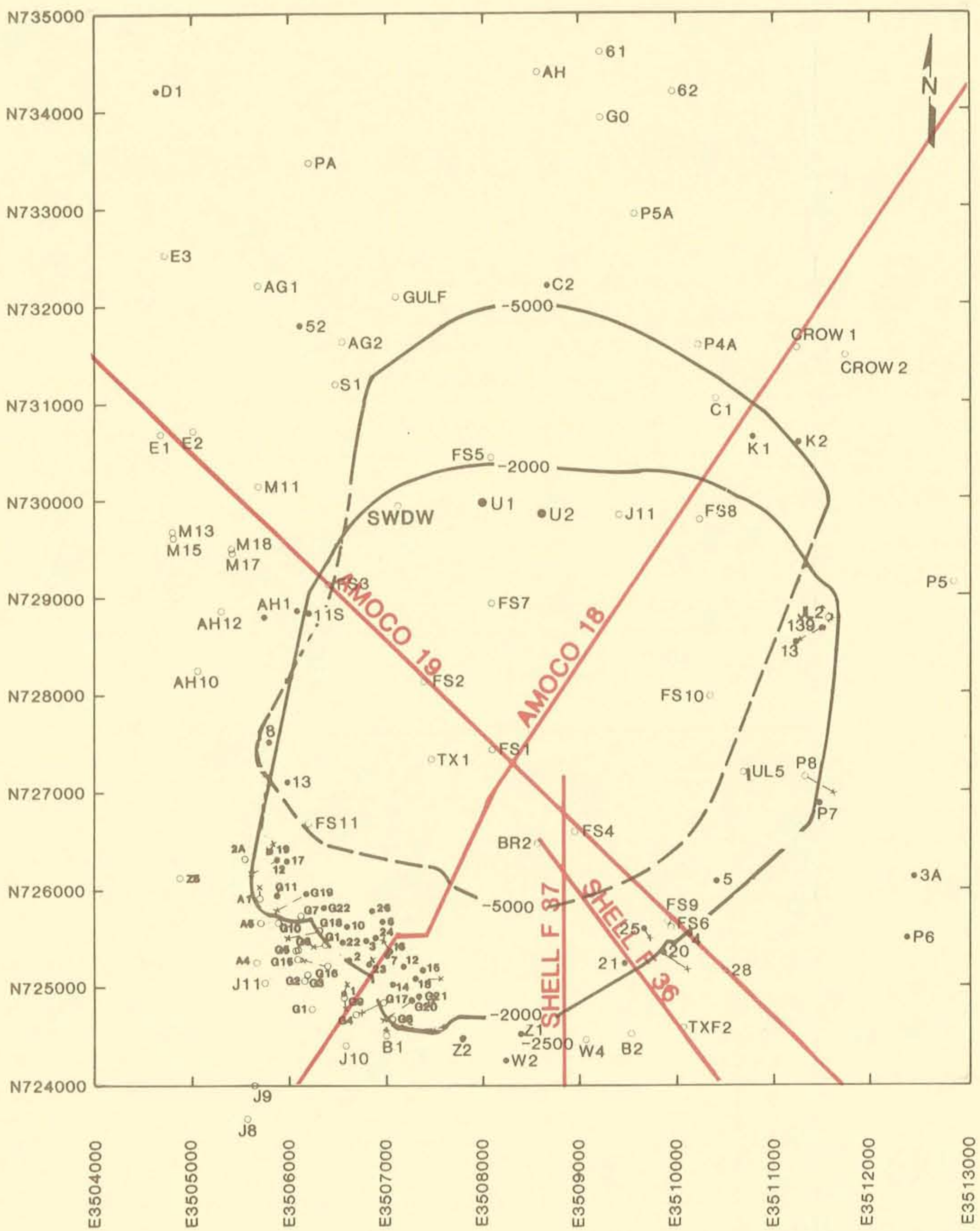

NOTES

1. SEE APPENDIX B FOR EXPLANATION OF WELL NUMBERS AND WELL LOCATIONS

LEGEND

- U1 — UNION OIL LPG CAVERN.
- SURFACE LOCATION OF WELL.
- G2 — BOTTOM HOLE LOCATION OF WELL.
- G2 — BOTTOM HOLE LOCATION OF SIDETRACK HOLE.
- G2 — DRILLED AS VERTICAL HOLE. NO BOTTOM HOLE LOCATION AVAILABLE.
- G2 — LOCATION OF WELL PENETRATING SALT.

1000 500 0 1000 2000

BIG HILL SALT DOME SEISMIC PROFILE REFERENCE MAP

Sandia National Laboratories

T. R. MAGORIAN

SEP 1981 FIG. 5-36

CHAPTER 6 - CAVERN LOCATIONS AND GEOTECHNICAL CONSIDERATIONS

The SPR Phase III expansion program calls for the construction of 140 MMB of storage capacity at Big Hill. The baseline plan developed by DOE-SPR calls for this storage capacity to be achieved by the construction of 14 10-MMB caverns through solution mining. The objective of the cavern location study was to determine the feasibility of constructing 14 10-MMB caverns on the south part of the dome through the use of (1) the dome definition developed in this site-characterization study, (2) DOE-specified guidelines, and (3) geotechnical criteria necessary to assure cavern structural integrity and stability.

Cavern Layout and Design Criteria

Some of the cavern layout and design criteria and guidelines for this study have been established by the DOE based on system requirements, SPR design consistency, and other studies. These guidelines and criteria include

1. Fourteen 10-MMB caverns, located preferably on the Amoco Production Company property on the south portion of the dome (Figure 2-1)

2. Five oil-withdrawal cycles

3. Initial maximum cavern diameter of ~230 ft

4. Cavern height of 2000 ft

5. Bottom of caverns not to exceed 6000 ft in depth

The remaining cavern design and spacing criteria are determined by geotechnical considerations of cavern structural adequacy and stability. These criteria are:

1. Pillar-to-diameter (P/D) ratio

2. Salt roof thickness-to-diameter (S/D) ratio

3. Distance from edge of cavern to edge of dome (E)

The following values of these criteria were used in the cavern location study:

1. $P/D \geq 1.78$

2. $S/D \geq 1$

3. $E \geq 300$ ft

These criteria are considered conservative based on our current knowledge, and some discussion of their basis will help put in perspective the following discussions on cavern size, spacing, and location.

Pillar-to-Diameter (P/D) Ratio

P/D ratio is the ratio of the thickness of the pillar (or web) between two caverns to the average diameter of the two caverns. It is inversely related to the stress in the web between two caverns for given pressures in the caverns. In determining P/ D for two or more adjacent caverns, we assume the operating conditions that produce the greatest pressure differential between the two caverns. Also, because caverns are rarely symmetrical or straight-walled, right-circular cylinders, a safety factor is included in the calculated P/D to account for such effects. Another consideration in determining P/D, especially for a large array of caverns in a dome, such as that planned for SPR, is the effect of salt creep and possible associated surface subsidence.

A P/D ratio of 1.78 was used in the design layout of SPR Phase II (Bryan Mound and West Hackberry) expansion caverns. It was a safe and conservative value at the time, although it was selected on the basis of a limited analysis, limited salt-properties data, and no long-term salt creep data.

More comprehensive analyses based on recently acquired salt properties from other SPR sites and the Waste Isolation Pilot Project (WIPP) site have been carried out since the SPR Phase II design (Hogan, 1980a; Whiting, 1980; Wawersik, et al, 1980a; Hilton, et al, 1980; Munson and Dawson, 1979; Benzley, 1980; and Wawersik, et al 1980b). Some additional data and experience have also been acquired from analyses and observations of SPR West Hackberry Cavern 6 (Benzley, 1980 and Wawersik, 1980b), and of Bayou Choctaw Caverns 15 and 17 (Hogan, 1980; Hilton, et al, 1980). Analyses of the elastic stress created by pressure differences in two relatively isolated adjacent caverns (zero brine-wellhead pressure in one and zero oil-wellhead pressure in the other), indicates that a P/D of much less than 1.78 is adequate to assure structural stability. However, calculations of secondary (long-term) creep for a large number of caverns in a dome with a P/D of 1.78 or less indicate a significant reduction of cavern volume and a potential for significant surface subsidence over 20- to 30-yr period. Therefore, until enough field data can be acquired to verify or disprove projected creep behavior, the continued use of a P/D of 1.78 is recommended and was used in the Big Hill cavern layout study.

Salt Roof Thickness-to-Diameter (S/D) Ratio

The ratio of the thickness of the salt roof over the cavern to the diameter of the cavern (S/D) is an expression of the structural adequacy of the salt roof. S/D must be great enough so that the salt roof is self-supporting; i.e., no tensile stresses are developed in the salt roof for worst-case pressures. For salt properties typical of nearly pure halite in the Gulf Coast salt domes, analyses indicate that an S/D ≥ 1 is adequate (Ney, 1981). For a cavern diameter of 270 ft (the diameter of the SPR caverns at the end of five withdrawal cycles), the minimum roof thickness is then 270 ft. This thickness of salt roof also provides adequate salt above the cavern for good cementation of the production casing in the salt. However, in practice the SPR Phase II caverns have been designed with a salt roof thickness of 450 ft. That value will therefore be used in the baseline cavern layout for Big Hill. In the case of Big Hill, little data are available to accurately define the elevation contour of the top of the salt over the south half of the dome. The lowest elevation of the top of the salt at the planned SPR cavern locations on the south half of the dome is estimated as 1800 ft below the surface. For the baseline cavern layout, the top of the caverns is 2250 ft below msl, which should provide at least 450 ft of salt roof. This results in an S/D of 1.7. If salt is encountered at a higher elevation during drilling of the first few cavern wells, the tops of the caverns should be set correspondingly higher to provide a larger edge-of-dome margin as discussed below.

There are several reasons it is desirable to construct the caverns as near the top of the salt as feasible, particularly at Big Hill. For a given cavern height, frictional losses and required pumping pressures are minimum for a minimum cavern depth both during leaching and oil fill and withdrawal. So there is a savings of power costs for a shallower cavern. Perhaps a more serious consideration is the increase in the rate of secondary salt creep with depth. Analyses based on data derived from laboratory tests of salt from the Bryan Mound and West Hackberry domes (Wawersik, et al, 1980a and 1980b) indicate an exponential relationship between secondary creep rate and stress (depth) as shown in Figure 6-1. Creep rate increases exponentially with depth because it is an exponential function of both stress and temperature, both of which increase with depth. Although Figure 6-1 is an approximation intended only to illustrate the general relationship between depth and creep rate, the difference in secondary creep rate between depths of 4500 ft and 5000 ft may be significant. Creep reduces cavern volume, which increases wellhead pressures and requires continuing bleedoff of brine or stored oil. Further, at the cavern depths being considered, long-term creep may result in significant surface subsidence. It is thus desirable to construct the caverns at the shallowest feasible depth to minimize creep rate.

It is also necessary to construct the caverns at the shallowest feasible depth because of the steep slope of the salt overhang on the south side of the Big Hill dome. As Figure 6-2 shows, for a given cavern diameter and height, cavern depth must be minimized to maintain the desired distance from the edge of the cavern to the edge of the dome for caverns on the southern periphery of the dome.

Edge of Cavern to Edge of Dome (E)

Our analyses (Ney, 1981) indicate that 50 ft of good quality (structurally competent) salt between the edge of cavern and the edge of the dome would be structurally adequate for zero surface-oil pressure (worst-case operating or accident conditions). However, the actual quality of salt near the dome edge at Big Hill is unknown. For Big Hill, where relatively little data are available to define the edge of the dome, a tolerance ±100 ft is associated with the geological interpretation of the dome edge at a depth of 5000 ft (maximum depth of sump). To account for these and other tolerances and uncertainties, a minimum edge distance of E = 300 ft is used in the cavern location layout, as shown in Figure 6-2.

Edge of Cavern to Property Line

According to the Texas Railroad Commission, no regulations specify or control the proximity of a storage cavern to the owner's property line in Texas. The Commission has informed us that the Texas state legislature is assigning authority to regulate storage cavern construction and operations to the Railroad Commission. Although no regulations in Texas control the spacing of storage caverns from property lines, in practice the cavern operators at Barber's Hill dome in Texas, for example, have constructed their caverns ~150 ft from their property lines.

Since P/D is the stability parameter controlling the distance between two adjacent caverns, it should be applied in determining distance from the caverns to the property line where there is enough salt for a cavern on adjacent property. For adjacent caverns 270 ft in diameter (the diameter of SPR caverns after five withdrawal cycles) and P/D = 1.78, the pillar width is 480 ft.

A cavern spacing of 190 ft from the north property line was chosen for the baseline cavern layout. As shown in Figure 6-3, if a cavern-to-property line distance of 190 ft is maintained by each property owner, the required pillar width of 480 ft will be achieved for caverns 270 ft in diameter. Even if Texas adopts a 100-ft spacing (as Louisiana has) and the adjoining property owner chooses to use this minimum spacing, he could still construct a cavern 190 ft in diameter without violating the P/D criterion of 1.78. (The diameter used in calculating P/D when the caverns are of different diameters is the average diameter of the two.) Larger cavern-to-property line spacings for the SPR caverns that would assure maintenance of required pillar width under all possible conditions were considered. But increasing the spacing of the caverns from the north property line shifts the whole cavern complex to the south and decreases the distance from the edge of the salt dome to the caverns on the bottom row. Because of the limited data upon which the salt contours are based, the distance from cavern to edge of dome is of much greater concern than increased spacing from the property line beyond the 190 ft.

Baseline Cavern Layout

Using the guidelines and geotechnical criteria outlined in this chapter, we have determined that it is feasible to construct 14 10-MMB storage caverns on the south portion of the Big Hill dome as shown in Figures 6-2 and 6-4. Figure 6-2 is not an accurate cross section of the dome but simply a schematic showing the required relationship of the planned SPR caverns to the top of the salt and the edge of the dome. The coordinates given in Figure 6-4 are for the center of the caverns. Figures 5-5, 5-6, and 5-7 are west-east cross sections through the three rows of the planned SPR caverns showing the relationship of the caverns to the salt-dome boundaries. Note that in all three of these cross sections (cavern rows) there appears to be space for an additional cavern on the west (left) side. The caverns were located nearer the east side of the dome because the risk of an unexpectedly deep overhang reentrant on the west flank of the dome is higher than on the east side, as indicated by the deeper D and E sands on the west flank.

No separate exploratory well program or geophysical exploration program is required to proceed with the design of the site and construction of the caverns according to this baseline layout. However, because the Big Hill dome is relatively unexplored and the geological interpretation of the salt contours is based on sparse data, exploratory extension of some cavern wells is recommended to verify the geological interpretations. Also, a comprehensive geophysical cavern well-logging and coring program is required to obtain salt and cap rock material properties and to complete characterization of the dome. The drilling extension and logging and coring programs are presented in detail later in this chapter.

Potential Expansion Cavern Layout

The feasibility of constructing additional caverns on the south portion of the dome was investigated. To provide the option of adding Phase IV expansion caverns after the construction of the Phase III caverns, the baseline cavern layout was maintained and the feasibility of adding caverns to the baseline was addressed. The same geotechnical criteria used in the baseline layout were used in the feasibility study of additional caverns for possible Phase IV expansion.

Figures 6-5 through 6-8 show the results of the feasibility study and the potential for expansion of the SPR site at Big Hill to a total of 19 caverns. Note that Figures 6-6, 6-7, and 6-8 are repeats of the sections shown in Figures 5-5, 5-6, and 5-7 with an additional cavern added to the west end of each row of caverns. The five additional caverns are numbered in order of geotechnically preferred cavern location. Cavern Location X3 would require the purchase of the 6-acre rectangular tract of land on the south side and west end of the Sabine Pass Terminal property (Figure 6-5). Amoco Well 8, west of Cavern X1, bottomed out in salt at a depth of 5200 ft, thus providing good well control for the location of this expansion cavern on the west end of the middle row of caverns (Figure 6-7). There appears to be about 400 ft of salt between Caverns X2 and X3 and the edge of the dome at a depth of 5000 ft. Amoco Wells 8 and 11 provide control for X2 in the top row of caverns (Figure 6-6). Caverns could be constructed at Locations X1, X2, and X3 without further geological or geophysical exploration, assuming that the exploratory extension drilling program outlined in the next section is implemented during drilling. Additional data defining the edge of the dome would be required before the construction of caverns at Locations X4 and X5.

Exploratory Extension of Cavern Wells

The Big Hill dome is relatively unexplored. Few wells have been drilled on the southern periphery of the dome that penetrate and/or exit the salt at the critical elevations required to accurately define the salt contours at the elevations of concern for cavern layouts. Salt contours at -4000 to -5000-ft elevations in particular were derived from geological interpretations of limited data. One method of verifying these interpretations is to drill exploratory holes 5000 to 6000 ft deep around the south side of the dome in a few critical places. The cost of such an exploratory program would be ~$4 to $5 million. An alternative to drilling exploratory holes is to drill 300-ft-deep extensions of the cavern wells that are adjacent to the dome edge as shown in Figure 6-9. This drilling extension program will help assure that the desired distance from the cavern to the edge of the dome is achieved. The additional cost of drilling an extension 300 ft deep would not exceed a few thousand dollars per well. This program is recommended for one of the wells in Caverns 101, 111, and 114. To confirm that the planned cavern layout is feasible, the wells for these three caverns should be drilled first.

The extension should be drilled to a depth 300 ft below the bottom of the cavern sump to ensure adequate salt thickness. Thirty feet of additional core should be taken from these extensions of the holes for lithological and mineralogical analyses. A complete set of geophysical well logs should also be run and analyzed. Precautions should be taken in case the hole is drilled through the salt into the underlying sediments. Strata near the salt overhang may be overpressured, and heavy drilling fluid may be required. The exploratory extension of the holes should be completely plugged with cement after analysis of the logs and visual inspection of the core. If the extended hole breaks out of the salt, the well should be pressure-tested after plugging the extension to make certain that there is no leak from the sediments to the cavern or vice versa.

Well-Logging and Coring Program

A comprehensive well-logging and coring program for Big Hill is essential to acquire data for completing geological characterization of the dome, to provide supporting data for the cavern leaching program, and to support a materials test program. In addition, analysis of water samples from the cap rock is required to evaluate potential long-term corrosion of the casing.

The following logs should be run in each cavern well:

Type of Log	Determination	Depth
4-arm caliper	borehole geometry	before each casing is set and to total depth in final configuration
cement bond log	casing to formation bond	all casing*
gyroscopic survey	borehole deviation	0 to total depth
casing collar	depths of casing collars	0 to total depth
gamma ray	radioactivity associated with shale or potassium-bearing evaporites	all salt
neutron log	lithology porosity, clay (hydrogen content)	0 to total depth
density log	bulk log density lithology, porosity	0 to total depth
sonic log	lithology, porosity	0 to total depth
seismic velocity	seismic velocity of cap rock and salt	0 to total depth in at least 4 wells

Additional logs that should be run under special circumstances include resistivity, dipmeter, and temperature.

Data should be obtained in both analog and digital form. The analog data should be analyzed immediately by the onsite geologist to determine if additional logs are warranted. Anomalous zones should be reported and sidewall samples of those zones taken. At least 24 sidewall samples should be taken in each hole and analyzed immediately.

Digital log data are required to take advantage of specialized computer programs to determine material properties, to generate combined data plots, and to determine formation lithology. A combination of sonic and density logs allows determination of mechanical properties like shear modulus and bulk compressibility. A combination of gamma-ray, sonic, neutron, density, and caliper logs allows for interpretation of the percentage of halite, sylvite, and insolubles.

If it should become necessary at some future time to do geological/geophysical exploration at Big Hill in connection with SPR development, good records of the seismic velocity of the cap rock and salt would prove invaluable. Such data can only be acquired before casing is installed.

---

*The cement bond log is not definitive in large (diameter >14 in.) casing. Therefore it is essential that good drilling, casing, and cementing records be available.

A program to collect and analyze drill cuttings should be maintained, with cuttings labeled and preserved. Drilling fluid should also be monitored.

Ideally, core taken from each hole should include a 30-ft core from the cap-rock/salt interface, a 60-ft core from the roof of the cavern, a 60-ft core from the middle elevation of the cavern, and a 60-ft core from the bottom of the 300-ft extension of the drillholes. The minimum coring program should consist of a 30-ft core from the -2200-ft elevation, the -3200-ft elevation, and the bottom of the 300-ft extension of the drillholes in one well each from Caverns 101, 111, and 114. If the minimum coring program is implemented, it is imperative that side wall sampling be flexible. Both coring and drilling in salt should be done with salt-saturated drilling fluid. The onsite geologist should inspect the core immediately and record a core analysis. The core should then be properly packaged for shipment by sealing it in a waterproof material, careful assembly into an appropriate shock-absorbing material, and packaging into a rigid container before shipment to the testing laboratory for detailed analysis. Determination of mechanical, chemical, and mineralogical properties supports structural modeling of the caverns, as well as the leaching program. The next section outlines the proposed material testing program.

Finally, as the drilling program progresses and new cap rock and top-of-salt data are acquired, the site geologist should modify the working contour maps on a timely basis to better prepare for upcoming drilling. Sandia will continue to update contour maps as information is received.

From the experience of the Union Oil Company with their storage cavern, it is known that some of the Big Hill cap-rock water is corrosive. Water samples from the cap rock are required to evaluate the potential corrosion of SPR well casing. Water samples should be taken from the cap-rock interval, one per hole, from several holes. Water is present in the vugs of the cap rock, which are also likely to be zones of lost circulation. If lost circulation occurs, the hole should be bailed to allow flushing of drilling fluid; a water sample should then be taken by means of a drill stem test and sent immediately for analysis.

Material Properties Program

A comprehensive material properties program similar to those done by Sandia for Bryan Mound and West Hackberry (Whiting, 1980 and Hilton, et al, 1980) will be needed to support cavern leaching and the analytical program for evaluating both near- and long-term structural stability of the caverns. When available, results of the material properties program should be incorporated into this site-characterization report.

The material properties program will provide a complete definition of the salt in the SPR cavern wells at selected intervals. This program will use core, sidewall samples, and drill cuttings in lab tests along with well logs to obtain the following chemical and mineralogical properties of the salt and brine:

Chemical and Mineralogical Properties

Solubility of salt at 22°C and 60°C

Percent of original sample insoluble in water

Percent of weight loss at 60°C

Background radiation

Complete sample mineralogy (through X-ray diffraction)

Complete sample mineralogy of insolubles (through X-ray diffraction)

Corrosive nature of the brine, materials in the brine of primary interest to the Environmental Protection Agency (EPA), and mineralogy of the brine

Percentage of potassium, calcium, magnesium

Percentage of lead, zinc, calcium, mercury, borate, chromium, selenium

Percentage of strontium, lithium, barium, nitrate, iodine, bromide

The following physical and mechanical properties of the salt should be obtained over the range of variables listed below:

Physical and Mechancial Properties

Density

Megascopic physical descriptions

Stress-strain behavior, onset of nonelastic behavior, strain hardening, strength

Young's modulus

Poisson's ratio

Thermal expansion

Elongation

P and S wave velocities

Variables

Temperature (°C): 22 and 60

Confinement (psi): 0, 500, 3000, 5000 (as time permits)

Load rate = 0.5 psi/s, 15 psi/s, constant strain rate

Moisture content and accessory minerals

Load path: triaxial compression ($\sigma_2 = \sigma_3$)

triaxial extension ($\sigma_2 = \sigma_1$) tension

Cyclic loading

Primary, secondary (steady-state) and tertiary (accelerated) creep (strain vs time) should be obtained over the following range of variables:

Temperature (°C): 22 and 60

Confinement (psi): 500, 3000, 5000 (as time permits)

Moisture content

Stress difference (at three values between 1000 and 4500)

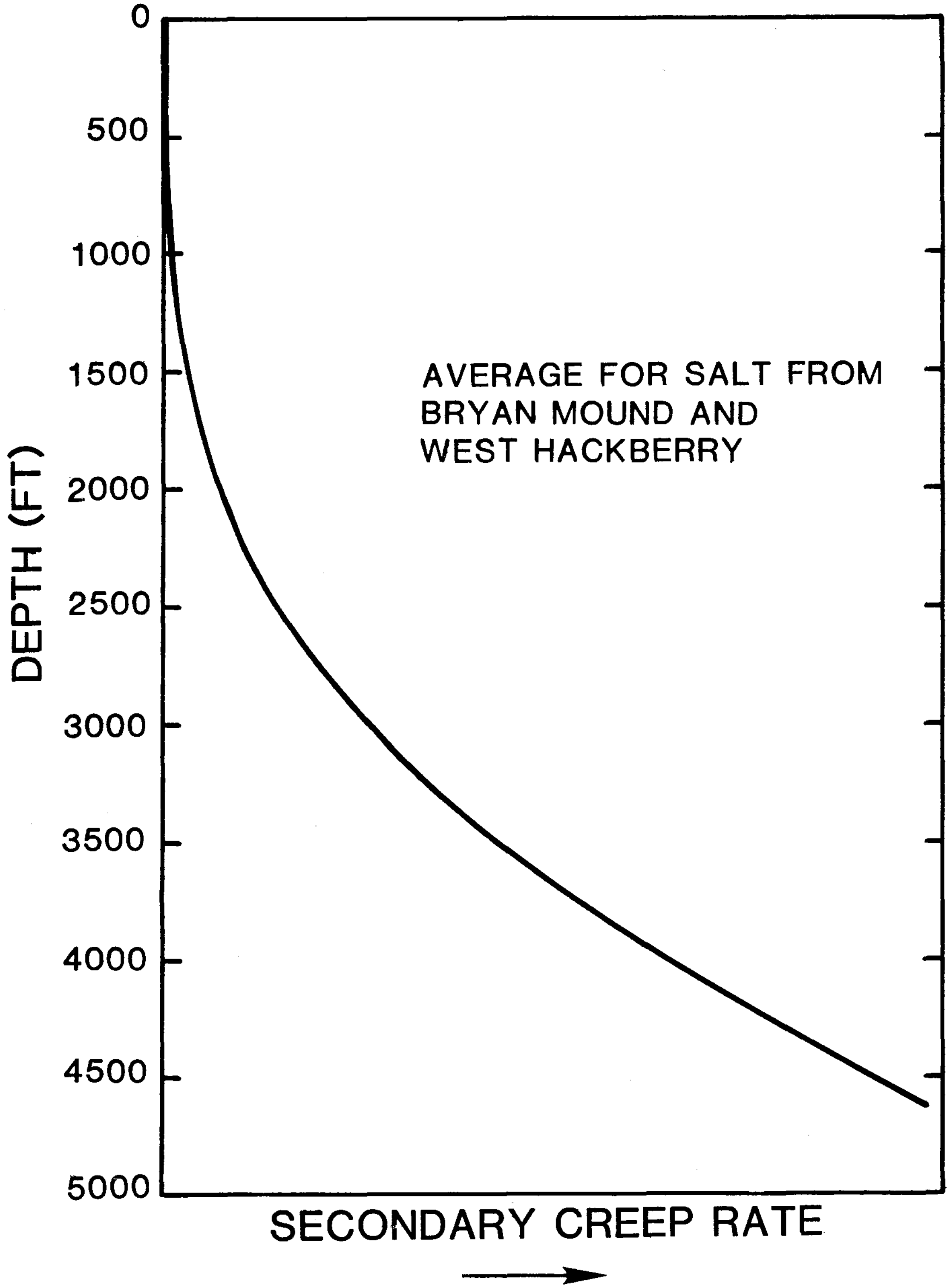

DEPTH VS SECONDARY CREEP RATE

Sandia National Laboratories

SEP 1981 FIG. 6-1

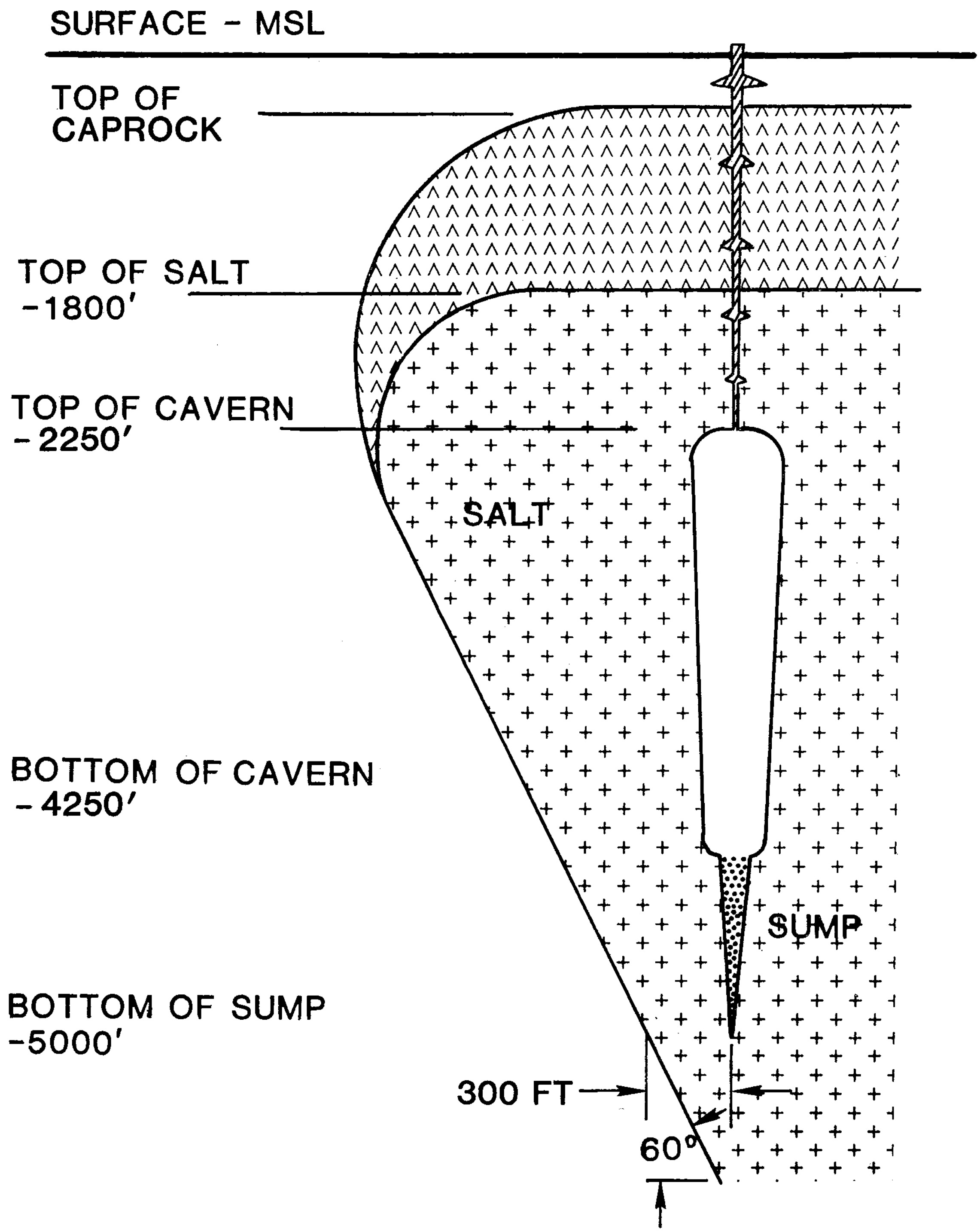

BIG HILL SALT DOME

CAVERN DESIGN AND LOCATION

Sandia National Laboratories

SEP 1981 FIG. 6-2

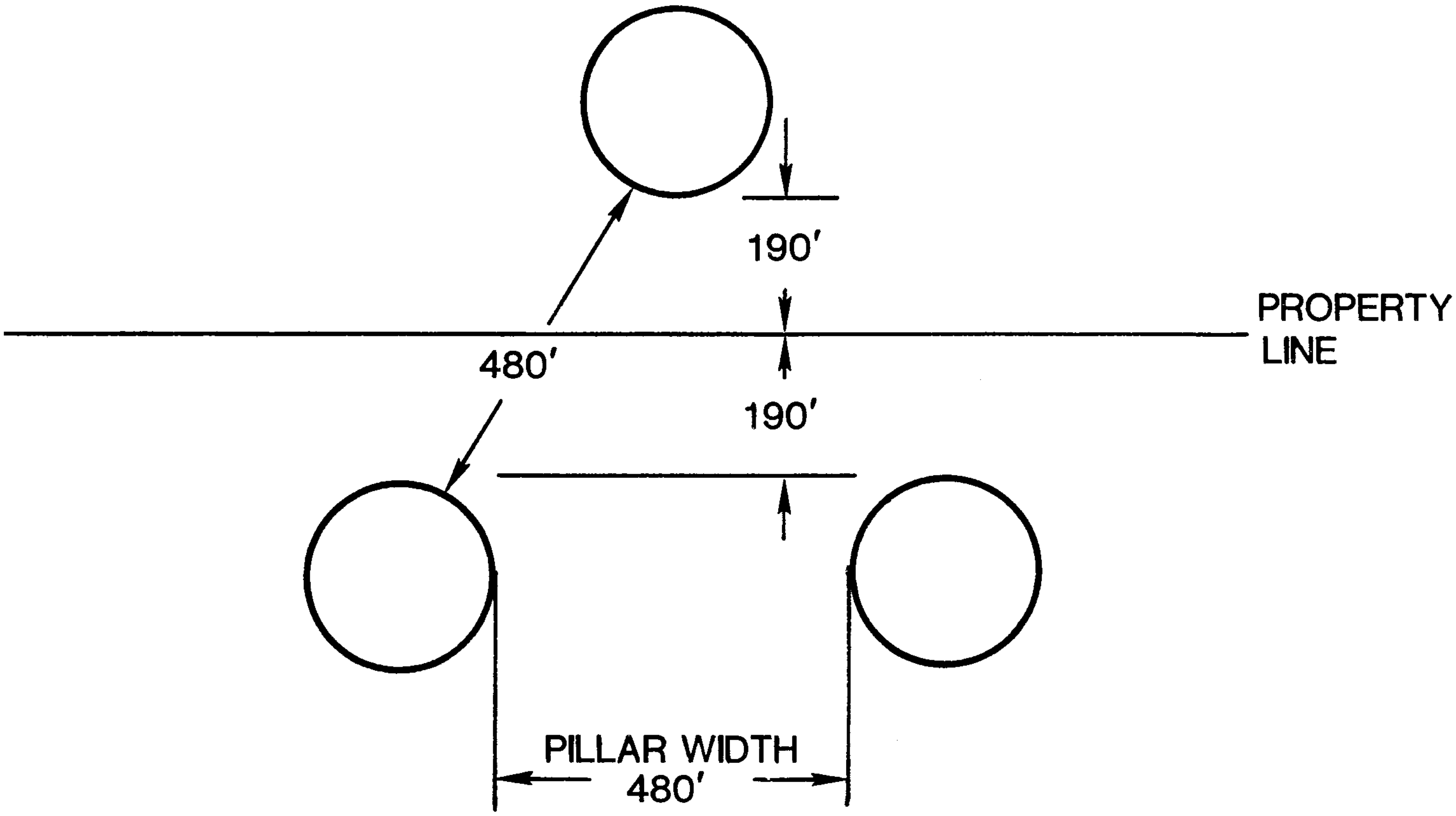

P/D = 1.78
CAVERN DIAMETERS = 270′

BIG HILL SALT DOME
CAVERN-TO-PROPERTY
LINE SPACING

Sandia
National
Laboratories

SEP 1981 FIG. 6-3

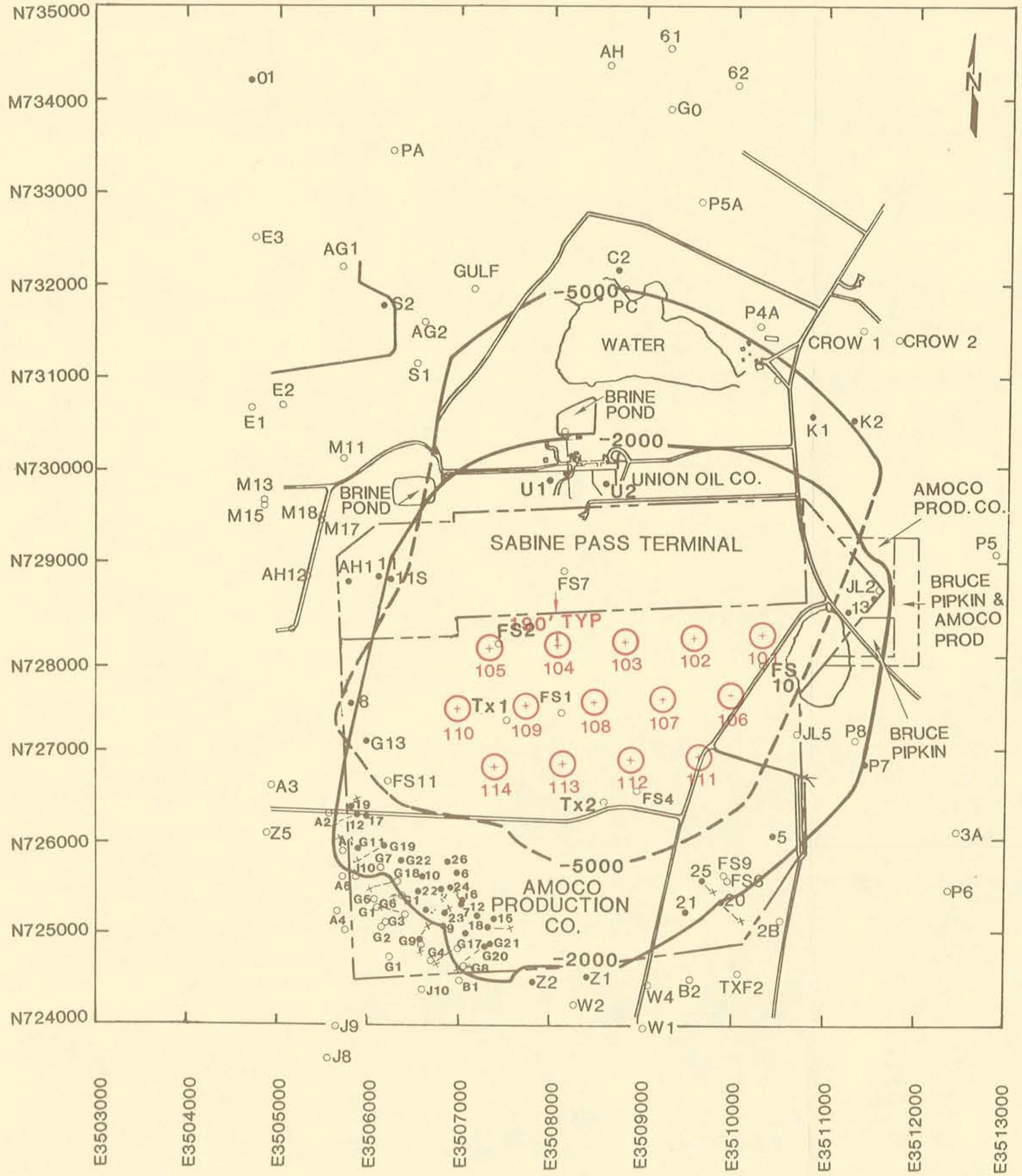

CAVERN LOCATION TABLE

CAV#	NORTH	EAST
101	728250.45	3510231.68
102	728214.66	3509482.52
103	728178.87	3508733.39
104	728143.09	3507984.23
105	728107.30	3507235.09
106	727583.79	3509888.10
107	727548.00	3509138.95
108	727512.21	3508389.79
109	727476.43	3507640.64
110	727440.65	3506891.51
111	726917.14	3509544.51
112	726881.34	3508795.35
113	726845.56	3508046.23
114	726809.77	3507297.08

1000 500 0 1000

DISTANCE IN FEET

BIG HILL SALT DOME
CAVERN LAYOUT
BASELINE

Sandia National Laboratories

SEP 1981 FIG. 6-4

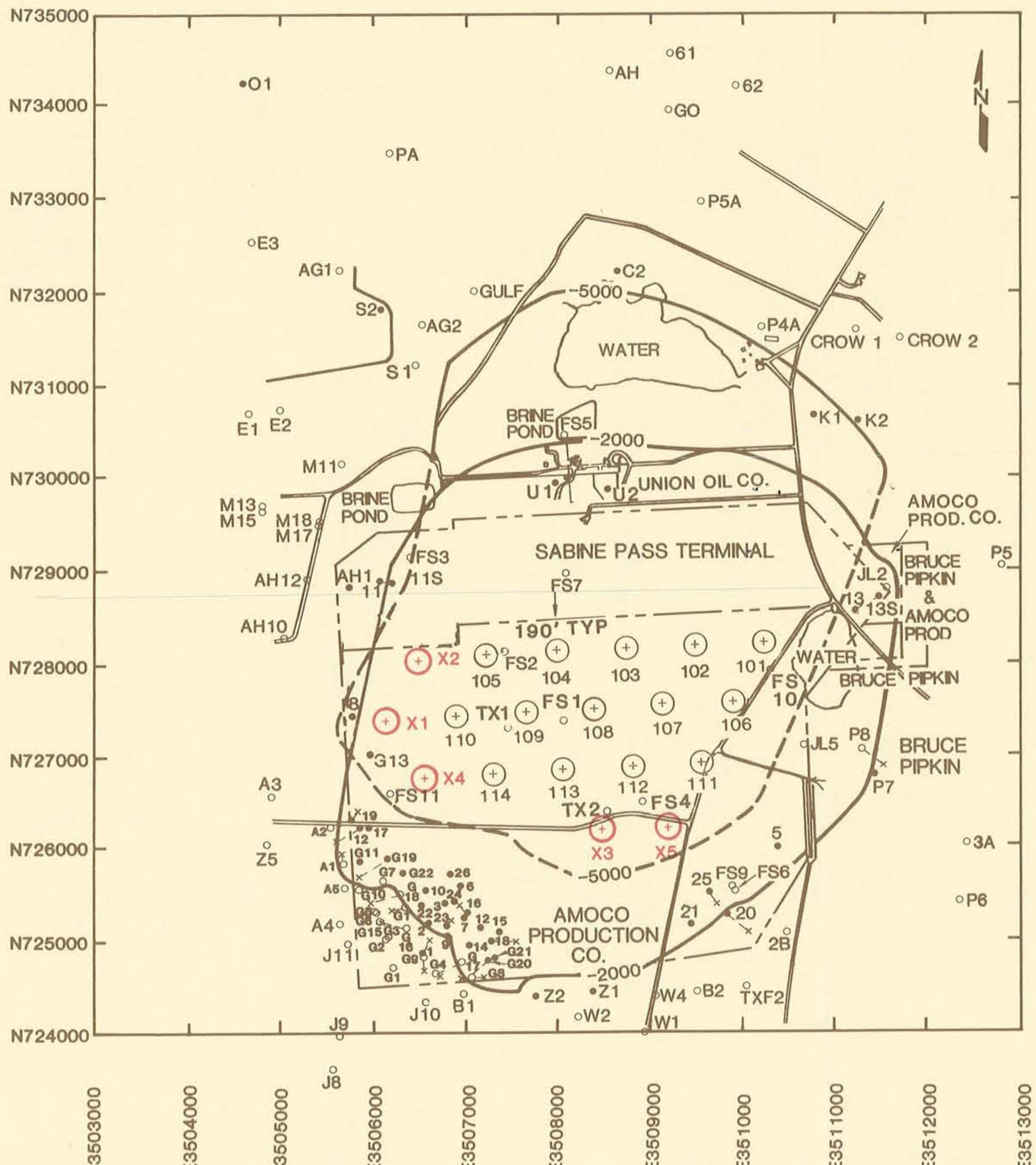

CAVERN LOCATION TABLE

CAV #	NORTH	EAST
101	728250.45	3510231.68
102	728214.66	3509482.52
103	728178.87	3508733.39
104	728143.09	3507984.23
105	728107.30	3507235.09
106	727583.79	3509888.10
107	727548.00	3509138.95
108	727512.21	3508389.79
109	727476.43	3507640.64
110	727440.65	3506891.51
111	726917.14	3509544.51
112	726881.34	3508795.35
113	726845.56	3508046.23
114	726809.77	3507297.08
X1	727404.86	3506142.36
X2	728071.52	3506485.95
X3	726214.68	3508451.79
X4	726773.99	3506547.09
X5	726250.46	3509201.77

1000 500 0 1000 2000

DISTANCE IN FEET

POTENTIAL EXPANSION CAVERN LAYOUT
BIG HILL SALT DOME

Sandia National Laboratories

SEP 1981 FIG. 6-5

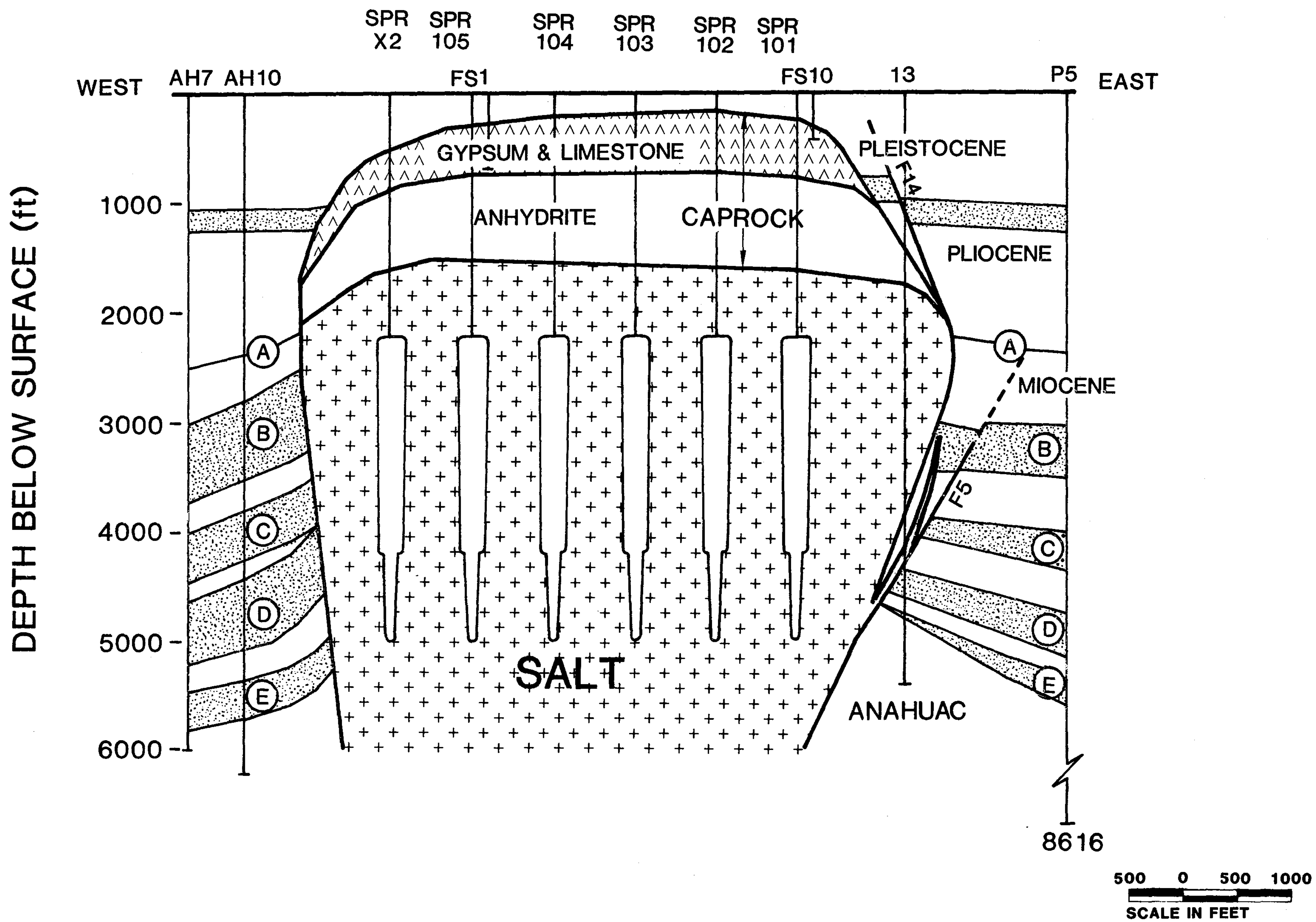

BIG HILL SALT DOME
WEST-EAST CROSS
SECTION NO. 1

Sandia National Laboratories

T.R. MAGORIAN

SEP. 1981 FIG. 6-6

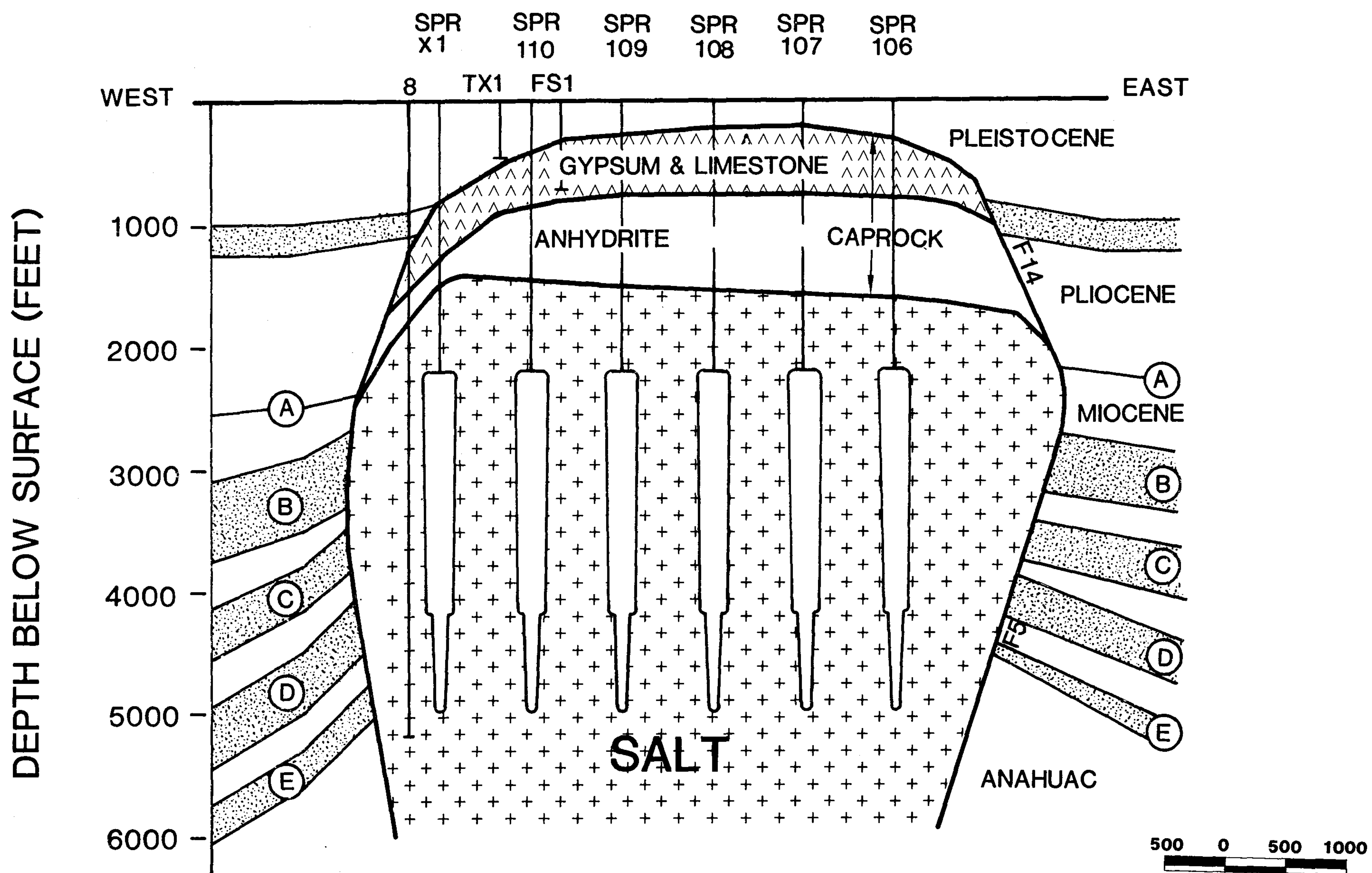

BIG HILL SALT DOME
WEST-EAST CROSS
SECTION NO. 2

Sandia National Laboratories

T.R. MAGORIAN

SEP 1981 FIG. 6-7

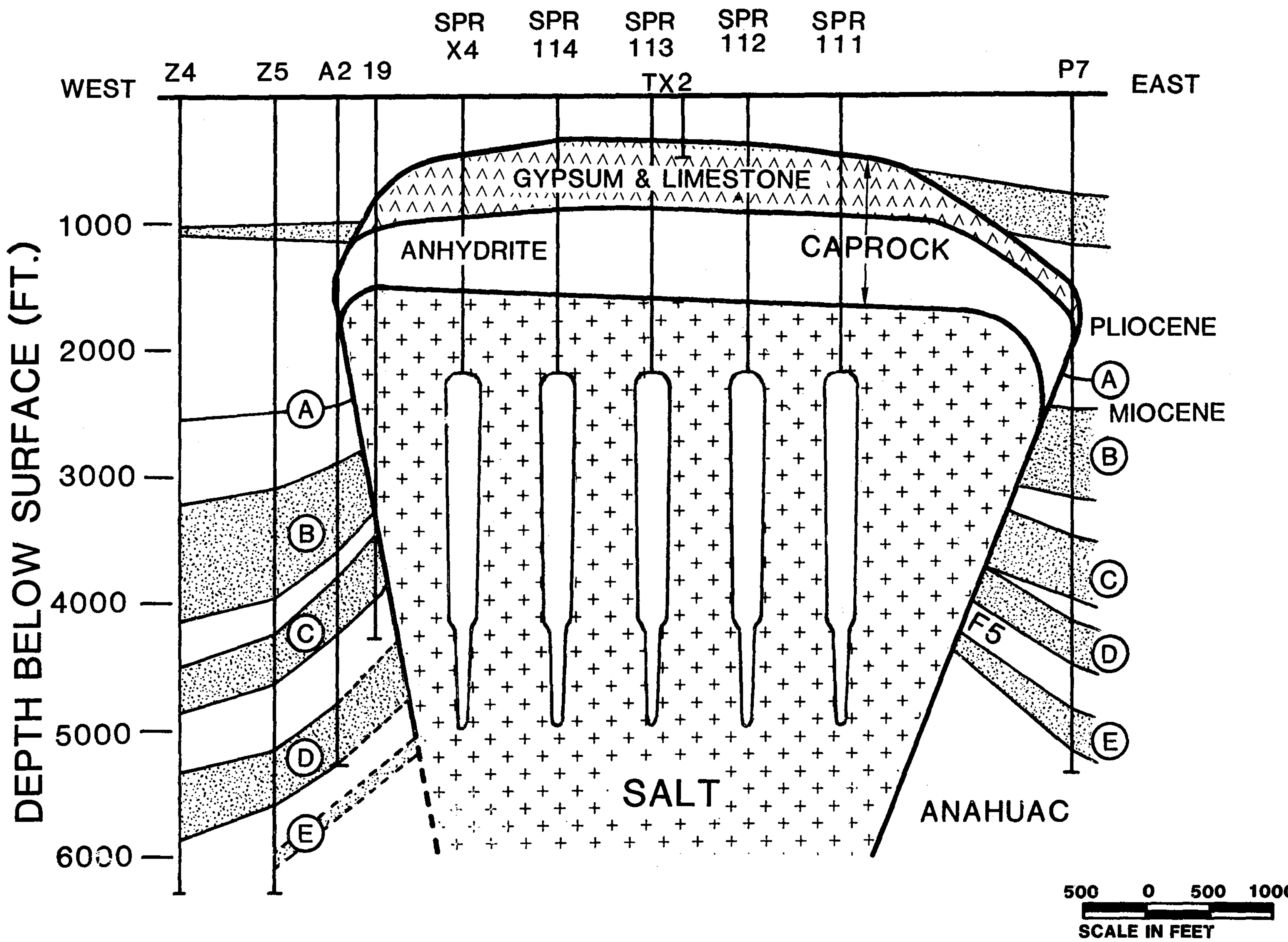

BIG HILL SALT DOME
WEST-EAST
CROSS SECTION NO. 3

Sandia National Laboratories

T.R. MAGORIAN

SEP 1981 FIG. 6-8

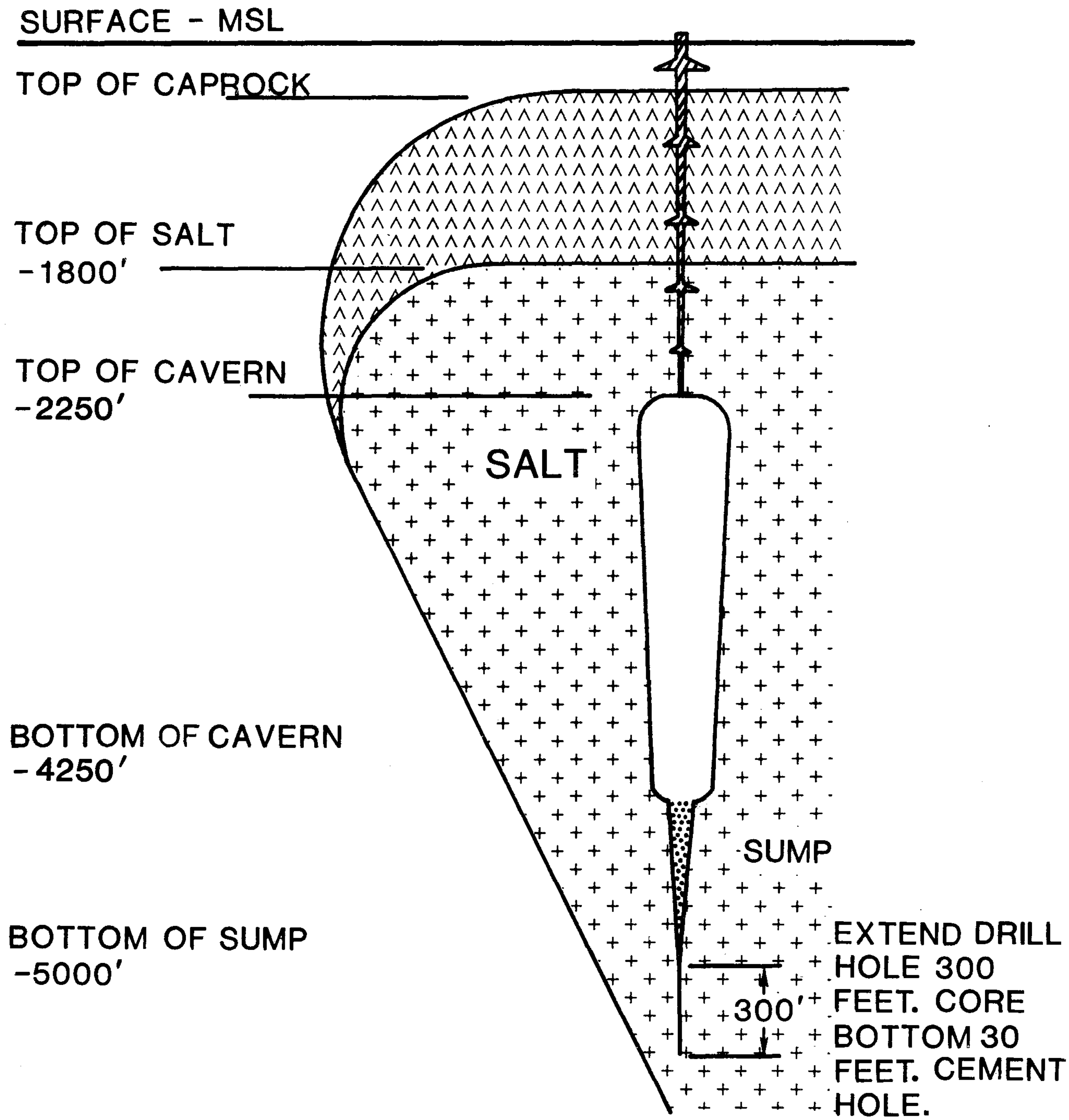

BIG HILL SALT DOME
EXPLORATORY EXTENSION
DRILLING

Sandia National Laboratories

SEP 1981 FIG. 6-9

CHAPTER 7 - NATURAL HAZARDS

Subsidence

Ground water withdrawal has caused some minor regional subsidence (0.2 to 1 ft) in the Big Hill area (Brown, et al, 1974). This type of subsidence will not adversely affect the SPR site. Minor subsidence because of oil withdrawal around the periphery of the dome can also be expected, but it appears unlikely to threaten SPR facilities.

The possibility of subsidence because of the formation of storage caverns has not been adequately determined. The importance of cavern spacing and roof thickness is discussed in detail in Chapter 6.

Earthquakes

The National Oceanic and Atmospheric Administration (NOAA) (1974) has classified the Big Hill area as having no reasonable expectancy of seismic activity (Figure 7-1). An earthquake data search by NOAA shows that no earthquakes have occurred in recorded history in the Big Hill area (PB/KBB, 1979). The data search covered a rectangle bounded by 28° 55' to 30° 19' north latitude and 90° 10' to 95° 45' west longitude. The Big Hill SPR site is at 29° 75' north latitude and 94° 25' west longitude.

Faulting

Two types of faults occur in the Gulf Coast area of Texas. First are gravity-related growth faults that are formed by slumping and consolidation of thick sections of geosynclinal sediments. Moving along these faults is a gradual slippage generally considered aseismic.

The other type of fault relates to the growth of salt domes. Most of the faults recognized in this study have been inactive since mid-Miocene; only one fault (see Chapter 5) could be considered active. The steeper slopes of the salt dome could also indicate active faulting. Again, this type of fault movement is not seismic but rather a silent, gradual movement that will not adversely affect the SPR site.

Floods and Hurricanes

Annual average precipitation at Big Hill is ~47 in. Flooding is common along the Gulf Coast of Texas in the area. A regional flood-insurance study by the Department of Housing and Urban Development (HUD, 1977) indicates that the maximum elevation of the 100-yr flood is ~15 ft above msl. Figure 7-2 indicates the area of the site that would be affected by the 100-yr flood.

Damage from hurricanes can result from both wind and water. Facilities, including wellheads, should be built to withstand the potential effects of hurricanes.

Figure 7-3 shows the area inundated by marine water during Hurricanes Carla in 1961 and Beulah in 1967. The maximum water elevation near Big Hill was ~8.6 ft during Carla, which made landfall at Port O'Connor, Texas, ~175 mi from the site. Maximum storm surge reported was 22 ft above msl reported at Port Lavaca (Brown, et al, 1974). Maximum high-water elevation during a hurricane in the northern hemisphere is immediately to the northeast of the eye of the hurricane because of counterclockwise winds. If a hurricane hit the coast immediately southwest of the site, the maximum high-water elevation would be somewhat higher than the maximum 100-yr non-hurricane-related flood because of the added impact of storm surge. Maximum high water elevation during a hurricane has not yet been determined, but was estimated by Bodine (1969) as 15.3 ft above msl. In addition, high waves added to the impact of storm surge could significantly increase the amount of flooding at Big Hill. The surface elevation at Cavern 114 is approximately 22 to 23 ft above msl. The remaining caverns lie at an elevation >25 ft msl.

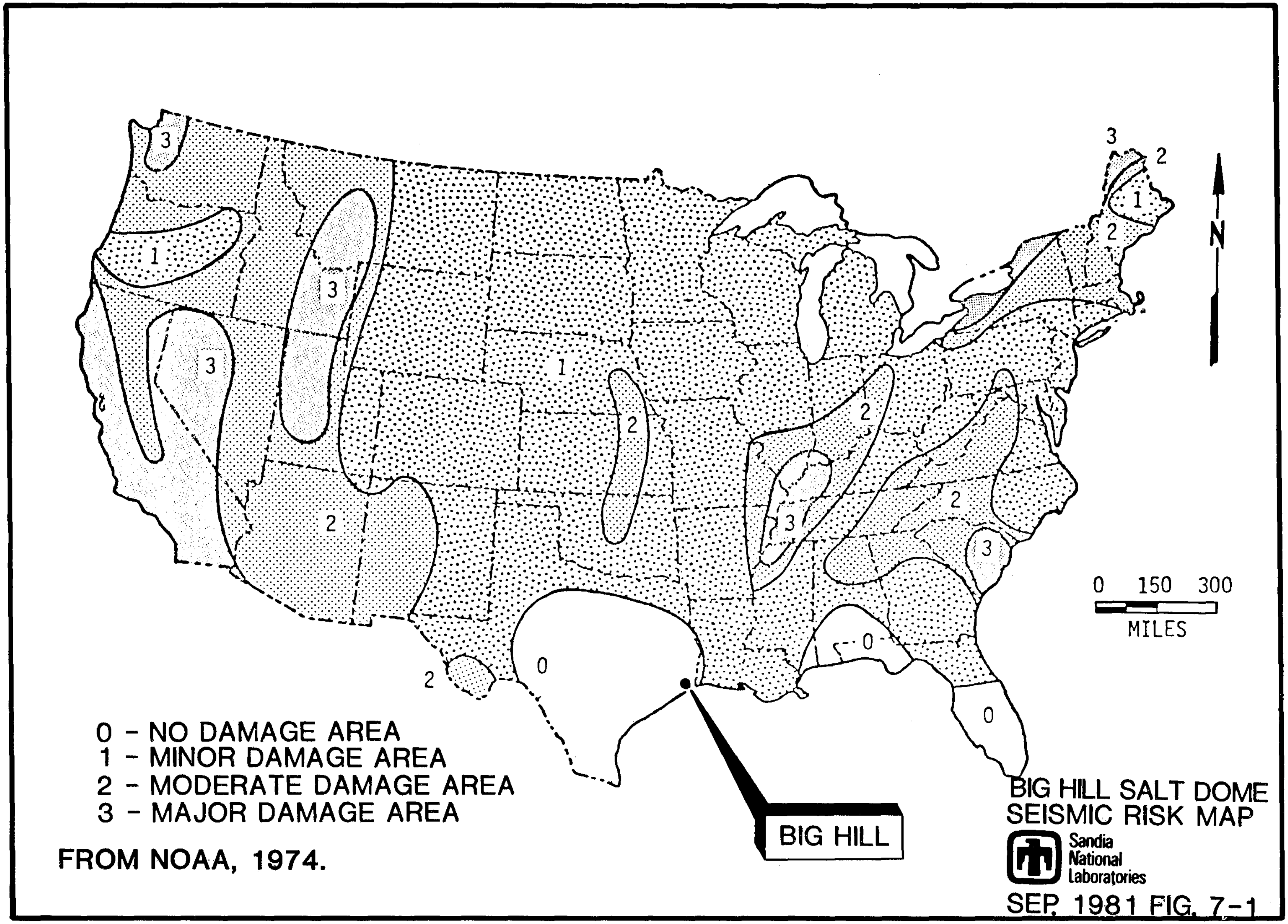

BIG HILL SALT DOME SEISMIC RISK MAP

SEP. 1981 FIG. 7-1

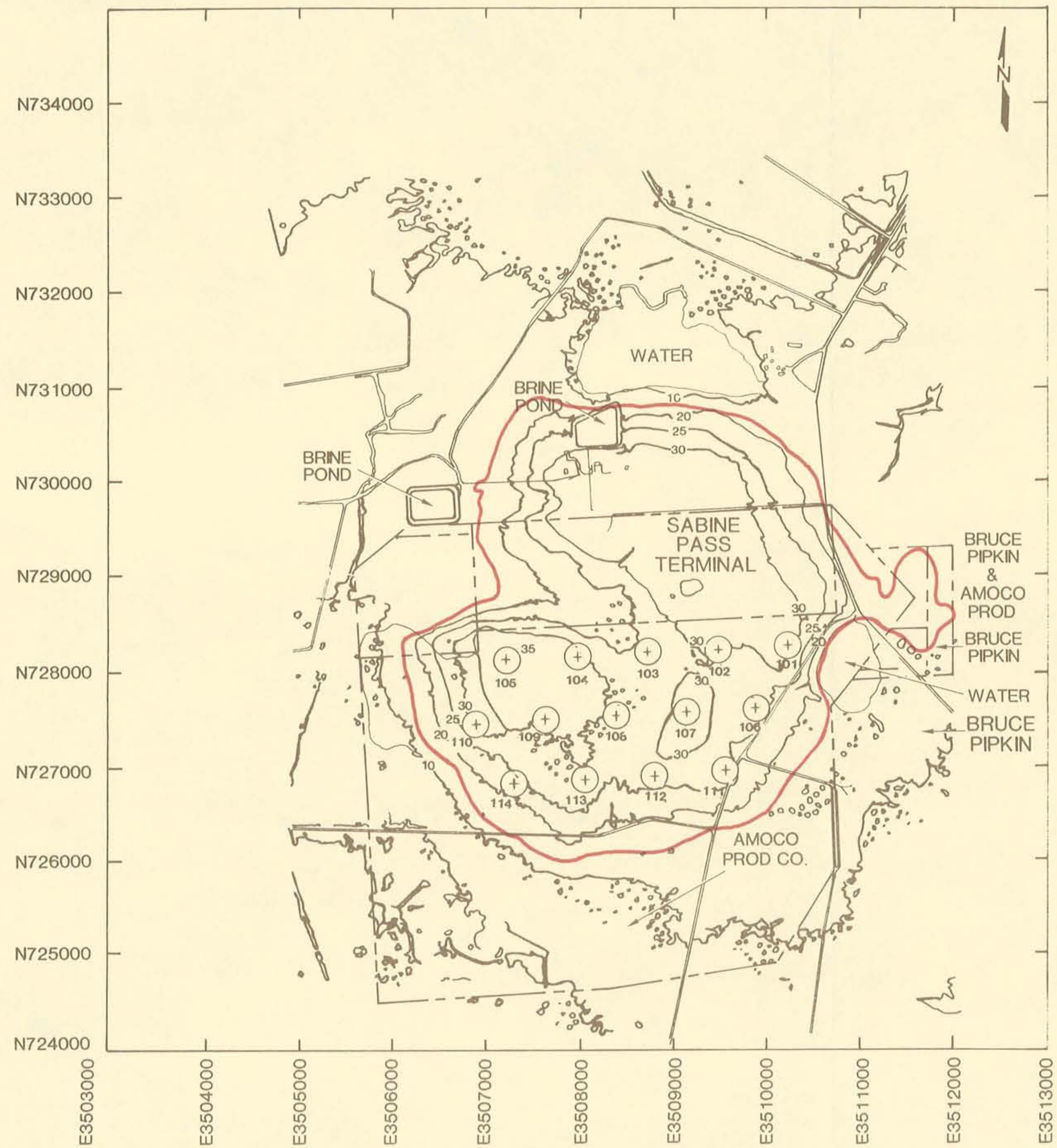

NOTE:
100 YEAR FLOOD LINE
APPROXIMATELY 15
FEET MEAN SEA LEVEL
(HUD, 1977).

LEGEND

- - - - PROPERTY LINE
—— 5 FOOT TOPOGRAPHIC CONTOUR
—— 100 YEAR FLOOD LINE

1000 500 0 1000 2000

DISTANCE IN FEET

BIG HILL SALT DOME
100 YEAR FLOOD
HAZARD MAP

Sandia National Laboratories

SEP 1981 FIG. 7-2

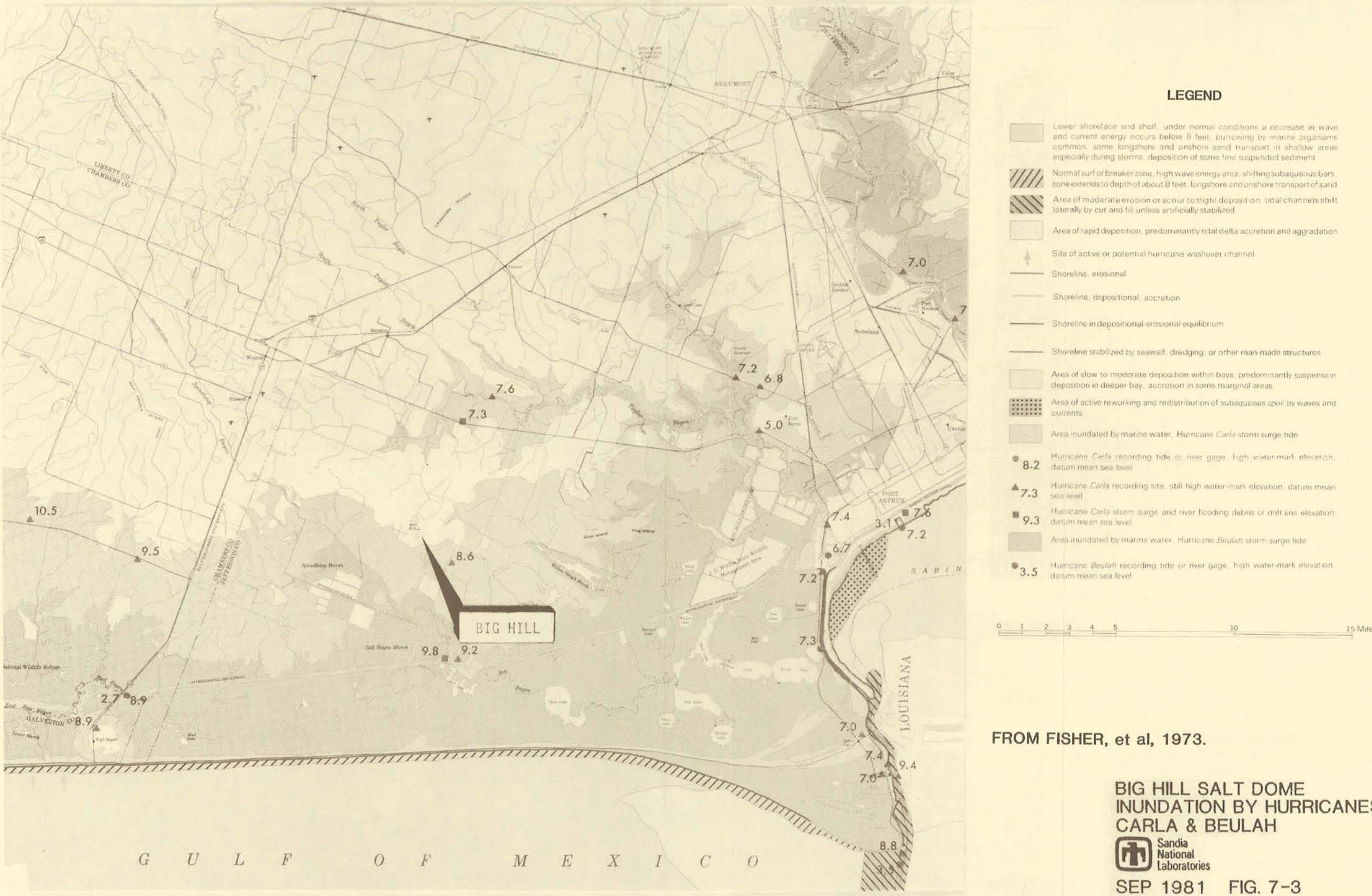

FROM FISHER, et al, 1973.

BIG HILL SALT DOME INUNDATION BY HURRICANES CARLA & BEULAH

Sandia National Laboratories

SEP 1981 FIG. 7-3

APPENDIX A

APPENDIX A

References and Bibliography

APPENDIX A

References and Bibliography

S. E. Benzley, Structural Analysis of West Hackberry No. 6 SPR Storage Cavern, SAND80-1904 (Albuquerque, NM: Sandia National Laboratories, August 1980).

H. A. Bernard and R. J. LeBlanc, Resume of the Quaternary Geology of the Northwestern Gulf of Mexico Province, in The Quaternary of the United States, ed H. E. Wright, Jr and D. G. Frey (Princeton: Princeton University Press, 1965, pp 137-185).

B. R. Bodine, Hurricane Surge Frequency Estimated for the Gulf Coast of Texas, Tech. Memo No. 26 (Ft Belvoir, VA: US Army Corps of Engineers, Coastal Engineerning Research Center, 1969).

L. F. Brown, R. A. Morton, J. H. McGowen, C. W. Kreitler, and W. L. Fisher, Natural Hazards of the Texas Coastal Zone (Austin, TX: University of Texas, in cooperation with Texas Coastal and Marine Council, 1974).

J. L. Crout, D. G. Symmank, and G. A. Peterson, Soil Survey of Jefferson Co, Texas, US Department of Agriculture, Soil Conservation Service, in cooperation with Texas A&M Agr. Expt. Sta., Soil Survey Ser. No. 21 (Washington, DC: US Dept. of Agriculture, 1960).

DOE, Final Environmental Impact Statement, Strategic Petroleum Reserve, Texoma Group Salt Domes, Cameron and Calcasieu Parishes, Louisiana and Jefferson County, Texas (Washington, DC: DOE, 1978).

R. S. Dollison, Big Hill Field, Jefferson County, Texas, Trans. Gulf Coast Assoc. Geol. Soc., Vol XV, pp 25-35, 1965.

Fenix & Scisson, Investigation of New Leached Caverns in Salt Domes, prepared for the DOE (Albuquerque, NM: Fenix & Scisson, 1973).

W. L. Fisher, L. F. Brown, Jr, J. H. McGowen, and C. G. Groat, Environmental Geologic Atlas of the Texas Coastal Zone--Beaumont-Port Arthur Area (Austin, TX: Texas Bureau of Econ. Geol., 1973).

H. N. Fisk, Geological Investigation of the Alluvial Valley of the Lower Mississippi River (Vicksburg, MI: US Army Corps of Engineers, 1944).

W. G. Gussow, Salt Diapirism, Importance of Temperature and Energy Source of Emplacement, in Diapirism and Diapirs. Amer. Assoc. Pet. Geol. Memoir No. 8, 1968.

M. T. Halbouty, Salt Domes, Gulf Region, United States and Mexico (2nd ed; Houston, TX: Gulf Publishing Co., 1979).

A. S. Henley, 1925, Big Hill Salt Dome, Jefferson County, Texas, Bull. Amer. Assoc. Pet. Geol., Vol 9, pp 590-593.

P. D. Hilton, et al, Interaction Effects of Storage Caverns in Salt, SAND79-0732 (Albuquerque, NM: Sandia National Laboratories, August 1980).

R. G. Hogan, ed, Strategic Petroleum Reserve (SPR) Geological Site Characterization Report, Bryan Mound Salt Dome, SAND80-7111 (Albuquerque, NM: Sandia National Laboratories, October 1980a).

R. G. Hogan, ed, Strategic Petroleum Reserve (SPR) Geological Site Characterization Report Bayou Choctaw Dome, SAND80-7140 (Albuquerque, NM: Sandia National Laboratories, December 1980b).

Department of Housing and Urban Development (HUD), Federal Insurance Administration, Flood Hazard Boundary Map, Jefferson County, Texas, Sheet 47 (Washington, DC: HUD, 1977).

P. H. Jones, A. N. Turcan, Jr, and H. E. Skibitzke, Geology and Ground-Water Resources of Southwestern Louisiana (Baton Rouge, LA: USGS Bull. No. 30, 1954).

D. H. Kupfer, Boundary Shear Zones in Salt Stocks, in Fourth Symposium on Salt (Cleveland, OH: Northern Ohio Geological Society, Vol 1, pp 215-225, 1974).

J. D. Martinez et al, An Investigation of the Utility of Gulf Coast Salt Domes for the Storage or Disposal of Radioactive Wastes, prepared for the DOE (Baton Rouge, LA: Institute for Environmental Studies, Louisiana State University, 1978).

D. E. Munson and P. R. Dawson, Constitutive Model for the Low Temperature Creep of Salt (With Application to WIPP), SAND79-1853 (Albuquerque, NM: Sandia National Laboratories, October 1979).

G. E. Murray, Geology of the Atlantic and Gulf Coastal Province of North America (New York: Harper and Brothers, 1961).

National Oceanic and Atmospheric Administration (NOAA) Earthquake History of the US, Publication 41-1 (Washington, DC: US Department of Commerce, 1974).

Memo from J. F. Ney, Sandia National Laboratories, to E. E. Chapple, DOE SPR-PMO, Minimum Thickness of Salt Between Edge-of-Dome and Storage Caverns, March 25, 1981.

H. Ode, Rheology of Salt, in Diapirism and Diapirs, Amer. Assoc. Pet. Geol. Memoir No. 8, 1968.

PB/KBB, Big Hill Complex, Planning Studies, Preliminary and Conceptual Design and Geotechnical Investigations, prepared for the DOE Strategic Petroleum Reserve Program under Contract DE-AC01-79RA31801 (Houston, TX: PB/KBB, August 1979).

F. W. B. Van Eysinga, Geologic Time Table (3rd ed; Amsterdam, Holland: Elsevier Scientific Publishing Co., 1975).

C. W. Walker, Nature and Origin of Caprock Overlying Gulf Coast Salt Domes, in Fourth Symposium on Salt (Cleveland, OH: Northern Ohio Geological Society, Vol 1, pp 169-195, 1974).

W. R. Wawersik, D. W. Hannum, and H. S. Lauson, Compression and Extension Data for Dome Salt from West Hackberry, LA, SAND79-0668 (Albuquerque, NM: Sandia National Laboratories, September 1980a).

W. R. Wawersik, D. W. Hannum, and H. S. Lauson, Compression and Extension Data for Dome Salt from West Hackberry, LA, SAND79-0668 (Albuquerque, NM: Sandia National Laboratories, September 1980b).

J. B. Wesselman and S. Aronow, Ground-Water Resources of Chambers and Jefferson Counties, Texas, Report 133, prepared by the USGS in cooperation with the Texas Water Development Board (Washington, DC: USGS, 1973).

G. H. Whiting, ed, Strategic Petroleum Reserve, Geological Site Characterization, West Hackberry Salt Dome, SAND80-7131 (Albuquerque, NM: Sandia National Laboratories, October 1980).

Oscar Wilhelm and Maurice Ewing, Geology and History of the Gulf of Mexico, Bull. Geol. Soc. Am., Vol 83, pp 575-600.

L. A. Wood, R. K. Gabrysch, and R. Marvin, Reconnaissance Investigation of the Ground-Water Resources of the Gulf Coast Region, Texas, Bull. 6305 prepared by the US Geological Survey (USGS) in cooperation with the Texas Water Commission (Washington, DC: USGS, 1963).

APPENDIX B

APPENDIX B

Well Data
and Well Control

Table B-1

Well Data

API No.	Operator	Well No.	Location	Total Depth (in feet)	Result	Logs	Date Completed
2020	Adams & Haggarty	Crow 1	N734500 E3508650	6238	Abandoned	Electric	3/16/62
2024	Texaco	Crow 1	N731010 E3510380	4604	Oil-cap rock production	Electric directional	3/27/51
2025	Texaco	Crow 2	N732170 E3508640	5444	Abandoned	Electric	7/1/56
2031	Stanolind	Pipkin A-4	N731580 E3510210	5490	Abandoned	Electric	11/15/37
2032	Stanolind	Pipkin A-5	N732925 E3505333	8294	Abandoned		
2033		Crow 2	N732925 E3505333	2600	Abandoned		
20351	Union Oil	LPG 1	N729959	3430	Cavern Well		4/20/57
20362	Union Oil	LPG 2	N729842 E3508590	3203	Cavern Well		5/9/61
20371	Union Oil	SWDW	N729938 E3507104	978	Brine Disposal	Drillers	10/10/56
2038	Freeport Sulphur	Staiti 2	N728120 E3507370	450	Exploratory Sulphur	Drillers	10/20/27
2039	Freeport Sulphur	Staiti 5	N730420 E3508080	700	Exploratory Sulphur	Drillers	12/15/27
2040	Freeport Sulphur	Staiti 7	N728915 E3508080	527	Exploratory Sulphur	Drillers	1/2/28
2041	Freeport Sulphur	Staiti 8	N729768 E3510217	610	Exploratory Sulphur	Drillers	1/16/28
2042	Freeport Sulphur	Staiti 10	E3510315 E3510315	510	Exploratory Sulphur	Drillers	2/9/28
2043	Guffey	Broussard G-1	N727900 3510509	1400	Abandoned		
2044	Texaco	Masterson 1	N730679 E3510760	4435	Abandoned		11/21/51
2045	Texaco	Masterson 2	N730569 E3511230	4697	Abandoned	Electric	6/16/53
2047		Crow 1	N731465 E3511700	1153	Abandoned		
2775	Pan Am (Stanolind)	Davidson 1	N734220 E3507610	10114	Abandoned	Electric	5/1/42
2776	McCarthy	Davidson 1E	N730670 E3504660	8457	Gas	Electric	12/9/55
2787	Adams & Haggarty	Marrs McLean 11	N730121 E3505652	5650	Abandoned	Electric	5/23/55
2789	Adams & Haggarty	Marrs McLean 13	N729654 E3504787	5932	Abandoned	Electric	8/22/61
2790	Adams & Haggarty	Marrs McLean 15	N729596 E3504782	6670	Oil	Electric	10/25/61
2791	Adams & Haggarty	Marrs McLean 16	N729120 E3502640	7824	Oil	Electric	4/23/62
2792	Adams & Haggarty	Marrs McLean 17	N729455 E3505391	7982	Oil	Electric	10/9/62
2793	Adams & Haggarty	Marrs McLean 18	N729479 E3505391	1550	Oil	Electric	10/19/62

Table B-1
(Cont)

API No.	Operator	Well No.	Location	Total Depth (in feet)	Result	Logs	Date Completed
2796	Adams & Haggarty	Pan Am 1	N728780 E3505723	5500	Oil	Electric	10/7/62
2797	Freeport Sulphur	Staiti 3	N729112 E3506376	1416	Exploratory Sulphur	Drillers	11/24/27
2803	Adams & Haggarty	Fitzhugh 10	N728240 E3505031	6153	Oil	Electric	7/25/61
2805	Adams & Haggarty	Fitzhugh 12	N728843 E3505269	5761	Oil	Electric	4/30/62
2824	Freeport Sulphur	Staiti 11	N726652 E3506184	1347	Exploratory Sulphur	Drillers	2/28/28
2829	Pan Am	Fitzhugh 5	N726095 E3504860	8500	Abandoned	Electric	2/19/43
2835	Jayred	Fitzhugh 9	N723970 E3505632	6615	Abandoned	Electric	8/15/62
2837	Pan Am	Fitzhugh 3	N721470 E3505920	8031	Abandoned	Electric	7/10/42
2870	Texas Exploration	Broussard 1	N727320 E3507450	482	Abandoned	Drillers	7/27/17
2871	Texas Exploration	Broussard 2	N726445 E3508543	548	Abandoned	Drillers	10/10/17
2872	Texas Exploration	Broussard 3	N725400 E3507500	1200	Abandoned	Drillers	1/3/18
2873	Texas Exploration Staiti	Broussard 4	N725000 E3507375	1358	Abandoned	Drillers	8/5/18
2874	Freeport Sulphur	Staiti 1	N727412 E3508080	656	Exploratory Sulphur	Drillers	10/24/27
2875	Freeport Sulphur	Staiti 4	N7265568 E3508930	1041	Exploratory Sulphur	Drillers	12/07/27
2876	Freeport Sulphur	Staiti 6	N725589 E3509920	1153	Exploratory Sulphur	Drillers	1/18/28
2877	Freeport Sulphur	Staiti 9	N725638 E3509892	1295	Exploratory	Drillers	2/19/28
2878	Houston Oil	Staiti 1	N725892 E3510650	1559	Abandoned	Drillers	11/07/23
2879	Houston Oil	Staiti 2	N725554 E3510426	1634	Abandoned	Drillers	6/29/23
2881	Chance & Caldwell	Fitzhugh 1	N724465 E3508068	1828	Abandoned	Electric	6/19/45
2882	Chance & Caldwell	Fitzhugh 2-A	N724445 E3507700	1720	Abandoned	Electric	11/16/45
2883	Chance & Caldwell	Fitzhugh 1-B	N724582 E3508263	1669	Abandoned	Electric	10/07/45
2884	Stanolind Oil	Fitzhugh 1	N724500 E35088379	5572	Oil	Electric	3/04/37
2885	Stanolind Oil	Fitzhugh 2	N724452 E3507775	4705	Abandoned	Electric	11/01/37
2887	Bering Co (Wynne)	Fitzhugh 1-A	N723970 E3509004	5540	Oil	Electric	11/17/49
2890	Bering Co. (Wynne)	Fitzhugh 4	N724444 E3509059	5101	Abandoned	Electric	12/04/50
2892	Texaco	Fitzhugh 2	N724552 E3510054	2922	Abandoned		3/20/20

Table B-1
(Cont)

API No.	Operator	Well No.	Location	Total Depth (in feet)	Result	Logs	Date Completed
2907	Stanolind Oil	McFaddin A-3	N726260 E3512350	6698	Abandoned	Electric	8/17/36
2909	Pan Am	Pipkin 2-B	N725143 E3510490	6414	Abandoned	Electric	8/18/37
2914	Texaco	Pipkin 6	N725630 E3512270	8800	Abandoned	Electric	4/06/53
2915	Texaco	Pipkin 7	N726850 E3511441	5254	Abandoned	Electric	8/28/53
2916	Texaco	Pipkin 8	N727010 E3511520	4829	Abandoned	Electric	1/15/54
3072	Sunset	Anderson 1	N731180 E3506450	1437	Abandoned	Electric	7/22/64
3073	Sunset	Anderson 2	N731780 E3506080	7913	Oil	Electric	8/29/64
3079	Goodale	Pan Am 1	N724760 E3506219	5995	Oil	Electric	8/19/64
3091	HNG	Davidson 2E	N730710 E3505280	6000	Abandoned	Electric	11/19/64
3093	Goodale Bertman	Pan Am 2	N725060 E3506140	5677	Oil	Electric	10/29/64
3094	Jayred	Fitzhugh 10	N724385 E3506577	5800	Oil	Electric	11/11/64
3121	Gulf	Anderson 1	N7231980 E3507080	5576	Abandoned	Electric	3/7/65
3128	Goodale	Pan Am 3	N725098 E3506169	1463	Oil	Electric	12/21/64
3129	Goodale	Pan Am 4	N724700 E3506681	4802	Oil	Electric	1/7/65
3130	Pan Am	Texas Exploration 1	N725067 E3506615	5500	Oil	Electric	4/16/65
3131	Goodale Bertman	Pan Am 5	N725363 E3506039	5413	Oil	Electric	4/14/65
3132	Goodale Bertman	Pan Am 6	N725363 E3506053	2583	Oil	Electric	3/14/65
3133	Jayred	Fitzhugh 11	N725020 E3305730	5650	Abandoned	Electric	1/9/65
3160	Goodale Bertman	Texas Exploration 7	N725708 E3506148	2600	SWDW	Electric	5/20/65
3180	Goodale Bertman	Texas Exploration 10	N725645 E3505858	5045	Oil		12/10/65
3181	Goodale Bertman	Texas Exploration 9	N724755 E3506560	4524	Oil	Electric	10/22/65
3215	Goodale Bertman	Texas Exploraton 11	N725921 E3505852	5000	Oil	Electric	4/15/66
3216	Goodale Bertman	Fitzhugh TAST	N726015 E3505676	5149	Oil	Electric	3/18/66
3225	Goodale Bertman	Fitzhugh 1-B	N724480 E3506700	4800	Oil	Electric	5/9/66
3236	Goodale Bertman	Fitzhugh 2-A	N726278 E3505525	5323	Oil	Electric	7/2/66

Table B-1
(Cont)

API No.	Operator	Well No.	Location	Total Depth (in feet)	Result	Logs	Date Completed
3237	Goodale Bertman	Fitzhugh 3-A	N726610 E3504910	6149	Abandoned	Electric	7/19/66
3238	Goodale Bertman	Texas Exploration 13	N727085 E3505957	1912	Abandoned	Electric	8/26/66
3239	Goodale Bertman	Fitzhugh 4-A	N725230 E3505644	5562	Abandoned	Electric	8/18/66
3244	Goodale Bertman	Fitzhugh 5-A	N725630 E3505700	5200	Abandoned	Electric	10/24/66
3257	Pan Am	Texas Exploration 2	N725245 E3506603	7111	Oil	Electric	1/25/67
3265	Pan Am	Texas Exploration 4	N725540 E3510112	5025	Oil	Electric	3/6/67
3266	Pan Am	Texas Exploration 3	N725458 E3506779	4900	Oil	Electric	3/24/67
3267	Pan Am	Texas Exploration 5	N726070 E3510390	4653	Abandoned	Electric	3/29/67
3269	Goodale Bertman	Fitzhugh 2B (was TX Exp 12)	N726151 E3505598	4273	Abandoned	Scout Ticket	2/20/67
3272	Pan Am	Texas Exploration 8	N727497 E3505768	5200	Abandoned	Electric	4/26/67
3274	Goodale Bertman	Fitzhugh 2-B	N724507 E3509519	5393	Abandoned	Electric	5/8/67
3282	Pan Am	Texas Exploration 7	N725307 E3506996	4687	Oil	Electric	5/27/67
3284	Goodale Bertman	Texas Exploration 14	N725390 E3506229	1618	Abandoned		
3289	Goodale Bertman	Texas Exploration 15	N725271 E3506068	4265	Oil	Electric	6/26/67
3290	Pan Am	Texas Exploration 9	N725096 E3506815	5000	Oil	Electric	7/1/67
3295	Goodale Bertman	Texas Exploration 16	N725271 E3506093	5202	Oil	Electric	7/26/67
3297	Pan Am	Texas Exploration 10	N725607 E3506571	6200	Oil	Electric	8/11/67
3299	Goodale Bertman	Texas Exploration 7	N724665 E3506731	4925	Oil	Electric	8/19/67
3303	Pan Am	Texas Exp 11 (ST)	N728850 E3506055	5066	Abandoned	Electric	9/7/67
3305	Pan Am	Texas Exploration 12	N725189 E3507164	4451	Oil	Scout Ticket	9/1/67
3308	Goodale Bertman	Texas Exploration 18	N725482 E3505974	5100	Oil	Electric	9/15/67
3309	Pan Am	Texas Exploration 14	N725010 E3507052	4400	Oil	Electric	9/25/67
3318	Pan Am	Texas Exploratio 13	N728518 E3511209	4464	Abandoned	Electric	11/10/67
3319	Goodale Bertman	Texas Exploration 19	N725647	4712	Oil	Electric Gamma ray	11/4/67
3322	Pan Am	Texas Exploration 15	N725150 E3507363	4050	OIl	Electric	11/4/67
3324	Goodale Bertman	Texas Exploration 20	N724622 E3506980	4549	Oil	Electric	12/15/67

Table B-1
(Cont)

API No.	Operator	Well No.	Location	Total Depth (in feet)	Result	Logs	Date Completed
3328	Pan Am	Texas Exploration 16	N725452 E3506940	4006	Oil	Electric	12/5/67
3338	Pan Am	Texas Exploration 18	N725052 E3507536	4000	Oil	Electric	1/22/68
3340	Pan Am	Texas Exploration 17	N726270 E3505951	4688	Oil now Salt water disposal	Electric	1/24/28
3346	Pan Am	Pipkin Crow	N731950 E3508750	4728	Abandoned	Electric	2/28/68
3354	Goodall Bertman	Texas Exploration 21	N724882 E3507323	4504	Oil	Electric Gamma ray	4/13/68
3355	Pan Am	Texas Exploration 19	N726479 E3505850	4300	Salt water disposal	Electric	4/24/68
3359	Goodale Bertman	Texas Exploration 22E	N725791 E3506330	4040	Oil	Gamma ray	5/18/68
3363	Goodale Bertman	Fitzhugh 8-A	N725450 E3504000	6730	Oil	Electric	6/23/68
3376	HNG	Davidson 3-E	N732500 E3504700	7003	Abandoned	Electric	8/6/68
3381	Goodale Bertman	Fitzhugh 9-A	N725300 E3504300	6451	Abandoned	Electric	9/3/68
30031	Pan Am	Texas Exploration 20	N725143 E3510081	5054	Oil	Electric	3/30/69
30032	Pan Am	Texas Exploration 21	N725232 E3509449	4435	Abandoned	Electric	7/18/69
30138	Amoco	Texas Exploration 22	N725440 E3506520	4115	Oil	Electric	8/6/71
30139	Amoco	Texas Exploration 23	N725220 E3806857	3900	Oil	Electric	9/29/71
30140	Amoco	Texas Exploration 24	N725481 E3506872	4000	Oil	Electric	8/11/71
30250	HNG	Anderson Guiterman 1	N732200 E3505680	7450	Oil	ISF/Sonic	10/19/73
30272	HNG	Anderson Guiterman 2	N731620 E3506520	5912	Abandoned	Electric	1/13/74
31274	Amoco	Texas Exploration 25	N725465 E3509722	4107	Abandoned	Electric	1/27/79
33325	Praire	McFaddin 1 Trust		8654	Abandoned	Electric	10/26/78
	Jefferson Lake Sulphur	JL1	N729827 E3509395	1161	Exploratory Sulphur	Drillers	1962
	Jefferson Lake Sulphur	JL2	N728758 E3511549	1504	Exploratory Sulphur		1962
	Jefferson Lake Sulphur	JL3	N724879 E3509050	1744	Exploratory Sulphur	Drillers	1962
	Jefferson Lake Sulphur	JL4	N728350 E3511994	2384	Exploratory Sulphur	Drillers	1962
	Jefferson Lake Sulphur	JL5	N727188 E3510671	1468	Exploratory Sulphur	Drillers	1962
	Stanolind	Pipkin A3	N726120 E3512452	6742	Abandoned	Electric	5/14/36

Table B-1
(Cont)

API No.	Operator	Well No.	Location	Total Depth (in feet)	Result	Logs	Cate Completed
	Jayred	Fitzhugh 8	N723640 E3505557		Abandoned	Electric	5/22/62
	Texaco	Pipkin 5	N729135 E3512835	8616	Abandoned	Electric	2/3/53
	Texaco	Pipkin 6	N725483 E3512376	8806	Abandoned	Electric	4/5/53

Table B-2

Well Control

API No.	Well No.	Map Symbol	Top Cap	Top Salt	Base Salt	L	PL	A	BF	B	AB	C	RL	D	SD	E	DR	M	F
3130	Amoco (Pan Am) TX Exploration 1	1	1600	1820	2665	880	1110	-	-	2730	3140	3590	3980	4260	4960	5130	-	-	
3257	Amoco (Pan Am) TX Exploration 2	2	1590	1935	2760							3000	3240	3825	4110	4765	5115	5802	
3266	Amoco (Pan Am) TX Exploration 3	3	1300	1630	2890	765	852							3430	4160				
3265	Amoco (Pan Am) TX Exploration 4	4	1380	1970	2910	1095	1250				3240	3500			4130	4490	4640		
3267	Amoco (Pan Am) TX Exploration 5	5	1300	1800	2935							3300	3435	3655	4105	4565			
3281	Amoco (Pan Am) TX Exploration 6	6		1815	3470	1008	1175										3830	4330	
3282	Amoco (Pan Am) TX Exploration 7	7	1315	1640	3010											3465	4335		
3272	Amoco (Pan Am) TX Exploration 8	8	1220	1850															
3290	Amoco (Pan Am) TX Exploration 9	9		2015	2660							3090	3603	4000	4399	4660			
3297	Amoco (Pan Am) TX Exploration 10	10		1710	2990									3195	3980	4277	4703	5290	
3303	Amoco (Pan Am) TX Exploration 11	11	1255	1630	3520	960	1190								3880	4255	4735		
3303	Amoco (Pan Am) TX Exploration 11ST	11ST			3550										3815	4140			
3318	Amoco (Pan Am) TX Exploration 13	13	1340	1730 to 3710 4120 to 4345		1000													
3318	Amoco (Pan Am) TX Exploration 13ST	13ST			2850 3330 to 3580								4080	4360					
3309	Amoco (Pan Am) TX Exploration 14	14			2740						2930	3110	3495	4040					
3322	Amoco (Pan Am) TX Exploration 15	15			3195												3790		
3328	Amoco (Pan Am) TX Exploration 16	16		1880	2990											3380			

Table B-2 (Cont)

API No.	Well No.	Map Symbol	Top Cap	Top Salt	Base Salt	L	PL	A	BF	B	AB	C	RL	D	SD	E	DR	M	F
3340	Amoco (Pan Am) TX Exploration 17	17		1280	3180						3480	3940	4320						
3338	Amoco (Pan Am) TX Exploration 18	18		1720	3030								3110	3360	3470	3710			
3355	Amoco (Pan Am) TX Exploration 19	19			3340							3550	3950						
3355	Amoco (Pan Am) TX Exploration 19ST	19ST			3260							3610	3960						
30031	Amoco (Pan Am) TX Exploration 20	20	1580	2670	2810	940	1195				2990	3300	3800	3950	4265	4445			
30031	Amoco (Pan Am) TX Exploration 20ST	20ST									3200		3740	3850	4100	4190	4755		
30032	Amoco (Pan Am) TX Exploration 21	21	1055	2060	3340	770	920							3660	3985	4090			
3359	Amoco (Pan Am) TX Exploration 22	22			2775								3405	3800					
30139	Amoco (Pan Am) TX Exploration 23	23			2810									3380					
30140	Amoco (Pan Am) TX Exploration 24	24			3030									3410					
31272	Amoco (Pan Am) TX Exploration 25	25		2620	3740														
31274	Amoco (Pan Am) TX Exploration 26	26			3235										3577	3880	4315	4898	
2884	Amoco (Pan Am) Fitzhugh 1	Z1		2120	2505							3160	3755						
2885	Amoco (Pan Am) Fitzhugh 2	Z2	1690	2165	2685	1045	1360				3125	3270	3995	4115					
2829	Amoco (Pan Am) Fitzhugh 5	Z5						2430	2795	2960	3715	4205		5230	5780	5950	6140	6960	
3346	Amoco (Pan Am) Pipkin Crow 1	PC				1020	1200	2260	2440	2590	3230	3335	3680	3710	3760	3880	4320		
3079	Goodale-Bertman Pan Am 1	G1				1050	1310	2420	2625	3002	3510	4015	4397	4635	5250	5405	5650		
3093	Goodale-Bertman Pan Am 2	G2				1055	1295	2400	2735	3030	3330	3800	4350	4610	5005	5162	5400		

Table B-2 (Cont)

API No.	Well No.	Map Symbol	Top Cap	Top Salt	Base Salt	L	PL	A	BF	B	AB	C	RL	D	SD	E	DR	M	F
3128	Goodale-Bertman Pan Am 3	G3				1055	1295												
3129	Goodale-Bertman Pan Am 4	G4				1080	1300	2235	2420	2960	3425	3703	4220	4710					
3131	Goodale-Bertman Pan Am 5	G5				1050	1280	2380	2745	3080	3370	3640	3990	4350	4820	4990	5250		
3132	Goodale-Bertman Pan Am 6	G6	1650			1050	1280												
3160	Goodale-Bertman TX Exploration 7	G7	1280			1070	1230												
3179	Goodale-Bertman TX Exploration 8	G8	1580	1650	2350	1100	1380			3080	3210	3450	3760	4170	4320	4870	4990		
3181	Goodale-Bertman TX Exploration 9	G9				1075	1300	2330	2530	2980	3350	3750	4140	4390					
3215	Goodale-Bertman TX Exploration 11	G11		1587	3050	1053	1260				3610	3950	4270	4385	4500	4640	4855		
3269	Goodale-Bertman Fitzhugh 2B	2B		1560	1790			2000	2260	2640	3530	3940	4180						
3238	Goodale-Bertman TX Exploration 13	G13	780	1390															
3284	Goodale-Bertman TX Exploration 14	G14																	
3289	Goodale-Bertman TX Exploration 15	G15	1810					2350	2500	2825	3180	3330	3865	4000					
3295	Goodale-Bertman TX Exploraton 16	G16	1810					2380	2690	2975	3280	3550	3780	4040	4730	4900			
3299	Goodale-Bertman TX Exploration 17	G17						2290	2550	2788	3300	3788	3912	4350	4720	4790			
3308	Goodale-Bertman TX Exploration 18	G18		2300	2820						3090	3385	3640	3760	4370	4550	4870		
3319	Goodale-Bertman TX Exploration 19	G19		2190	3025						3100	3745	4070	4100	4140	4430			
3324	Goodale-Bertman TX Exploration 20	G20	1530	2105	2670						2900	3120		3760	3830	4200			
3354	Goodale-Bertman TX Exploration 21	G21	1360	1690	2790								3430	3590	3725	4105			

Table B-2 (Cont)

API No.	Well No.	Map Symbol	Top Cap	Top Salt	Base Salt	L	PL	A	BF	B	AB	C	RL	D	SD	E	DR	M	F
3359	Goodale-Bertman TX Exploration 22	G22	1470	1820	3050								3720						
3216	Goodale-Bertman Fitzhugh A1	A1	1630			1030	1265	2390	2625	2930	3610	3940	4330	4535	4720	4800	4980		
3236	Goodale-Bertman Fitzhugh A2	A2	1560			1030	1285	2465	2750	3400	3695	3865	4150	4220	4700	4990			
3237	Goodale-Bertman Fitzhugh A3	A3				1025	1275	2400	2665	2860	3505	3840	4350	4605	5065	5190	5965		
3239	Goodale-Bertman Fitzhugh A4	A4				1040	1305	2455	2660	2970	3590	4270	4570	4610	4960	5185	5355		
3244	Goodale-Bertman Fitzhugh A5	A5				1033	1275	2392	2610	2830	3440	4015	4570	4770	4910	5005			
3225	Goodale-Bertman Fitzhugh B1	B1				1088	1360	2320	2635	2990	3380	3720	4150	4590					
3274	Goodale-Bertman Fitzhugh B2	B2	2145							2530	3100	3520	4080	4305	4495	4600	5145		
2796	Adams & Haggarty Amoco (Pan Am)1	AH1		3080	3550								3600	4100	4555	4820	5390		
2803	Adams & Haggarty Fitzhugh 10	AH10				1047	1230	2390	2635	2850	3580	3870	4270	4630	5120	5265	5750		
2805	Adams & Haggarty Fitzhugh 12	AH12				1045	1240	2335	2575	2730	3860	3825	4110	4510	4970	5150	5665		
2787	Adams & Haggarty Marrs McLean 11	M11				990	1190	2300	2420	2760	3375	3550	3975	4085	4695	5020	5565		
2790	Adams & Haggarty Marrs McLean 15	M15						2410	2660	2865	3820	4150	4360	4770	5090	5395	5705	6575	
2792	Adams & Haggarty Marrs McLean 17	M17				997	1220	2325	2580	2740	3520	3705	4170	4315	4853	5060	5470	6270	
2789	Adams & Haggarty Marrs McLean 18	M18				1001	1203												
2020	Adams & Haggarty Crow 1	AH				970	1470	2395	2785	2980	3850	4140	4700	5070	5570	5705	6150		
3072	Sunset Anderson 1	S1				970	1055												
3072	Sunset Anderson 2	S2		7630		1040	1250	2350	2695	3070	3630	3810	4350	4570	4880	5040	5735	6440	
30250	HNG Anderson Guiterman 1	AG1						2470	2870	3075	3955	4260	4770	4950	5235	5560	6110	6890	8350
30272	HNG Anderson Guiterman 2	AG2													5260	4550	6140	6920	

Table B-2 (Cont)

API No.	Well No.	Map Symbol	Top Cap	Top Salt	Base Salt	L	PL	A	BF	B	AB	C	RL	D	SD	E	DR	M	F
2776	McCarty (HNG) Davidson E1	E1						2400	2905	3200	3820	4205	4505	4740	5045	5240	5900	6620	
3091	HNG Davidson E2	E2				975	1200	2335	2590	3195	3730	3930	4260	4500	4870	5230	5740		
3376	HNG Davidson E3	E3					1220	2350	2630	3200	3925	4165	4710	4890	5335	5570	6125		
3121	Gulf Anderson 1	Gulf					1400	2250	2350	2920	3390	3845	4150	4265	4590	4715	5300		
2772	Pace	PA						2350	2455	2810	3770	4180	4690	5030	5550	5650	6215	6930	
2021	Goldrus	GO				970	1450	2380	2600	2950	3710	4115	4440	4760	4980	5100	5795		
2023	6TH 1	6-1				960	1450	2295	2590	2930	3760	4205	4595	4670	5165	5250	5860		
2022	6TH 2	6-2				990	1400	2210	2465	2880	3935	4230	4625	4750	5145	5495	6160		
2887	Bering (Wayne) Fitzhugh 1A	W1						2355	2650	2810	3250	3660	4100	4265	4515	4635	4270		
2775	Stanolind Davidson 1	D1	10,113																
2885	Stanolind Fitzhugh	W2						2470	2710	2950	3260	3820	4010	4140	4360	4510			
2907	Stanolind McFaddin 3A	W3						2400	2665	2900	3210	3550	4005	4280	4490	4795			
	Stanolind Pipkin 3A	3A						2305	2650	2825	3210	3540	3970	4400	4945	5340	6065		
2907	Stanolind McFaddin 3ST	W3A									3210	3510	3900	4095	4370	4515	4750		
2890	Bering (Wynne) Fitzhugh 4	W4	1930	2140 to 2280 2815 to 2940								3215	3610	3980	4050	4290	4780		
	Jayred Fitzhugh 8	J8						2550	2905	3450	4180	4430	5290	5575	6090	6230	6450		
2835	Jayred Fitzhugh 9	J9				1075	1250	2578	2915	3380	4000	4520	5030	5310	5835	5975	6190		
3094	Jayred Fitzhugh 10	J10				1082	1290	2400	2730	3150	3490	3950	4560	4960	5450	5630			
3133	Jayred Fitzhugh 11	J11				1050	1320	2455	2845	3000	3490	3970	4510	4740	5095	5250	5430		
33325	Prairie McFaddin 1	Prairie 1						2310	2685	3140	3490	3805	4675	4785	5410	5890	6275	7785	
2024	Texaco Crow 1	C1						1860	1970	2465	3070	3190	3540	3750	4005	4165			
2025	Texaco Crow 2	C2		5190		1010	1270	2010	2100	2525	3115	3220	3360	3635	3960	4085	4895		
2892	Texaco Fitzhugh 2	TXF2																	

Table B-2 (Cont)

API No.	Well No.	Map Symbol	Top Cap	Top Salt	Base Salt	L	PL	A	BF	B	AB	C	RL	D	SD	E	DR	M	F
2044	Texaco Masterson 1	K1	1460	3180		940	1120												
2045	Texaco Masterson 2	K2		4370						2080	2925	3250	3480	3690	3895	3970			
	Texaco Pipkin 5	P5						2320	2650	2950	3800	3990	4410	4550	4970	5270	5560	7060	
2914	Texaco Pipkin 6	P6					1150	2330	2590	2710	3250	3630	4040	4490	5160	5460	6165	7650	
2915	Texaco Pipkin 7ST	P7	1480	1725(?)	1890(?)	815	1180				3010	3435	3940	4105	4440	4685	5080		
2916	Texaco Pipkin 8	P8								2405	3050	3130	3525	3705	4145	4325	4540		
2374	Freeport Sulphur Staiti 1	FS1	1256																
2038	Freeport Sulphur Staiti 2	FS2	199																
2797	Freeport Sulphur Staiti 3	FS3	1146																
2875	Freeport Sulphur Staiti 4	FS4	367																
2039	Freeport Sulphur Staiti 5	FS5	268																
2876	Freeport Sulphur Staiti 6	FS6	1123																
2040	Freeport Sulphur Staiti 7	FS7	293																
2041	Freeport Sulphur Staiti 8	FS8	405																
2877	Freeport Sulphur Staiti 9	FS9	1095																
2042	Freeport Sulphur Staiti 10	FS10	316																
2824	Freeport Sulphur Staiti 11	FS11	1147																
2870	TX Exploration Broussard 1	TX1	233																
2871	TX Exploration Broussard 2	TX2	334																
2872	TX Exploration Broussard 3	TX3	1152																
2873	TX Exploration Broussard 4	TX4	1251																

Table B-2 (Cont)

API No.	Well No.	Map Symbol	Top Cap	Top Salt	Base Salt	L	PL	A	BF	B	AB	C	RL	D	SD	E	DR	M	F
	Jefferson Lake Sulphur 1	JL1	278																
	Jefferson Lake Sulphur 2	JL2	1068																
	Jefferson Lake Sulphur 3	JL3	1431																
	Jefferson Lake Sulphur 4	JL4																	
	Jefferson Lake Sulphur 5	JL5	1413																
2878	Houston Oil Staiti 1	H1	233																
2879	Houston Oil Staiti 2	H2	334																
2037	Union Oil	SWDW	795																
2035	Union Oil LPG1	U1		1630															
2036	Union Oil LPG2	U2		1700															

L Lafayette Gravel
PL Pliocene Sand
A Miocene Sand
BF Lagarto Clay
B Oakville Sand
AB *Amphistegina* B Shale
C Catahoula Sand
RL Robulus L Shale
D Main Sand
SD *Siphonina davisi* Shale
E Lower Sand
DR *Discorbis* restricted Shale

APPENDIX C

APPENDIX C

List of Contacts

APPENDIX C

List of Contacts

United Aerial Mapping	San Antonio	Ben Meitzen
PB/KBB, Inc.	Houston	Thayne Depuey Joe Cella Gene Ford Mark Stiener
Amoco Production Co.	Houston	Ted Wenzeler Tom Pinkstaff
DOE SPR-PO	Washington, DC	Dick Smith
DOE SPR-PMO	New Orleans	Ed Chapple Bob Mazurkiewicz Bob Mosely Larry Rousseau Leon Stepp Joyce Terrling Don Whittington
Texas Railroad Commission	Houston	Elva Fleckenstine Paul Stagg W. L. Gabelmann, Jr.
Texas Railroad Commission	Austin	Bob Harris
Texas Dept of Water Resources	Orange	David Buchannan
Texas Dept of Water Resources	Austin	Bob Bluntzer N. A. Jeier Mike Howard
Texas Bur. Economic Geology	Austin	Lee Jirik Jerry Wermund Frank Brown
Sabine Pass Terminal (Internorth, Inc.)	Houston	John Chauche Jerry Duffey
Union Oil Co	Beaumont	Ron Thompson

DISTRIBUTION:

US Department of Energy (3)
Strategic Petroleum Reserve
Program Office
1000 Independence Ave., SW
Washington, DC 20585
Attn: H. Jones
L. Pettis
R. Smith

US Department of Energy (13)
Strategic Petroleum Reserve
Project Management Office
900 Commerce Rd East
New Orleans, LA 70123
Attn: C. C. Johnson
G. A. Stafford
C. L. Steinkamp
E. E. Chapple (7)
J. Guarisco (2)
E. A. Crabtree

Aerospace Corp
880 Commerce Rd West, Suite 300
New Orleans, LA 70123
Attn: K. Henrie

Aerospace Corp
P. O. Box 92957
Los Angeles, CA 90009
Attn: G. F. Kuncir

Jacobs/D'Appolonia Engineers (2)
6226 Jefferson Hwy, Suite B
New Orleans, LA 70123
Attn: H. Kubicek
P. Campbell

Amoco Production Co.
P.O. Box 3092
Houston, TX 77001
Attn: T. J. Winzeler

Sabine Pass Terminal
P.O. Box 4420
Houston, TX 77210
Attn: J. G. Chauche

PB/KBB, Inc
11999 Katy Freeway #600
Houston, TX 77079
Attn: V. Lepardo

T. R. Magorian
133 South Drive
Amherst, NY 14226

Union Oil Co.
P.O. Box 237
Nederland, TX 77627
Attn: R. Thompson

4000 A. Narath
4500 E. H. Beckner
4540 M. L. Kramm
4543 J. F. Ney
4543 R. J. Hart
4543 T. S. Ortiz
4543 File (10)
8214 M. A. Pound
3141 L. J. Erickson (5)
3151 W. L. Garner (3)
For DOE/TIC (Unlimited Release)
DOE/TIC (25)
(C. Dalin, 3154-3)